Biomimetic total synthesis of peroxide-derived secondary metabolites from marine sponges

A thesis submitted for the award of Doctor of Philosophy (PhD)
on 31 May 2016 by

Matthew D. Norris, BSc(Hons)

from the School of Chemical and Physical Sciences,
Flinders University of South Australia

Declaration

I certify that this thesis does not incorporate without acknowledgment any material previously submitted for a degree or diploma in any university; and that to the best of my knowledge and belief it does not contain any material previously published or written by another person except where due reference is made in the text.

Matthew D. Norris

31 May 2016

Acknowledgements

Throughout my doctoral studies, I have been very fortunate to have the support and guidance of friends, family and mentors around me. Without these people, I could not have learned, explored or grown to the extent I have in the past four years.

I owe special thanks to my doctoral advisor Dr Michael Perkins. We have had an outstandingly productive working relationship, which has led to many published works of critical interest. He has continually challenged my approach to research and scientific reasoning, especially in the context of synthetic chemistry. He has always encouraged my creativity and helped me to realise the challenges faced and nuances presented in creative and innovate design. His support on an intellectual and professional level has been invaluable to my growth. I look forward to working with Michael well into the future.

The School of Chemical and Physical Sciences, including all academic staff, postgraduate students and technical support staff have provided ongoing support through resources and technical assistance; opportunities for professional growth and development; and a uniquely supportive community and environment. The School has been a steady platform on which I have been capable of launching into a successful early career, and for this I am endlessly grateful. I also acknowledge generous financial support through award of the MF and MH Joyner PhD Scholarship in Science.

My special thanks also to Dr Erik Sorensen and the Department of Chemistry, Princeton University for the enthusiasm, encouragement and hospitality I had the pleasure of receiving when studying in the United States. Working in Erik's laboratory has expanded my knowledge and awareness of the global community of chemistry well beyond the text with which I can communicate in this thesis. I

will always remember my days at Princeton and am very pleased to be a part of the alumni community. This outstanding opportunity would not have been possible without the support and guidance of the Australian–American Fulbright Commission and award of the Australian Fulbright Alumni (WG Walker) Postgraduate Scholarship.

Most importantly, I owe my greatest thanks to my family. They have supported me above and beyond the capabilities of any financial or academic institution. My Mum and Dad have always provided everything I need to achieve my best, and for this I am eternally grateful! My brother Jacob has been my roomy throughout my PhD at Flinders and we have had the best time together, inside and outside of studying. My partner Angie, who has always stuck by my side, even travelled all the way to the United States to see me! Our PhD journeys would not have been the same without each other. Congratulations, Dr!

To all my family, friends and colleagues, who have supported me through everything – we have completed this doctoral thesis together.

Published work

The following is a list of peer-reviewed articles and conference presentations resulting from the work presented in this thesis.

Peer-reviewed articles

1. M. D. Norris and M. V. Perkins, "A biomimetic cascade for the formation of the methyl [2(5*H*)-furanylidene]ethanoate core of spongosoritin A and the gracilioethers," *Tetrahedron*, 2013, **69**, 9813–9818. Cited by 7.

2. M. D. Norris, "Trifluoroacetic acid (TFA)," *Synlett*, 2015, **26**, 418–419. Cited by 1.

3. M. D. Norris, M. V. Perkins and E. J. Sorensen, "Biomimetic total synthesis of gracilioethers B and C," *Org. Lett.*, 2015, **17**, 668–671. Cited by 12.

4. M. D. Norris and M. V. Perkins, "Structural diversity and chemical synthesis of peroxide and peroxide-derived polyketide metabolites from marine sponges," *Nat. Prod. Rep.* 2016, **33**, 861–880. Cited by 1.

5. M. D. Norris and M. V. Perkins, "Total synthesis of plakilactones B, C and *des*-hydroxyplakilactone B by the oxidative cleavage of gracilioether furanylidenes," *J. Org. Chem.* 2016, **81**, 6848–6854.

Conference presentations

1. M. D. Norris and M. V. Perkins, "Toward a total synthesis of spongosoritin A and the gracilioethers: a biomimetic cascade for the formation of the hydrofurenone core," short talk at the 19th International Conference on Organic

Synthesis and 24th Royal Australian Chemical Institute Organic Conference, Melbourne, Australia.

2. M. D. Norris, E. J. Sorensen and M. V. Perkins, "Accessing the structural complexity of rare natural medicines: biomimicry in chemical synthesis," invited poster presentation at the Australian-American Fulbright Symposium, Canberra, Australia.

3. M. D. Norris and M. V. Perkins, "Biomimetic total synthesis of gracilioether furanylidenes and preliminary studies into their oxidation," short talk at the Royal Australian Chemical Institute Adelaide Synthetic Chemistry Symposium, Adelaide, Australia.

4. M. D. Norris and M. V. Perkins, "Strategy for a biomimetic total synthesis of the covalent PPARγ agonists gracilioether B and plakilactone C," short talk at the 248th American Chemical Society National Meeting, San Francisco, United States.

5. M. D. Norris and M. V. Perkins, "Biomimetic total synthesis of gracilioether and plakilactone marine natural products," poster presentation at the 24th International Symposium Synthesis in Organic Chemistry, Royal Society of Chemistry, Cambridge, United Kingdom.

6. M. D. Norris and M. V. Perkins, "A divergent and nature-inspired strategy for the total synthesis of gracilioether furanylidenes and plakilactone butenolides: building a sturdy platform to probe SARs," poster presentation at the RACI Medicinal Chemistry and Chemical Biology Conference, Sydney, Australia.

Thesis summary

This doctoral thesis reports the first enantioselective total synthesis and structural elucidation of six natural products, each isolated from the extracts of marine sponges collected near Japan, Fiji and the Caribbean Islands. These compounds, named gracilioether B, gracilioether C, *des*-hydroxygracilioether C, plakilactone B, *des*-hydroxyplakilactone B and plakilactone C are considered potential targets for the treatment of type II diabetes, have promising levels of antimalarial activity and exhibit some selectivity for cytotoxicity against cancer cells. Their structures, including the relative and absolute configuration of each, were assigned in this study by matching the nuclear magnetic resonance spectra, high-resolution mass data and specific rotation of several synthetic isomers to that reported for the natural material. This is the first and only time in the chemical literature that these important natural compounds have been synthesised in a laboratory and matched unequivocally to the spectral data of original samples.

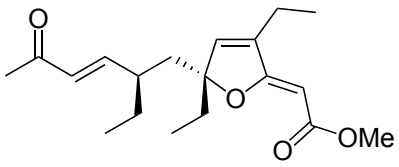

gracilioether B

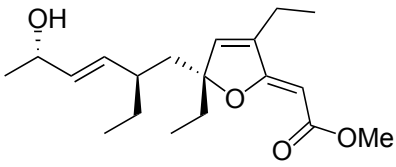

gracilioether C

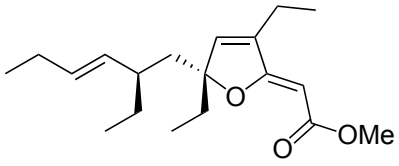

des-hydroxygracilioether C

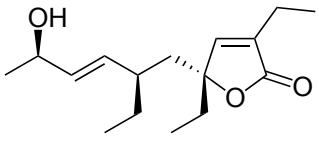

plakilactone B

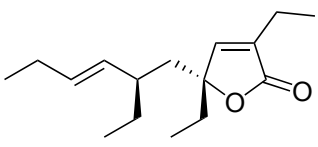

des-hydroxyplakilactone B

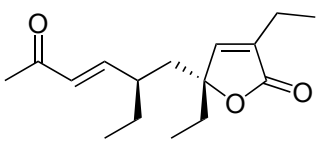

plakilactone C

This thesis also demonstrates a critical understanding of the compound class through a comprehensive review of relevant literature, which has produced new insight to the biosynthetic origin of the gracilioether furanylidenes and plakilactone butenolides from related endoperoxides; and driven development of the methodology reported herein. Notably, the present study is the first to suggest that plakortin endoperoxides, gracilioether furanylidenes and plakilactone butenolides isolated from marine sponges are inextricably linked through their biosynthesis, non-enzymatic dehydrative ring contraction and oxidative scission.

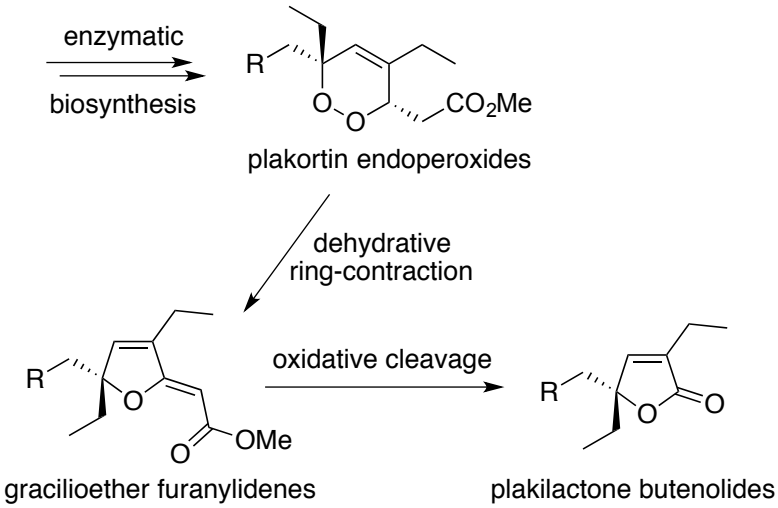

Each target compound was reached through a careful series of synthetic transformations that were selected, trialled and optimised to increase overall yield and to minimise difficult, unnecessary and wasteful procedures. These efforts have produced an expeditious and versatile synthetic route to the natural products, which is amenable to the synthesis of many natural and synthetic analogues of the gracilioethers and plakilactones. At the centrepiece of this approach is a facile biomimetic transacetalisation/dehydration cascade reaction of an advanced synthetic precursor, which was engineered to deliver the unsaturated 'furanylidene' heterocycle of the gracilioethers in a single operation. This in turn, was accessed through an unprecedented sodio-lithio aldol reaction of a substituted β-ketoester and hindered neo-pentyl aldehyde substrate. Finally, a novel and chemoselective oxidative cleavage reaction of the gracilioether furanylidenes with pyridinium chlorochromate (Corey-Suggs reagent) facilitated direct access to the plakilactone butenolides.

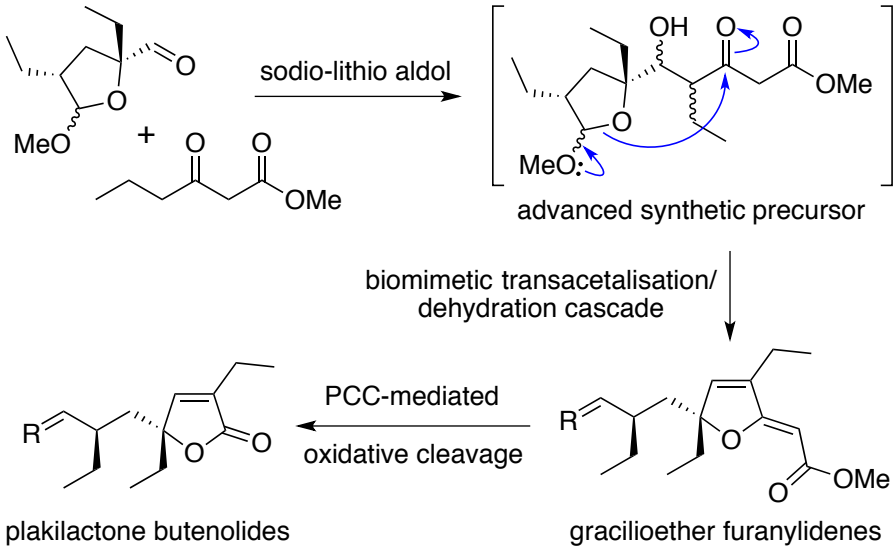

The results presented herein are of significant value for further exploring the use and appropriation of the gracilioether furanylidenes and plakilactone butenolides for target identification and drug development in a pharmaceutical setting.

Glossary of abbreviations and non-standard terms

[M]	Metal complex
[α]	Specific rotation
[θ]	Ellipticity
1D	One-dimensional
2D	Two-dimensional
Ac	Acetyl
AD	Asymmetric dihydroxylation
AIBN	Azobisisobutyronitrile
aq	Aqueous
Ar	Aromatic
ATP	Adenosine triphosphate
bipy	2,2'-Bipyridine
Bn	Benzyl
brsm	Based on recovered starting material
Bz	Benzoyl
c	Concentration (g/100mL)
CBS	Corey-Bakshi-Shibata
CD	Circular dichroism
COSY	Correlation spectroscopy
d	Days (when used in the context of time elapsed)
d	Doublet multiplicity (when used in the context of NMR spectroscopy)
Daipen	1,1-bis(4-Methoxyphenyl)-3-methylbutane-1,2-diamine
DBU	1,8-Diazabicycloundec-7-ene
DCC	Dicyclohexylcarbodiimide
DCE	1,2-Dichloroethane

DDQ	2,3-Dichloro-5,6-dicyano-1,4-benzoquinone
$(DHQ)_2PHAL$	Hydroquinidine 1,4-phthalazinediyl diether
DIBAL	Diisobutylaluminium hydride
DIPA	Diisopropylamine
DIPEA	Diisopropylethylamine
DMAP	4-Dimethylaminopyridine
DMF	Dimethylformamide
DMP	Dess-Martin periodinane
DMPU	1,3-Dimethyl-3,4,5,6-tetrahydro-2-pyrimidinone
DMSO	Dimethylsulfoxide
DNA	Deoxyribonucleic acid
dr	Ratio of diastereomers
DT_{50}	Half dissipation concentration
E	Electrophile (non-italicised)
EC_{50}	Half maximal effective concentration
ee	Enantiomeric excess
Enz	Enzyme
ESI	Electrospray ionisation
Et	Ethyl
fod	1,1,1,2,2,3,3-Heptafluoro-7,7-dimethyl-4,6-octanedionate
FTIR	Fourier transform infrared
h	Hours
HMBC	Heteronuclear multiple-bond correlation spectroscopy
HOBT	1-Hydroxybenzotriazole
HRMS	High-resolution mass spectrometry
HSQC	Heteronuclear single-quantum coherence spectroscopy
HWE	Horner-Wadsworth-Emmons
IC_{50}	Half maximal inhibitory concentration
^{i}Pr	2-Propyl
J	Coupling constant
LC/MS	Liquid chromatography/mass spectrometry
LDA	Lithium diisopropylamide
LHMDS	Lithium bis(trimethylsilyl)amide

lit.	Literature
M	Molecular ion (when used in the context of mass spectrometry)
m	Multiplet (when used in the context of NMR spectroscopy)
*m*CPBA	3-Chloroperoxybenzoic acid
Me	Methyl
MIC	Minimum inhibitory concentration
min	Minutes
modp	2-(5-Mercapto-1,3,4-oxadiazol-2-yl)phenol
MOM	Methoxymethyl
mp	Melting point
MPA	Methoxyphenylacetate
MS	Molecular sieves
MTPA	Methoxy(trifluoromethyl)phenylactate
N/A	Not applicable
^{n}Bu	1-Butyl
NMO	4-Methylmorpholine *N*-oxide
NMR	Nuclear magnetic resonance
NOE	Nuclear Overhauser effect
NOESY	Nuclear Overhauser effect spectroscopy
p	Pentet multiplicity
PCC	Pyridinium chlorochromate
PG	Protecting group
PGME	Phenylglycine methyl ester
Ph	Phenyl
PHB	4-Hydroxybenzyl
PMB	4-Methoxybenzyl
PMP	4-Methoxyphenyl
pol	Polymerase
PPARγ	Peroxisome proliferator-activated receptor γ
PPTS	Pyridinium 4-toluenesulfonate
PXR	Pregnane-X-receptor
PyBoP	Benzotriazolyloxytri(pyrrolidinyl) phosphonium hexafluorophosphate
q	Quartet multiplicity

quant.	Quantitative yield
R	Any group with the prescribed limitations
r.t.	Room temperature (20 °C)
R_f	Retention factor
ROE	Rotating frame nuclear Overhauser effect
ROESY	Rotating frame nuclear Overhauser effect spectroscopy
s	Singlet multiplicity (when used in the context of NMR spectroscopy)
s	Seconds (when used in the context of time elapsed)
salen	2,2'-Ethylenebis(nitrilomethylidene)diphenol
SAR	Structure-activity relationship
satd	Saturated
t	Triplet multiplicity
TBAF	Tetrabutylammonium fluoride
TBS	*tert*-Butyldimethylsilyl
^{t}Bu	2,2-Dimethylpropyl
TES	Triethylsilyl
Tf	Trifluoromethanesulfonyl
TFA	Trifluoroacetic acid or trifluoroacetyl
TFE	2,2,2-Trifluoroethanol
thd	2,2,6,6-Tetramethyl-3,5-heptanedionate
THF	Tetrahydrofuran
TLC	Thin layer chromatography
TMS	Trimethylsilyl
TPAP	Tetrapropylammonium perruthenate
Ts	4-Toluenesulfonyl
UV	Ultraviolet
Xylbinap	2,2'-bis[bis(3,5-Dimethylphenyl)phosphino]-1,1'-binaphthyl
Δ	Difference
δ_C	Chemical shift of carbon nuclei (ppm)
δ_H	Chemical shift of hydrogen nuclei (ppm)
ν_{max}	Wavenumber of maximum absorption (cm^{-1})

Table of contents

1. Introduction

There is a global demand for the relief of human suffering and disadvantage caused by infectious diseases, the proliferation of cancerous tumours and physiological disorders of the body. For hundreds of years we have continued to develop a better understanding of how to treat these ailments through patient care, surgical methods and traditional medicines derived from plant and animal material. Scientific research has now advanced to a molecular level and our understanding of the biophysical and biochemical processes that regulate bodily functions and disorders is growing at a remarkable pace. The discovery and application of vaccine technologies, small-molecule antibiotics, chemotherapies and radiotherapies have reduced suffering and increased the quality of life for millions. However, the emergence of antibiotic resistance; identification of more complex neurological and cardiovascular disorders; and the on-going threat of cancer metastasis presents an urgent need to further understand, prevent and repair the existing and emerging illnesses that continue to threaten human life.

Inspired by the use of natural medicines from plant and animal material, small molecule therapeutics are one of the most effective targets for treating infectious diseases, cancers and physiological disorders. It is often discovered that specific chemical components of natural medicines interact with the biochemical processes of pathogenic bacteria or disfunctional metabolic pathways in the human body to regulate cellular mechanisms, promoting or repressing the action of associated enzymes and proteins. This can help to manage physiological deficiencies or arrest cancer cell proliferation and the spread of infectious microorganisms throughout the body.

The efficacy of natural medicines can also be modulated or enhanced by manipulating their electronic and spatial structure through chemical

modification. Many of the therapeutic drugs available in the clinic are either derived from natural product scaffolds through chemical modification of the parent structure or are synthesised by analogy; and a number have risen purely through chemical synthesis. Thus, the ability to construct complex molecular frameworks from smaller chemical building blocks, the 'art of chemical synthesis' is fundamental for drug identification, development and optimisation.

This thesis details an effort to understand and apply new ideas, theories and methods at the cutting edge of chemical synthesis toward the goal of producing new small-molecule treatments for infectious diseases, human cancers and physiological disorders. The work is inspired by the structural complexity and promising therapeutic potential of peroxide and peroxide-derived metabolites isolated from marine sponges. The topic is of special interest given award of the 2015 Nobel Prize in Medicine to researchers who discovered and developed the endoperoxide metabolite artemisinin as a first-line defence against malaria (Figure 1.1).

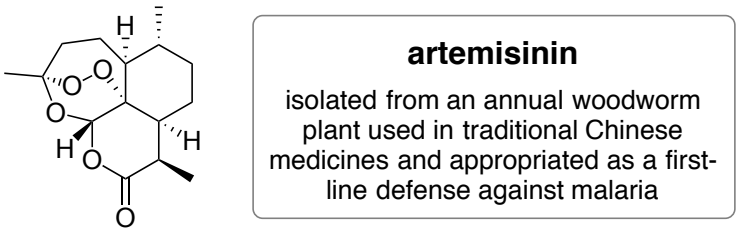

Figure 1.1: Structure of artemisinin, an antimalarial natural product that was the subject of the 2015 Nobel Prize in Medicine.

The work described herein is focused on developing a better understanding of the biosynthesis of the peroxide-derived metabolites gracilioethers B and C (Figure 1.2); and to develop an effective strategy for their total synthesis using this insight. The compounds are of great significance because they are known to be agonists of peroxisome proliferator-activated receptor γ, a pharmacological target for the treatment of type II diabetes; exhibit moderate activity against chloroquine-resistant strains of *Plasmodia* (malaria); and show cytotoxicity against a number of cancer types, with some observed selectivity above non-tumorous cells. The natural products have a complex molecular structure and few methods have been developed to address the challenges associated with

their chemical synthesis. Furthermore, the low availability of these compounds from natural sources prevents their supply through specimen extraction.

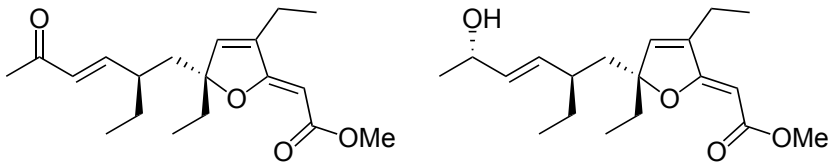

gracilioether B **gracilioether C**

isolated from marine sponges of the genera *Plakortis*, *Plakinastrella* and *Agelas*; novel target compounds for the treatment of type II diabetes, chloroquine-resistant strains of *Plasmodia* and cancer cell types

Figure 1.2: Structure of gracilioether B and C, polyketide metabolites isolated from marine sponges of the genera *Plakortis*, *Plakinastrella* and *Agelas*.

The thesis is presented in five major chapters, each detailing an original contribution to the field of synthetic chemistry. The first major chapter (Chapter 2) is a comprehensive and critical review of the current literature on peroxide and peroxide-derived polyketide metabolites. The review summarises published literature to the date of thesis submission and includes many of the candidate's contributions, which are placed in the context of the surrounding literature. The candidate's insight to this literature is also presented as a critical discussion in many parts. The second major chapter (Chapter 3) presents a revised theory for the non-enzymatic biosynthesis of the sponge metabolites gracilioethers B, C and spongosoritin A (a related compound). This theory is drawn from relevant literature that was previously disconnected and is supported through the synthesis of a model substrate to the natural products. The third major chapter (Chapter 4) outlines the progression of ideas and experiments that ultimately led to the discovery of a viable synthetic route to construct the natural products; and the fourth major chapter (Chapter 5) details the first enantioselective total synthesis of gracilioethers B and C using this approach. Finally, the fifth major chapter (Chapter 6) expands on all previous work to report the first enantioselective total synthesis and structural elucidation of four related sponge metabolites with additional comments on their biosynthetic origin.

Where possible, these chapters are presented as articles prepared for peer review and publication in reputable scientific outlets, with each chapter progressing fluently to the next. In accordance with the Flinders University rules and guidelines for thesis presentation, these published chapters are linked by a conceptual statement at the beginning and summary at the end of each chapter. Presenting this work in its peer-reviewed and published form illustrates the candidate's commitment to organising, writing and presenting research results in a timely manner and at an international standard, while being held accountable by peers and experts in the field. The candidate researched, planned, executed and prepared each of these chapters and published articles with full intellectual and practical contribution with due guidance and only minor textual editing from co-authors throughout manuscript preparation and final publishing, as stated at the beginning of each chapter.

2. Peroxide and peroxide-derived metabolites

In a global search for novel drug candidates to treat infectious diseases, cancers and human physiological disorders (Chapter 1), endoperoxide-containing metabolites have attracted significant interest as promising therapeutic leads. Recently, the 2015 Nobel Prize in Medicine was awarded to researchers who discovered and developed the antimalarial sesquiterpene lactone endoperoxide artemisinin, a natural product isolated from an annual woodworm plant used in traditional Chinese medicines. After the rise of peroxide antimalarial agents in the 1980s and with the increasing risk of chloroquine and mefloquine resistant strains, efforts have turned to the isolation and biological analysis of other peroxide metabolites, especially from the extracts of marine sponges. Now, more than 40 years since the isolation of artemisinin, scientific literature is rich with a diverse range of peroxide and peroxide-derived metabolites from marine sponges. Their unique structural elements and compelling therapeutic potential drive further research to understand their chemistry and biology; and to discover how these novel compounds might be useful in the treatment of human diseases.

Chapter 2 details the 'structural diversity and chemical synthesis of peroxide and peroxide-derived polyketide metabolites from marine sponges' as prepared in an article with the same title and published in the refereed journal *Natural Product Reports*, Royal Society of Chemistry on 10 May 2016 (DOI: 10.1039/c5np00142k). The candidate researched, planned, executed and prepared the following chapter/published article with full intellectual and practical contribution with due guidance and only minor textual editing from co-authors throughout manuscript preparation and final publishing; and is listed as the primary author of this work.

2.1 Structural diversity and chemical synthesis of peroxide and peroxide-derived polyketide metabolites from marine sponges

Marine sponges are widely known as a rich source of natural products, especially of polyketide origin, with a wealth of chemical diversity. Within this vast collection, peroxide and peroxide-derived secondary metabolites have attracted significant interest in the fields of natural product isolation and chemical synthesis for their structural distinction and promising *in vitro* antimicrobial and anticancer properties. In this review, peroxide and peroxide-derived polyketide metabolites isolated from marine sponges in the past 35 years are summarised. Efforts toward their synthesis are detailed with a focus on methods that utilise or attempt to elucidate the complex biosynthetic interrelationships of these compounds beyond enzymatic polyketide synthesis (Figure 2.1). Recent isolations, advances in synthetic methodology and theories of biogenesis are highlighted and critically evaluated.

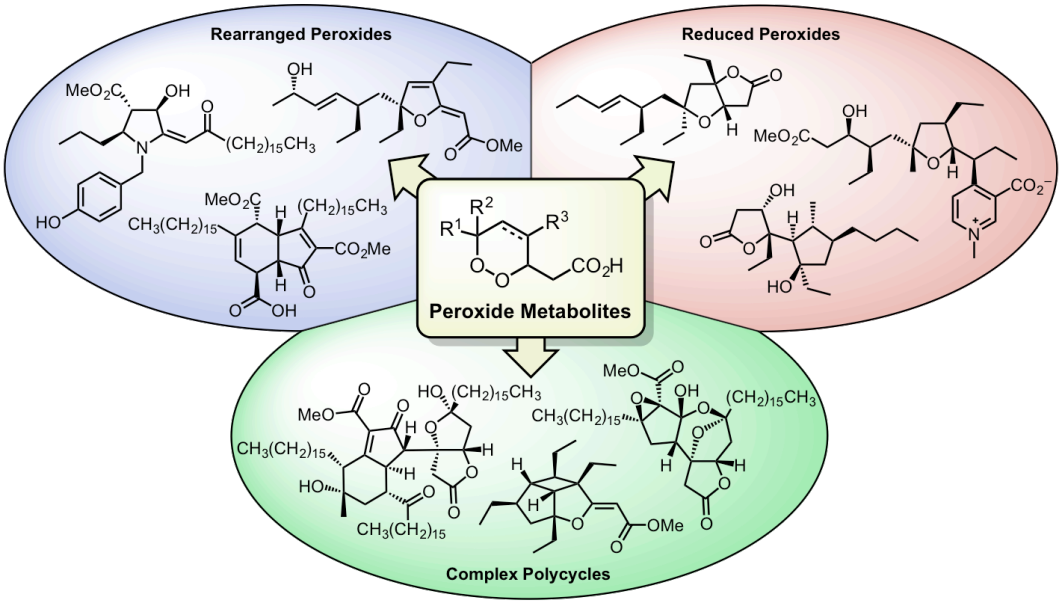

Figure 2.1: An artistic illustration of chemical literature on the topic: structural diversity and chemical synthesis of peroxide and peroxide-derived polyketide metabolites from marine sponges.

2.2 Introduction

Organic extracts of marine sponges from all corners of the globe often exhibit promising *in vitro* antimicrobial and anticancer properties, prompting further exploration to identify and characterise the constituent metabolites. In 1978, Faulkner examined the crude ethanol extracts of *Plakortis halichondrioides* and attributed the sample's notable growth inhibition of *Staphylococcus aureus* and *Escherichia coli* to the major product isolated, plakortin.[1] Structural elucidation by spectroscopic methods and chemical degradation revealed 1,2-dioxane **1** as the identity of plakortin (Figure 2.2).[2] Near the same time, a novel peroxyketal metabolite, chondrillin (**2**), was isolated from a marine sponge of the genus *Chondrilla*.[3] Compound **2** and a number of natural analogues were shown to be cytotoxic against mouse leukaemia cells and were activators of sarcoplasmic reticulum Ca^{2+} ATPase.[4,5]

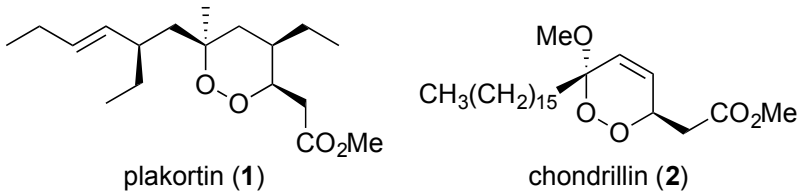

plakortin (**1**) chondrillin (**2**)

Figure 2.2: Plakortin (**1**) and chondrillin (**2**), polyketide endoperoxides from marine sponges of the genus *Plakortis* and *Chondrilla*.

With unique peroxyheterocyclic core structures and compelling therapeutic potential, compounds **1** and **2** have inspired numerous research programs in the fields of natural product isolation, chemical synthesis and medicinal chemistry since the late 1970s. The class has now expanded to include many new peroxide and peroxide-derived heterocycles and carbocycles with biological significance; and novel structural elements that have been targeted in the development of new synthetic methodology. A number of review articles on this topic have appeared in recent years. Most have focused on structural determination and biological analyses of marine endoperoxides;[6–13] and one from 2004 focused on methods developed for their chemical synthesis.[14] However, none have detailed the complex biosynthetic interrelationships of these compounds beyond enzymatic polyketide synthesis. Now, we present a critical review discussing the structural elucidation, chemical synthesis and therapeutic potential of this important

compound class, with special focus on their intriguing structural similarities and differences from a biogenetic perspective.

This review summarises the peroxide and peroxide-derived metabolites of polyketide origin reported since the discovery of **1** and **2**. Theories of biogenesis, both generally accepted and speculative; and examples of the use of chemical synthesis to demonstrate or utilise this understanding, are highlighted. Notably, it appears that the occurrence of many structurally novel polyketides in this family can be attributed to non-enzymatic modification or rearrangement of peroxide progenitors, which themselves are formed in enzymatic condensation and hydroperoxidation processes. This article is therefore presented in four parts: the first section (Section 2.3) summarises peroxide metabolites; the second section (Section 2.4) discusses related compounds most likely derived from base-mediated rearrangement; the third section (Section 2.5) details natural products that appear to arise from endoperoxide reduction; and the fourth section (Section 2.6) comments on the therapeutic potential of this compound class. Additionally, oxidative adducts are discussed where necessary.

2.3 Peroxide metabolites from marine sponges

Since the discovery of **1** and **2**, a suite of related metabolites have been isolated from marine sponges. These include plakorin (**3**),[4] xestins A (**4**), B (**5**),[5] manadoperoxides A–C, D (**6**), E–K,[15–17] manadodioxans A–E,[18] haterumadioxins A (**7**), B (**8**),[19] plakortenone (**9**),[20] plakortides E–O, P (**10**), Q–U, Z, AA,[20–32] plakorstatin 1 and 2 (**11**),[33] monotriajaponides B, C, D (**12**),[34] plakinic acids A (**13**), B–P,[32,35–43] plakortolides A–O, P (**14**), Q–W,[40–48] plakortoperoxides A1 (**15**), A2 (**16**), B–D,[48] capucinoate A (**17**),[49] plakortisinic acid (**18**),[50] andavadoic acid (**19**),[46] and related compounds (Figure 2.3).[6,7,13,51–62] Following global interest in antimalarial peroxide natural products such as artemisinin,[63,64] compounds in this class are routinely screened for *in vitro* activity against strains of *Plasmodia* (Section 2.6.1).[11,12,65,66] Testing for cytotoxic action against cancer cell types is also commonplace (Section 2.6.2).[8–10] Despite many encouraging results, the availability of marine endoperoxides is usually very poor and methods for their chemical synthesis are still in development.

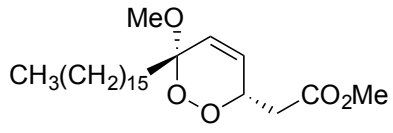

plakorin (**3**)

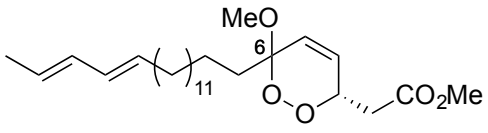

xestin A (6*R*) (**4**)
xestin B (6*S*) (**5**)

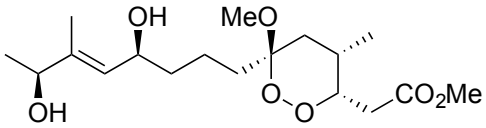

manadoperoxide D (**6**)

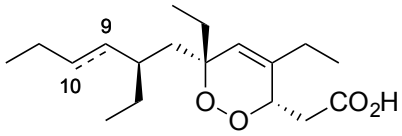

$\Delta_{9,10}$ haterumadioxin A (**7**)
haterumadioxin B (**8**)

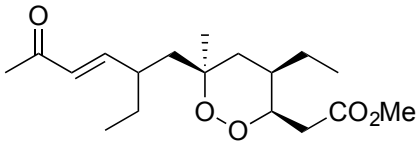

plakortenone (**9**)

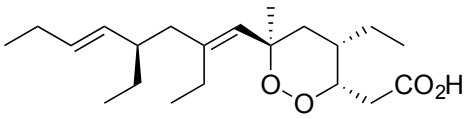

plakortide P (**10**)

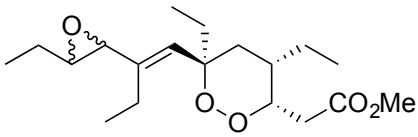

plakorstatin 1 and 2 (**11**)

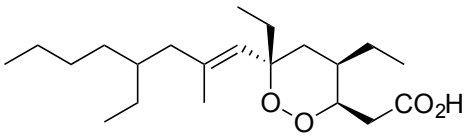

monotriajaponide D (**12**)

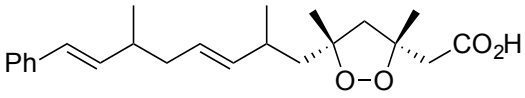

plakinic acid A (**13**)

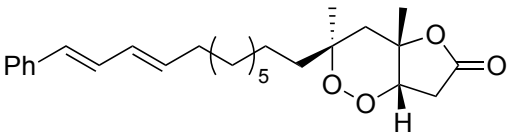

plakortolide P (**14**)

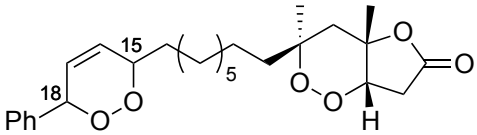

plakortoperoxide A1 (15*R*,18*R*) (**15**)
plakortoperoxide A2 (15*S*,18*S*) (**16**)

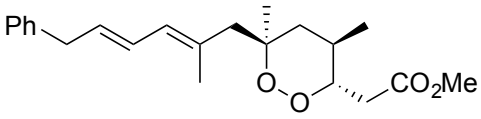

capucinoate A (**17**)

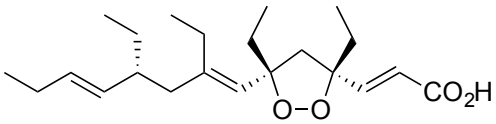

plakortisinic acid (**18**)

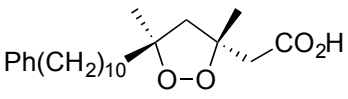

andavadoic acid (**20**)

Figure 2.3: Selected peroxide metabolites of polyketide origin isolated from marine sponges (absolute stereochemistry not implied).

2.3.1 Peroxide biosynthesis

Importantly, all the above-mentioned endoperoxides are isolated as optically active compounds and are thus believed to arise from the enzymatic inclusion of molecular oxygen to an unsaturated polyketide scaffold. Capon first proposed a model for enzymatic hydroperoxidation of 2,5-dienoic acids to yield straight-chain peroxides (**20**), which then undergo oxa-Michael cyclisation to generate enantiomerically enriched 1,2-dioxanes (Scheme 2.1).[67] The model was initially developed to illustrate biosynthesis of the norterpene peroxide sigmosceptrellin D,[67,68] but has since been extended to rationalise the formation of other polyketide endoperoxides, including those related to plakortin.[47] Recently, metagenomic analyses of several marine sponges have provided insight to the complexity of the metabolic processes of these organisms and their symbiotic microbiome.[69,70]

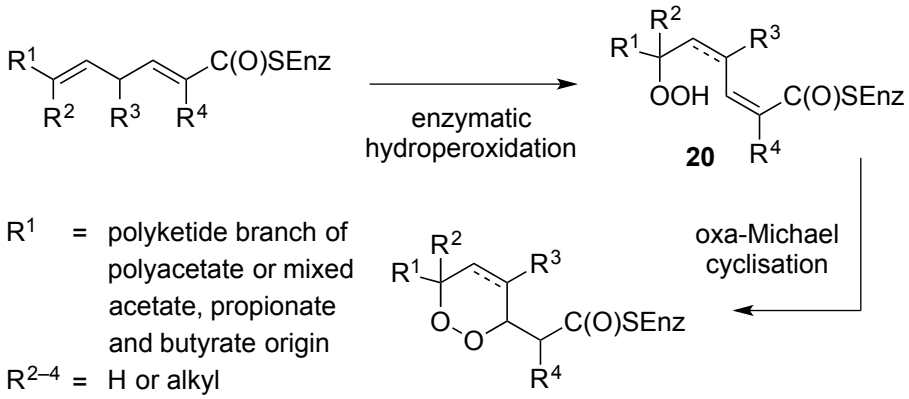

Scheme 2.1: Biosynthesis of polyketide endoperoxides based on Capon's model.

2.3.2 Chemical synthesis of peroxide metabolites

Natural products of this family, characterised by highly substituted peroxyheterocyclic core structures with specific absolute configuration, present unique challenges as targets in the field of chemical synthesis. A variety of approaches have been explored, most involving molecular oxygen or hydrogen peroxide as key reagents to construct the endoperoxide system.

Cobalt(II)-catalysed peroxysilylation developed by Mukaiyama and Isayama[71,72] is used extensively to generate open hydroperoxide substrates, which are poised for cyclisation to 5- and 6-membered rings. Although the oxidation itself proceeds with little facial selectivity, stereocontrol in the subsequent cyclisation event has proven

effective. Inspired by Capon's model (Section 2.3.1), Harwood accessed compound **21** by peroxysilylation of olefin **22** and effected oxa-Michael cyclisation to the pendant α,β-unsaturated ester yielding a number of stereoisomers related to mycaperoxide B (Scheme 2.2).[73,74] Similarly, Mukaiyama's method allowed the synthesis of lactone **23**, which underwent conjugate-base elimination and oxa-Michael cyclisation to construct both plakortolide E (**24**) and *ent*-plakortolide I (**25**) in 2012 (Scheme 2.3).[75] The asymmetric total synthesis of **24** and **25** prompted clarification of the relative and absolute configuration of the natural products.[47,75,76] Campiani and co-workers were able to obtain peroxysilane **26** by the same methodology, before initiating 6-*exo*-tet hydroperoxide cyclisation to dioxane **27** (Scheme 2.4).[77–79] In a number of subsequent steps, the first total synthesis of 9,10-dihydroplakortin (**28**) was accomplished and its absolute configuration was confirmed.[77–79] Notably, the relative and absolute configuration of **28** and its dehydro analogue **1** were established from the natural material through application of Kusumi's and Mosher's methods to selected products of chemical degradation (Scheme 2.5).[2] Lanthanide-induced shift experiments of alcohol **29** with $Eu(fod)_3$ were also used to assign the relative stereochemistry of **1**.[1] Finally, Vatéle employed a similar hydroperoxide cyclisation approach toward the synthesis of andavadoic acid (**19**), effecting oxidation of olefin **30** to peroxysilyl ether **31**, which was followed by 5-*exo*-tet cyclisation to dioxolane intermediate **32** (Scheme 2.6).[80–82]

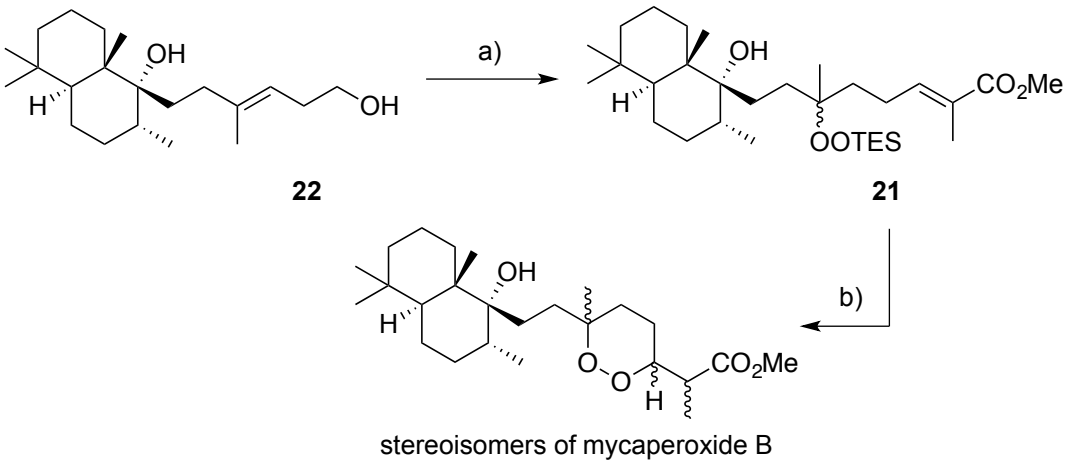

Scheme 2.2: Synthesis of mycaperoxide B diastereomers by Mukaiyama–Isayama peroxidation and cyclisation. a) O_2, $Co(modp)_2$, Et_3SiH, DCE, r.t.; then DMP, CH_2Cl_2, r.t., 2 h; then $(CH_3)C(PPh_3)CO_2Me$, CH_2Cl_2, r.t., overnight, 21% over 3 steps; b) PPTS, EtOH, r.t., 6 h; then Et_3N, MeOH, r.t., 2 d, 8% over 2 steps.

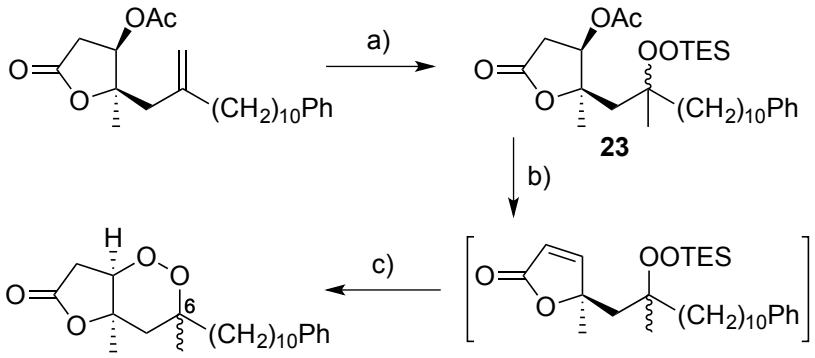

Scheme 2.3: Synthesis of plakortolide E (**24**) and *ent*-plakortolide I (**25**) by Mukaiyama–Isayama peroxidation and cyclisation. a) O_2, $Co(thd)_2$, Et_3SiH, DCE, r.t., 2 h, 94%; b) DBU, THF, 0 °C, 3 h; then c) TFE, TBAF, 0 °C, 3 h, 75% over 2 steps.

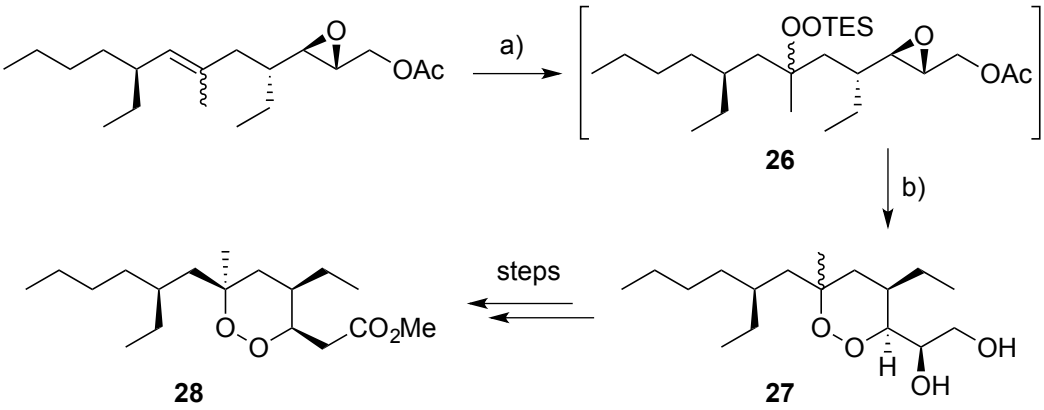

Scheme 2.4: Synthesis of 9,10-dihydroplakortin (**28**) by Mukaiyama–Isayama peroxidation and 6-*exo*-tet cyclisation. a) O_2, $Co(thd)_2$, Et_3SiH, DCE, r.t., 5 h; then b) Amberlyst, CH_2Cl_2, r.t., 18 h; then K_2CO_3, MeOH, 0 °C, 3 h, 78% over 3 steps.

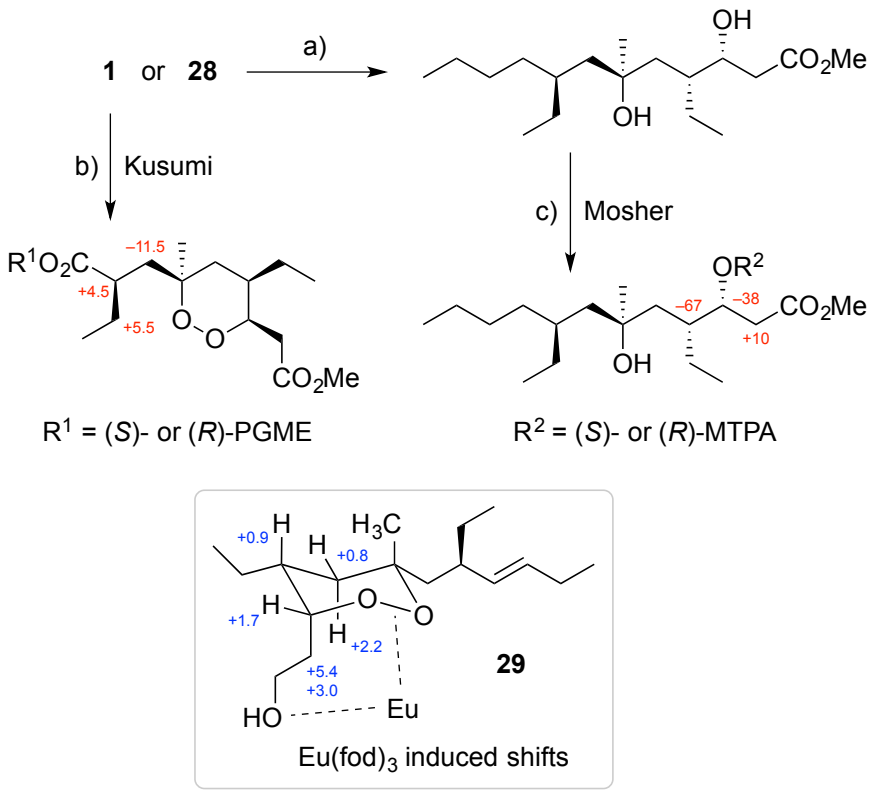

Scheme 2.5: Application of Kusumi's and Mosher's methods to determine the absolute configuration of plakortin (**1**) and dihydroplakortin (**28**); and Eu(fod)$_3$ induced shift data to determine relative configuration of **1**. Change in chemical shift due to Kusumi's and Mosher's method expressed as shift of (*R*)-PGME or (*R*)-MTPA compound subtracted from shift of (*S*)-PGME or (*S*)-MTPA compound (in Hz) and shown as red numbers. Change in shift due to incorporation of Eu(fod)$_3$ (in ppm) shown as blue numbers. a) H_2 (1 atm), 10% Pd/C, EtOH, r.t., 5 h; b) $KMnO_4$, $NaIO_4$, Na_2CO_3, ^{t}BuOH, H_2O, 37 °C, 20 h; then (*S*)- or (*R*)-PGME hydrochloride, PyBoP, HOBT, *N*-methylmorpholine, DMF, r.t., 3 h, 76% over 2 steps (for both (*S*)- and (*R*)-PGME amide); c) (*S*)- or (*R*)-MTPA chloride, pyridine, r.t., overnight, 88% (for both (*S*)- and (*R*)-MTPA ester). PGME = phenylglycine methyl ester; PyBoP = benzotriazolyloxytri(pyrrolidinyl) phosphonium hexafluorophosphate; HOBT = 1-hydroxybenzotriazole; MTPA = methoxy(trifluoromethyl)phenylactate.

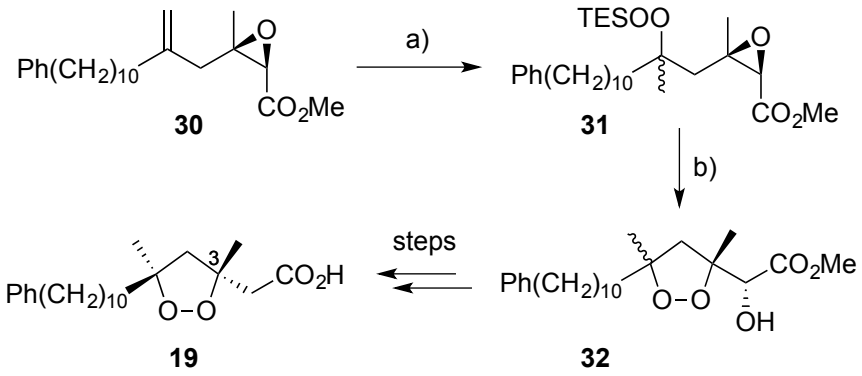

Scheme 2.6: Synthesis of andavadoic acid (**19**) by Mukaiyama–Isayama peroxidation and 5-*exo*-tet cyclisation. a) O_2, $Co(thd)_2$, Et_3SiH, DCE, r.t., 3–4 h, 86%; b) K_2CO_3, MeOH, 0 °C, 3 h, 64%.

Wong and co-workers took a different approach to the synthesis of 1,2-dioxolanes *en route* to plakortide E (**33**), constructing a pivotal [3.2.1]-peroxybicycle intermediate (**34**) using Feldman's[83–85] method for vinyl cyclopropane oxygenation (Scheme 2.7).[86] Thus, irradiation of lactone *rac*-**35** with a 300W sunlamp in the presence of catalytic Ph_2Se_2 and AIBN under an atmosphere of oxygen effected near quantitative oxidation to *rac*-**34**. Selective reduction of the lactone ester and lipase-

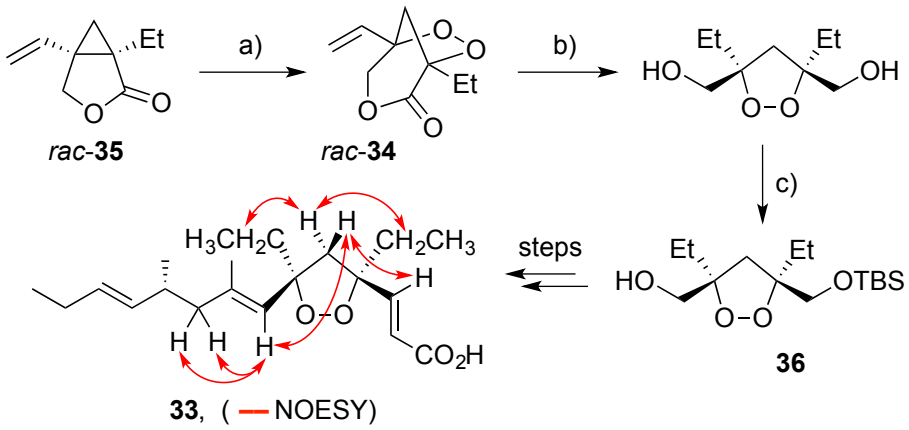

Scheme 2.7: Synthesis of plakortide E (**33**) by Feldman vinyl cyclopropane oxygenation. Selected NOESY correlations of natural **33** shown as red arrows. a) O_2, Ph_2Se_2, AIBN, MeCN, 300W lamp, r.t., 99%; b) $LiBH_4$, THF, 0 °C; then $KO_2CN{=}NCO_2K$, AcOH, CH_2Cl_2, 0 °C (three cycles), 70% over 2 steps; c) TBSCl, imidazole, DMAP, DMF, 0 °C to r.t.; then lipase, vinyl acetate, hexane, 29 h, 32% over 2 steps.

mediated kinetic resolution gave TBS ether **36** in >99% *ee*, before completing the synthesis over several steps. Using this approach, four stereoisomers of plakortide E were synthesised, establishing the relative and absolute configuration of the natural product as (4*S*,6*R*,10*R*)-**33** (selected NOESY correlations of the natural material shown in Scheme 2.7).[22] A similar method was later used to establish the first asymmetric total synthesis of epiplakinic acid F.[87]

Endoperoxide substrates have also been successfully constructed from suitable straight-chain dienes by [4+2] cycloaddition with singlet oxygen.[88] Jung[89] and Taylor[90] have each prepared peroxylactone analogues from diene precursors and a racemic synthesis of 6-*epi*-plakortolide E (*rac*-**25**) was completed in 2002 (Scheme 2.8).[89] Steliou used a similar approach for the synthesis of two cytotoxic endoperoxides isolated from *Plakortis angulospiculatus* in 1990.[91,92] Garson effected photooxygenation of natural plakortolide P (**14**), yielding synthetic plakortoperoxide A1 (**15**) and A2 (**16**) as a 1:1 mixture (Scheme 2.9).[48] Snider constructed the peroxyketal diastereomers **2** and **3** by photooxygenation of ketone **37**, presumably via the enolic tautomer **38** (Scheme 2.10).[93–95] The first asymmetric synthesis of **2** and **3** was later achieved by photooxygenation of enantio-enriched allyl alcohols followed by hydroperoxide rearrangement.[96–98] Peroxyketal structures related to **1–3** were also synthesised by Fattorusso and co-workers using manganese(III) acetate catalysed addition of molecular oxygen to β-ketoester and olefin substrates.[99,100]

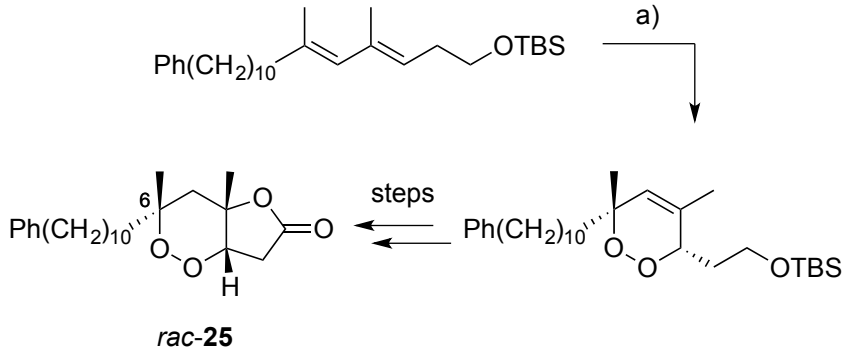

rac-**25**

Scheme 2.8: Synthesis of 6-*epi*-plakortolide E (*rac*-**25**) by [4+2] cycloaddition of singlet oxygen. a) O_2, rose bengal, CH_2Cl_2, MeOH, 500W lamp, 0 °C, 6 h.

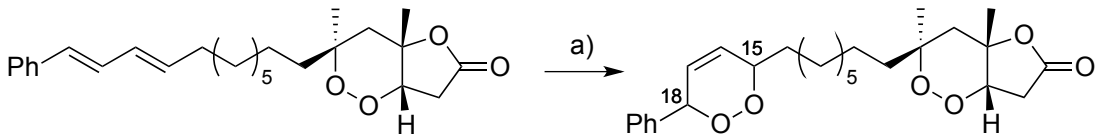

14 **15** (15*R*,18*R*) and **16** (15*S*,18*S*), ~1:1

Scheme 2.9: Conversion of natural plakortolide P (**14**) to plakortoperoxides A1 (**15**) and A2 (**16**) by [4+2] cycloaddition of singlet oxygen. a) O_2, rose bengal bis(triethylammonium) salt, CH_2Cl_2, 500W lamp, 5 °C, 3 h, 62%.

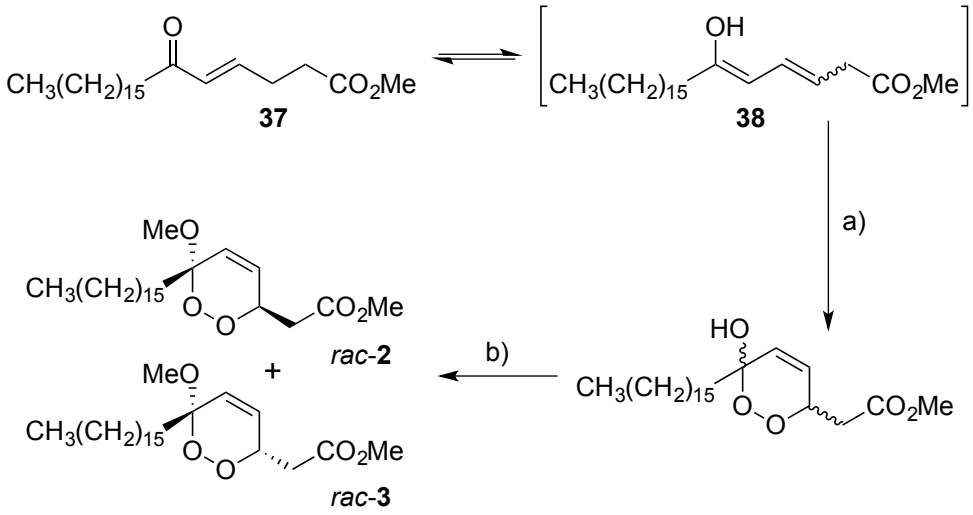

Scheme 2.10: Snider's racemic synthesis of chondrillin (**2**) and plakorin (**3**) by [4+2] oxygenation. a) O_2, rose bengal lactone, 275W lamp, CH_2Cl_2, MeOH, r.t., 12 h, 73%; b) $TsOH.H_2O$, MeOH, r.t., 80 h, 98%.

Other methods developed for the synthesis of peroxide scaffolds have involved the use of hydrogen peroxide rather than molecular oxygen.[101–103] Dussault completed the synthesis of a series of plakinic acid A (**13**) stereoisomers (including **39**) by advancing enantio-enriched α-hydroxyepoxides such as **40** (accessed by Sharpless asymmetric epoxidation of the corresponding allyl alcohol) to oxetane **41**, before regioselective ring opening with hydrogen peroxide (Scheme 2.11).[104,105] Ring closure and acetate homologation were then achieved over a number of steps. Earlier, Bloodworth developed an effective double peroxymercuration-demercuration strategy for the synthesis of 1,2-dioxolanes, including a natural saturated analogue (**42**) of the plakinic acids (Scheme 2.12).[106] Most recently, Deng and co-workers developed an enantioselective and organocatalytic method for the peroxidation of unsaturated ketones and aldehydes using cinchona alkaloid derviatives.[107–109]

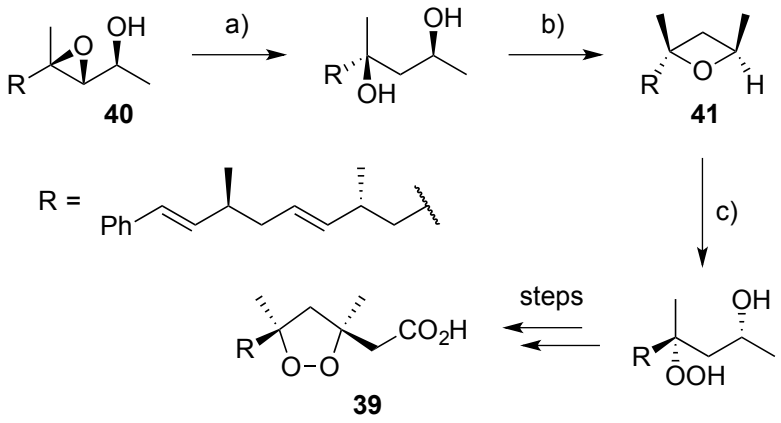

Scheme 2.11: Synthesis of an isomer (**39**) of plakinic acid A (**13**). a) Red-Al, THF, 0 °C, overnight, 97%; b) ^{t}BuOK, TsCl, THF, r.t., 3 h, then NaH, 0 °C, overnight, 72%; c) H_2O_2, TMSOTf, Et_2O, THF, –78 °C, 45 min.

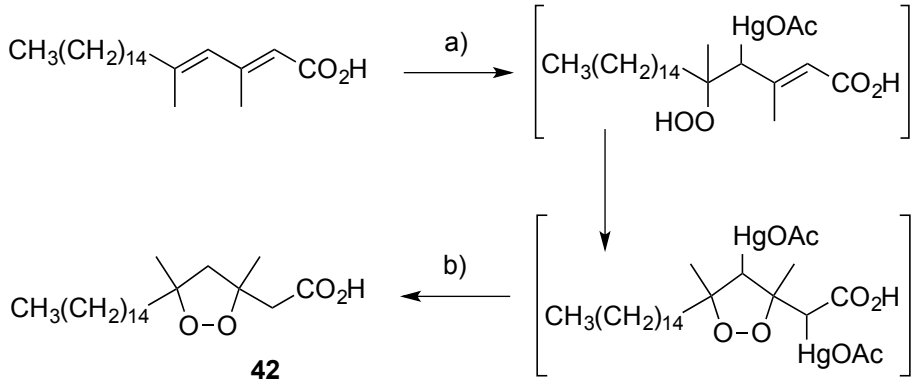

Scheme 2.12: Synthesis of a plakinic acid analogue (**42**) by peroxymercuration-demercuration. a) H_2O_2, H_2O, $Hg(OAc)_2$, then b) $NaBH_4$, NaOH.

2.4 Metabolites derived from peroxide rearrangement

The base-catalysed rearrangement of dialkyl peroxides was first reported in the early 1950s when Kornblum and DeLaMare discovered that 1-phenylethyl *tert*-butylperoxide (**43**) decomposes in the presence of catalytic KOH, KOEt or piperidine to yield acetophenone and *tert*-butanol (Figure 2.4).[110,111] The reaction was rationalised by abstraction of a proton from the less substituted α-peroxy carbon, followed either by stepwise or concerted elimination across the C–O bond. The instability of peroxide scaffolds, including 1,2-dioxanes, to base-mediated rearrangement has led to the occurrence and isolation of many rearranged endoperoxide metabolites related to **1**–**3**.

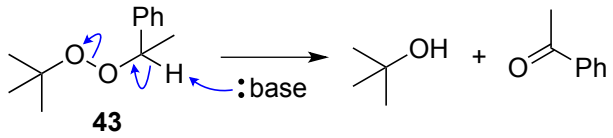

43

Figure 2.4: Base-catalysed rearrangement of 1-phenylethyl *tert*-butylperoxide (**43**).

2.4.1 Untenone A and plakortic acid

Untenone A (**44**)[112] and plakortic acid (**45**)[113] were each isolated from *Plakortis* marine sponges in 1993 and 2001, respectively (Figure 2.5). Although **44** and **45** appear to be quite different, both are closely related to chondrillin (**2**) and plakorin (**3**), sharing the same elemental composition and oxidation pattern of the central carbon chain. After completing a racemic total synthesis of **2** and **3** in the early 1990s (Section 2.3.2), Snider studied the base-catalysed structural rearrangements of the two diastereomers and found that they decompose via distinct pathways.[95] The findings of Snider's study have, in retrospect, provided insight to the biosynthesis of **44** and **45**.[114]

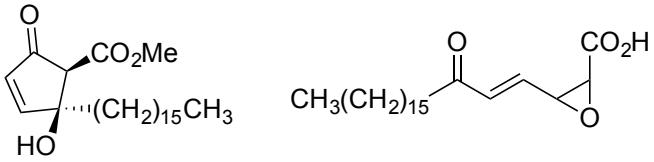

44

reported structure of plakortic acid (**45**)

Figure 2.5: Untenone A (**44**) and plakortic acid (**45**) from *Plakortis* marine sponges.

In a model system, Snider found that the rearrangement of peroxyketal heterocycles **46** and *epi*-**46** (analogues of **2** and **3**) is critically dependent on their relative stereochemistry. As shown in Scheme 2.13, the conformation in which the C6 alkyl substituent of **46** (a methyl analogue of **2**) is pseudoequatorial places the C3 dioxane hydrogen antiperiplanar to the adjacent 1,2-dioxane bond. This facilitates Kornblum-DeLaMare rearrangement to yield methyl ester **47** (R = Me) before rapid aldol addition to give cyclopentenone *rac*-**48**, a methyl analogue of untenone A (**44**). In contrast, the conformation in which the C6 alkyl substituent of *epi*-**46** (a methyl analogue of **3**) is pseudoequatorial places the C3 acetate group antiperiplanar to the O–O bond (Scheme 2.14). This allows nucleophilic attack of the α-keto acetate carbon to the peroxide yielding oxirane **49**, a structural analogue of plakortic acid (**45**).[115] It is therefore apparent that natural **44** and **45** are likely to be derived from the

rearrangement of **2** and **3**, respectively. It is also important to note that **44** was isolated as a racemate[112,116,117] and **45** in enantio-enriched form,[113] which is consistent with the presented theory of biogenesis.

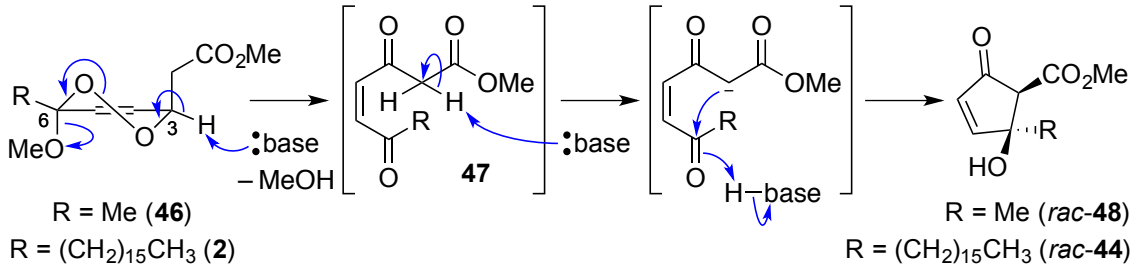

Scheme 2.13: Kornblum–DeLaMare rearrangement and intramolecular aldol of chondrillin (**2**) analogue **46**.

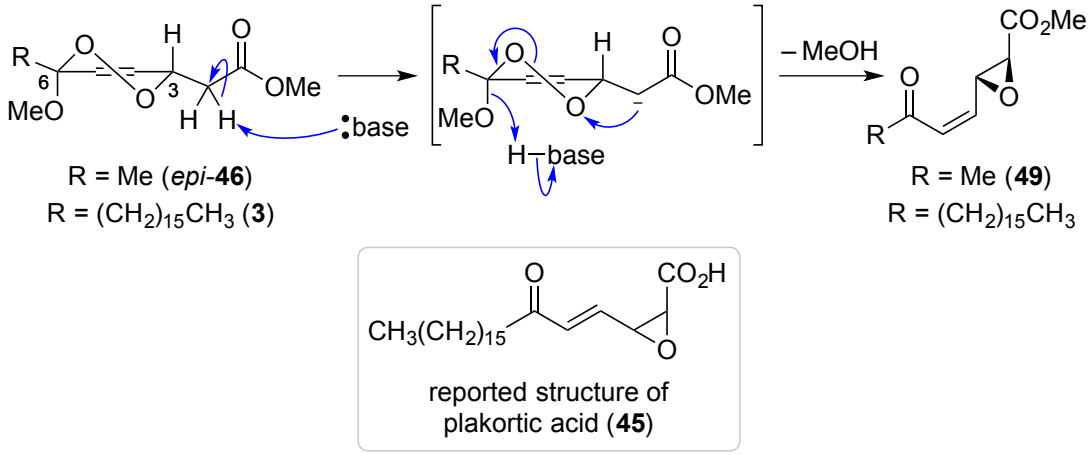

Scheme 2.14: Base-mediated decomposition of plakorin (**3**) analogue *epi*-**46**.

Inspired by Snider's work, Whitehead developed a synthesis of untenone A (**44**) by *in situ* generation of methyl ester (*Z*)-**50**, the postulated biosynthetic intermediate linking **2** and **44** (Scheme 2.15).[118–120] Thus, oxidation of synthetic plakorsin A (**51**, Section 2.5.4)[113] gave bismethyl acetal **52**, which on hydrolysis underwent aldol cyclisation yielding *rac*-**44**, directly. After developing an efficient total synthesis, Whitehead's study into the reactivity of *rac*-**44** was pivotal in elucidating biosynthesis of the manzamenone family of oxylipin dimers (Section 2.4.2). Both racemic and asymmetric total syntheses of untenone A (**44**) were also accomplished by Takeda,[121] Asami[116] and Yamada;[117] with each approach targeting modification of 5-membered carbocycles introduced in the early stages of synthesis.

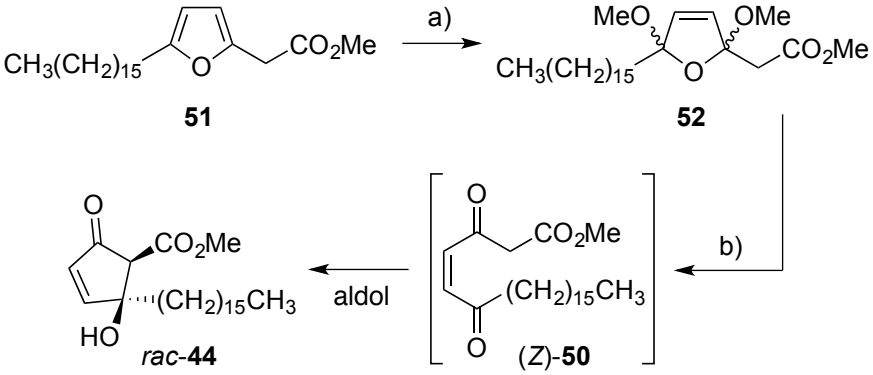

Scheme 2.15: Whitehead's biomimetic synthesis of untenone A (**44**). a) Br_2, Na_2CO_3, MeOH, Et_2O, r.t., 1 h, 79%; b) H_2SO_4, dioxane, H_2O, r.t., 1 h, then Na_2CO_3, H_2O, r.t., 30 min, 62%.

2.4.2 Manzamenones A–H, J–O and untenolide A

Manzamenones A–F (**53**–**58**)[122] and H (**59**)[123] were isolated by Kobayashi and co-workers from *Plakortis* sponges collected near Okinawa, Japan in 1992 and 1993 (Figure 2.6). They share a common [4.3.0]-carbobicyclic structure differing only by the carboxy substituent at C5. Manzamenone A (**53**) was found to be a potent inhibitor of DNA polymerase β[124,125] and manzamenones B (**54**) and E (**57**) are inhibitors of T-cell protein tyrosine phosphatase.[126]

Initial speculation on the biosynthesis of **53**–**58** considered that the cyclohexene ring system may be constructed in a hetero-bimolecular [4+2] cycloaddition of untenone A (**44**) and a suitable diene counterpart.[122,123] However, Whitehead postulated that **53**–**58** are in fact homodimers of untenone A (**44**).[118–120,127] Heating a neat sample of synthetic *rac*-**44** (Section 2.4.1) to it's melting point (72 °C) caused dehydration to the anti-aromatic cyclopentadiene **60** followed by rapid [4+2] homo-dimerisation to give *endo*-adduct *rac*-**61** *in situ* (Scheme 2.16). Retro-Dieckmann fragmentation of the bridgehead carbonyl with uptake of water as an incident nucleophile yielded *rac*-**62**, whose relative stereochemistry was determined by x-ray crystallography and detailed NMR analysis.[120] The spectral data obtained for **62** matched that of natural manzamenone A, thus prompting stereochemical reassignment of the original structure (**53**) at C2 and C5. Whitehead also completed the synthesis of manzamenones C and F from *rac*-**62** resulting in a similar revision of the original structures **55** and **58**.[128] The apparent pre-disposition of **44** to undergo dehydrative dimerisation yielding **62**

demonstrates beyond doubt that this process is responsible for the occurrence of **53**–**58** in the extracts of marine sponges.[129]

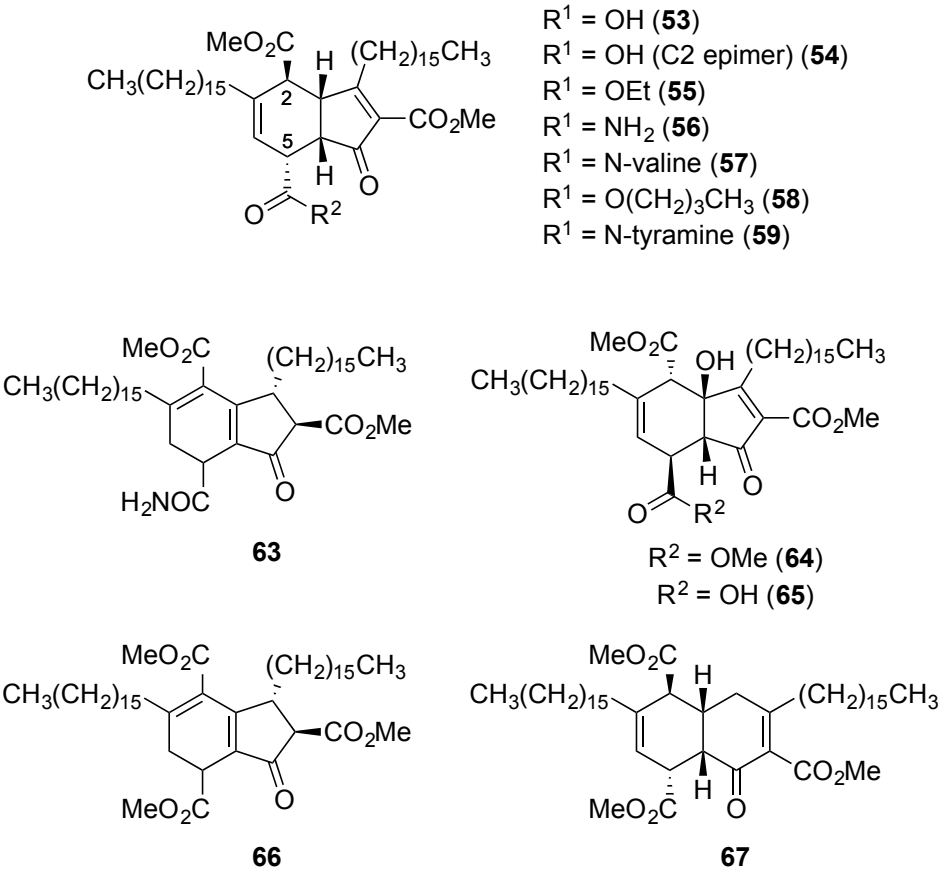

Figure 2.6: Reported structures of manzamenone A–F (**53**–**58**), G (**67**), H (**59**), J (**63**) and L–N (**64**–**66**).

Manzamenones J (**63**)[130] and L–N (**64**–**66**),[131] also isolated from *Plakortis* sponges, were determined to have the same carbocyclic structure as **53**–**58** with a different oxidation pattern of the central core and thus, are likely to be directly related (Figure 2.6). However, manzamenone G (**67**)[123] was reported as an unusual structural analogue with one carbon more than that expected for a dimer related to chondrillin (**2**). The structure of manzamenone G (**67**)[123] was only tentatively assigned and its biosynthetic origin remains unclear.

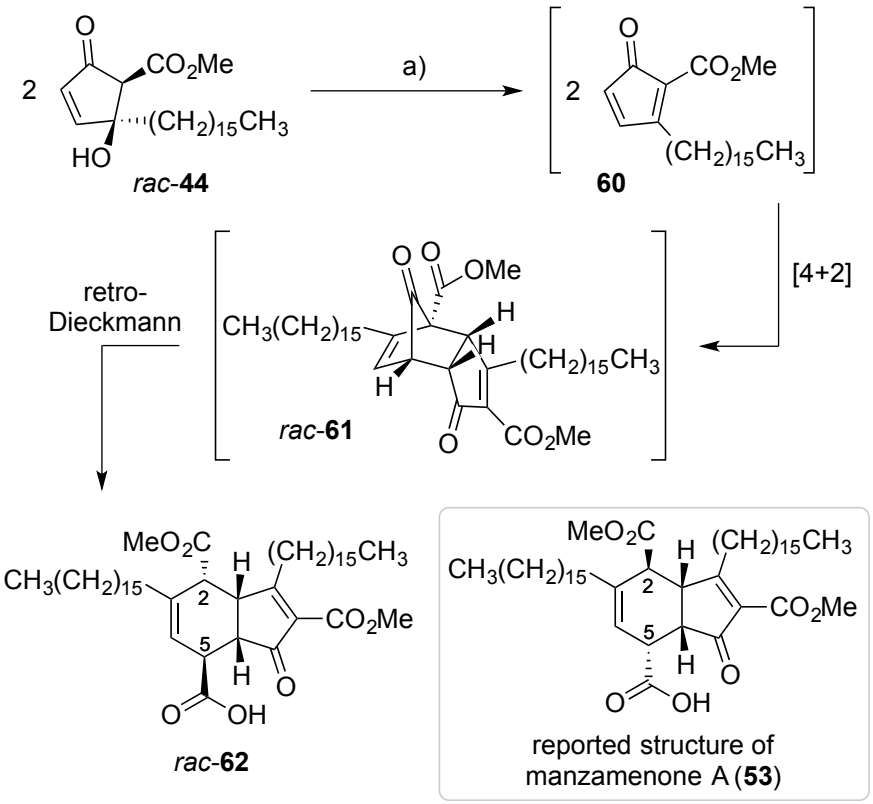

Scheme 2.16: Whitehead's biomimetic synthesis and structural elucidation of manzamenone A (**62**). a) neat, 72 °C, 24 h, 48%.

Manzamenone K (**68**),[130,132] O (**69**)[133] and untenolide A (**70**)[134] also appear to be related to **2** and **3**, yet are structurally distinct from **53**–**58** and **63**–**67** (Scheme 2.17). The central structure common to each natural product (**68**–**70**) was verified by x-ray crystallography[134] and ROE spectroscopy (selected ROESY correlations of compound **69** as in Scheme 2.17);[133] and found to consist of two structural elements that appear to be derived from **2** or **3** linked by a single C–C bond (most clearly seen in **68**). The compounds were isolated as racemic or are presumed to have a very low level of enantiomeric excess (pseudo-racemic), suggesting that they may arise from non-enzymatic dimerisation of an achiral intermediate similar to manzamenones A–F (**53**–**58**) and H (**59**). However, if derived from **2** and **3** it appears that a single reduction event has occurred at some stage during construction of the central scaffold. Kobayashi reported that **70** is likely to be related to **68** by oxidation and cyclisation; and **69** is likely to be related to **68** via condensation with intermediate (*Z*)-**50** (derived from **2**).[133–135] Despite the complexity of these unique oxylipin natural products, no further studies have commented on the biosynthesis or attempted chemical synthesis of **68**–**70**.

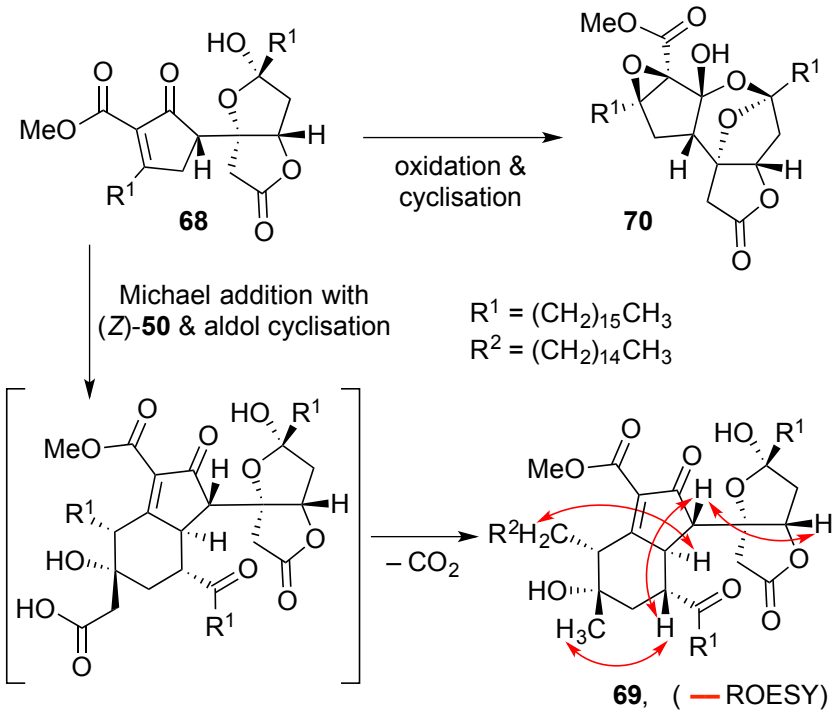

Scheme 2.17: Structures and postulated conversion of manzamenone K (**67**) to manzamenone O (**69**) and untenolide A (**70**). Selected ROESY correlations of compound **69** shown as red arrows.

2.4.3 Plakoridines A–C

Kobayashi and co-workers also isolated three fatty acid containing alkaloids from *Plakortis* marine sponges collected near Okinawa. Plakoridine A (**71**),[136] found to be an inhibitor of DNA polymerase,[124] and the less active compounds plakoridines B (**72**)[130] and C (**73**),[137] each contain a central carbon chain with a C16 aliphatic tail common to all peroxyketal-derived natural products related to chondrillin (**2**, Scheme 2.18).

Whitehead postulated that **71** and **72** are biosynthetically related to (*E*)-**50**,[138] an intermediate derived from plakorsin A (**51**).[139] In a single experiment, tyramine and aldehyde **74** condensed to generate imine **75** *in situ* before addition of (*E*)-**50** (itself prepared by bromine-mediated oxidation of synthetic **51**) to give *rac*-**71** as a 3:1 mixture of C3 epimers (Scheme 2.18).[127,138,140] Over 11 days at room temperature, **75** and (*E*)-**50** were presumed to undergo an intermolecular Mannich reaction followed by Michael ring closure to afford heterocycle **76**. An internal redox process, resulting in reduction of the cyclopentanone carbonyl and oxidation of the neighbouring α-amino

methine, then followed to yield *rac*-**71**. The relative configuration of the pyrrolidine ring was established through the analysis of vicinal coupling constants and NOE spectroscopy (key NOESY correlation of compound *rac*-**71** shown in Scheme 18). Hexadecyl aldehyde (**77**) was also advanced to *rac*-**72** using this method, demonstrating that natural **71** and **72** are most likely related to **51**. Furthermore, Ma's asymmetric synthesis of (2*S*,3*S*,4*R*)-**71** in 2000 showed that natural plakoridine A (**71**) was isolated as a racemate,[141] which is consistent with Whitehead's theory of biogenesis. Stafford also reported a racemic synthesis of a plakoridine A lactam in 1995.[142]

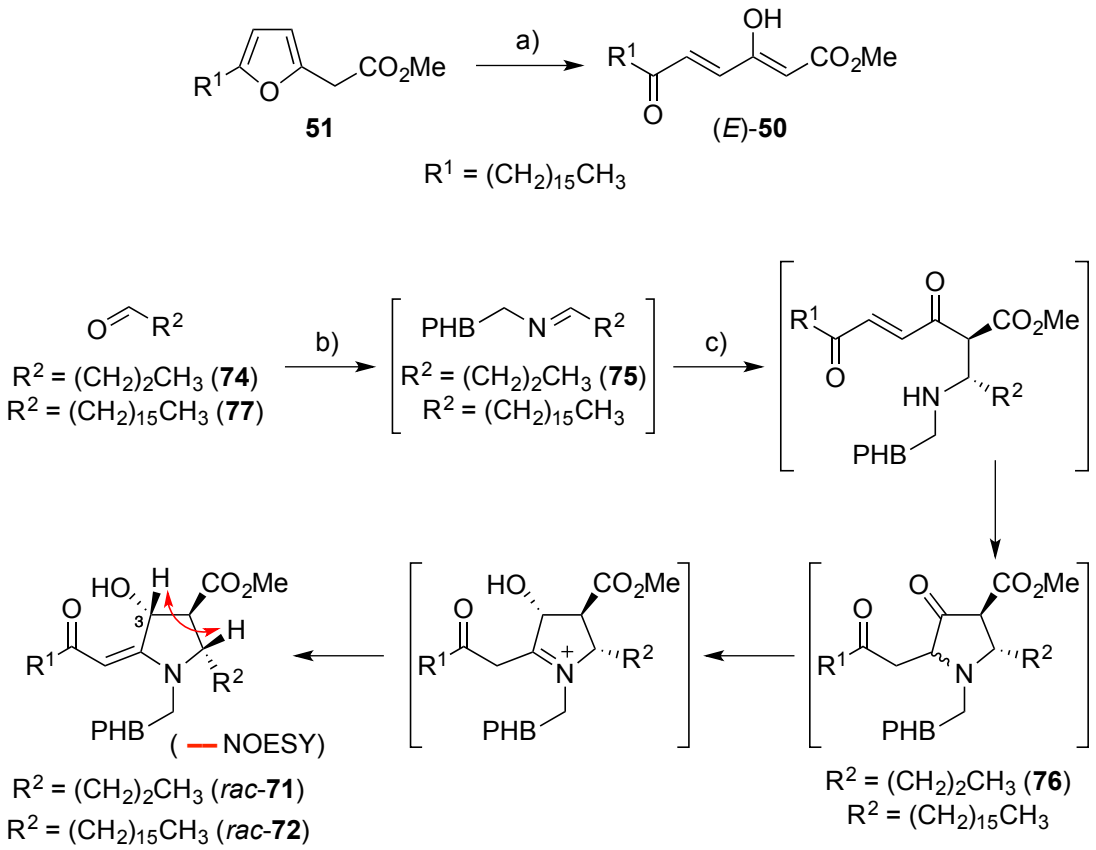

Scheme 2.18: Whitehead's biomimetic synthesis of plakoridine A (**71**) and B (**72**) from plakorsin A (**51**). Key NOESY correlation of compound *rac*-**71** shown as a red arrow. a) Br_2, Me_2CO, H_2O, –20 °C to –10 °C, 6 h, 63%; b) tyramine, $CDCl_3$, r.t., 3 h, then $MgSO_4$, r.t., 30 min, then c) (*E*)-**50**, r.t., 11 d, 43% (beginning with **74**) and 36% (beginning with **77**). PHB = *p*-hydroxybenzyl.

Plakoridine C (**73**) is structurally distinct from **71** and **72**; and appears to be derived from an intermediate related to **2** or **3** by addition of piperideine or δ-lactam (Figure 2.7).[137] To date, there is no published work on the synthesis of **73**.

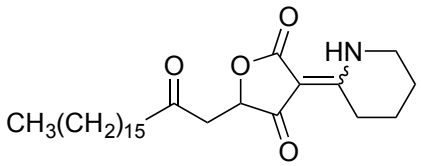

73, ~1:1 (*E*:*Z*)

Figure 2.7: Plakoridine C (**73**) isolated from a *Plakortis* marine sponge near Okinawa, Japan.

2.4.4 Gracilioethers B–D, plakilactones A–H and related compounds

The base-catalysed rearrangements of dialkyl peroxides related to and including plakortin (**1**), which are structurally distinct from **2** and **3**, yield furan-containing polyketide metabolites by ring contraction of the 1,2-dioxane motif. Faulkner discovered that treating **1** with NaOMe in MeOH induced rearrangement to tetrahydrofuran **78**, presumably by ring closure of epoxide intermediate **79** (Scheme 2.19).[1] This general reaction of unsaturated dialkyl peroxides has been used in the synthesis of polyether tetrahydrofuran compounds;[143] and **78** has itself been linked to the sponge metabolite **80**, as a likely biogenetic precursor.[2] By extension, Faulkner rationalised biosynthesis of the [2(5*H*)-furanylidene]ethanoate (furanylidene) metabolite **81** from peroxide **82** through formation of epoxide **83** (Scheme 2.20).[144] However, Snider's work on the stereochemical dependence of base-catalysed rearrangements of 4,5-unsaturated-1,2-dioxane peroxyketals (Section 2.4.1) suggests that the conversion of **82** to **81** is likely to proceed by Kornblum-DeLaMare rearrangement via hydroxy-β-ketoester **84** (Scheme 2.21).[114] We believe a similar mechanistic course is most likely in the biosynthesis of gracilioethers B–D,[145,146] spongosoritin A,[147,148] spiroplakortone,[149] glanvillic acids A, B[49] and related compounds.[51,150–152]

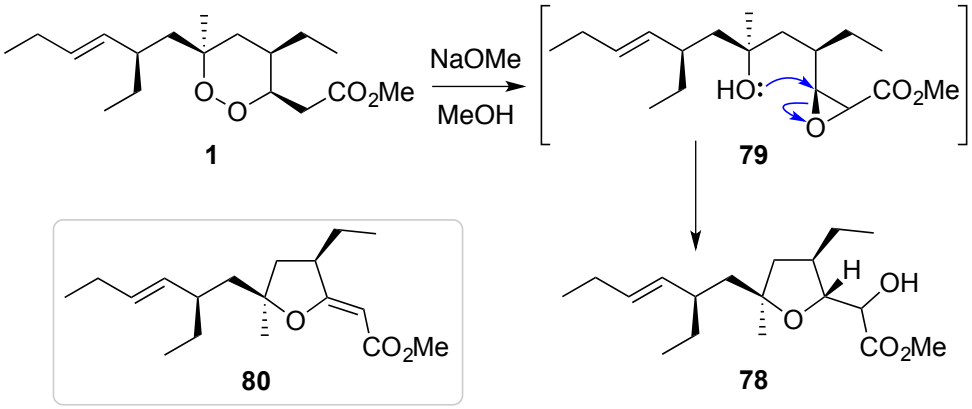

Scheme 2.19: An observed ring contraction of plakortin (**1**).

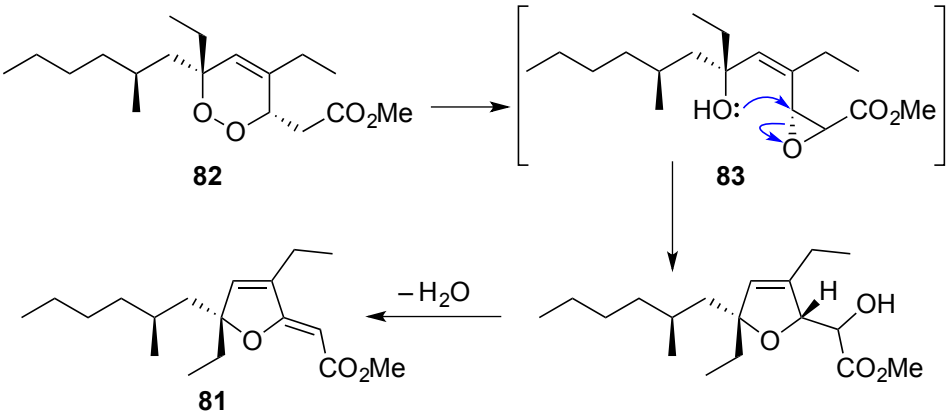

Scheme 2.20: Faulkner's hypothesis for ring contraction of peroxide **82** to furanylidene **81**.

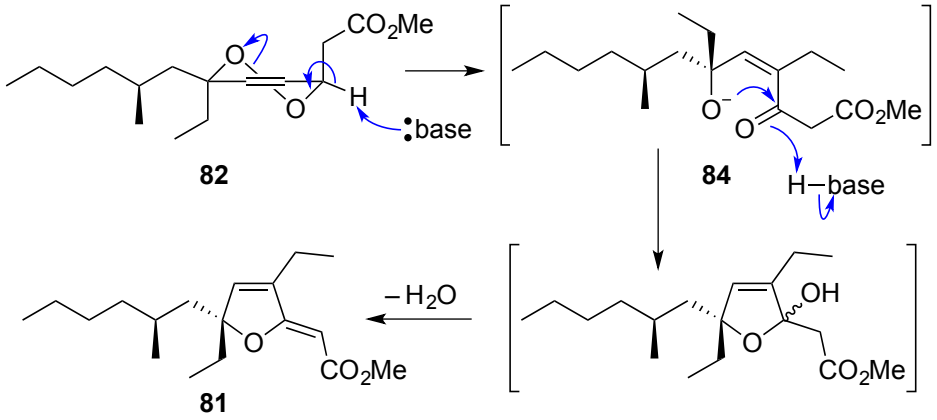

Scheme 2.21: Postulated Kornblum-DeLaMare rearrangement of peroxide **82** to furanylidene **81**.

We have recently demonstrated the utility of targeting such hydroxy-β-ketoester intermediates in the synthesis of furanylidene compounds (Chapters 3 and 5) and have reported the total synthesis of gracilioethers B (**85**) and C (**86**) using this approach (Scheme 2.22).[153] Methyl acetal **87** (a synthetic analogue of **84**) was converted into furanylidene **88** by transacetalisation to intermediate **89** and dehydration to the conjugated system. Compounds **85** and **86** are known agonists of peroxisome proliferator-activated receptor γ (PPARγ);[146] and the related metabolite *des*-hydroxygracilioether C (**90**) was found to be cytotoxic against HCT-116 cells (human colon carcinoma).[31] Ohira and co-workers completed a racemic total synthesis of **90** in 2005 using reactions of alkylidenecarbenes.[154]

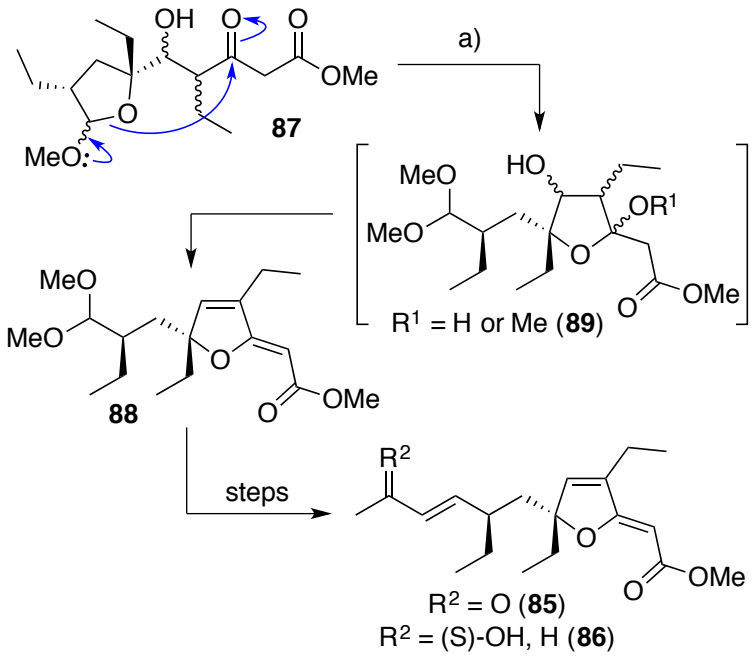

Scheme 2.22: Biomimetic total synthesis of gracilioethers B (**85**) and C (**86**); and a possible biogenetic link to the plakilactone metabolites via oxidative cleavage of the furanylidene heterocycle. a) AcCl, MeOH, $CH(OMe)_3$, 20 °C, 15 h, 74% over 2 steps (first step not shown).

Plakilactones A–H[146] and *des*-hydroxyplakilactone B (**91**) were isolated from *Plakinastrella mamillaris* in 2012 along with a number of furanylidene natural products, including gracilioethers B (**85**), C (**86**) and *des*-hydroxygracilioether C (**90**). The structural similarity of the plakilactone butenolides and gracilioether furanylidenes would appear to suggest that they are related by oxidative cleavage of the furanylidene enol ether, although this possible relationship is yet to be demonstrated (Scheme 2.22).

2.4.5 *Gracilioethers A, E–K and hippolachnin A*

Gracilioethers A[145] and E–K[155,156] are complex polycyclic metabolites that also appear to be oxidative adducts of the furanylidene heterocycles, although the biosynthetic origins of these compounds remains unclear. The structure and absolute configuration of gracilioether A (**92**) was determined by chemical derivatisation and detailed NMR analysis of the resulting acetonide **93** (Scheme 2.23); and the structures of related natural products have been assigned accordingly. Wong recently demonstrated [4+2] addition of singlet oxygen to a reactive bicyclic diene (*rac*-**94**), forging the peroxy-tricyclic core of **92**, before completing total synthesis of gracilioether F (*rac*-**95**, Scheme 2.24).[157] Brown also completed a total synthesis of **95** in 2014 using a ketene–alkene [2+2] cycloaddition reaction and Baeyer-Villiger oxidation; and a carboxylic acid directed C–H oxidation to install each of the lactone rings.[158] The related metabolite gracilioether K (**96**), whose structure was determined through detailed NMR analysis (selected ROESY correlations of compound **96** shown

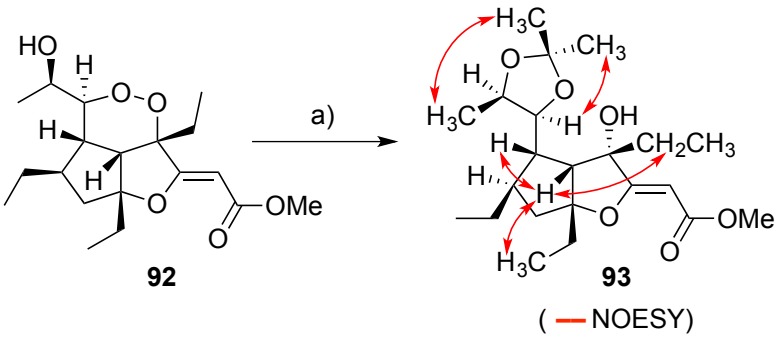

Scheme 2.23: Structural and stereochemical elucidation of gracilioether A (**92**) through chemical derivatisation and detailed NMR analysis. Selected NOESY correlations of compound **93** shown as red arrows. a) Zn, Et_2O, AcOH, r.t., overnight; then $(CH_3)_2C(OCH_3)_2$, PPTS, CH_2Cl_2, r.t., overnight.

in Scheme 2.25) and by application of Mosher's method, is believed to arise from Kornblum-DeLaMare ring contraction and oxa-Michael cyclisation of (11*S*)-gracilioether A (**97**, Scheme 2.25),[156] which itself may be constructed from gracilioether C (**86**) by inclusion of molecular oxygen.

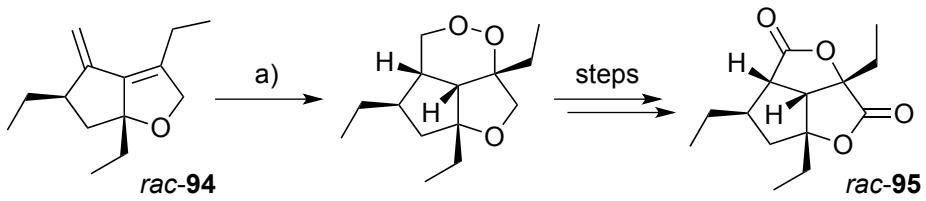

Scheme 2.24: Wong's synthesis of racemic gracilioether F (*rac*-**95**) by [4+2] oxygenation of diene *rac*-**94**. a) O_2 (bubbled), methylene blue, CH_2Cl_2, sunlamp (200–300W), 0–5 °C, 2 h.

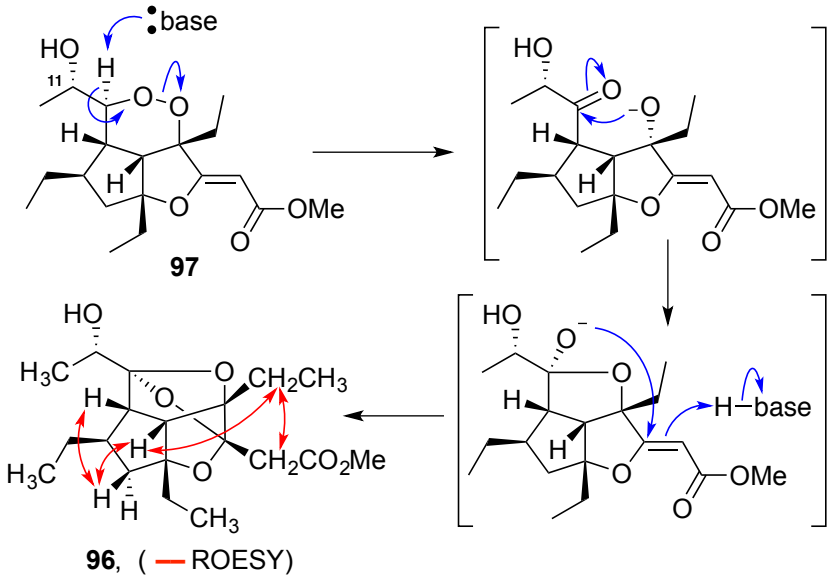

Scheme 2.25: Postulated base-catalysed rearrangement of (11*S*)-gracilioether A (**97**) to gracilioether K (**96**). Selected ROESY correlations of compound **96** shown as red arrows.

Hippolachnin A (**98**), isolated from *Hippospongia lachne* in 2013, also bears a unique tricyclic structure with a highly substituted cyclobutane ring (Scheme 2.26).[159] It appears that **98** arises biosynthetically from an intramolecular [2+2] cycloaddition of **90**, which itself was isolated from the same sponge extract.[159] In turn, **90** is expected to arise from the dehydrative ring contraction of haterumadioxin A (**7**) methyl ester.[160] Carreira completed the first total synthesis of *rac*-**98** in 2015 constructing a pivotal cyclobutene intermediate **99** (Scheme 2.26)[161] *en route* to the natural product (selected NOESY correlations of natural **98** shown in Scheme 2.26);[159] and later extended the approach to achieve a racemic total synthesis of gracilioethers E (*rac*-**100**) and F (*rac*-**95**).[162] Brown and Wood recently published a collaborative project, which detailed the

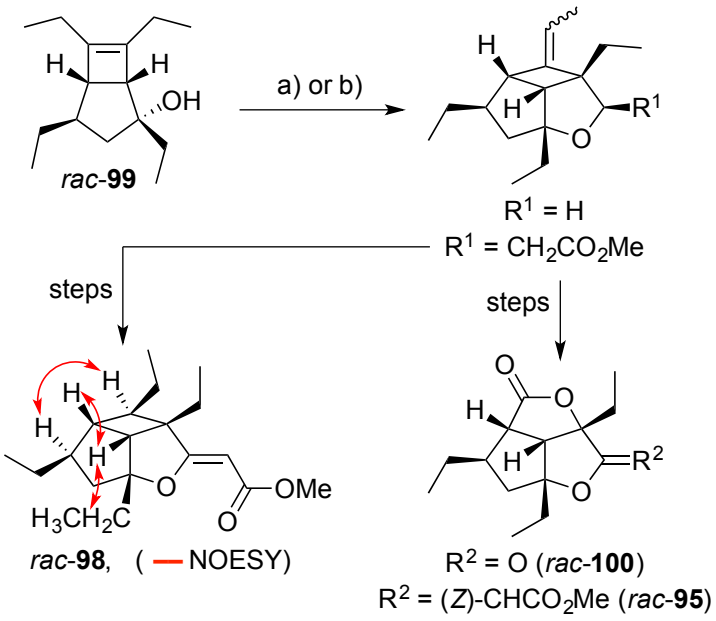

Scheme 2.26: Carreira's racemic synthesis of hippolachnin A (*rac*-**98**), gracilioether E (*rac*-**100**) and F (*rac*-**95**) from cyclobutene intermediate **99**. Selected NOESY correlations of natural **98** shown as red arrows. a) $(CH_2O)_n$, $Sc(OTf)_3$, $CHCl_3$, –78 °C to r.t., 28 h, 61% brsm (for R^1 = H); b) (*E*)-methyl-3-methoxyacrylate, PPTS, 80 °C, 4.5 d; then BF_3·2AcOH, CH_2Cl_2, THF, r.t., 20 h, 62% over 2 steps (for $R^1 = CH_2CO_2Me$).

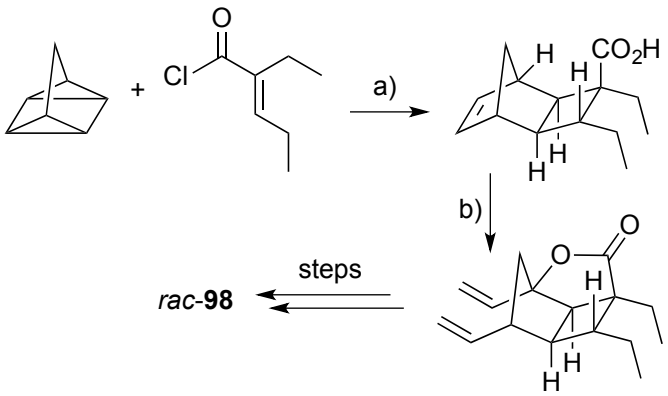

Scheme 2.27: Brown and Wood's synthesis of racemic hippolachnin A (*rac*-**98**) via quadricyclane cycloaddition and carboxylic acid directed C–H oxidation. a) 140 °C (microwave irradiation), 4 h, then NaOH, r.t., 24 h, 50%; b) ethylene (1 atm), Grubbs I, CH_2Cl_2, r.t., 7 h; then $PhSO(CH_2)_2SOPh$·$Pd(OAc)_2$, Cr(salen)Cl, *p*-benzoquinone, dioxane, H_2O, 60 °C, 24 h, 64% over 2 steps.

total synthesis of *rac*-**98** in only six steps through an enabling quadricyclane cycloaddition and late-stage carboxylic acid directed C–H oxidation, similar to that developed in Brown's earlier synthesis of *rac*-**95** (Scheme 2.27).[163] Ghosh has also been successful in accessing the central tricyclic core, effecting a [2+2] enone-alkene cycloaddition of a synthetic butenolide related to **90**.[164]

2.5 Metabolites derived from peroxide reduction

Iron(II)-mediated reduction has been identified as a likely biological mode of action of peroxide metabolites related to **1** and **2**. On treatment with $FeCl_2$, 9,10-dihydroplakortin (**28**) undergoes reductive cleavage of the 1,2-dioxane to give alkoxyradical **101**, followed by 1,5-H atom transfer from the branched alkyl chain and "chloro-Fenton"[37,165] reaction yielding the isolated chlorides **102** (Scheme 2.28).[166] Peroxyketals such as **103** also undergo reduction with iron(II) followed by radical

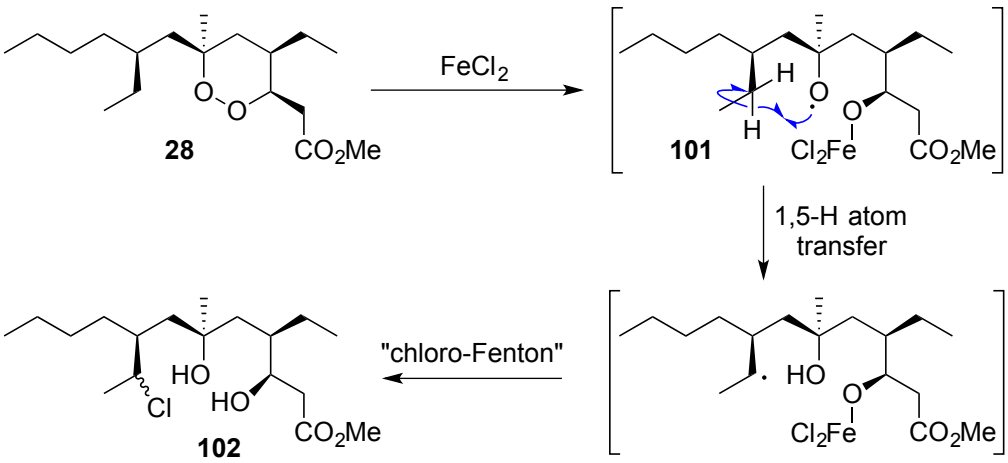

Scheme 2.28: Reaction of 9,10-dihydroplakortin (**28**) with iron(II) chloride.

fragmentation with C–C bond scission to generate γ-hydroxyesters (by quenching of intermediate **104**) or the corresponding lactones (Scheme 2.29),[166] which themselves are isolated from marine sponge extracts.[5,113,167] In each case, it is the resultant carbon-centered radical that is believed to cause cell damage and the cytotoxic effect of these metabolites.[99,103,168]

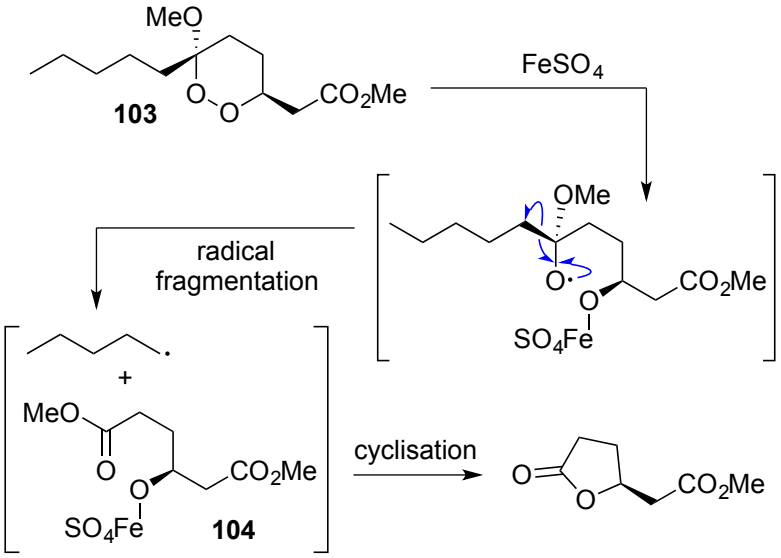

Scheme 2.29: Reaction of peroxyketal **103** with iron(II) sulfate and cyclisation.

2.5.1 Plakortethers A–G and simplakidine A

Plakortin (**1**) is known to undergo iron(II)-mediated reduction like dihydro-analogue **28**, with concomitant 5-*exo-trig* radical cyclisation of alkoxyradical **105** to the pendant olefin (Scheme 2.30).[166] When treated with $FeCl_2$, **106** is then presumed to undergo "chloro-Fenton" reaction yielding the isolated tetrahydrofuran adducts **107** and **108**, the latter isolated in 2002 from extracts of *Plakortis simplex* and named plakortether C (**108**).[169] A series of co-isolates, plakortethers A (**109**), B (**110**), D–G (**111**–**114**)[169] and simplakidine A (**115**)[170] are all reported to share a similar carbon framework, indicating that each analogue most likely arises from the reductive ring opening of **1**, with the termination of radical **106** taking a different mechanistic course in each case (Figure 2.8). Plakortethers A (**109**), B (**110**), D (**111**) and E (**112**) are cytotoxic against the RAW 264-7 (murine macrophage) cell line in the range 7–12 μg/mL;[169] and an asymmetric total synthesis of **113** and **114** was completed by Novikov and co-workers in 2009, exploiting symmetrical aspects of the central carbon frame.[171]

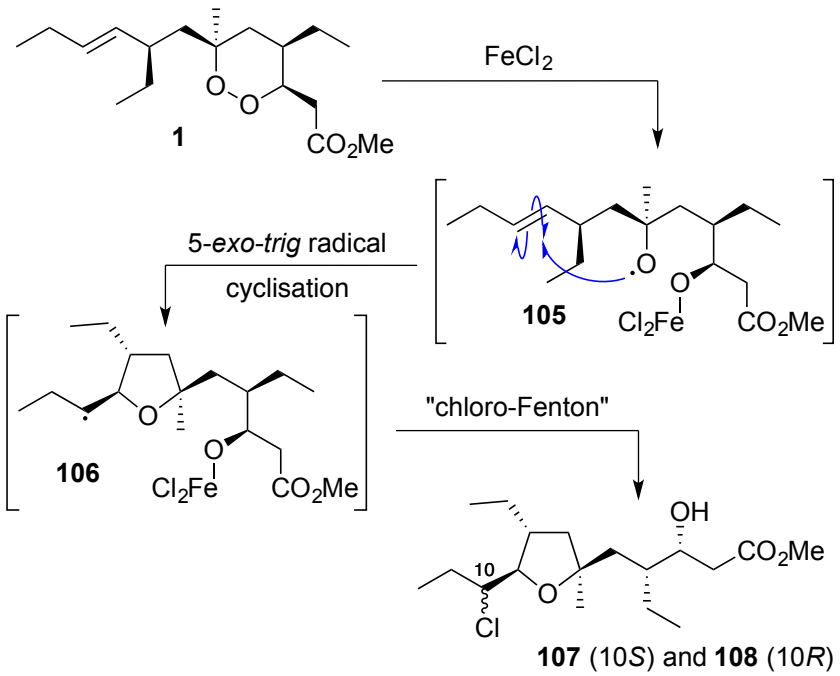

Scheme 2.30: Reaction of plakortin (**1**) with iron(II) chloride yielding plakortether C (**108**).

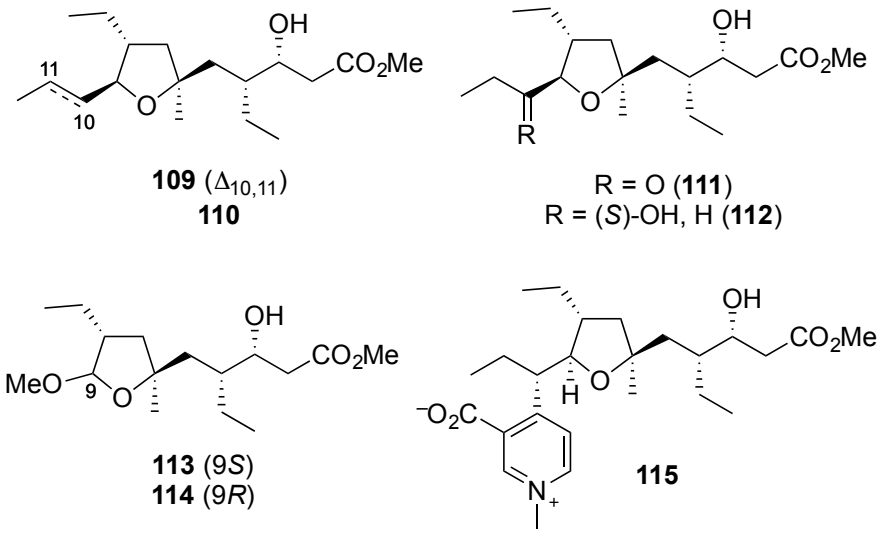

Figure 2.8: Plakortethers A (**109**), B (**110**), D–G (**111**–**114**) and simplakidine A (**115**) from *Plakortis simplex*.

2.5.2 Simplextones A and B

Simplextones A (**116**) and B (**117**),[172] recently isolated from *Plakortis simplex*, have an unprecedented skeletal arrangement with a substituted cyclopentane carbocycle connected to a γ-lactone motif by a single C–C bond (Scheme 2.31). Their structures and absolute configuration were determined by x-ray crystallography, application of

Mosher's method, detailed NMR analysis (selected NOESY correlations of compound **116** shown in Scheme 2.31) and quantum chemical calculation of the CD spectra.[172] The continuous carbon backbone of **116** and **117** is remarkably similar to that of **1** and hence, the plakortethers. We speculate that simplextones A (**116**) and B (**117**) may in fact result from reductive ring opening, radical cyclisation and lactonisation of the known endoperoxides haterumadioxin B (**8**)[19] and **118**,[143] respectively (Scheme 2.31).

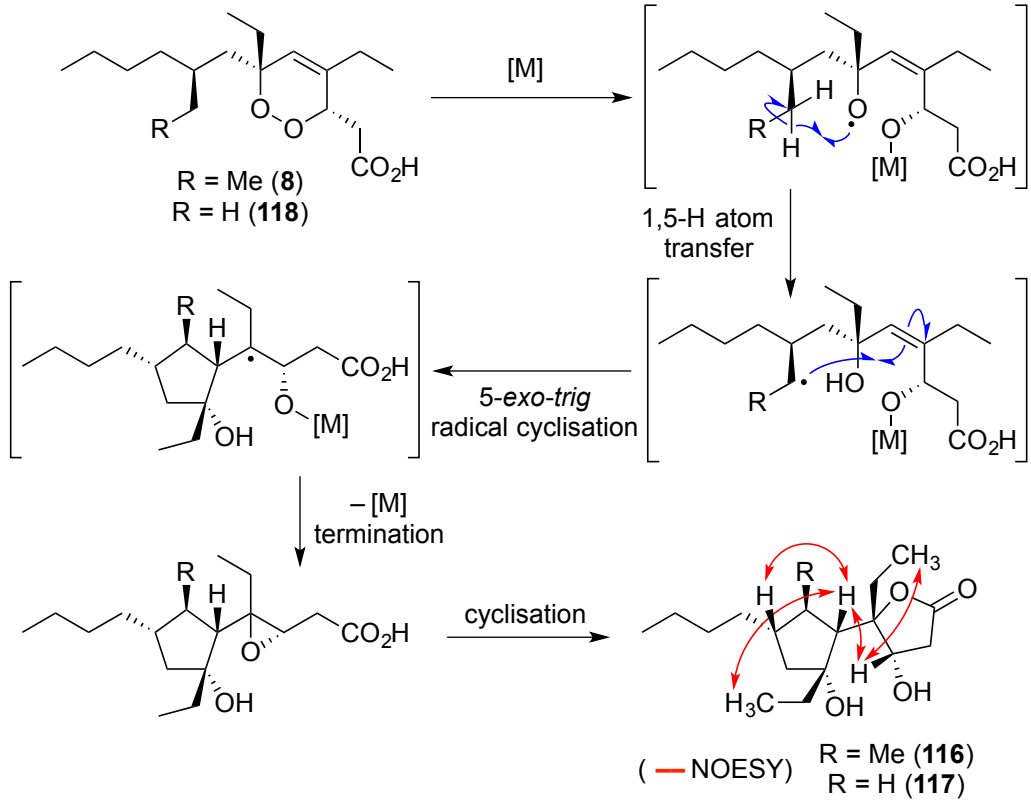

Scheme 2.31: Postulated biosynthesis of simplextones A (**116**) and B (**117**) from haterumadioxin B (**8**) and endoperoxide **118**, respectively. Selected NOESY correlations of compound **116** shown as red arrows. M = metal.

2.5.3 Plakortones A–F, L, N, P and simplexolides A–E

Plakortones A–F, L, N and P[22,27,47,173] were isolated from marine sponges of the genera *Plakortis* and *Plakinastrella*. Each natural product is characterised by a common 2,6-dioxabicyclo[3.3.0]octan-3-one (furanolactone) motif, yet two distinct pathways of biogenesis have been identified. Following their synthesis of plakortide E (**33**, Section 2.3.2), Wong and co-workers[86] demonstrated the facile conversion of **33** into plakortone B (**119**) by reduction to diol **120**, itself related to a natural product isolated in 1993,[174]

oxa-Michael cyclisation and lactonisation (Scheme 2.32). Impressively, this conversion was achieved with full stereocontrol for the desired bicyclic framework (NOESY correlations of natural **119** shown in Scheme 2.32)[22] providing strong evidence that natural **119** is derived from the reduction of **33**. In contrast, through application of Mosher's method to determine the absolute configuration of plakortolide L (**121**), Garson found that *seco*-anologue **122** undergoes dehydration and oxa-Michael cyclisation to yield plakortone L (**123**), directly (Scheme 2.33).[47] The relative structures and absolute configurations of plakortolide L and plakortone L were thus determined as (3*S*,4*S*,6*S*)-**121** and (3*S*,4*S*,6*S*)-**123**, respectively; and the biogenesis of **123** from **121** was implicated. Plakortones A–D are activators of cardiac sarcoplasmic reticulum Ca^{2+} ATPase at micromolar concentrations[22] and plakortones B–F exhibit *in vitro* cytotoxicity against WEHI 164 murine fibrosarcoma cells.[173]

It is also interesting to note that plakortolide B (**124**), a structural homologue of **121**, has been accessed directly from plakinic acid I (**125**) on treatment with $FeCl_2$, presumably through a complex "chloro-Fenton" reaction (Scheme 2.34).[37] The conditions also gave rise to the expected chloride **126**, which was advanced to napthyl amide **127** and used to determine absolute configuration of the remaining stereocenter with a novel analytical technique, liposomal circular dichroism.[37]

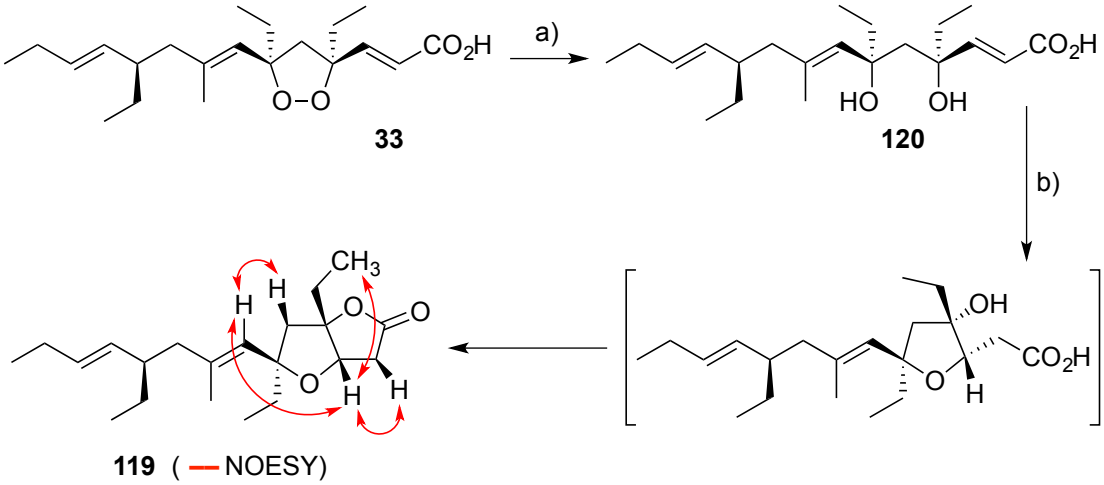

Scheme 2.32: Synthesis of plakortone B (**119**) from plakortide E (**33**). Selected NOESY correlations of natural **119** shown as red arrows. a) Zn, AcOH, CH_2Cl_2, 0 °C to r.t., 2 h, 99%; b) DBU, toluene, reflux, overnight, 90%.

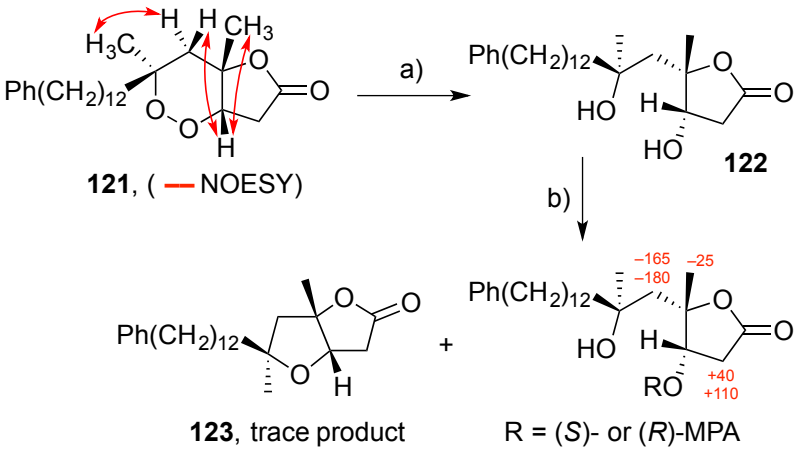

Scheme 2.33: Conversion of natural plakortolide L (**121**) to plakortone L (**123**). Change in chemical shift, expressed as shift of (*R*)-MPA compound subtracted from shift of (*S*)-MPA compound (in Hz) and shown as red numbers. a) Zn, AcOH, Et_2O, r.t., 16 h, 83%; b) (*S*)- or (*R*)-MPA, DCC, DMAP, CH_2Cl_2, r.t., overnight. MPA = methoxyphenyl acetate.

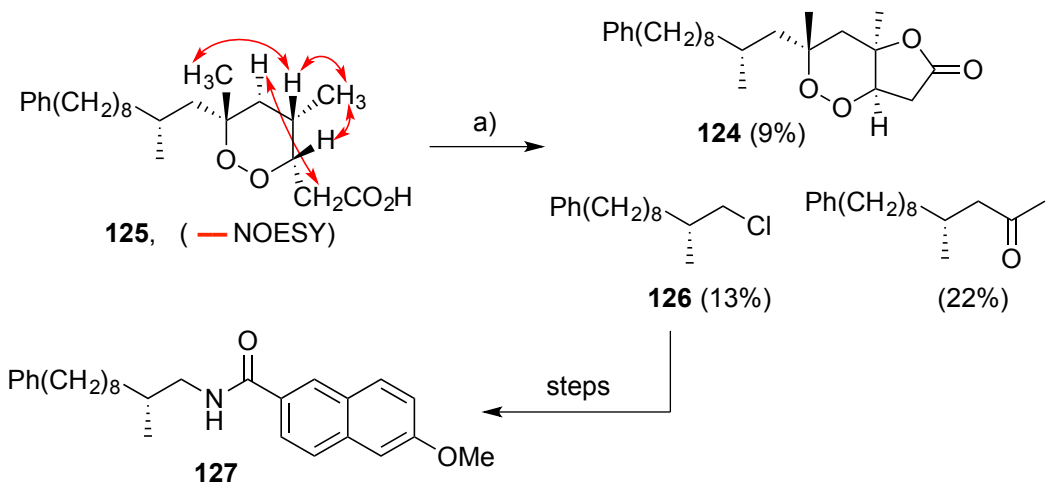

Scheme 2.34: Assigning the remote stereocenter of plakinic acid I (**125**) by chemical derivatisation and liposomal circular dichroism. Also, biomimetic conversion of plakinic acid I (**125**) to plakortolide B (**124**) through a complex "chloro-Fenton" reaction. Key NOESY correlations of compound **125** shown as red arrows. a) $FeCl_2$, CH_3CN, H_2O, r.t., 45 min.

Semmelhack[175,176] and Kitching[177–180] have independently developed palladium-mediated carbonylation reactions of diols such as **128** (which can be considered a structural analogue of **120**, the putative biosynthetic intermediate relating **33** and **119**) in the synthesis of plakortone natural products (Scheme 2.35).[176] Wong also completed the

total synthesis of **119** independent to that of **33**, constructing the furanolactone system by oxa-Michael cyclisation and transesterification of a suitable butenolide (once again, drawing upon the intermediacy of a diol similar to **120**, Scheme 2.36).[181,182] In other works, Mehta constructed the core bicycle from simple Morita-Baylis-Hillman adducts;[183] Thornhill used an intramolecular Wittig reaction to build the furanolactone core;[184] Ohira successfully effected iodolactonisation of a dihydrofuran to construct plakortone E;[185] and most recently, Sugimura developed a [3+2] annulation strategy for the total synthesis of **123**.[186]

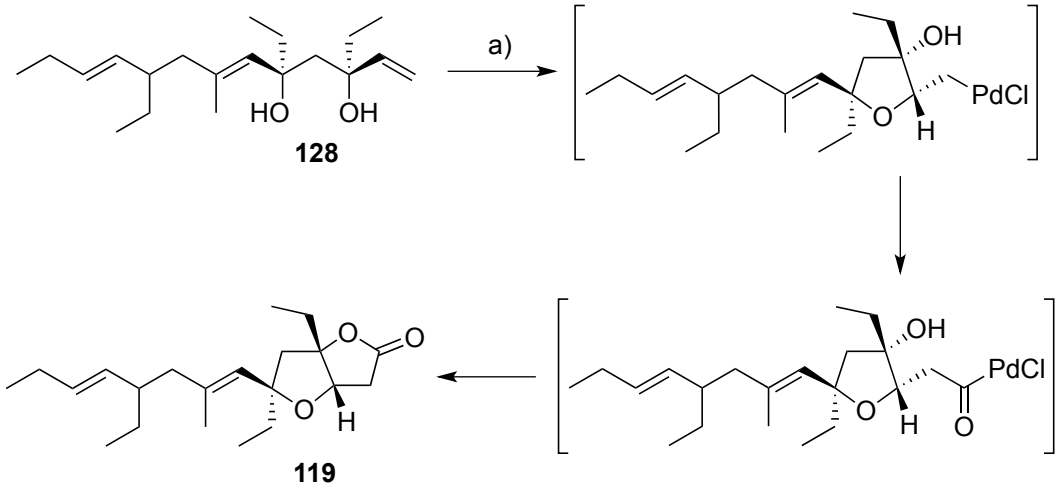

Scheme 2.35: Synthesis of plakortone B (**119**) by palladium(II)-mediated carbonylation. a) $PdCl_2$, $CuCl_2$, NaOAc, AcOH, CO (1 atm), 23 °C, 24 h, 75%.

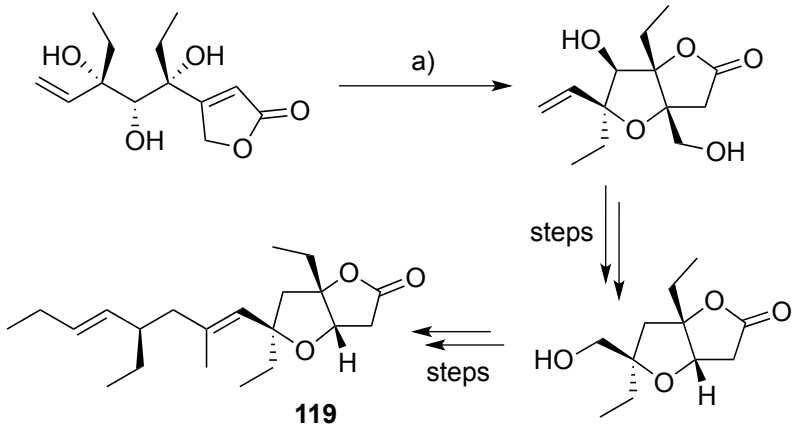

Scheme 2.36: Synthesis of plakortone B (**119**) by oxa-Michael cyclisation and transesterification. a) DBU, toluene, reflux, 72 h, 90%.

Simplexolides A–E (**129–133**, Figure 2.9)[152] represent interesting structural analogues of the plakortone natural products, which appear to arise from the tertiary alcohol dehydration of reduced peroxylactones analogous to compound **122** (Scheme 2.33).

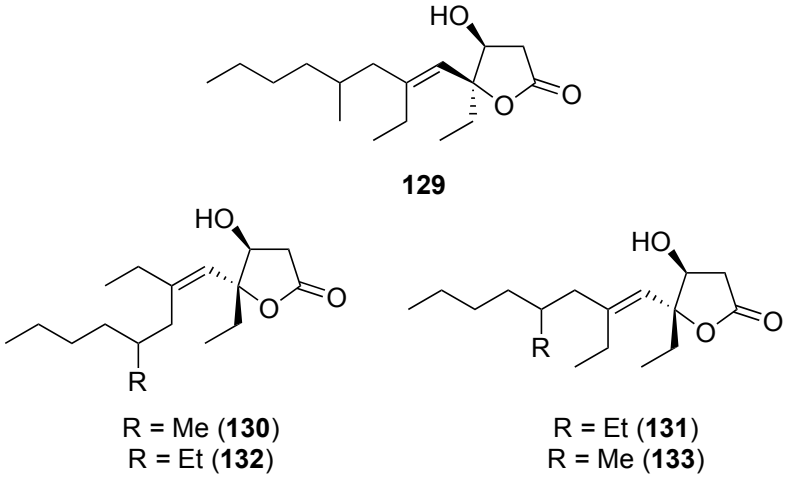

Figure 2.9: Simplexolides A–E (**129–133**) from *Plakortis simplex*.

2.5.4 Plakorsins A, B and plakevulin A

Plakorsins A (**51**), B[113] and plakevulin A (**134**)[187–190] were each isolated from *Plakortis* sponges and share a carbon framework that appears to be related to chondrillin (**2**, Scheme 2.37). While it is clear that plakorsin A (**51**) is likely to arise from the reduction of **2** itself, the biosynthetic origin of plakevulin A (**134**) is less certain. Due to their structural similarity, it has been suggested that **134** may arise by enzymatic reduction of untenone A (**44**).[187] However, we speculate that **134** may be generated from the reduction and intramolecular aldol cyclisation of **2** (Scheme 2.37), in a process analogous to the accepted biosynthesis of **44** (Section 2.4.1). Furthermore, the absolute configuration of plakevulin A (**134**) at C3, as determined by asymmetric synthesis,[189,190] matches that of chondrillin (**2**).

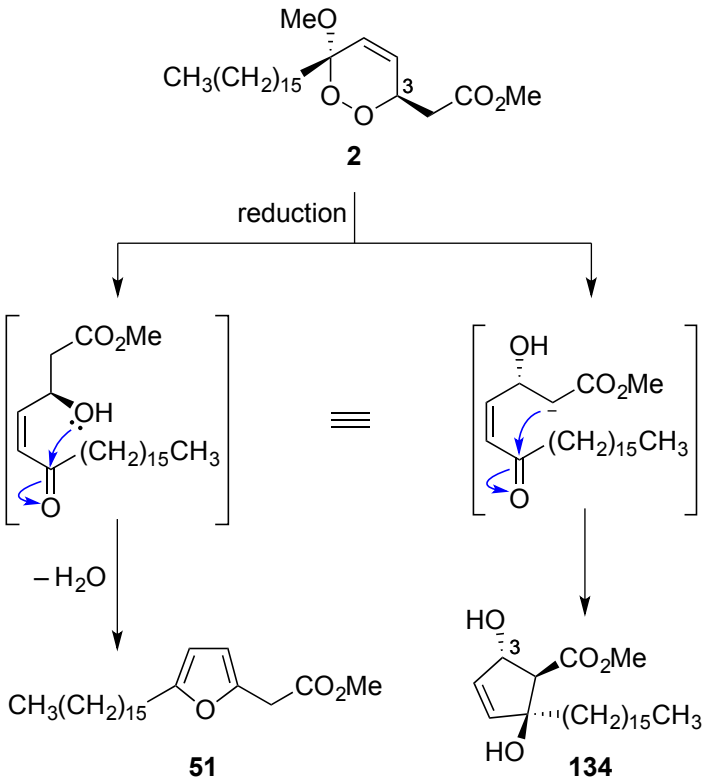

Scheme 2.37: Postulated reduction and cyclisation reactions of chondrillin (**2**) to give plakorsin A (**51**) and plakevulin A (**134**).

2.6 Therapeutic potential and biological activity

Continued interest in the isolation, structural elucidation and chemical synthesis of peroxide and peroxide-derived sponge metabolites is fuelled by their potential for development as therapeutic agents in the treatment of infectious diseases, cancers and physiological disorders. Many of the compounds presented in this review have promising activity for one or more therapeutic targets, and some exhibit selectivity for these targets against other microorganisms and non-tumour cells. However, the cytotoxicity of polyketide endoperoxides is often a factor that must be considered in the hope of producing desirable lead compounds. While a number of research groups have recently begun to address this challenge, managing the cytotoxicity of peroxide and peroxide-derived sponge metabolites remains an ongoing difficulty.

Potency has widely been attributed to the presence of 1,2-dioxane heterocycles, normally appended with a terminal acetate group, through their action as an oxidant. The rearranged congeners, where the peroxide functional group is lost, are typically less

active for the desired target and also tend to have lower levels of cytotoxicity.[24,44,51,144] Endoperoxides appended with a free acid are normally more potent than their corresponding esters.[25,29,32,35,62] In some instances, the esterification of peroxyacids and their rearrangement to non-peroxide containing homologues has been attributed to prolonged storage in alcoholic solvents during specimen extraction.[29,51]

2.6.1 Infectious diseases

Since the discovery of peroxide metabolites as effective antimalarial agents, plakortin (**1**) and its related compounds have been routinely screened for antiplasmodial activity, especially against chloroquine-resistant strains. Although their mechanisms of action are still unclear, a number of studies have focused on understanding the structural requirements and limitations of plakortin-related 1,2-dioxanes as novel targets for treating malaria.

Plakortin (**1**) and its dihydro analogue **28** show good activity against the chloroquine sensitive D10 strain (IC_{50} 1.12–1.26 μM) and chloroquine resistant W2 strain (IC_{50} 0.74–0.76 μM) of *Plasmodium falciparum*.[65] Greater potency for the resistant strain follows the same trend as artemisinin and further demonstrates that polyketide endoperoxides do not share the same mechanism of resistance as chloroquine.[65] Recently, detailed studies on the structure-activity relationships (SARs) of plakortin (**1**) and plakortin-related scaffolds have shown that the formation of discrete carbon centered radicals plays a key role in their effect.[166,191] Other SAR studies on the dioxane scaffold have generated novel synthetic compounds, which maintain antiprotozoal activity and significantly reduce cytotoxicity.[88,99–101] Schwarzer recently discovered that plakortin (**1**) can induce lipid-peroxidation and a marked increase of the lipoperoxide breakdown product 4-hydroxynonenal, which conjugates to *P. falciparum* proteins critically involved in its cellular function.[66]

Manadoperoxides A–K were evaluated extensively for antitrypansomal activity. Most showed excellent activity against *Trypanosoma brucei rhodesiense* including manadoperoxide I (IC_{50} 0.062 μg/mL) and K (IC_{50} 0.087 μg/mL) with low levels of cytotoxicity against HMEC-1 (IC_{50} >10 μg/mL).[15–17] Interestingly, Taglialatella-Scafati found that manadoperoxide B (**135**) had greater potency against *T. b. rhodesience* (IC_{50} 0.003 μg/mL) compared to *P. falciparum* (IC_{50} 2.30 μg/mL), whereas peroxyplakoric ester B_3 (**136**) had greater potency against *P. falciparum* (IC_{50} 0.040 μg/mL) compared

to *T. b. rhodesience* (IC_{50} 3.61 μg/mL); and that notably, they only differ by the placement of methyl groups on an otherwise identical core structure (Figure 2.10).[16] Furthermore, the isomeric compound **137** maintained activity against *T. b. rhodesience* (IC_{50} 0.011 μg/mL) but had increased cytotoxicity against L6 cells (IC_{50} 3.80 μg/mL).[17] Further SAR-based studies revealed the importance of the peroxyketal heterocycle and length of the lipophilic tether for antiprotozoal activity.[15–17]

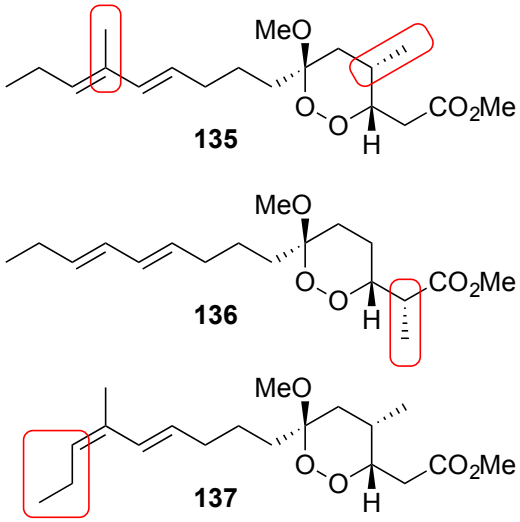

Figure 2.10: The minor structural differences of manadoperoxide B (**135**), peroxyplakoric ester B_3 (**136**) and 12-isomanadoperoxide B (**137**), which greatly effect their antiprotozoal activity and cytotoxicity.

Plakortide endoperoxides have similarly attracted interest as potential therapeutic agents for tropical diseases. Plakortide F was active against *P. falciparum* (IC_{50} 0.39–0.48 μg/mL) and cytotoxic against a number of cancer cell lines *in vitro*, but failed to prolong life expectancy when treating *Plasmodium* infected mice.[27] In the same study, plakortone G was found to be highly cytotoxic with no apparent selectivity. Plakortide P (**10**) had antiparasitic activity against *Leishmania chagasi* (IC_{50} 0.5–1.9 μg/mL) with low toxicity against human macrophages (IC_{50} 16.6 μg/mL);[20] and plakortide I, possessing an unsaturated ketone, was effective when tested against *P. falciparum* (IC_{50} 0.57 μg/mL) but inactive against a panel of other pathogenic bacteria and fungi.[26] Plakortide E (**24**) was also found to be a non-competitive, slow-binding and reversible inhibitor of rhodesain from *T. B. rhodesience* (IC_{50} 5 μM) without cytotoxic effects against J774.1 macrophages at 100 μM.[30]

Recently, the novel endoperoxide metabolite gracilioether H was reported to be active against the chloroquine resistant FC29 strain (IC_{50} 3.3 μM) of *P. falciparum* with low cytotoxicity for vero cells (DT_{50} 324 μM).[160]

Other metabolites in this class have also been tested for activity against pathogenic fungi and bacteria with promising results. Plakinic acid M was active toward a number of *Cryptococcus* fungi (MIC_{90} 2.4–13 μM);[32] manzamenone O (**69**) was effective against *Micrococcus luteus* (MIC 4 μg/mL), *Apergillis niger* (IC_{50} 8 μg/mL) and *Trichophyton mentagrophytes* (IC_{50} 8 μg/mL);[133] and hippolachnin A (**98**) was shown to have potent antifungal activity against *Cryptococcus neoformans*, *Trichophyton rubrum* and *Microsporum gypseum* (MIC 0.4 μM).[155]

2.6.2 Anticancer activity

The cytotoxic effects of many peroxide and peroxide-derived sponge metabolites have prompted numerous studies into their suitability as anticancer leads. Costa-Lotufo found that plakortide P (**14**) and a number of structural analogues were cytotoxic against HCT-116 cells, causing arrest at the G_2/M stage.[31] However, the co-isolated furanylidenes *des*-hydroxygracilioether C (**90**) and spongosoritin A induced arrest at the G_0/G_1 stage, indicating that the two structural subclasses have distinct modes of antimitotic action. Furthermore, while the peroxides showed low selectivity for tumour cells compared to non-tumour cells, compound **90** was more selective with IC_{50} 8.1 μM for HCT-116 and IC_{50} >163 μM for MRC-5 cells.[31] Plakinic acids A–D and a number of structural analogues were found to be remarkably cytotoxic against L1210 murine leukemia (IC_{50} 0.003–0.052 μg/mL);[39] and endoperoxide **138** showed significant *in vitro* cytotoxicity against P388 cells (IC_{50} 0.055 μg/mL), but failed to induce a response *in vivo*.[49,91]

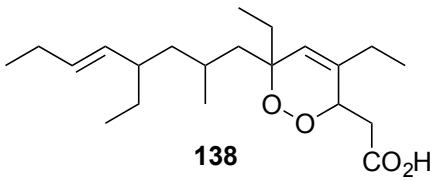

138

Figure 2.11: Endoperoxide **138**, a cytotoxic metabolite.

Other work has specifically targeted the inhibition of DNA polymerase (pol) enzymes. Manzamenone A (**53**) showed inhibition of polα (IC_{50} 1.9 μM), β (IC_{50} 3.2 μM) and human terminal deoxynucleotidyltransferase (IC_{50} 2.5 μM).[124,125] Untenone A (**44**) demonstrated greater selectivity for polα (IC_{50} 4.3 μM);[125] plakevulin A (**134**) was a moderate inhibitor of polγ (IC_{50} 7.5 μg/mL);[187] and a number of synthetic analogues of plakoridine A (**71**) and B (**72**) showed greater inhibition of polα and β than the natural products.[127]

2.6.3 Physiological disorders

Peroxide-derived sponge metabolites have also been reported as useful compounds for the investigation of a range of physiological disorders, including type II diabetes, heart failure and inflammation. Gracilioether B (**85**) and plakilactone C were recently shown to be selective covalent agonists of peroxisome proliferator-activated receptor γ (PPARγ, EC_{50} 2–5 μM), a known pharmacological target for the treatment of type II diabetes, undergoing thio-Michael addition of the lower binding domain cysteine residue to the unsaturated ketone of the natural products.[146] Both compounds were found to regulate the expression of PPARγ-dependent genes in the liver and inhibit the generation of inflammatory mediators.[146] In contrast, gracilioether C (**86**) was found to be a non-covalent agonist (EC_{50} 10 μM) and its *des*-hydroxy homologue (**90**) a non-covalent antagonist.[146] In a separate study, manzamenones B (**54**) and E (**57**) showed inhibition of T-cell protein tyrosine phosphatase (IC_{50} 2.5–3.2 μM) and protein tyrosine phosphatase-1B (IC_{50} 10.8–13.5 μM), also implicated in the treatment of type II diabetes.[126]

Plakortone D activated sarcoplasmic reticulum Ca^{2+} ATPase (EC_{50} 2.8 μM), a protein associated with cardiac muscle relaxation abnormalities, improving calcium uptake at a similar level to that reported for gingerol.[22] 3-*epi*-Plakortin was also found to be an activator, while the longer chain co-isolates plakortides F–H were less active.[23] Interestingly, the ability of polyketide endoperoxides to stimulate calcium uptake is also suggested to play a role in their antimitotic and antifungal activity.[31,192]

Finally, gracilioethers E (**100**), G and I–K were found to be agonists of pregnane-X-receptor, a novel pharmacological target for the treatment of various inflammatory and metabolic disorders, when administered in combination with rifaximin.[162]

2.7 Concluding remarks

Since their discovery in the late 1970s, plakortin (**1**) and chondrillin (**2**) have been the centerpiece of a global research effort to uncover, elucidate and synthesise peroxide and peroxide-derived metabolites from marine sponges. Literature in the chemical sciences is now laced with novel polyketide substances related to **1** and **2** and synthetic methods to effectively construct and arrange their unique and often complex structural components. These efforts, especially those targeting the chemical synthesis of peroxide-derived natural products, have increasingly become inspired by a desire to understand the fascinating decomposition pathways and inherent structural rearrangements of these peroxide substrates. Their potential as therapeutic agents for a wide range of infectious diseases, cancers and physiological disorders adds further motivation for the investigation of this class of compound. Incredibly, investigations in the field to date places the sponge metabolites chondrillin (**2**) and plakorin (**3**) as sole non-enzymatic progenitors to the natural products untenone A (**44**), plakortic acid (**45**), plakorsin A (**51**), manzamenone A–F (**53**–**58**) and H (**59**) with many others expected. Furthermore, plakortin (**1**) and 4,5-unsaturated-1,2-dioxane analogues such as haterumadioxin A (**7**) and B (**8**), are thought to be directly responsible for the occurrence of plakortethers A–G (**108**–**114**), simplakidine A (**115**), gracilioethers B (**85**), C (**86**), D, hippolachnin A (**98**) and spiroplakortone plus many more.

However, efforts to elucidate the biosynthesis of peroxide-related metabolites have only begun. Understanding the assembly of complex polycyclic structures such as gracilioethers A (**92**), E (**100**), F (**95**), G–J, K (**96**), manzamenones K (**68**), O (**69**), untenolide A (**70**), simplextones A (**116**) and B (**117**) remains a challenge of significant novelty and interest. Feasible preparation of such intricate substrates on the scale required in a pharmaceutical context will undoubtedly be aided by consideration of how they are assembled in nature.

2.8 Chapter summary

Chapter 2 is a comprehensive and critical review of current literature on the non-enzymatic biosynthesis, chemical synthesis and therapeutic potential of peroxide and peroxide-derived polyketide metabolites from marine sponges. It is a timely account of literature on the topic since the 2015 Nobel Prize in Medicine was awarded for

discovery and development of the antimalarial endoperoxide, artemisinin. It is also a contemporary review, including literature references to the date of thesis submission; and places the candidate's key contributions (Chapters 3 and 5), which are the subject of this thesis, in the context of the surrounding literature.

Notably, the efforts of many research programs over the past 35 years are collated, analysed and presented with additional comments from the candidate's perspective. Interpretation of this literature, through considering dehydrative ring contraction of 4,5-unsaturated-1,2-dioxane scaffolds as a key step in the biosynthesis of related structures, has provided a clear platform to advance the field of research. This hypothesis, drawn from prior literature, inspired a novel design for the chemical synthesis of furanylidene-containing metabolites (Chapter 3), which also provides tangible evidence to the elucidation of their biosynthetic origins.

2.9 References and notes

1. M. D. Higgs and D. J. Faulkner, *J. Org. Chem.*, 1978, **43**, 3454.
2. F. Cafieri, E. Fattorusso, O. Taglialetella-Scafati and A. Ianaro, *Tetrahedron*, 1999, **55**, 7045.
3. R. J. Wells, *Tetrahedron Lett.*, 1976, **30**, 2637.
4. T. Murayama, Y. Ohizumi, H. Nakamura, T. Sasaki and J. Kobayashi, *Experientia*, 1989, **45**, 898.
5. E. Quinoa, E. Kho, L. V. Manes, P. Crews and G. J. Bakus, *J. Org. Chem.*, 1986, **51**, 4260.
6. D. A. Casteel, *Nat. Prod. Rep.*, 1992, **9**, 289.
7. D. A. Casteel, *Nat. Prod. Rep.*, 1999, **16**, 55.
8. M. Jung; H. Kim; K. Lee and M. Park, *Mini-Rev. Med. Chem.*, 2003, **3**, 159.
9. V. M. Dembitsky; T. A. Gloriozova and V. V. Poroikov, *Mini-Rev. Med. Chem.*, 2007, **7**, 571.
10. V. M. Dembitsky, *Eur. J. Med. Chem.*, 2008, **43**, 223.
11. E. Fattorusso and O. Taglialatela-Scafati, *Mar. Drugs*, 2009, **7**, 130.
12. E. Fattorusso and O. Taglialatela-Scafati, *Phytochem. Rev.*, 2010, **9**, 515.
13. D.-Z. Liu and J.-K Liu, *Nat. Prod. Bioprospect.*, 2013, **3**, 161.
14. F. Rahm, P. Y. Hayes and W. Kitching, *Heterocycles*, 2004, **64**, 523.

15. C. Fattorusso, M. Persico, B. Calcinai, C. Cerrano, S. Parapini, D. Taramelli, E. Novellino, A. Romano, F. Scala, E. Fattorusso and O. Taglialatela-Scafati, *J. Nat. Prod.*, 2010, **73**, 1138.
16. G. Chianese, E. Fattorusso, F. Scala, R. Teta, B. Calcinai, G. Bavestrello, H. A. Dien, M. Kaiser, D. Tasdemir and O. Taglialatela-Scafati, *Org. Biol. Chem.*, 2012, **10**, 7197.
17. G. Chianese, F. Scala, B. Calcinai, C. Cerrano, H. A. Dien, M. Kaiser, D. Tasdemir and O. Taglialatela-Scafati, *Mar. Drugs*, 2013, **11**, 3297.
18. M. Gushiken, I. Kagiyama, H. Kato, T. Kuwana, F. Losung, R. E. P. Mangindaan, N. J. de Voogd and S. Tsukamoto, *J. Nat. Med.*, 2015, **69**, 595.
19. N. Takada, M. Watanabe, A. Yamada, K. Suenaga, K. Yamada, K. Ueda and D. Uemura, *J. Nat. Prod.*, 2001, **64**, 356.
20. M. H. Kossuga, A. M. Nascimento, J. Q. Reimao, A. G. Tempone, N. N. Taniwaki, K. Veloso, A. G. Ferreira, B. C. Cavalcanti, C. Pessoa, M. O. Moraes, A. M. S. Mayer, E. Hajdu and R. G. S. Berlinck, *J. Nat. Prod.*, 2008, **71**, 334.
21. C. Festa, S. De Marino, M. V. D'Auria, O. Taglialatela-Scafati, E. Deharo, S. Petek and A. Zampella, *Tetrahedron*, 2013, **69**, 3706.
22. A. D. Patil, A. J. Freyer, M. F. Bean, B. K. Carte, J. W. Westley, R. K. Johnson and P. Lahouratate, *Tetrahedron*, 1996, **52**, 377.
23. A. D. Patil, A. J. Freyer, B. Carte, R. K. Johnson and P. Lahouratate, *J. Nat. Prod.*, 1996, **59**, 219.
24. B. Harrison and P. Crews, *J. Nat. Prod.*, 1998, **61**, 1033.
25. E. Fattorusso, O. Taglialatela-Scafati, M. Di Rosa and A. Ianaro, *Tetrahedron*, 2000, **56**, 7959.
26. J.-F. Hu, H.-F. Gao, M. Kelly and M. T. Hamann, *Tetrahedron*, 2001, **57**, 9379.
27. D. J. Gochfeld and M. T. Hamann, *J. Nat. Prod.*, 2001, **64**, 1477.
28. M. del Sol Jimenez, S. P. Garzon and A. D. Rodriguez, *J. Nat. Prod*, 2003, **66**, 655.
29. F. Berrue, O. P. Thomas, C. F.-L. Bon, F. Reyes and P. Amade, *Tetrahedron*, 2005, **61**, 11843.
30. S. Oli, U. R. Abdelmohsen, U. Hentschel and T. Schirmeister, *Mar. Drugs*, 2014, **12**, 2614.
31. E. A. Santos, A. L. Quintela, E. G. Ferreira, T. S. Sousa, F. d. C. L. Pinto, E. Hajdu, M. S. Carvalho, S. Salani, D. D. Rocha, D. V. Wilke, M. d. C. M. Torres,

P. C. Jimenez, E. R. Silveira, J. J. La Clair, O. D. L. Pessoa and L. V. Costa-Lotufo, *J. Nat. Prod.*, 2015, **78**, 996.

32. M. T. Jamison, D. S. Dalisay and T. F. Molinski, *J. Nat. Prod.*, 2016, **79**, 555.
33. G. R. Pettit, T. Nogawa, J. C. Knight, D. L. Doubek and J. N. A. Hooper, *J. Nat. Prod.*, 2004, **67**, 1611.
34. M. Yanai, S. Ohta, E. Ohta, T. Hirata and S. Ikegami, *Bioorg. Med. Chem.*, 2003, **11**, 1715.
35. D. W. Phillipson and K. L. Rinehart, *J. Am. Chem. Soc.*, 1983, **105**, 7735.
36. J. S. Sandler, P. L. Colin, J. N. A. Hooper and D. J. Faulkner, *J. Nat. Prod.*, 2002, **65**, 1258.
37. D. S. Dalisay, T. Quach, G. N. Nicholas and T. F. Molinski, *Angew. Chem. Int. Ed.*, 2009, **48**, 4367.
38. D. S. Dalisay, T. Quach and T. F. Molinski, *Org. Lett.*, 2010, **12**, 1524.
39. B. S. Davidson, *J. Org. Chem.*, 1991, **56**, 6722.
40. B. S. Davidson, *Tetrahedron Lett.*, 1991, **32**, 7167.
41. P. A. Horton, R. E. Longley, M. Kelly-Borges, O. J. McConnell and L. M. Ballas, *J. Nat. Prod.*, 1994, **57**, 1374.
42. Y. Chen, K. B. Killday, P. J. McCarthy, R. Schimoler, K. Chilson, C. Selitrennikoff, S. A. Pomponi and A. E. Wright, *J. Nat. Prod.*, 2001, **64**, 262.
43. C. Jimenez-Romero, I. Ortiz, J. Vicente, B. Vera, A. D. Rodriguez, S. Nam and R. Jove, *J. Nat. Prod.*, 2010, **73**, 1694.
44. M. Varoglu, B. M. Peters and P. Crews, *J. Nat. Prod.*, 1995, **58**, 27.
45. T. L. Perry, A. Dickerson, A. A. Khan, R. K. Kondru, D. N. Beratan, P. Wipf, M. Kelly and M. T. Hamann, *Tetrahedron*, 2001, **57**, 1483.
46. A. Rudi, R. Afanii, L. G. Gravalos, M. Aknin, E. Gaydou, J. Vacelet and Y. Kashman, *J. Nat. Prod.*, 2003, **66**, 682.
47. K. W. L. Yong, J. J. De Voss, J. N. A. Hooper and M. J. Garson, *J. Nat. Prod.*, 2011, **74**, 194.
48. K. W. L. Yong, L. K. Lambert, P. Y. Hayes, J. J. De Voss and M. J. Garson, *J. Nat. Prod.*, 2012, **75**, 351.
49. D. E. Williams, T. M. Allen, R. van Soest, H. W. Behrisch and R. J. Andersen, *J. Nat. Prod.*, 2001, **64**, 281.
50. R. Mohammed, J. Peng, M. Kelly, M. Yousaf, E. Winn, S. Odde, Z. Bie, A. Xie, R. J. Doerksen and M. T. Hamann, *Aust. J. Chem.*, 2010, **63**, 877.

51. D. B. Stierle and D. J. Faulkner, *J. Org. Chem.*, 1979, **44**, 964.
52. M. Kobayashi, K. Kondo and I. Kitagawa, *Chem. Pharm. Bull.*, 1993, **41**, 1324.
53. A. Rudi, R. Talpir, Y. Kashman, Y. Benayahu and M. Schleyer, *J. Nat. Prod.*, 1993, **56**, 2178.
54. S. I. Toth and F. J. Schmitz, *J. Nat. Prod.*, 1994, **57**, 123.
55. J. C. Braekman, D. Daloze, S. De Groote, J. B. Fernandes and R. W. M. Van Soest, *J. Nat. Prod.*, 1998, **61**, 1038.
56. A. Fontana, M. Ishibashi and J. Kobayashi, *Tetrahedron*, 1998, **54**, 2041.
57. A. Fontana, A. Ishibashi, H. Shigemori and J. Kobayashi, *J. Nat. Prod.*, 1998, **61**, 1427.
58. E. Manzo, M. L. Ciavatta, D. Melck, P. Schupp, N. de Voogd and M. Gavagnin, *J. Nat. Prod.*, 2009, **72**, 1547.
59. Y. Feng, R. A. Davis, M. Sykes, V. M. Avery, D. Camp and R. J. Quinn, *J. Nat. Prod.*, 2010, **73**, 716.
60. J. S. Oh, B. S. Hwang, O.-H. Kang, D.-Y. Kwon and J.-R. Rho, *Mar. Drugs*, 2013, **11**, 4407.
61. B. S. Hwang and J.-R. Rho, *J. Kor. Magn. Reson.*, 2013, **17**, 47.
62. T. R. Hoye, W. M. Alarif, S. S. Basaif, M. Abo-Elkarm, M. T. Hamann, A. E. Wahba and S.-E. N. Ayyad, *Arkivoc*, 2015 (v), 164.
63. J. H. McKerrow, *Nat. Prod. Rep.*, 2015, **32**, 1610.
64. L. Y. Kong and R. X. Tan, *Nat. Prod. Rep.*, 2015, **32**, 1617.
65. E. Fattorusso, S. Parapini, C. Campagnuolo, N. Basilico, O. Taglialatela-Scafati and D. Taramelli, *J. Antimicrob. Chemother.*, 2002, **50**, 883.
66. O. A. Skorokhod, D. Davalos-Schafler, V. Gallo, E. Valente, D. Ulliers, A. Notarpietro, G. Mandili, F. Novelli, M. Persico, O. Taglialatela-Scafati, P. Arese and E. Schwarzer, *Free Radic. Biol. Med.*, 2015, **89**, 624.
67. S. P. D. Ovenden and R. J. Capon, *J. Nat. Prod.*, 1999, **62**, 214.
68. R. J. Capon, *Eur. J. Org. Chem.*, 2001, 633.
69. G. Della Sala, T. Hochmuth, V. Costantino, R. Teta, W. Gerwick, L. Gerwick, J. Piel and A. Mangoni, *Environ. Microbiol. Rep.*, 2013, **5**, 809.
70. G. Della Sala, T. Hochmuth, R. Teta, V. Costantino and A. Mangoni, *Mar. Drugs*, 2014, **12**, 5425.
71. S. Isayama and T. Mukaiyama, *Chem. Lett.*, 1989, 573.
72. S. Isayama, *Bull. Chem. Soc. Jpn.*, 1990, **63**, 1305.

73. E. M. P. Silva, R. J. Pye, C. Cardin and L. M. Harwood, *Synlett*., 2010, 509.
74. E. M. P. Silva, R. J. Pye, G. D. Brown and L. M. Harwood, *Eur. J. Org. Chem*., 2012, 1209.
75. B. Barnych and J.-M. Vatéle, *Org. Lett*., 2012, **14**, 564.
76. K. W. L. Yong, B. Barnych, J. J. De Voss, J.-M. Vatéle and M. J. Garson, *J. Nat. Prod*., 2012, **75**, 1792.
77. S. Gemma, F. Marti, E. Gabellieri, G. Campiani, E. Novellino and S. Butini, *Tetrahedron Lett*., 2009, **50**, 5719.
78. S. Gemma, E. Gabellieri, S. S. Coccone, F. Marti, O. Taglialatela-Scafati, E. Novellino, G. Campiani and S. Butini, *J. Org. Chem*., 2010, **75**, 2333.
79. S. Gemma, S. Kunjir, S. S. Coccone, M. Brindisi, V. Moretti, S. Brogi, E. Novellino, N. Basilico, S. Parapini, D. Taramelli, G. Campiani and S. Butini, *J. Med. Chem*., 2011, **54**, 5949.
80. B. Barnych and J.-M. Vatéle, *Synlett*, 2011, **13**, 1912.
81. B. Barnych, B. Fenet and J.-M. Vatéle, *Tetrahedron*, 2013, **69**, 334.
82. As reproduced in Scheme 6, 5-*exo*-tet cyclisation of **31** was drawn in ref. 81 to give **32** with retention of configuration at C3. However, in a personal communication with the authors of this work (B. Barnych), it has been verified that this reaction should proceed with inversion at C3 and that compound **32** should be drawn with (3*S*) configuration, as suggested below. Consequently, the absolute configuration of natural andavadoic acid (**19**) is in fact (3*S*,5*R*).

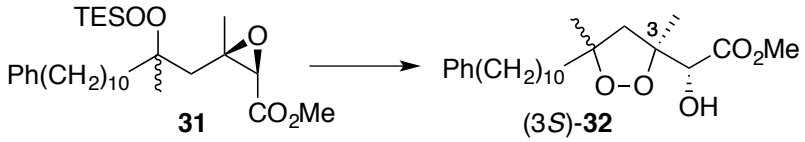

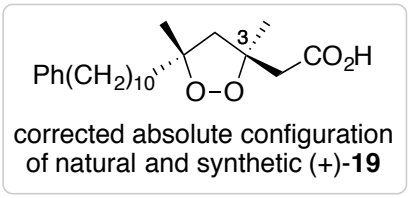

83. K. S. Feldman and M. Pravez, *J. Am. Chem. Soc*., 1986, **108**, 1328.
84. K. S. Feldman and R. E. Simpson, *J. Am. Chem. Soc*., 1989, **111**, 4878.
85. K. S. Feldman and C. M. Kraebel, *J. Org. Chem*., 1992, **57**, 4574.
86. X.-Y. Sun, X.-Y. Tian, Z.-W. Li, X.-S. Peng and H. N. C. Wong, *Chem. Eur. J*., 2011, **17**, 5874.

87. X.-Y. Tian, J.-W. Han, Q. Zhao and H. N. C. Wong, *Org. Biol. Chem.*, 2014, **12**, 3686.

88. C. Fattorusso, M. Persico, N, Basilico, D. Taramelli, E. Fattorusso, F. Scala and O. Taglialetela-Scafati, *Bioorg. Med. Chem.*, 2011, **19**, 312.

89. M. Jung, J. Ham and J. Song, *Org. Lett.*, 2002, **4**, 2763.

90. O. Zvarec, T. D. Avery, D. K. Taylor and E. R. T. Tiekink, *Tetrahedron*, 2010, **66**, 1007.

91. S. P. Gunasekera, M. Gunasekera, G. P. Gunawardana, P. McCarthy and N. Burres, *J. Nat. Prod.*, 1990, **53**, 669.

92. G. Yao and K. Steliou, *Org. Lett.*, 2002, **4**, 485.

93. B. B. Snider and Z. Shi, *J. Org. Chem.*, 1990, **55**, 5669.

94. B. B. Snider and Z. Shi, *J. Am. Chem. Soc.*, 1992, **114**, 1790.

95. B. B. Snider, Z. Shi, S. V. O'Neil, K. D. Kreutter and T. L. Arakaki, *J. Org. Chem.*, 1994, **59**, 1726.

96. P. Dussault, A. Sahli and T. Westermeyer, *J. Org. Chem.*, 1993, **58**, 5469.

97. P. H. Dussault and K. R. Woller, *J. Am. Chem. Soc.*, 1997, **119**, 3824.

98. P. H. Dussault, C. T. Eary and K. R. Woller, *J. Org. Chem.*, 1999, **64**, 1789.

99. M. Persico, A. Quintavalla, F. Rondinelli, C. Trombini, M. Lombardo, C. Fattorusso, V. Azzarito, D. Taramelli, S. Parapini, Y. Corbett, G. Chianese, E. Fattorusso and O. Taglialatela-Scafati, *J. Med. Chem.*, 2011, **54**, 8526.

100. M. Persico, S. Parapini, G. Chianese, C. Fattorusso, M. Lombardo, L. Petrizza, A. Quintavalla, F. Rondinelli, N. Basilico, D. Taramelli, C. Trombini, E. Fattorusso and O. Taglialatela-Scafati, *Eur. J. Med. Chem.*, 2013, **70**, 875.

101. N. Murakami, M. Kawanishi, S. Itagaki, T. Horii and M. Kobayashi, *Bioorg. Med. Chem. Lett.*, 2002, **12**, 69.

102. N. Murakami, M. Kawanishi, H. M. Mostaqul, J. Li, S. Itagaki, T. Horii and M. Kobayashi, *Bioorg. Med. Chem. Lett.*, 2003, **13**, 4081.

103. M. Kawanishi, N. Kotoku, S. Itagaki, T. Horii and M. Kobayashi, *Bioorg. Med. Chem.*, 2004, **12**, 5297.

104. P. H. Dussault, T. K. Trullinger and F. Noor-e-Ain, *Org. Lett.*, 2002, **4**, 4591.

105. P. Dai, T. K. Trullinger X. Liu and P. H. Dussault, *J. Org. Chem.*, 2006, **71**, 2283.

106. A. J. Bloodworth, B. D. Bothwell, A. N. Collins and N. L. Maidwell, *Tetrahedron Lett.*, 1996, **37**, 1885.

107. X. Lu; Y. Liu; B. Sun; B. Cindric and L. Deng, *J. Am. Chem. Soc*., 2008, **130**, 8134.

108. L. Hu; X. Lu and L. Deng, *J. Am. Chem. Soc*., 2015, **137**, 8400.

109. For a recent review on asymmetric peroxidation, see G. D. Sala and A. Lattanzi, *ACS Catal*., 2014, **4**, 1234.

110. N. Kornblum and H. E. DeLaMare, *J. Am. Chem. Soc*., 1951, **73**, 880.

111. N. Kornblum and H. E. DeLaMare, *J. Am. Chem. Soc*., 1952, **74**, 3079.

112. M. Ishibashi, S. Takeuchi and J. Kobayashi, *Tetrahedron Lett*., 1993, **34**, 3749.

113. Y.-C. Shen, C. V. S. Prakash and Y.-H. Kuo, *J. Nat. Prod*., 2001, **64**, 324.

114. M. D. Norris and M. V. Perkins, *Tetrahedron*, 2013, **69**, 9813.

115. Epoxides **45** and **49** are reported to have a *syn*-oxirane, *E*-olefin and *anti*-oxirane, *Z*-olefin arrangement, respectively; although the data presented in literature is not directly comparable (see ref. 95 and 113). Since natural plakortic acid was originally co-isolated with **3** and base-mediated rearrangement of **3** appears to be likely, we speculate that the correct structure of natural plakortic acid may in fact be the acid of oxirane **49**, where R = $(CH_2)_{15}CH_3$ (Scheme 14 in text).

116. M. Asami, T. Ishizaki and S. Inoue, *Tetrahedron Lett*., 1995, **36**, 1893.

117. H. Miyaoka, T. Watanuki, Y. Saka and Y. Yamada, *Tetrahedron*, 1995, **51**, 8749.

118. S. Al-Busafi, M. G. B. Drew, T. Sanders and R. C. Whitehead, *Tetrahedron Lett*., 1998, **39**, 1647.

119. S. Al-Busafi and R. C. Whitehead, *Tetrahedron Lett*., 2000, **41**, 3467.

120. S. Al-Busafi, J. R. Doncaster, M. G. B. Drew, A. C. Regan and R. C. Whitehead, *J. Chem. Soc., Perkin Trans. 1*, 2002, 476.

121. K. Takeda, I. Nakayama and E. Yoshii, *Synlett*, 1994, **3**, 178.

122. S. Tsukamoto, S. Takeuchi, M. Ishibashi and J. Kobayashi, *J. Org. Chem.,* 1992, **57**, 5255.

123. J. Kobayashi, S. Tsukamoto, S. Takeuchi and M. Ishibashi, *Tetrahedron*, 1993, **49**, 5955.

124. M. Perpelescu, M. Tsuda, M. Suzuki, S. Yoshida and J. Kobayashi, *Natural Medicines*, 2004, **58**, 86.

125. F. Saito, R. Takeuchi, T. Kamino, K. Kuramochi, F. Sugawara, K. Sakaguchi and S. Kobayashi, *Bioorg. Med. Chem. Lett*., 2004, **14**, 1975.

126. Y. Wakuda, T. Kubota, H. Shima, T. Okada, S. Mitsuhashi, N. Aoki, K. Kikuchi and J. Kobayashi, *Mar. Drugs*, 2006, **4**, 9.

127. J. R. Doncaster, L. L. Etchells, N. M. Kershaw, R. Nakamura, H. Ryan, R. Takeuchi, K. Sakaguchi, A. Sardarian and R. C. Whitehead, *Bioorg. Med. Chem. Lett.,* 2006, **16**, 2877.

128. We expect that a similar structural reassignment is likely for compounds **56**, **57** and **59**.

129. Compounds **53–56**, **58** and **59** (excluding **57**, which has a valine residue attached) were reported with low magnitudes of optical rotation indicating that they may in fact have been isolated as pseudo-racemic. This is consistent with Whitehead's theory of biogenesis.

130. S. Takeuchi, T. Kikuchi, S. Tsukamoto, M. Ishibashi and J. Kobayashi, *Tetrahedron*, 1995, **51**, 5979.

131. T. Kubota, Y. Ishiguro, A. Takahashi-Nakaguchi, J. Fromont, T. Gonoi and J. Kobayashi, *Bioorg. Med. Chem. Lett.*, 2013, **23**, 244.

132. N. Tanaka, M. Asai, T. Kusama, J. Fromont and J. Kobayashi, *Tetrahedron Lett.*, 2015, **56**, 1388.

133. N. Tanaka, M. Asai, A. Takahashi-Nakaguchi, T. Gonoi, J. Fromont and J. Kobayashi, *Org. Lett.*, 2013, **15**, 2518.

134. Y. Ishiguro, T. Kubota, J. Fromont, M. Shiro and J. Kobayashi, *Tetrahedron Lett.*, 2010, **51**, 4023.

135. The acid of (*Z*)-**50** (or (*E*)-**50**, Section 3.3) may decarboxylate prior to condensation with **68**.

136. S. Takeuchi, M. Ishibashi and J. Kobayashi, *J. Org. Chem.*, 1994, **59**, 3712.

137. Y. Ishiguro, T. Kubota, K. Ishiuchi, J. Fromont and J. Kobayashi, *Tetrahedron Lett.*, 2009, **50**, 3202.

138. L. L. Etchells, A. Sardarian and R. C. Whitehead, *Tetrahedron Lett.*, 2005, **46**, 2803.

139. In turn, plakorsin A (**51**) is expected to arise from the reduction of **2** or **3** (Section 4.4).

140. L. L. Etchells, M. Helliwell, N. M. Kershaw, A. Sardarian and R. C. Whitehead, *Tetrahedron*, 2006, **62**, 10914.

141. D. Ma and H. Sun, *Tetrahedron Lett.*, 2000, **41**, 1947.

142. J. A. Stafford, *Tetrahedron Lett.*, 1995, **36**, 681.

143. P. A. Bartlett and C. Chapuis, *J. Org. Chem.*, 1986, **51**, 2799.
144. R. S. Compagnone, I. C. Pina, H. R. Rangel, F. Dagger, A. I. Suarez, M. V. R. Reddy and D. J. Faulkner, *Tetrahedron*, 1998, **54**, 3057.
145. R. Ueoka, Y. Nakao, S. Kawatsu, J. Yaegashi, Y. Matsumoto, S. Matsunaga, K. Furihata, R. W. M. van Soest and N. Fusetani, *J. Org. Chem.*, 2009, **74**, 4203.
146. C. Festa, G. Lauro, S. De Marino, M. V. D'Auria, M. C. Monti, A. Casapullo, C. D'Amore, B. Renga, A. Mencarelli, S. Petek, G. Bifulco, S. Fiorucci and A. Zampella, *J. Med. Chem.*, 2012, **55**, 8303.
147. R. J. Capon, S. Singh, S. Ali and S. Sotheeswaran, *Aust. J. Chem.*, 2005, **58**, 18.
148. R. A. Epifanio, L. S. Pinheiro and N. C. Alves, *J. Braz. Chem. Soc.*, 2005, **16**, 1367.
149. G. Chianese, B.-B. Gu, F. Yang, W.-H. Jiao, Y.-W. Guo, H.-W. Lin and O. Taglialetella-Scafati, *RSC Adv.*, 2015, **5**, 63372.
150. D. B. Stierle and D. J. Faulkner, *J. Org. Chem.*, 1980, **45**, 3396.
151. Faulkner also isolated hemiacetal adducts related to **80** (ref. 51), which indicates that Kornblum-DeLaMare rearrangement may also be a prevalent decomposition pathway for saturated 1,2-dioxanes.
152. X.-F. Liu, Y. Shen, F. Yang, M. T. Hamann, W.-H. Jiao, H.-J. Zhang, W.-S. Chen and H.-W. Lin, *Tetrahedron*, 2012, **68**, 4635.
153. M. D. Norris, M. V. Perkins and E. J. Sorensen, *Org. Lett.*, 2015, **17**, 668.
154. M. Akiyama, Y. Isoda, M. Nishimoto, A. Kobayashi, D. Togawa, N. Hirao, A. Kuboki and S. Ohira, *Tetrahedron Lett.*, 2005, **46**, 7483.
155. C. Festa, S. De Marino, M. V. D'Auria, E. Deharo, G. Gonzalez, C. Deyssard, S. Petek, G. Bifulco and A. Zampella, *Tetrahedron*, 2012, **68**, 10157.
156. C. Festa, C. D'Amore, B. Renga, G. Lauro, S. De Marino, M. V. D'Auria, G. Bifulco, A. Zampella and S. Fiorucci, *Mar. Drugs*, 2013, **11**, 2314.
157. X.-Y. Shen, X.-S. Peng and H. N. C. Wong, *Org. Lett.*, 2016, **18**, 1032.
158. C. M. Rasik and M. K. Brown, *Angew. Chem., Int. Ed.*, 2014, **53**, 14522.
159. S.-J. Piao, Y.-L. Song, W.-H. Jiao, F. Yang, X.-F. Liu, W.-S. Chen, B.-N. Han and H.-W. Lin, *Org. Lett.*, 2013, **15**, 3526.
160. Interestingly, monotriajaponide A, isolated in 2003 (ref. 34) appears to represent a *des*-hydroperoxy precursor related to haterumadioxin A (**7**).
161. S. A. Ruider, T. Sandmeier and E. M. Carreira, *Angew. Chem., Int. Ed.*, 2015, **54**, 2378.

162. S. A. Ruider and E. M. Carreira, *Org. Lett.*, 2016, **18**, 220.
163. M. E. McCallum, C. M. Rasik, J. L. Wood and M. K. Brown, *J. Am. Chem. Soc.*, 2016, **138**, 2437.
164. R. Datta, R. J. Dixon and S. Ghosh, *Tetrahedron Lett.*, 2016, **57**, 29.
165. D. T. Sawyer, J. P. Hage and A. Sobkowiak, *J. Am. Chem. Soc.*, 1995, **117**, 106.
166. O. Taglialetela-Scafati, E. Fattorusso, A. Romano, F. Scala, V. Barone, P. Cimino, E. Stendardo, B. Catalanotti, M. Persico and C. Fattorusso, *Org. Biomol. Chem.*, 2010, **8**, 846.
167. F. S. De Guzman and F. J. Schmitz, *J. Nat. Prod.*, 1990, **53**, 926.
168. C. Fattorusso, G. Campiani, B. Catalanotti, M. Persico, N. Basilico, S. Parapini, D. Taramelli, C. Campagnuolo, E. Fattorusso, A. Romano and O. Taglialetela-Scafati, *J. Med. Chem.*, 2006, **49**, 7088.
169. C. Campagnuolo, E. Fattorusso, O. Taglialatela-Scafati, A. Ianaro and B. Pasino, *Eur. J. Org. Chem.*, 2002, 61.
170. C. Campagnuolo, C. Fattorusso, E. Fattorusso, A. Ianaro, B. Pisano and O. Taglialatela-Scafati, *Org. Lett.*, 2003, **5**, 673.
171. J. P. John, J. Jost and A. V. Novikov, *J. Org. Chem.*, 2009, **74**, 6083.
172. X.-F. Liu, Y.-L. Song, H.-J. Zhang, F. Yang, H.-B. Yu, W.-H. Jiao, S.-J. Piao, W.-S. Chen and H.-W. Lin, *Org. Lett.*, 2011, **13**, 3154.
173. F. Cafieri, E. Fattorusso, O. Taglialatela-Scafati, M. Di Rosa and A. Ianaro, *Tetrahedron*, 1999, **55**, 13831.
174. A. Rudi and Y. Kashman, *J. Nat. Prod.*, 1993, **56**, 1827.
175. M. F. Semmelhack and P. Shanmugam, *Tetrahedron Lett.*, 2000, **41**, 3567.
176. M. F. Semmelhack, R. J. Hooley and C. M. Kraml, *Org. Lett.*, 2006, **8**, 5203.
177. G. C. Paddon-Jones, N. L. Hungerford, P. Hayes and W. Kitching, *Org. Lett.*, 1999, **1**, 1905.
178. P. Y. Hayes and W. Kitching, *J. Am. Chem. Soc.*, 2002, **124**, 9718.
179. P. Y. Hayes and W. Kitching, *Heterocycles*, 2004, **62**, 173.
180. P. Y. Hayes, S. Chow, F. Rahm, P. V. Bernhardt, J. J. De Voss and W. Kitching, *J. Org. Chem.*, 2010, **75**, 6489.
181. H.-K. Lee and H. N. C. Wong, *Chem. Commun.*, 2002, 2114.
182. X.-G. Xie, X.-W. Wu, H.-K. Lee, X.-S. Peng, and H. N. C. Wong, *Chem. Eur. J.*, 2010, **16**, 6933.
183. G. Mehta, B. A. Bhat and T. H. S. Kumara, *Tetrahedron Lett.*, 2009, **50**, 6597.

184. C. Bittner, A. Burgo, P. J. Murphy, C. H. Sung and A. J. Thornhill, *Tetrahedron Lett*., 1999, **40**, 3455.

185. M. Akiyama, Y. Isoda, M. Nishimoto, M. Narazaki, H. Oka, A. Kuboki and S Ohira, *Tetrahedron Lett*., 2006, **47**, 2287.

186. H. Sugimura, S. Sato, K. Tokudome and T. Yamada, *Org. Lett*., 2014, **16**, 3384.

187. M. Tsuda, T. Endo, M. Perpelescu, S. Yoshida, K. Watanabe, J. Fromont, Y. Mikami and J. Kobayashi, *Tetrahedron*, 2003, **59**, 1137.

188. F. Saito, R. Takeuchi, T. Kamino, K. Kuramochi, F. Sugawara, K. Sakaguchi, S. Kobayashi, M. Tsudad and J. Kobayashi, *Tetrahedron Lett*., 2004, **45**, 8069.

189. K. Kuramochi, F. Saito, R. Takeuchi, T. Era, M. Takemura, J. Kobayashi, K. Sakaguchi, S. Kobayashi and F. Sugawara, *Tetrahedron*, 2006, **62**, 8006.

190. H. Mizutani, M. Watanabe and T. Honda, *Synlett*, 2005, 793.

191. G. Chianese, M. Persico, F. Yang, H.-W. Lin, Y.-W. Guo, N. Basilico, S. Parapini, D. Taramelli, O. Taglialatela-Scafati and C. Fattorusso, *Bioorg. Med. Chem*., 2014, **22**, 4572.

192. T. Xu, Q. Feng, M. R. Jacob, B. Avula, M. M. Mask, S. R. Baerson, S. K. Tripathi, R. Mohammed, M. T. Hamann, I. A. Khan, L. A. Walker, A. M. Clark and A. K. Agarwal, *Antimicrob. Agents Chemother*., 2011, **55**, 1611.

3. Development of a biomimetic cascade reaction

A thorough and critical review of current literature (Chapter 2) revealed an opportunity to explore the chemical basis of marine sponge metabolites with a methyl [2(5*H*)-furanylidene]ethanoate (furanylidene) core structure, such as gracilioethers B, C and spongosoritin A. Careful analyses of contrasting literature led to a revised mechanism for the dehydrative ring contraction of suggested endoperoxide progenitors, and a synthetic model was constructed to demonstrate this relationship. This new mechanistic insight into the biosynthetic origin of the furanylidene structural subclass unveiled a convenient synthetic intermediate *en route* to construction of the heterocyclic core, which allowed controlled assembly of the central structure in a single cyclisation/double dehydration cascade reaction.

Chapter 3 details 'a biomimetic cascade for the formation of the methyl [2(5*H*)-furanylidene]ethanoate core of spongosoritin A and the gracilioethers' as prepared in an article with the same title and published in the refereed journal *Tetrahedron*, Elsevier on 9 September 2013 (DOI: 10.1016/j.tet.2013.09.006). Preliminary results to the findings presented in this chapter were collected and disclosed in a thesis for award of the candidate's previous degree (M. D. Norris, 2011, "Studies in organic methodology: a biomimetic approach to plakortin natural products," Flinders University). Although on the same topic, all results presented in this chapter were obtained during doctoral candidature and expand the previous study to one of greater depth. The candidate researched, planned, executed and prepared the following chapter/published article with full intellectual and practical contribution with due guidance and only minor textual editing from co-authors throughout manuscript preparation and final publishing; and is listed as the primary author of this work.

3.1 A biomimetic cascade for the formation of the methyl [2(5*H*)-furanylidene]ethanoate core of spongosoritin A and the gracilioethers

The polyketide secondary metabolites spongosoritin A and gracilioethers A–C contain a unique methyl [2(5*H*)-furanylidene]ethanoate core. A synthetic model of a suspected biosynthetic intermediate to these natural products was constructed in seven steps and 48% overall yield. This model undergoes a facile cyclisation/double dehydration cascade to give the desired furanylidene motif, with the required (2*Z*) isomer obtained in >9:1 dr when an ethyl substituent is located at C3' of the furanylidene.

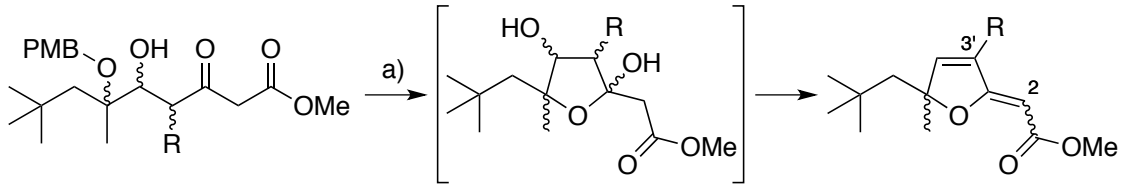

Scheme 3.1: A biomimetic cascade for the formation of the methyl [2(5*H*)-furanylidene]ethanoate core of spongosoritin A and the gracilioethers. a) DDQ, pH 7 phosphate buffer, CH_2Cl_2, r.t., 3 h; then TFA, CH_2Cl_2, r.t., 48 h.

3.2 Introduction

The gracilioethers A (**92**), B (**85**) and C (**86**)[1] are a recently (2009) isolated series of polyketide natural products from the marine sponge *Agelas gracilis*. Their unusual structures and seemingly related relative and absolute stereochemistries were determined by spectroscopic and chemical methods. Compounds **92**, **85** and **86** were found to have significant antimalarial activity against *Plasmodium falciparum* with IC_{50} values of 0.5–10 mg/mL, while gracilioether B also showed antiprotozoan activity against *Leishmania major* with 68% inhibition at 10 mg/mL.[1] Since their first isolation, **92**, **85** and **86** have also been reported as constituents in the chloroform extracts of *Plakinastrella mamillaris* along with an array of congeners; gracilioethers D–K and

plakilactones A–F.[2–4] A number of these compounds were found to act as selective agonists or antagonists of peroxisome proliferator-activated receptor γ (PPARγ).[2]

The gracilioethers and other related metabolites, such as spongosoritin A (**139**)[5] and the homologous compounds **81**, **140** and **141**[6,7] all contain a methyl [2(5*H*)-furanylidene]ethanoate 'furanylidene' moiety, unique to this family (Figure 3.1). Although the biosynthetic origins of these compounds are unclear,[8] they appear to be formed by the decomposition of unsaturated 1,2-dioxane precursors as proposed by Faulkner and co-workers.[7,9] Whilst reporting their isolation from Palauan marine sponges of the genus Plakortis, Faulkner suggested that furanylidene **81** may arise from the base-catalysed rearrangement of peroxide **82**, as shown in Scheme 3.2.[7] This type of rearrangement has been observed for both saturated and unsaturated 1,2-dioxane analogues and has proven to be useful in synthesis.[9–11]

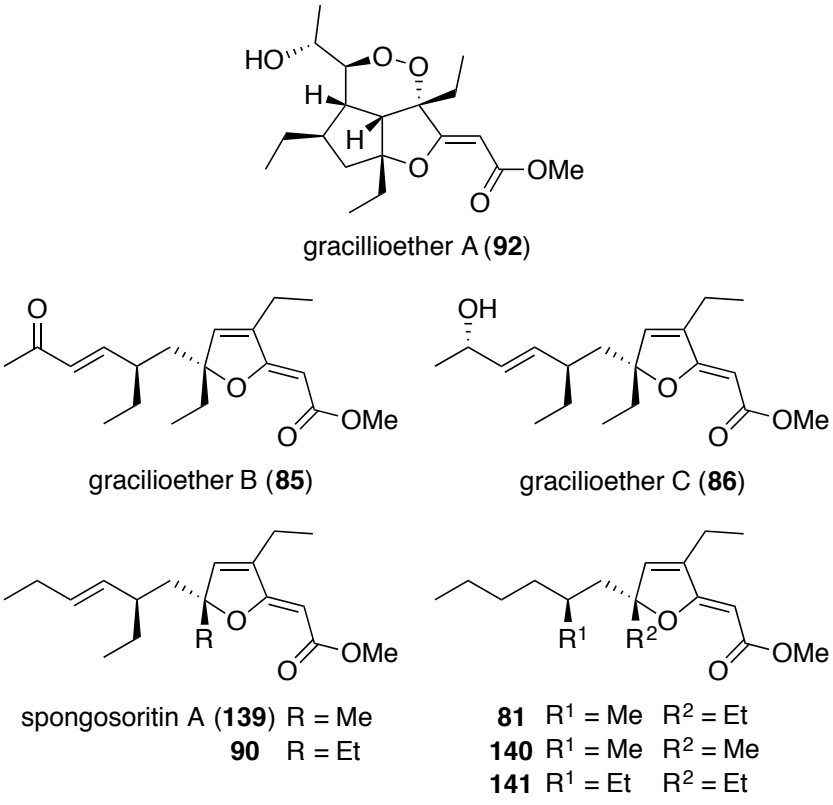

Figure 3.1: Polyketide secondary metabolites containing the furanylidene core structure.

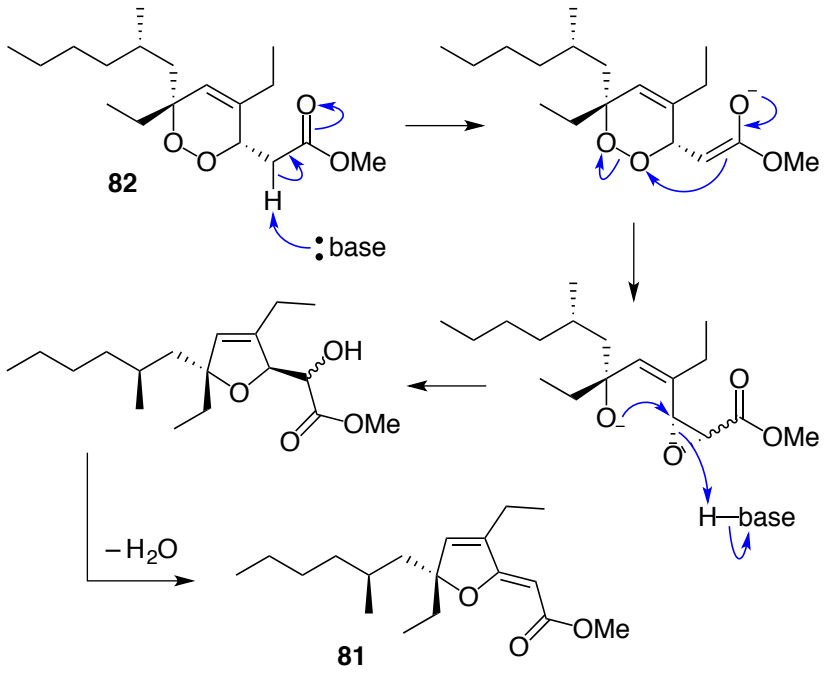

Scheme 3.2: Faulkner's hypothesis of base-catalysed rearrangement of peroxide **82** to furanylidene **81**.

3.3 Results and Discussion

Based on the elegant work of Snider,[11,12] which showed a stereochemical dependence for the base-catalysed cleavage of unsaturated peroxyketals, we propose an alternative pathway for the formation of furanylidene **81**. Peroxide **82** was reported to have a *syn*-relationship of the larger alkyl substituent on C6 and alkyl group on C3. Thus the conformation of **82** in which the larger of the two C6 alkyl groups is pseudoequatorial places the C3 aliphatic dioxane hydrogen in a pseudoequatorial position. This hydrogen is then antiperiplanar to the adjacent peroxide bond facilitating Kornblum–DeLaMare rearrangement[13] analogous to that reported by Snider,[11] as shown in Scheme 3.3. We therefore propose β-ketoester **84** as an alternative intermediate in the formation of furanylidene **81** from peroxide **82**. Furthermore, we envisage that this linear adduct could be a viable intermediate in developing concise chemical syntheses of furanylidene-containing natural products including gracilioethers A–C and spongosoritin A.

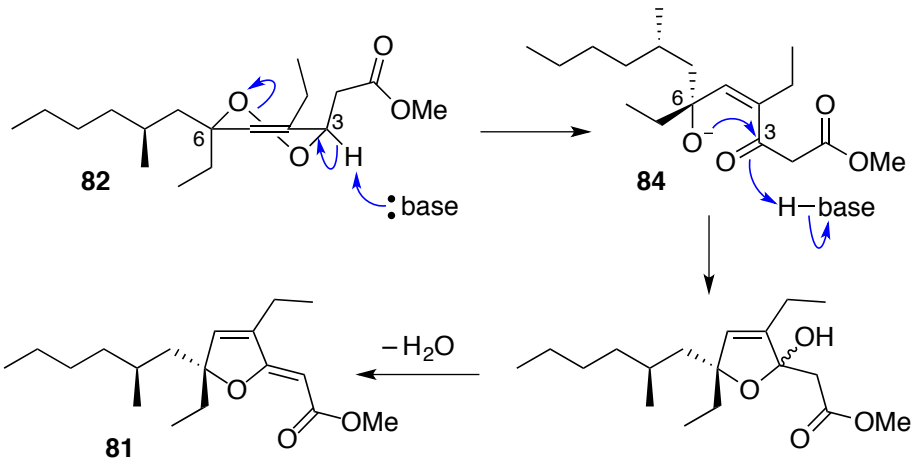

Scheme 3.3: Suggested rearrangement of peroxide **82** to furanylidene **81** via β-ketoester intermediate **84**.

With the aim of developing an efficient method for total synthesis, we proposed a model system to demonstrate the cyclisation and dehydration of a suitable β-ketoester intermediate (Scheme 3.4). We envisaged that furanylidene **142** could be accessed by acid-mediated cyclisation and double dehydration of β-ketoester **143**, a hydrated congener of **84**. This in turn, may be produced in a lithium aldol reaction of the corresponding α-hydroxy aldehyde and β-ketoester fragments **144** and **145**, respectively. The required aldehyde could be crafted in a number of steps from commercially available olefin **146**, which we used as the starting material in our synthesis.

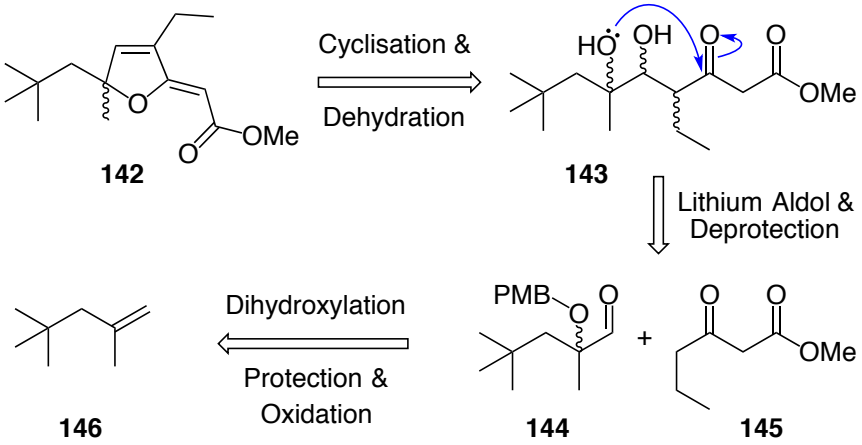

Scheme 3.4: Retrosynthetic analysis of a model furanylidene structure.

To investigate the scope of the cyclisation cascade we began from olefins **146** and **147**. Diols **148** and **149** were thus obtained in excellent to moderate yield by the

epoxidation and acid-mediated ring opening of olefins **146** and **147**, respectively (Scheme 3.5).[14] Selective protection of the hindered tertiary alcohol was achieved in a two step procedure by the condensation of anisaldehyde dimethyl acetal, to give the corresponding acetals of **148** and **149**, followed by reduction with DIBAL.[15] Swern oxidation established aldehydes **144** and **152**, which were then subject to an aldol reaction with the sodio-lithio dianion enolate of methyl 3-oxohexanoate (**145**) and/or methyl acetoacetate.[16] After some optimisation of our original method, we were able to obtain the full carbon structure of model precursors **153–155** in good yields, under the conditions specified in Scheme 3.5.

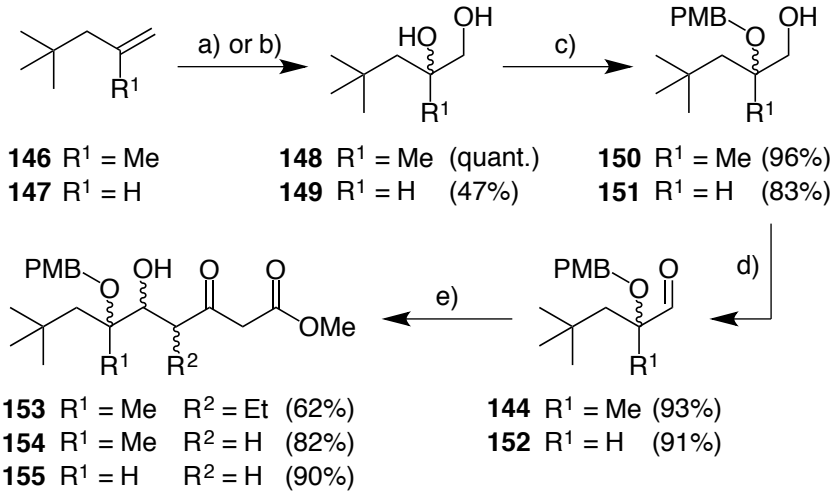

146 R^1 = Me
147 R^1 = H

148 R^1 = Me (quant.)
149 R^1 = H (47%)

150 R^1 = Me (96%)
151 R^1 = H (83%)

153 R^1 = Me R^2 = Et (62%)
154 R^1 = Me R^2 = H (82%)
155 R^1 = H R^2 = H (90%)

144 R^1 = Me (93%)
152 R^1 = H (91%)

Scheme 3.5: Synthesis of model precursors **153–155**. a) *m*CPBA, H_2O, r.t., 5 h, then H_2SO_4, r.t., 15 h (for **146**); or b) *m*CPBA, CH_2Cl_2, 30 °C, 24 h, then H_2SO_4, H_2O, THF, 55 °C, 24 h (for **147**); c) $PMPCH(OMe)_2$, TFA, CH_2Cl_2, r.t., 24 h; then DIBAL, CH_2Cl_2, 0 °C, 2 h; d) $(COCl)_2$, DMSO, CH_2Cl_2, –78 °C, 30 min, then Et_3N, –78 °C, 20 min; e) methyl 3-oxohexanoate (**145**) (treated with NaH and ^{n}BuLi), THF, 0 °C to 40 °C, 24 h; or methyl acetoacetate (treated with NaH and ^{n}BuLi), THF, –78 °C to r.t., 3 h.

Attempted oxidation of compounds **153–155** with DDQ in a biphasic mixture of CH_2Cl_2 and H_2O failed to affect removal of the PMB group. Rather, oxidation with internal capture of the neighbouring secondary hydroxyl to the PMB group yielded the corresponding 1,3-dioxolanes of compounds **153–155**. In the most efficient method found, these crude intermediates were not purified and simply treated with TFA in CH_2Cl_2 for 48 h. This allowed hydrolysis and concomitant cyclisation/double dehydration (Scheme 3.6). Gratifyingly, the reaction of precursor **153** yielded the

desired (2*Z*) furanylidene isomer **142** in 86% over two steps and >9:1 dr, as determined by ^{1}H NMR. The (*Z*)-geometry about the exocyclic olefin was evidenced by a strong NOE enhancement for the C2 alkenyl proton and methylene protons of the ethyl substituent at C3' on the furanylidene (Figure 3.2). This observation was also reported by Capon[5] in elucidating the (2*Z*)-geometry of spongosoritin A.

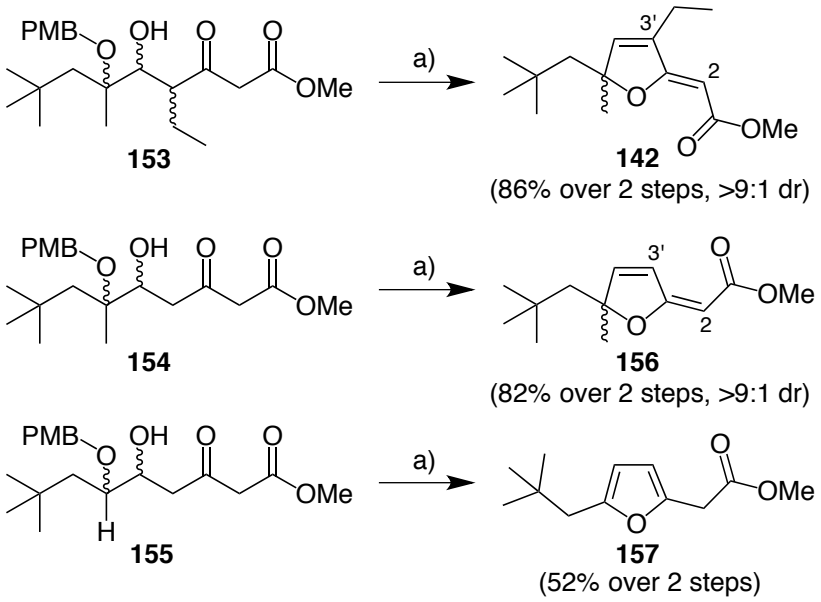

Scheme 3.6: Cyclisation/double dehydration cascade of protected model precursors **153**–**155**. a) DDQ, pH 7 phosphate buffer, CH_2Cl_2, r.t., 3 h or 7 days (for **155**), then TFA, CH_2Cl_2, r.t., 48 h.

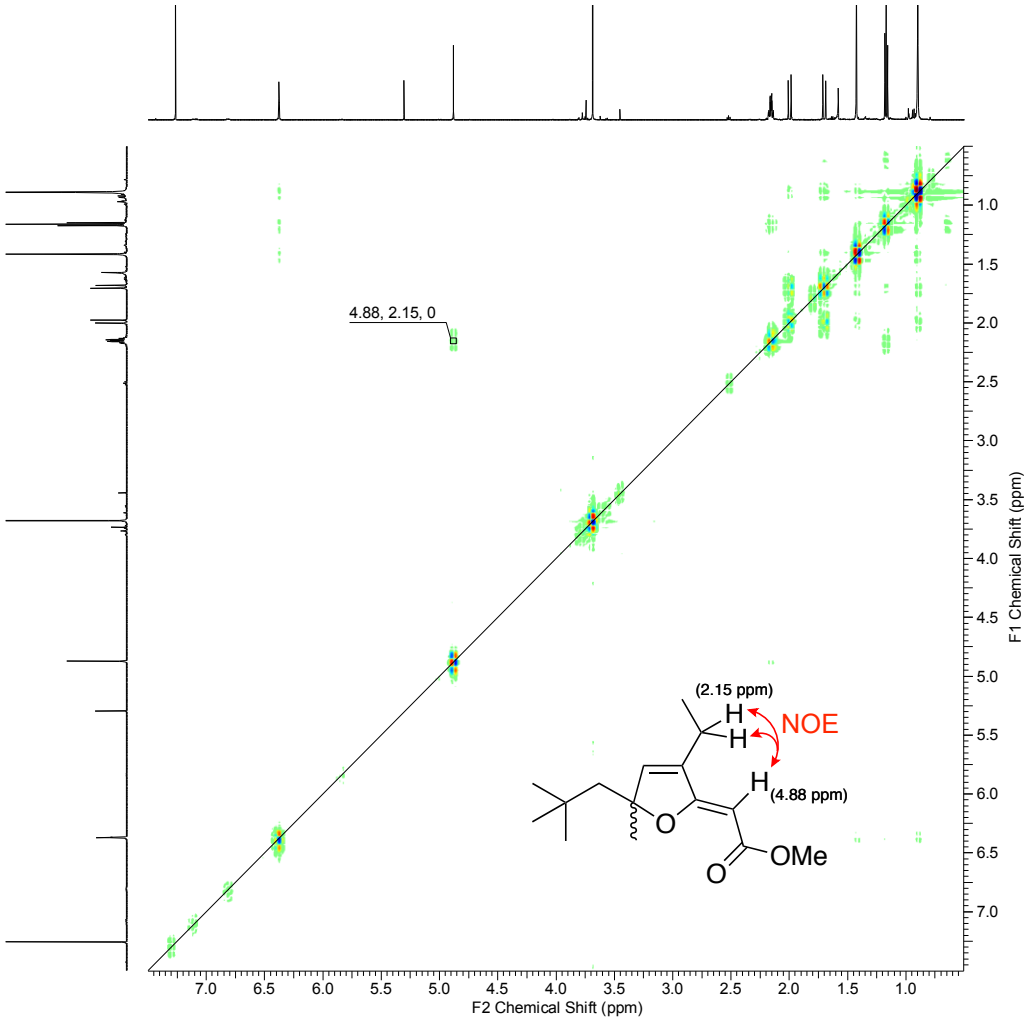

Figure 3.2: NOESY spectrum of furanylidene **142** with 1D ^{1}H NMR (600 MHz, $CDCl_3$) projections as evidence of the depicted stereochemical relationship.

Reaction of precursor **154** also gave the furanylidene core structure in excellent yield, but with >9:1 dr for (2*E*) isomer **156**. No NOE enhancement was observed for the C2 and C3' alkenyl protons of **156** and all relevant ^{1}H resonances closely matched those observed for the minor (2*E*) isomer formed in the preparation of **154**. The (2*Z*) isomer of compound **156** was found as a minor product in the reaction of **154** and similarly, all relevant ^{1}H resonances closely matched those of (2*Z*) isomer **142**. Interestingly, DDQ treatment and acidic hydrolysis of precursor **155** led exclusively to the formation of furan **157**, a structural motif present in the glanvillic acids.[17] This result shows that our synthetic approach is amenable to the synthesis of related aromatic furan structures and that these might also arise via β-ketoester intermediates rather than the proposed[17] epoxide.

We rationalise this substrate dependence on product formation by the reaction pathways outlined in Scheme 3.7. Initial cyclisation and loss of the hemiketal hydroxyl gives the stable alkyloxonium cation **158**. Deprotonation then yields olefins **159** and **160**, which exist in equilibrium via the oxonium intermediate **158**. While the formation of unsaturated ester **159** would be expected to be thermodynamically favoured, olefin **160** facilitates formation of the highly stabilised allylic oxonium cation **161**. When R^1 = H, loss of this proton from **161** (R^1, R^2 = H) gives aromatic furan **157** as the thermodynamic product but when R^1 = Me the 'furanylidene' structural motif forms. Under the acidic reaction conditions, it is expected that (2*Z*) and (2*E*) furanylidene isomers exist in equilibrium via cation **161**. When R^2 = Et steric hindrance favours formation of (2*Z*) isomer **142** (>9:1 dr) and when the steric bulk is decreased (R^2 = H) the equilibration favours the (2*E*) isomer **156** (>9:1 dr). Thus, selective formation of compounds **142**, **156** and **157** demonstrates the relative thermodynamic stability of these systems given their respective R^1 and R^2 substituents.

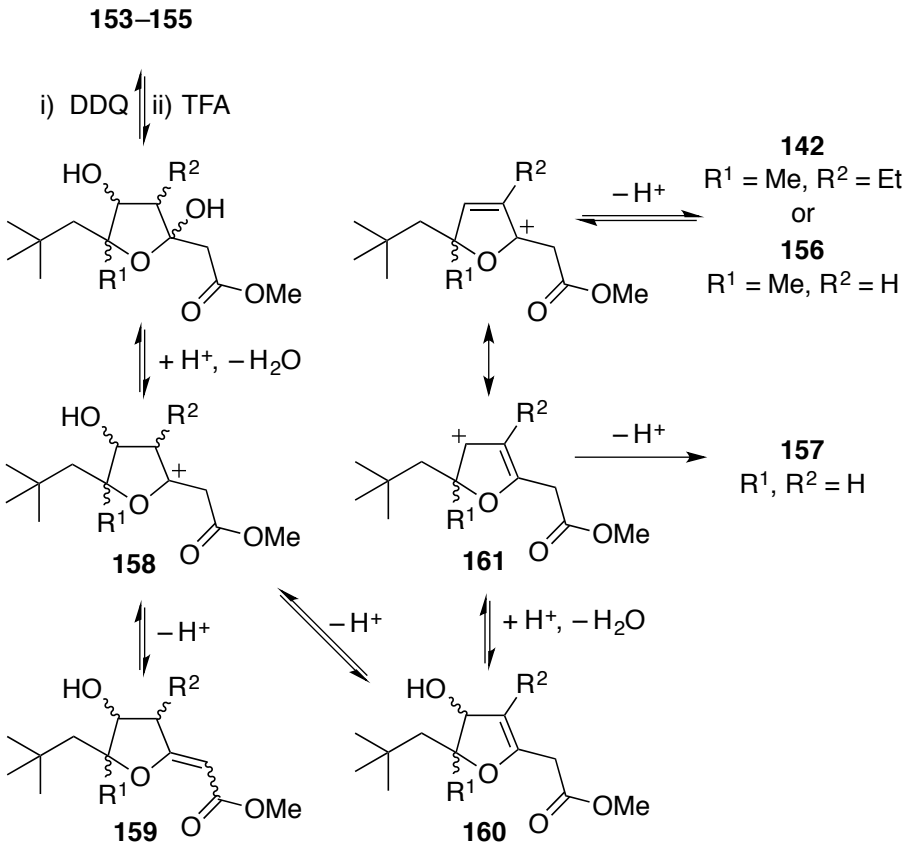

Scheme 3.7: Suggested reaction pathways for the acid-mediated cyclisation/double dehydration of precursors **153**–**155**.

3.4 Concluding remarks

Compounds **153–155** were constructed to model a suspected biosynthetic intermediate in the formation of polyketide secondary metabolites bearing the furanylidene core. Deprotection of the C6 hydroxyl of **153** by DDQ oxidation and acidic hydrolysis occurred with concomitant cyclisation/double dehydration to furnish desired (2*Z*) furanylidene **142** in excellent yield (86%) and >9:1 dr. We are currently investigating this facile synthetic approach with the aim to develop an efficient method for total synthesis of gracilioethers A (**92**), B (**85**) and C (**86**). Further results will be reported in due course.

3.5 Preparative procedures and analytical data

3.5.1 General experimental details

All reactions without water as a solvent were carried out under an atmosphere of nitrogen in flame-dried glassware. CH_2Cl_2 and Et_3N were distilled over CaH_2; and THF and Et_2O were distilled over sodium and benzophenone. All other solvents were used as commercial reagent grade. Analytical thin layer chromatography was performed on Merck Keiselgel $60F_{254}$ silica aluminium backed sheets, monitored by an UV lamp and developed in potassium permanganate. Column chromatography was performed on Merck Keiselgel (particle size: 0.040–0.063 mm) 230–400 mesh silica or Silicycle SiliaFlash P60 silica gel (60 Å pore size, 40–63 μm particle size, 230–400 mesh) treated with pH 7 phosphate buffer (0.94 g KH_2PO_3 and 3.27 g $Na_2HPO_3.7H_2O$ in 100 mL H_2O per 1000 g silica). Electrospray Ionisation (ESI) mass spectra were recorded using a Waters Synapt HDMS or LC/MS equipped with a time-of-flight mass analyser and data is reported as the observed molecular ion. Infrared spectra were recorded on an FTIR spectrometer with the absorptions reported in wavenumbers (cm^{-1}). Melting points were recorded on a Barloworld melting point apparatus.

^1H NMR spectra were recorded at 400 MHz, 500 MHz or 600 MHz and ^{13}C NMR spectra at 100 MHz, 125 MHz or 150 MHz on Bruker NMR Spectrometers. Where $CDCl_3$ is used as the solvent and internal lock, spectra are referenced to residual $CHCl_3$ (δ_H 7.26) for ^1H NMR and $CDCl_3$ (δ_C 77.0) for ^{13}C NMR. Where CD_3OD is used as the solvent and internal lock, spectra are referenced to residual CD_3OH (δ_H 3.30) for

^{1}H NMR and CD_3OD (δ_C 49.0) for ^{13}C NMR. Where C_6D_6 is used as the solvent and internal lock, spectra are referenced to residual C_6D_6 (δ_C 128.0) for ^{13}C NMR. Chemical shift values are reported in parts per million and coupling constants are reported in hertz (Hz). ^{1}H multiplicity, as observed in 1D ^{1}H NMR spectra, is reported using the abbreviations s = singlet, d = doublet, t = triplet, q = quartet, p = pentet, m = multiplet. Structural and stereochemical assignments, where required, were made using COSY, HSQC, HMBC and NOESY 2D NMR experiments.

*3.5.2 2,4,4-Trimethylpentan-1,2-diol (**148**)*

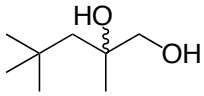

To a rapidly stirred suspension of 2,4,4-trimethylpent-1-ene (2.00 g, 17.8 mmol) and distilled water (70 mL) at room temperature was added *m*CPBA (6.35 g, 50–60%, 22.9 mmol) in small portions. The mixture was stirred at room temperature for 5 h before adding H_2SO_4 (1.8 mL, 3.0 M aq). After a further 15 h stirring solid NaOH was added until solution was achieved. The aqueous mix was saturated with NaCl and extracted with EtOAc. The combined extracts were washed with $Na_2S_2O_5$ (satd aq), brine, dried (Na_2SO_4) and concentrated *in vacuo*. Purification by column chromatography yielded the *title compound* (2.60 g, quant.) as white crystals: mp 59–60 °C; R_f (40% Et_2O/CH_2Cl_2) 0.25; ν_{max} (thin film) 3385, 2953, 1473, 1366, 1302, 1249, 1199, 1107, 1049, 948, 913, 883 cm^{-1}; δ_H (600 MHz, $CDCl_3$) 3.46 (1H, d, *J* 10.8 Hz, C*H*$_A$H$_B$OH), 3.36 (1H, d, *J* 10.8 Hz, CH$_A$*H*$_B$OH), 2.19 (2H, s, O*H*), 1.54 (1H, d, *J* 14.8 Hz, (CH$_3$)$_3$CC*H*$_A$H$_B$), 1.43 (1H, d, *J* 14.8 Hz, (CH$_3$)$_3$CCH$_A$*H*$_B$), 1.29 (3H, s, C(OH)C*H*$_3$), 1.04 (9H, s, (C*H*$_3$)$_3$); δ_C (150 MHz, $CDCl_3$) 74.3, 71.3, 50.6, 31.5, 31.1, 24.8; HRMS (ESI): MNa^+, found 169.1207. $C_8H_{18}NaO_2^+$ requires 169.1204.

*3.5.3 4,4-Dimethylpentan-1,2-diol (**149**)*

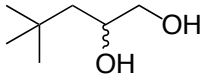

To a stirred solution of 4,4-dimethylpent-1-ene (1.50 mL, 10.4 mmol) in CH_2Cl_2 (20 mL) at room temperature was added *m*CPBA (3.20 g, 50–60%, 11.5 mmol) in small portions. The mixture was stirred at 30 °C for 24 h before careful concentration *in vacuo*. The crude residue was diluted in THF (5 mL) and stirred at room temperature for

the addition of H_2SO_4 (0.35 mL, 3.0 M aq) before heating at 55 °C for a further 24 h. Once cooled to room temperature, Et_2O (40 mL) followed by $Na_2S_2O_5$ (1.0 g, 5.3 mmol) and $NaHCO_3$ (1.7 g, 20 mmol) were added in small portions. The mixture was stirred at 45 °C for another 2 h before the addition of Na_2SO_4 (2.0 g). All solids were filtered (washing with excess Et_2O) and the resulting solution was concentrated onto a small quantity of silica (for column chromatography) *in vacuo*. Purification by column chromatography yielded the *title compound* (0.65 g, 47%) as a volatile colourless oil: R_f (50% Et_2O/CH_2Cl_2) 0.21; ν_{max} (thin film) 3377, 2953, 1468, 1365, 1249, 1199, 1087, 1042, 1013, 912, 879, 847 cm^{-1}; δ_H (600 MHz, $CDCl_3$) 4.24 (1H, s, O*H*), 3.86 (1H, s, O*H*), 3.77–3.73 (1H, m, C*H*OH), 3.46 (1H, dd, *J* 11.3, 3.0 Hz, C$H_A$$H_B$OH), 3.30 (1H, dd, *J* 11.3, 8.5 Hz, $CH_A$$H_B$OH), 1.29 (1H, dd, *J* 14.5, 7.7 Hz, $(CH_3)_3CCH_A$$H_B$), 1.16 (1H, dd, *J* 14.5, 3.0 Hz, $(CH_3)_3CCH_A$$H_B$), 0.91 (9H, s, $(CH_3)_3$); δ_C (150 MHz, $CDCl_3$) 69.7, 67.8, 46.3, 29.9 (two overlapping peaks).

*3.5.4 2-[(4-Methoxybenzyl)oxy]-2,4,4-trimethylpentan-1-ol (**150**)*

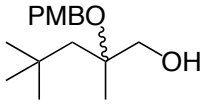

To a stirred solution of **148** (4.70 g, 32.1 mmol) in CH_2Cl_2 (200 mL) at room temperature was added anisaldehyde dimethylacetal (8.60 mL, 50.5 mmol) and TFA (0.50 mL, 6.5 mmol). The mixture was stirred at room temperature for 24 h before diluting with CH_2Cl_2 (100 mL) and quenching with the addition of $NaHCO_3$ (satd aq). The organic layer was separated and aqueous extracted with CH_2Cl_2. The combined extracts were washed with brine, dried (Na_2SO_4) and concentrated *in vacuo*. Flash chromatography to remove excess anisaldehyde yielded the acetal congener of **148** (4-(2,2-dimethylpropyl)-2-(4-methoxyphenyl)-4-methyl-1,3-dioxolane) as an inseparable 1:1 mixture of stereoisomers: R_f (10% EtOAc/hexanes) 0.32; ν_{max} (thin film) 2955, 2838, 1615, 1517, 1467, 1394, 1303, 1249, 1170, 1074, 1035, 989, 933, 896, 830 cm^{-1}; δ_H (400 MHz, $CDCl_3$) 7.42 (2H, dt, *J* 8.7, 2.4 Hz), 6.91 (2H, dt, *J* 8.7, 2.4 Hz), 5.86 (0.5H, s), 5.82 (0.5H, s), 3.87 (0.5H, d, *J* 7.7 Hz), 3.86 (0.5H, d, *J* 7.7 Hz), 3.81 (3H, s), 3.78 (0.5H, d, *J* 7.9 Hz), 3.73 (0.5H, d, *J* 7.9 Hz), 1.85 (0.5H, d, *J* 14.5 Hz), 1.83 (0.5H, d, *J* 14.5 Hz), 1.70 (0.5H, d, *J* 14.5 Hz), 1.62 (0.5H, d, *J* 14.5 Hz), 1.48 (1.5H, s), 1.46 (1.5H, s), 1.06 (4.5H, s), 1.04 (4.5H, s); δ_C (100 MHz, $CDCl_3$) 160.3, 160.2, 131.9, 130.6, 128.0 (two overlapping peaks), 113.7, 113.6, 103.2, 102.0, 82.4, 82.2, 78.2, 76.9,

55.2 (two overlapping peaks), 52.5, 51.3, 31.3 (two peaks), 31.0, 30.9, 26.6, 24.3. The crude residue was diluted in CH_2Cl_2 (250 mL) and stirred at 0 °C for the addition of DIBAL (73.0 mL, 1.0 M in PhMe, 73.0 mmol). The mixture was stirred at 0 °C for 2 h before diluting with CH_2Cl_2 and quenching with the addition of HCl (3.0 M aq). The organic layer was separated and aqueous extracted with CH_2Cl_2. The combined extracts were washed with brine, dried (Na_2SO_4), passed through a small pad of silica (washing with excess CH_2Cl_2) and concentrated *in vacuo* to yield the *title compound* (8.21 g, 96% over 2 steps) as a colourless oil: R_f (10% Et_2O/CH_2Cl_2) 0.35; ν_{max} (thin film) 3446, 2952, 2836, 1613, 1587, 1514, 1465, 1381, 1365, 1302, 1248, 1173, 1108, 1039, 823 cm^{-1}; δ_H (600 MHz, $CDCl_3$) 7.26 (2H, d, *J* 8.7 Hz, Ar*H*), 6.88 (2H, d, *J* 8.7 Hz, Ar*H*), 4.40 (1H, d, *J* 10.6 Hz, C*H*$_a$H$_b$Ar), 4.35 (1H, d, *J* 10.6 Hz, CH$_a$*H*$_b$Ar), 3.80 (3H, s, OC*H*$_3$), 3.57 (1H, d, *J* 11.3 Hz, C*H*$_a$H$_b$OH), 3.52 (1H, d, *J* 11.3 Hz, CH$_a$*H*$_b$OH), 1.92 (1H, s, O*H*), 1.72 (1H, d, *J* 14.9 Hz, (CH$_3$)$_3$CC*H*$_A$H$_B$), 1.52 (1H, d, *J* 14.9 Hz, (CH$_3$)$_3$CCH$_A$*H*$_B$), 1.35 (3H, s, C(OPMB)C*H*$_3$), 1.04 (9H, s, (C*H*$_3$)$_3$); δ_C (150 MHz, $CDCl_3$) 158.9, 131.1, 129.0, 113.8, 78.9, 68.2, 63.1, 55.2, 47.6, 31.6, 30.9, 21.6; HRMS (ESI): MNa^+, found 289.1785. $C_{16}H_{26}NaO_3^+$ requires 289.1780.

*3.5.5 2-[(4-Methoxybenzyl)oxy]-4,4-dimethylpentan-1-ol (**151**)*

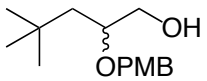

Compound **149** (0.58 g, 4.4 mmol) was subject to the same procedure as **148** (in the synthesis of **150**) on a 4.4 mmol scale to firstly produce the acetal congener of **149** (4-(2,2-dimethylpropyl)-2-(4-methoxyphenyl)-1,3-dioxolane) as an inseparable 3:2 mixture of stereoisomers: R_f (15% EtOAc/hexanes) 0.41; δ_H (400 MHz, $CDCl_3$) 7.40 (2H, dt, *J* 9.5, 2.5 Hz), 6.90 (2H, dt, *J* 9.5, 2.5 Hz), 5.87 (0.4H, s), 5.75 (0.6H, s), 4.32–4.24 (1.4H, m), 4.11 (0.6H, t, *J* 7.0 Hz), 3.81 (3H, s), 3.57 (0.6H, t, *J* 7.5 Hz), 3.53 (0.4H, t, *J* 7.0 Hz), 1.79 (0.6H, dd, *J* 14.2, 6.5 Hz), 1.75 (0.4H, dd, *J* 14.3, 7.0 Hz), 1.52 (0.6H, dd, *J* 4.2, 5.5 Hz), 1.41 (0.4H, dd, *J* 14.3, 4.7 Hz), 0.98 (9H, s); δ_C (100 MHz, $CDCl_3$) 160.3, 160.1, 130.9, 130.3, 128.0, 127.7, 113.7 (two peaks), 103.5, 102.7, 75.2, 74.0, 71.9, 71.1, 55.3 (two overlapping peaks), 47.0, 46.9, 30.0 (four peaks); n_{max} (thin film) 2955, 2837, 1615, 1517, 1466, 1366, 1303, 1249, 1170, 1079, 1035, 969, 827; then finally yield the *title compound* (0.92 g, 83% over 2 steps) as a colourless oil: R_f (CH_2Cl_2) 0.20; ν_{max} (thin film) 3433, 2954, 2837, 1613, 1587, 1514, 1466, 1365, 1365,

1302, 1249, 1174, 1038, 822 cm^{-1}; δ_H (600 MHz, $CDCl_3$) 7.27 (2H, dt, *J* 9.5, 2.5 Hz, Ar*H*), 6.88 (2H, dt, *J* 9.5, 2.5 Hz, Ar*H*), 4.52 (1H, d, *J* 10.9 Hz, CH_AH$_B$Ar), 4.44 (1H, d, *J* 10.9 Hz, CH$_A$$H_B$Ar), 3.80 (3H, s, OC$H_3$), 3.72 (1H, dd, *J* 11.5, 3.5 Hz, CH_AH$_B$OH), 3.59–3.55 (1H, m, C*H*OPMB), 3.48 (1H, dd, *J* 11.5, 6.0 Hz, CH$_A$$H_B$OH), 1.86 (1H, s, O*H*), 1.60 (1H, dd, *J* 14.7, 5.4 Hz, $(CH_3)_3$CCH_AH$_B$), 1.35 (1H, dd, *J* 14.7, 9.5 Hz, $(CH_3)_3$CCH$_A$$H_B$), 0.95 (9H, s, $(CH_3)_3$); δ_C (150 MHz, $CDCl_3$) 159.2, 130.4, 129.4, 113.9, 77.3, 70.6, 65.7, 55.3, 45.0, 30.0, 29.8; HRMS (ESI): MNa^+, found 275.1626. $C_{15}H_{24}NaO_3^+$ requires 275.1623.

*3.5.6 2-[(4-Methoxybenzyl)oxy]-2,4,4-trimethylpentanal (**144**)*

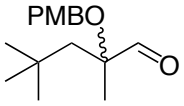

To a stirred solution of DMSO (2.0 mL, 29 mmol) in CH_2Cl_2 (70 mL) at –78 °C was added $(COCl)_2$ (7.4 mL, 2.0 M in CH_2Cl_2, 15 mmol). The mixture was stirred at –78 °C for 20 min before the addition of **150** (2.51 g, 9.4 mmol) in CH_2Cl_2 (50 mL), followed by Et_3N (8.0 mL, 57.4 mmol) after another 30 min. Once warmed (20 min) to room temperature, the reaction was quenched with the addition of NH_4Cl (satd aq). The organic layer was separated and aqueous extracted with CH_2Cl_2. The combined extracts were dried (Na_2SO_4) and concentrated *in vacuo*. Purification by column chromatography (CH_2Cl_2) yielded the *title compound* (2.31 g, 93%) as a colourless oil: R_f (CH_2Cl_2) 0.65; ν_{max} (thin film) 2954, 2837, 1734, 1614, 1515, 1466, 1365, 1302, 1248, 1173, 1107, 1036, 823 cm^{-1}; δ_H (600 MHz, $CDCl_3$) 9.80 (1H, s, C*H*O), 7.30 (2H, d, *J* 8.6 Hz, Ar*H*), 6.88 (2H, d, *J* 8.6 Hz, Ar*H*), 4.48 (1H, d, *J* 10.9 Hz, CH_AH$_B$Ar), 4.43 (1H, d, *J* 10.9 Hz, CH$_A$$H_B$Ar), 3.80 (3H, s, OC$H_3$), 1.76 (2H, dd, *J* 17.9, 14.9 Hz, $(CH_3)_3$CCH_2), 1.38 (3H, s, C(OPMB)CH_3), 0.98 (9H, s, $(CH_3)_3$); δ_C (150 MHz, $CDCl_3$) 206.1, 159.0, 130.6, 128.7, 113.7, 83.9, 65.5, 55.2, 50.1, 31.5, 31.1, 20.7; HRMS (ESI): MNa^+, found 287.1623. $C_{16}H_{24}NaO_3^+$ requires 287.1623.

*3.5.7 2-[(4-Methoxybenzyl)oxy]-4,4-dimethylpentanal (**152**)*

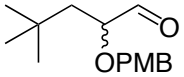

Compound **151** (0.89 g, 3.5 mmol) was subject to the same procedure as **150** (in the synthesis of **144**) on a 3.5 mmol scale to yield the *title compound* (0.80 g, 91%) as a

colourless oil: R_f (CH_2Cl_2) 0.48; ν_{max} (thin film) 2956, 2867, 2837, 1732, 1613, 1586, 1515, 1466, 1395, 1303, 1250, 1175, 1110, 1036, 822 cm^{-1}; δ_H (600 MHz, $CDCl_3$) 9.59 (1H, d, *J* 2.5 Hz, C*H*O), 7.28 (2H, dt, *J* 9.5, 2.5 Hz, Ar*H*), 6.89 (2H, dt, *J* 9.5, 2.5 Hz, Ar*H*), 4.55 (1H, d, *J* 11.0 Hz, CH_AH_BAr), 4.44 (1H, d, *J* 11.0 Hz, CH_AH_BAr), 3.83 (1H, ddd, *J* 8.3, 3.4, 2.5 Hz, C*H*OPMB), 3.81 (3H, s, OCH_3), 1.57 (1H, dd, *J* 14.6, 8.3 Hz, $(CH_3)_3CCH_AH_B$), 1.50 (1H, dd, *J* 14.6, 3.4 Hz, $(CH_3)_3CCH_AH_B$), 0.96 (9H, s, $(CH_3)_3$); δ_C (150 MHz, $CDCl_3$) 203.9, 159.5, 129.9, 129.3, 113.9, 82.0, 72.1, 55.3, 43.1, 30.4, 30.0; HRMS (ESI): MNa^+, found 273.1468. $C_{15}H_{22}NaO_3^+$ requires 273.1467.

*3.5.8 Methyl 4-ethyl-5-hydroxy-6-[(4-methoxybenzyl)oxy]-6,8,8-trimethyl-3-oxononanoate (**153**)*

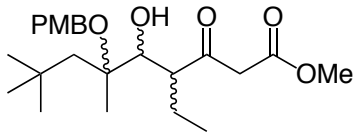

NaH (0.10 g, 60% in mineral oil, 2.4 mmol) was washed with hexane and suspended in THF (4 mL). To the stirred slurry at 0 °C was added methyl acetobutyrate (0.17 g, 1.2 mmol), followed by ^{n}BuLi (0.57 mL, 1.95 M in hexane, 1.1 mmol) after 30 min. The mixture was stirred at 0 °C for a further 30 min before warming to room temperature and transferring the supernatant via cannula to a stirred solution of **144** (0.15 g, 0.6 mmol) in THF (1.5 mL) (care was taken not to transfer excess NaH). The resulting mixture was stirred at 40 °C for 24 h before quenching with the addition of NH_4Cl (satd aq). The organic layer was separated and aqueous extracted with Et_2O. The combined extracts were washed with brine, dried (Na_2SO_4) and concentrated *in vacuo*. Purification by column chromatography yielded the *title compound* (0.15 g, 62%) as a mixture of stereoisomers: R_f (15% EtOAc/hexane) 0.23; ν_{max} (thin film, combined isomers) 3515, 2954, 2875, 2837, 1746, 1702, 1613, 1587, 1515, 1464, 1439, 1383, 1303, 1249, 1174, 1111, 1037, 823 cm^{-1}; δ_H (600 MHz, $CDCl_3$) 7.23 (2H, dt, *J* 8.7, 2.4 Hz, Ar*H*), 6.86 (2H, dt, *J* 8.7, 2.4 Hz, Ar*H*), 4.36 (1H, d, *J* 10.3 Hz, CH_AH_BAr), 4.16 (1H, d, *J* 10.3 Hz, CH_AH_BAr), 3.97–3.95 (1H, m, C*H*OH), 3.80 (3H, s, $ArOCH_3$), 3.66 (3H, s, CO_2CH_3), 3.55 (1H, d, *J* 15.5 Hz, $CH_AH_BCO_2CH_3$), 3.34 (1H, d, *J* 15.5 Hz, $CH_AH_BCO_2CH_3$), 2.88 (1H, ddd, *J* 8.8, 7.5, 4.0 Hz, $CHCH_2CH_3$), 2.26 (1H, d, *J* 6.6 Hz, O*H*), 1.78–1.70 (2H, m, CH_2CH_3), 1.66 (1H, d, *J* 14.6 Hz, $(CH_3)_3CCH_AH_B$), 1.60 (1H, d, *J* 14.6 Hz, $(CH_3)_3CCH_AH_B$), 1.38 (3H, s, $C(OPMB)CH_3$), 1.05 (9H, s, $(CH_3)_3$), 0.88 (3H,

t, *J* 7.5 Hz, CH_2CH_3); δ_C (150 MHz, $CDCl_3$) 204.7, 167.6, 158.9, 130.6, 129.5, 113.6, 80.8, 75.1, 63.3, 55.2, 54.0, 52.1, 49.7, 46.1, 31.8, 30.9, 21.9, 21.7, 11.4. R_f (15% EtOAc/hexane) 0.28; δ_H (600 MHz, $CDCl_3$) 7.17 (2H, d, *J* 8.6 Hz, Ar*H*), 6.85 (2H, d, *J* 8.6 Hz, Ar*H*), 4.41 (1H, d, *J* 10.8 Hz, CH_AH_BAr), 4.30 (1H, d, *J* 10.8 Hz, CH_AH_BAr), 3.79 (3H, s, OCH_3), 3.78 (1H, dd, *J* 8.9, 2.3 Hz, C*H*OH), 3.61 (3H, s, CO_2CH_3), 3.53 (1H, d, *J* 8.9 Hz, O*H*), 3.35 (1H, d, *J* 15.6 Hz, $CH_AH_BCO_2CH_3$), 3.30 (1H, d, *J* 15.6 Hz, $CH_AH_BCO_2CH_3$), 2.79 (1H, td, *J* 7.2, 2.3 Hz, C*H*CH_2CH_3), 1.91 (1H, d, *J* 14.2 Hz, $(CH_3)_3CCH_AH_B$), 1.80 (1H, dq, *J* 14.6, 7.3 Hz, $CH_AH_BCH_3$), 1.72 (1H, dq, *J* 14.6, 7.3 Hz, $CH_AH_BCH_3$), 1.51 (1H, d, *J* 14.2 Hz, $(CH_3)_3CCH_AH_B$), 1.38 (3H, s, C(OPMB)CH_3), 1.02 (9H, s, $(CH_3)_3$), 0.95 (3H, t, *J* 7.3 Hz, CH_2CH_3); δ_C (150 MHz, $CDCl_3$) 207.8, 167.5, 158.8, 130.7, 128.9, 113.7, 80.9, 78.3, 63.3, 55.2, 52.0, 51.8, 50.3, 46.2, 31.7, 30.5, 24.1, 21.8, 12.1. R_f (15% EtOAc/hexane) 0.34; δ_H (600 MHz, $CDCl_3$) 7.19 (2H, d, *J* 8.6 Hz, Ar*H*), 6.85 (2H, d, *J* 8.6 Hz, Ar*H*), 4.40 (1H, d, *J* 10.5 Hz, CH_AH_BAr), 4.29 (1H, d, *J* 10.5 Hz, CH_AH_BAr), 3.79 (3H, s, OCH_3), 3.71 (1H, dd, *J* 7.7, 2.6 Hz, C*H*OH), 3.68 (1H, d, *J* 7.7 Hz, O*H*), 3.63 (3H, s, CO_2CH_3), 3.48 (1H, d, *J* 15.5 Hz, $CH_AH_BCO_2CH_3$), 3.24 (1H, d, *J* 15.5 Hz, $CH_AH_BCO_2CH_3$), 2.94 (1H, td, *J* 7.2, 2.6 Hz, C*H*CH_2CH_3), 1.80 (1H, dq, *J* 14.6, 7.2 Hz, $CH_AH_BCH_3$), 1.72 (1H, d, *J* 14.8 Hz, $(CH_3)_3CCH_AH_B$), 1.67 (1H, dq, *J* 14.6, 7.2 Hz, $CH_AH_BCH_3$), 1.45 (3H, s, C(OPMB)CH_3), 1.40 (1H, d, *J* 14.8 Hz, $(CH_3)_3CCH_AH_B$), 1.03 (9H, s, $(CH_3)_3$), 0.94 (3H, t, *J* 7.2 Hz, CH_2CH_3); δ_C (150 MHz, $CDCl_3$) 208.8, 167.4, 158.9, 130.7, 129.5, 113.6, 81.3, 80.3, 64.5, 55.2, 52.0, 51.3, 50.7, 48.1, 31.8, 31.1, 24.2, 20.8, 12.0; HRMS (ESI, combined isomers): $M(-H)^-$, found 407.2441. $C_{23}H_{35}NaO_6^-$ requires 407.2434.

*3.5.9 Methyl 5-hydroxy-6-[(4-methoxybenzyl)oxy]-6,8,8-trimethyl-3-oxononanoate (**154**)*

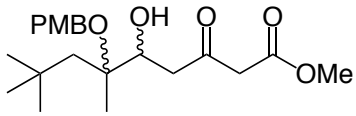

NaH (0.31 g, 60% in mineral oil, 7.6 mmol) was washed with hexane and suspended in THF (20 mL). To the stirred slurry at 0 °C was added methyl acetoacetate (0.37 mL, 3.4 mmol), followed by ^{n}BuLi (1.4 mL, 2.05 M in hexane, 2.8 mmol) after 30 min. The mixture was stirred at 0 °C for a further 30 min before cooling to –78 °C and adding a solution of **144** (0.43 g, 1.6 mmol) in THF (5 mL). After warming to room temperature, stirring continued for 3 h before quenching with the addition of NH_4Cl

(satd aq). The organic layer was separated and aqueous extracted with Et_2O. The combined extracts were washed with brine, dried (Na_2SO_4) and concentrated *in vacuo*. Purification by column chromatography yielded the *title compound* (0.50 g, 82%) as an inseparable 1:1 mixture of stereoisomers: R_f (5% Et_2O/CH_2Cl_2) 0.40; ν_{max} (thin film) 3546, 3055, 2956, 1748, 1716, 1613, 1514, 1438, 1324, 1302, 1266, 1174, 1075, 1035, 896, 824 cm^{-1}; δ_H (600 MHz, $CDCl_3$) 7.22 (2H, d, *J* 8.6 Hz), 6.86 (2H, d, *J* 8.6 Hz), 4.43 (0.5H, d, *J* 10.6 Hz), 4.39 (1H, s), 4.34 (0.5H, d, *J* 10.6 Hz), 4.26 (0.5H, dd, *J* 9.7, 1.7 Hz), 4.24 (0.5H, dd, *J* 7.8, 4.1 Hz), 3.79 (3H, s), 3.72 (1.5H, s), 3.71 (1.5H, s), 3.53–3.52 (2H, m), 2.79–2.68 (2H, m), 2.54 (1H, s), 1.74 (0.5H, d, *J* 14.9 Hz), 1.64 (0.5H, d, *J* 15.1 Hz), 1.49 (0.5H, d, *J* 15.1 Hz), 1.35 (0.5H, d, *J* 14.9 Hz), 1.35 (1.5H, s), 1.33 (1.5H, s), 1.04 (4.5H, s), 1.03 (4.5H, s); δ_C (150 MHz, $CDCl_3$) 203.2, 203.0, 167.5, 158.9, 130.9, 130.8, 129.0, 128.9, 128.8, 128.6, 113.7 (two peaks), 80.0, 79.9, 71.6, 71.3, 63.2 (two peaks), 55.2 (two peaks), 53.4, 52.3, 49.8, 49.7, 45.4, 45.2, 44.8, 44.7, 31.7 (two peaks), 31.1, 31.0, 20.4, 20.3; HRMS (ESI): MNa^+, found 403.2081. $C_{21}H_{32}NaO_6^+$ requires 403.2097.

*3.5.10 Methyl 5-hydroxy-6-[(4-methoxybenzyl)oxy]-8,8-dimethyl-3-oxononanoate (**155**)*

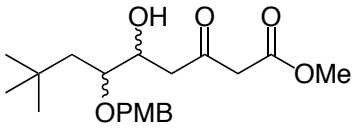

Compound **152** (0.20 g, 0.8 mmol) was subject to the same procedure as **144** (in the synthesis of **154**) on a 0.8 mmol scale to yield the *title compound* (0.27 g, 90%) as an inseparable 3:2 mixture of stereoisomers: R_f (10% Et_2O/CH_2Cl_2) 0.28; ν_{max} (thin film) 3502, 2954, 2868, 1747, 1716, 1613, 1514, 1466, 1438, 1404, 1365, 1324, 1303, 1249, 1174, 1073, 1035, 822 cm^{-1}; δ_H (600 MHz, $CDCl_3$) 7.26 (0.8H, dt, *J* 9.2, 2.5 Hz), 7.23 (1.2H, dt, *J* 9.5, 2.4 Hz), 6.88–6.86 (2H, m), 4.66 (0.4H, d, *J* 10.7 Hz), 4.50 (0.6H, d, *J* 10.7 Hz), 4.48 (0.4H, d, *J* 10.7 Hz), 4.42 (0.6H, d, *J* 10.7 Hz), 4.26–4.22 (1H, m), 3.80 (1.8H, s), 3.80 (1.2H, s), 3.74 (1.2H, s), 3.73 (1.8H, s), 3.59 (0.4H, dt, *J* 7.7, 2.6 Hz), 3.54 (0.4H, d, *J* 15.8 Hz), 3.51 (0.6H, dd, *J* 7.0, 3.5 Hz), 3.50 (0.4H, d, *J* 15.8 Hz), 3.47 (0.6H, d, *J* 15.8 Hz), 3.44 (0.6H, d, *J* 15.8 Hz), 2.85 (0.4H, dd, *J* 17.2, 9.0 Hz), 2.80 (0.6H, dd, *J* 17.2, 3.3 Hz), 2.68 (0.6H, dd, *J* 17.2, 9.0 Hz), 2.64 (0.4H, dd, *J* 17.2, 3.3 Hz), 2.61 (1H, s), 1.62 (0.6H, dd, *J* 14.5, 3.5 Hz), 1.45 (0.4H, dd, *J* 14.8, 7.7 Hz), 1.36 (0.6H, dd, *J* 14.5, 7.0 Hz), 1.23 (0.4H, dd, *J* 14.8, 2.6 Hz), 0.97 (5.4H, s), 0.94 (3.6H, s); δ_C (150 MHz, $CDCl_3$) 203.4, 203.3, 167.4, 159.2 (two peaks), 130.5, 130.2, 129.6,

129.5, 128.6, 113.9, 113.8 (two peaks), 79.4, 77.7, 71.7, 71.2, 70.7, 68.1, 55.3, 52.4 (two peaks), 49.8, 49.6, 45.4, 44.4, 44.1, 42.8, 30.1 (two peaks), 30.0, 29.9; HRMS (ESI): MNa^+, found 389.1930. $C_{20}H_{30}NaO_6^+$ requires 389.1940.

*3.5.11 Methyl (2Z)-[5-(2,2-dimethylpropyl)-3-ethyl-5-methyl-2(5H)-furanylidene] ethanoate (**142**)*

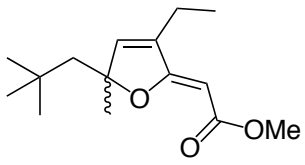

To a rapidly stirred suspension of **153** (0.14 g, 0.4 mmol), CH_2Cl_2 (10 mL) and pH 7 phosphate buffer solution (2.0 mL) at room temperature was added DDQ (0.11 g, 0.5 mmol). The mixture was stirred at room temperature for 3 h before diluting with CH_2Cl_2 and quenching with the addition of $NaHCO_3$ (satd aq). The organic layer was separated and aqueous extracted with CH_2Cl_2. The combined extracts were washed with brine, dried (Na_2SO_4), filtered through a small pad of buffered silica (washing with excess Et_2O) and concentrated *in vacuo* to give the acetal congener of **153** (methyl 4-[5-(2,2-dimethylpropyl)-2-(4-methoxyphenyl)-5-methyl-1,3-dioxolan-4-yl]-3-oxohex-anoate) as a complicated mixture of isomers. The crude acetal was diluted with CH_2Cl_2 (10 mL) and stirred at room temperature for the addition of TFA (0.05 mL, 0.3 mmol). The mixture was stirred at room temperature for 48 h before quenching with the addition of $NaHCO_3$ (satd aq). The organic layer was separated and aqueous extracted with CH_2Cl_2. The combined extracts were washed with brine, dried (Na_2SO_4) and concentrated *in vacuo*. Purification by column chromatography yielded the *title compound* (0.076 g, 86% over 2 steps) as a yellow oil: R_f (CH_2Cl_2) 0.35; ν_{max} (thin film) 2952, 1714, 1685, 1627, 1435, 1364, 1271, 1169, 1144, 1062, 975, 895, 849, 805 cm^{-1}; δ_H (400 MHz, $CDCl_3$) 6.37 (1H, s, C*H*=CCH_2CH_3), 4.88 (1H, s, C*H*CO_2CH_3), 3.68 (3H, s, OC*H*$_3$), 2.15 (2H, q, *J* 7.4 Hz, C*H*$_2$$CH_3$), 1.99 (1H, d, *J* 15.0 Hz, $(CH_3)_3CCH_AH_B$), 1.70 (1H, d, *J* 15.0 Hz, $(CH_3)_3CCH_AH_B$), 1.42 (3H, s, CC*H*$_3$), 1.16 (3H, t, *J* 7.4 Hz, CH_2CH_3), 0.90 (9H, s, (C*H*$_3$)$_3$), peaks for minor (2*E*) isomer observed at 6.33 (1H, s, C*H*=C(Et)C=CH) and 5.15 (1H, s, C*H*CO_2CH_3); δ_C (150 MHz, $CDCl_3$) 171.1, 166.9, 142.4, 137.4, 95.4, 84.5, 51.4, 50.5, 31.0, 30.7, 28.2, 18.4, 11.7; HRMS (ESI): MNa^+, found 275.1626. $C_{15}H_{24}NaO_3^+$ requires 275.1623.

*3.5.12 Methyl (2E)-[5-(2,2-dimethylpropyl)-5-methyl-2(5H)-furanylidene]ethanoate (**156**)*

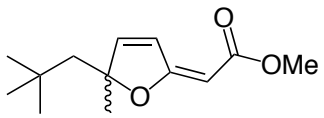

154 (0.26 g, 0.7 mmol) was subject to the same procedure as **153** (in the synthesis of **142**) on a 0.7 mmol scale to yield the *title compound* (0.11 g, 80% over two steps) as a yellow oil: R_f (20% EtOAc/hexane) 0.35; ν_{max} (thin film) 2953, 2872, 1704, 1636, 1575, 1435, 1397, 1301, 1272, 1188, 1115, 1044, 952, 811 cm^{-1}; δ_H (600 MHz, $CDCl_3$) 7.20 (1H, d, *J* 5.9 Hz, C*H*=CHC=CH), 6.76 (1H, d, *J* 5.9 Hz, CH=C*H*C=CH), 5.20 (1H, s, C*H*CO_2CH_3), 3.67 (3H, s, OC*H*$_3$), 1.90 (1H, d, *J* 15.1 Hz, $(CH_3)_3CCH_AH_B$), 1.69 (1H, d, *J* 15.1 Hz, $(CH_3)_3CCH_AH_B$), 1.36 (3H, s, C*H*$_3$), 0.87 (9H, s, $(CH_3)_3$), peaks for minor (2*Z*) isomer observed at 6.69 (1H, d, *J* 5.7 Hz, C*H*=CHC=CH), 6.04 (1H, d, *J* 5.7 Hz, CH=C*H*C=CH) and 4.91 (1H, s, C*H*CO_2CH_3); δ_C (150 MHz, $CDCl_3$) 173.6, 168.7, 149.7, 122.3, 94.6, 87.6, 51.4, 50.7, 31.0, 30.6, 28.1; HRMS (ESI): MNa^+, found 247.1310. $C_{13}H_{20}NaO_3^+$ requires 247.1310.

*3.5.13 Methyl 2-[5-(2,2-dimethylpropyl)furan]ethanoate (**157**)*

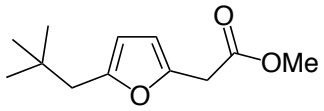

155 (0.40 g, 1.1 mmol) was subject to the same procedure as **153** (in the synthesis of **142**) on a 1.1 mmol scale with 2.0 equivalents of DDQ and 7 days reaction time in the first (oxidation) step to yield the *title compound* (0.12 g, 52% over 2 steps) as a pale yellow oil: R_f (15% EtOAc/hexane) 0.44; ν_{max} (thin film) 2955, 2906, 2868, 1748, 1561, 1476, 1437, 1365, 1341, 1225, 1170, 1014, 975, 913, 789, 734 cm^{-1}; δ_H (600 MHz, $CDCl_3$) 6.10 (1H, d, *J* 3.1 Hz, C*H*=C$CH_2CO_2CH_3$), 5.92 (1H, d, *J* 3.1 Hz, $(CH_3)_3CCH_2C$=C*H*), 3.70 (3H, s, OC*H*$_3$), 3.64 (2H, s, C*H*$_2CO_2CH_3$), 2.45 (2H, s, $(CH_3)_3CCH_2$), 0.91 (9H, s, $(CH_3)_3$); δ_C (150 MHz, $CDCl_3$) 170.1, 154.4, 145.6, 108.4, 107.7, 52.1, 42.1, 34.0, 31.5, 29.3; HRMS (ESI): MNa^+, found 233.1156. $C_{12}H_{18}NaO_3^+$ requires 233.1154.

3.6 Reagent of choice, trifluoroacetic acid

Following the development of this methodology, the candidate prepared a short article highlighting the use of trifluoroacetic acid in organic synthesis, especially as a catalyst for multi-bond forming processes. This article, titled 'Trifluoroacetic acid (TFA),' was published as a 'Spotlight' in the refereed journal *Synlett*, Georg Thieme Verlag on 23 January 2015 (DOI: 10.1055/s-0034-1379995). Although not included in the body of this thesis, the article is available on the publisher's website.

3.7 Chapter summary

The results presented in Chapter 3 contribute to a better understanding of the chemical basis and biosynthetic origin of sponge metabolites with a methyl [2(5*H*)-furanylidene]ethanoate (furanylidene) core structure. New mechanistic insight, obtained from a detailed review of relevant literature, implicated hydroxy β-ketoesters (such as compound **84**) as valuable intermediates for the assembly of these complex heterocyclic frameworks; and a synthetic model was constructed to demonstrate the utility of this approach. A number of related compounds were investigated for reactivity on treatment with an acid catalyst (trifluoroacetic acid) and each were found to undergo a facile cyclisation/double dehydration cascade yielding discrete furan-based products. When the structural elements of these synthetic precursors were aligned with that expected for the furanylidene natural products, the desired ring system was accessed in excellent yield and with remarkable control for the correct configurational isomer. This would appear to provide tangible evidence of the postulated biosynthetic conversion.

Finally, optimisation of a pivotal sodio-lithio aldol reaction to construct the required hydroxy β-ketoester scaffold; and validation of the subsequent acid-catalysed rearrangement to produce furanylidene heterocycles with a desired stereochemical outcome, provides a clear platform to develop an effective strategy for the total synthesis of natural products in this important structural subclass.

3.8 References and notes

1. R. Ueoka, Y. Nakao, S. Kawatsu, J. Yaegashi, Y. Matsumoto, S. Matsunaga, K. Furihata, R. W. M. van Soest and N. Fusetani, *J. Org. Chem.*, 2009, **74**, 4203.
2. C. Festa, G. Lauro, S. De Marino, M. V. D'Auria, M. C. Monti, A. Casapullo, C. D'Amore, B. Renga, A. Mencarelli, S. Petek, G. Bifulco, S. Fiorucci and A. Zampella, *J. Med. Chem.*, 2012, **55**, 8303.
3. C. Festa, S. De Marino, M. V. D'Auria, E. Deharo, G. Gonzalez, C. Deyssard, S. Petek, G. Bifulco and A. Zampella, *Tetrahedron*, 2012, **68**, 10157.
4. C. Festa, C. D'Amore, B. Renga, G. Lauro, S. De Marino, M. V. D'Auria, G. Bifulco, A. Zampella and S. Fiorucci, *Mar. Drugs*, 2013, **11**, 2314.
5. R. J. Capon, S. Singh, S. Ali and S. Sotheeswaran, *Aust. J. Chem.*, 2005, **58**, 18.
6. D. B. Stierle and D. J. Faulkner, *J. Org. Chem.*, 1980, **45**, 3396.
7. R. S. Compagnone, I. C. Pina, R. R. Hector, F. Dagger, A. I. Suarez, M. V. R. Reddy and D. J. Faulkner, *Tetrahedron*, 1998, **54**, 3057.
8. F. Rahm, P. Y. Hayes and W. Kitching, *Heterocycles*, 2004, **64**, 523.
9. M. D. Higgs and D. J. Faulkner, *J. Org. Chem.*, 1978, **43**, 3454.
10. P. Bartlett and C. Chapius, *J. Org. Chem.*, 1986, **51**, 2799.
11. B. B. Snider, Z. Shi, S. V. O'Neil, K. D. Kreutter and T. L. Arakaki, *J. Org. Chem.*, 1994, **59**, 1726.
12. S. Al-Busafi, J. R. Doncaster, M. G. B. Drew, A. C. Regan and R. C. Whitehead, *J. Chem. Soc., Perkin Trans. 1*, 2002, 476.
13. N. Kornblum and H. DeLaMare, *J. Am. Chem. Soc.*, 1951, **73**, 880.
14. F. Fringuelli, R. Germani, F. Pizzo and G. Savelli, *Synth. Commun.*, 1989, **19**, 1939.
15. D. A. Evans, B. D. Allison, M. G. Yang and C. E. Masse, *J. Am. Chem. Soc.*, 2001, **123**, 10840.
16. S. N. Huckin and L. Weiler, *Can. J. Chem.*, 1974, **52**, 2157.
17. D. E. Williams, T. M. Allen, R. van Soest, H. W. Behrisch and R. J. Andersen, *J. Nat. Prod.*, 2001, **64**, 281.

4. An effective divergent strategy for total synthesis

With an insight to the biosynthesis of furanylidene-containing metabolites (Chapter 2) and through developing an effective method to construct their unique heterocyclic ring system (Chapter 3), a generic strategy for the total synthesis of these compounds was designed. Three features of this strategy were considered central to its value in a research setting: first, the synthesis must be designed to generate targets as a single enantiomer; second, the synthesis must be achievable to a satisfactory yield with minimal steps; and third, the synthesis must be amenable to the construction of a variety of related compounds.

Chapter 4 details the evolution of an effective divergent strategy for the biomimetic total synthesis of gracilioether furanylidenes, which ultimately led to the development of a successful route to the natural products gracilioethers B and C (Chapter 5). The results presented in Chapter 4, with the exclusion of any results that are mentioned in Chapter 5, have not been prepared for publication in any scientific journal to the date of thesis submission. Preparative procedures and analytical data presented in Sections 4.7.10–13 were collected by the candidate at the Department of Chemistry, Princeton University while enrolled externally at Flinders University and with the support of the Fulbright Alumni (WG Walker) Postgraduate Scholarship.

4.1 A divergent strategy for the biomimetic total synthesis of gracilioether furanylidenes

The discovery and optimisation of an enabling sodio-lithio aldol reaction of substituted β-ketoesters with hindered α-oxygenated neo-pentyl aldehydes; and the facile cyclisation/dehydration cascade reactions of the resulting alcohols to yield furanylidene ring systems under thermodynamic control (Chapter 3),[1] provided a unique opportunity to design an effective strategy for the total synthesis of furanylidene-containing natural products. Furthermore, the inspiration for this design, a revised hypothesis (mechanism) for the biosynthesis of furanylidene metabolites from related endoperoxides, represents a novel approach to their chemical synthesis.

Disassembling the unsaturated heterocycle of a target furanylidene (**162**) to an acyclic system such as **163**, which in turn can be constructed by the sodio-lithio aldol reaction of commercially available ester **145** and synthetic aldehyde **164** (Scheme 4.1), appears to simplify the challenges associated with constructing this motif. If these operations are successful in a broader context than those of the synthetic model presented in Chapter 3, it may also be possible to access a late stage intermediate (**162**) appended with an appropriate synthetic handle, R (Scheme 4.1). Ideally, this latent functional group would allow the synthesis of many related furanylidene-containing natural products, with a different end-game strategy for each selected target. Adopting a divergent approach may also provide an opportunity to synthesise unnatural derivatives of the furanylidene metabolites and to study their pharmacological structure-activity relationships. This may be especially useful in probing the structural requirements and limitations of lipophilic tethers in producing favourable antimitotic properties.[2]

Accordingly, the success of this design relies on the suitability of aldehyde **164** for the subsequent transformations. A number of candidate substrates were generated in the hope of producing a versatile late-stage synthetic intermediate, **162** (Sections 4.3, 4.4 and 4.5). Based on the stereochemical elucidation of (6*R*,8*R*)-*des*-hydroxygracilioether C (**90**) by chemical degradation of the natural material[3] and through its total synthesis;[4] and the expectation that related gracilioether furanylidenes share the same relative and absolute configuration through a similar enzymatic biosynthesis, the corresponding aldehyde (2*R*,4*R*)-**164** was targeted. A search of the literature revealed lactone **165** as an

advantageous starting point (Section 4.2) and all considered routes to aldehyde **164** began with this compound.

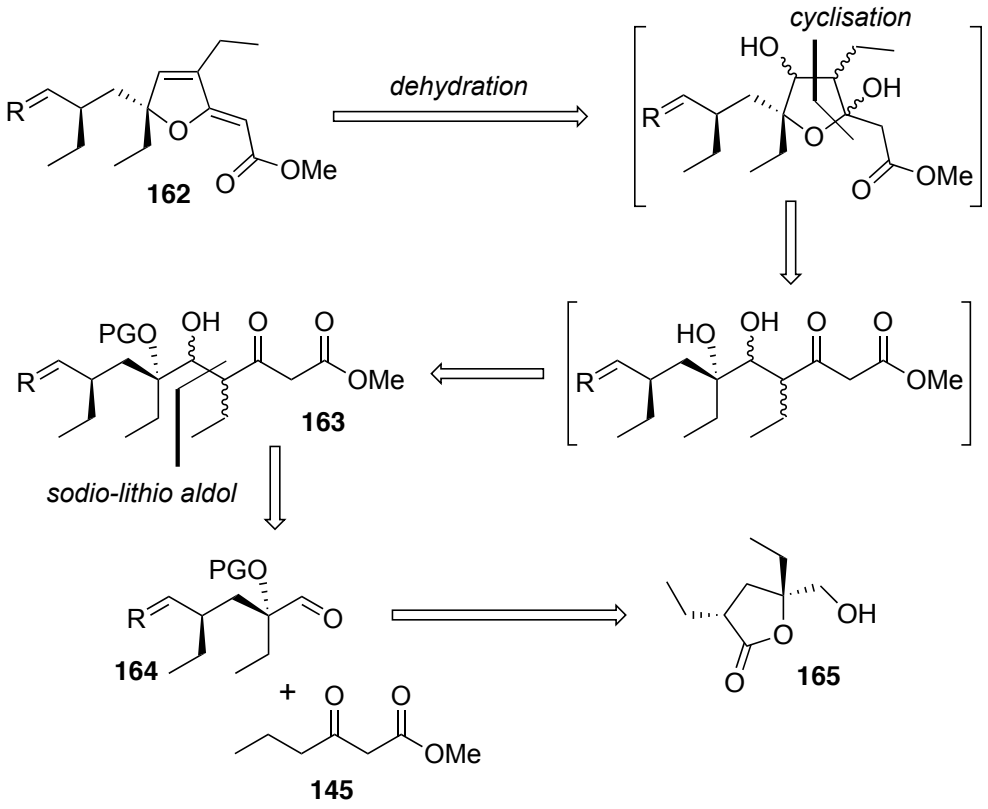

Scheme 4.1: An effective divergent strategy for the biomimetic total synthesis of furanylidene-containing metabolites.

4.2 Installing the common non-contiguous stereocenters

One of the many advantages of targeting lactone **165** is the early installation of non-contiguous stereocenters, which are presumed to be common for all related gracilioether furanylidenes. Forging this configuration at an early stage and as a single enantiomer avoids the need to create these centers through more complex enantioselective reactions in the later stages of total synthesis. It also allows any potential challenges with the purification of minor stereoisomers to be addressed sooner and before constructing more elaborate and/or sensitive substrates.

En route to the bis-spiroacetal moiety of the polyether antibiotic CP44,161, Brimble reported unexpected selectivity in the dihydroxylation of olefin **166** with catalytic K_2OsO_4 and $(DHQ)_2PHAL$ under the well-known Sharpless conditions to

afford lactone **167** (Scheme 4.2).[5] Evidently, dihydroxylation of olefin **166** proceeded with opposite facial selectivity to that predicted by Sharpless' mnemonic to give diol **168** *in situ*, which underwent rapid cyclisation with loss of the pendant norephedrine-derived oxazolidinone. Although this was not a desired stereochemical outcome in Brimble's study, the relative and absolute configuration of lactone **167** matches that required for the strategy outlined in Section 4.1.

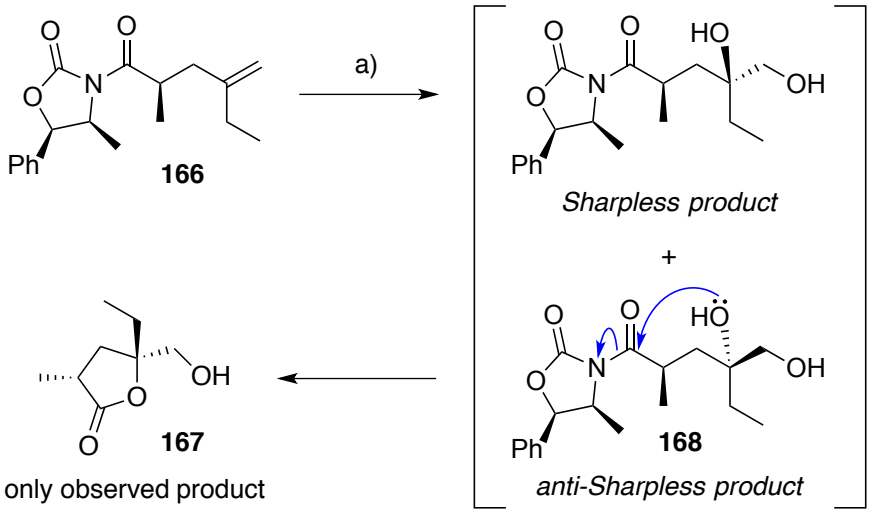

Scheme 4.2: Unexpected facial selectivity in the Sharpless dihydroxylation of olefin **166**. a) K_2CO_3, $K_3Fe(CN)_6$, $(DHQ)_2PHAL$, K_2OsO_4, ^tBuOH, H_2O, 0 °C, 77%.

Presumably, association of the $(DHQ)_2PHAL$ alkaloid ligands with olefin **166** and OsO_4 is influenced by either or both the tethered norephedrine oxazolidinone and neighbouring methyl group in such a way that dihydroxylation occurs at the *Si* face. Given the practical difficulty in obtaining norephedrine chiral building blocks, which are also used to synthesise illicit amphetamine-based drugs, benzyl oxazolidinone **169** was considered a more suitable target for oxidation to lactone **165** (Scheme 4.3), provided that it maintains similar facial selectivity to **166**.

Alkylation of the readily available oxazolidinone **170** with known allyl iodide 2-(iodomethyl)but-1-ene [5] yielded olefin **169** in 80% (see Section 5.5.2 for preparative procedure and analytical data for **169**) and with excellent selectivity for the expected isomer (Scheme 4.3). Oxidation with commercially available AD-mix-α in ^tBuOH and H_2O at 0–5 °C was sluggish with catalyst loadings under 0.17 mol%, but was efficient at this loading or above. Monitoring the reaction by thin layer chromatography and NMR spectroscopy showed the conversion of olefin **169** as a 9:1 mixture of isomers.

Full conversion was achieved after 15 h and flash chromatography afforded lactones **165** and **171** as an inseparable mixture (see Section 5.5.3 for preparative procedure and analytical data for **165**). The relative configuration of each lactone was established by close comparison of the NMR data to that reported by Brimble for lactone **167** (Table 4.1).[5] Despite the clear disadvantage that stereochemical purity could not be achieved through bench top chromatography, the ease of accessing lactone **165** as a major configurational isomer using Brimble's method was worthy of compromise at this stage. Furthermore, it was anticipated that the minor isomer might be more easily separable after further chemical modification. Synthesis of lactone **165** following Brimble's method without modification also yielded the desired *syn* isomer with 9:1 selectivity demonstrating that the benzyloxazolidinone tether has a similar directing capability to the norephedrine-derived auxiliary.

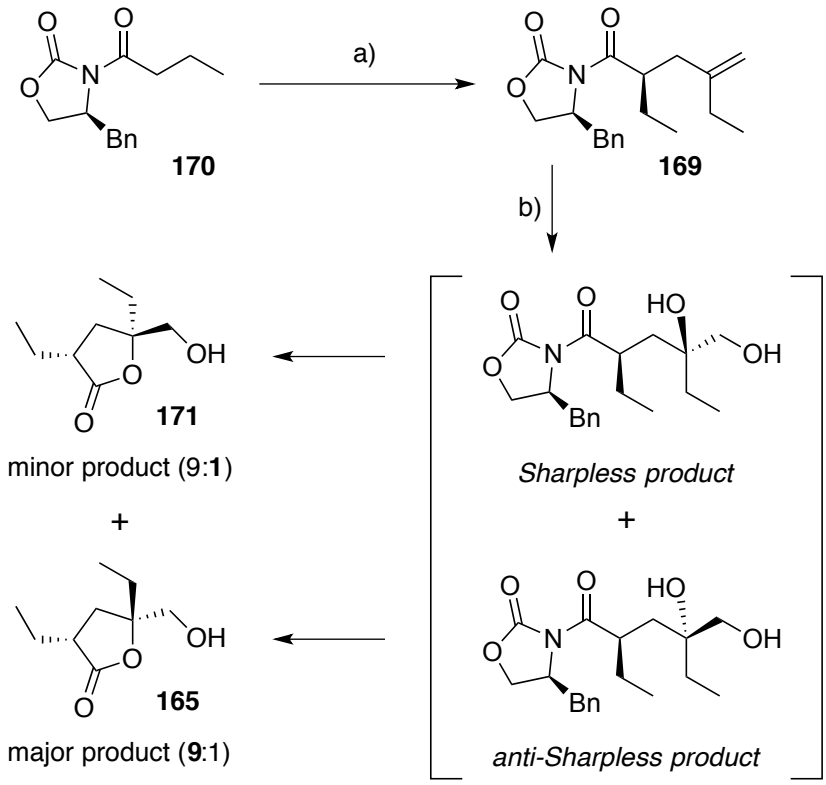

Scheme 4.3: Dihydroxylation/lactonisation of olefin **169** with good selectivity for *syn*-lactone **165**, corresponding to the anti-Sharpless dihydroxylation product. a) LDA, THF, –78 °C to r.t., 20 min, then 2-(iodomethyl)but-1-ene, –78 °C to r.t., 3 h, 80 %; b) AD-mix-α (0.17 mol% K_2OsO_4), ^{t}BuOH, H_2O, 0 °C, 15 h, 99%.

Table 4.1: Tabulated ^{1}H NMR data of **165** and **171** (major and minor isomers) with direct comparison to Brimble's lactones *syn*-**167** and *anti*-**167** (most significant similarities and differences highlighted in blue).

	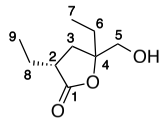		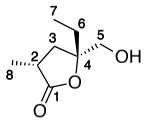	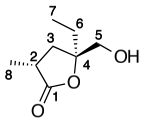
Carbon	**165** (major isomer)	**171** (minor isomer; observed peaks)	Brimble's *syn*-lactone (*syn*-**167**)[5]	Brimble's *anti*-lactone (*anti*-**167**)[5]
	δ_H (500 MHz, $CDCl_3$) (ppm)	δ_H (500 MHz, $CDCl_3$) (ppm)	δ_H (200 MHz, $CDCl_3$) (ppm)	δ_H (200 MHz, $CDCl_3$) (ppm)
2	2.67 (1H, tdd, *J* 10.2, 9.3, 4.7 Hz)	2.82 (1H, m)	2.91–2.69 (1H, m)	3.04–2.87 (1H, m)
3	**2.12 (1H, dd, *J* 12.9, 10.2 Hz)**	**2.35 (1H, dd, *J* 13.0, 10.1 Hz)**	**2.19 (1H, dd, *J* 12.9, 9.9 Hz)**	**2.43 (1H, dd, *J* 13.0, 10.0 Hz)**
	1.99 (1H, dd, *J* 12.9, 10.2 Hz)	**1.72 (1H, dd, *J* 10.1, 6.0 Hz)**	**1.95 (1H, dd, *J* 12.9, 9.9 Hz)**	**1.76–1.66 (1H, overlapping)**
5	**3.75 (1H, dd, *J* 12.2, 4.3Hz)**	**3.70 (1H, dd, *J* 11.9, 5.0 Hz)**	**3.75 (1H, dd, *J* 12.2, 4.8 Hz)**	**3.72 (1H, d, *J* 12.0 Hz)**
	3.46 (1H, dd, *J* 12.2, 7.3 Hz)	**3.58 (1H, dd, *J* 11.9, 4.6 Hz)**	**3.45 (1H, dd, *J* 12.2, 7.4 Hz)**	**3.58 (1H, d, *J* 12.0 Hz)**
6	1.69 (2H, q, *J* 7.6 Hz)		1.69 (2H, q, *J* 7.5 Hz)	1.76–1.66 (2H, overlapping)
7	0.95 (3H, t, *J* 7.5 Hz)		0.94 (3H, t, *J* 7.5 Hz)	0.94 (3H, t, *J* 7.5 Hz)
8	1.91 (1H, dtd, *J* 13.8, 7.5, 4.6 Hz)		1.29 (3H, d, *J* 7.0 Hz)	1.26 (3H, d, *J* 7.3 Hz)
	1.54 (1H, ddt, *J* 13.8, 9.3, 7.5 Hz)			
9	0.99 (3H, t, *J* 7.5 Hz)		N/A	N/A

4.3 First-generation 'alcohol' approach

With a method to construct the desired absolute and relative configuration of the central non-contiguous stereocenters, attention turned to the design of aldehyde **164** and methods to advance lactone **165** toward this target. Analogous to the approach outlined in Chapter 3, the first strategy was aimed at constructing **172**, with a PMB ether at the tertiary oxygenated carbon and a silyloxy ether as the synthetic handle (Scheme 4.4). It was envisaged that the sodio-lithio aldol reaction of aldehyde **173** with methyl 3-oxohexanoate (**145**) would cleanly afford the corresponding alcohol **172**, which on DDQ oxidation and acidic hydrolysis would undergo cyclisation and double dehydration to the desired furanylidene motif with concomitant acid hydrolysis of the silyl ether. Functionalisation of the resulting furanylidene alcohol (**174**) would then allow the total synthesis of several target metabolites.

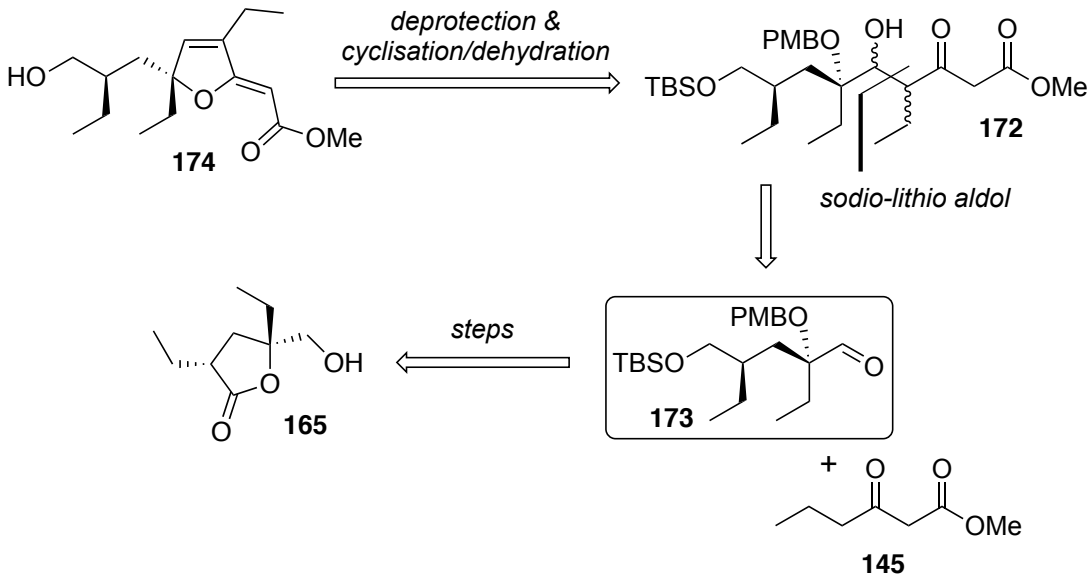

Scheme 4.4: A first-generation approach to the total synthesis of gracilioether furanylidenes via alcohol **172**.

To begin, a 9:1 mixture of lactone **165** and **171** was reduced with $LiBH_4$ in Et_2O to give triol **175** in the same ratio, which were also inseparable by bench top chromatography (Scheme 4.5). Selective protection of the hindered tertiary hydroxyl was achieved by analogy to the model system (Chapter 3) through condensation with anisaldehyde dimethyl acetal to dioxolane **176**, followed by TBS protection of the remaining primary alcohol giving silyl ether **177** and selective reduction with DIBAL to

afford **178**. While the latter two conversions were achieved without any significant difficulty, acetal protection of triol **175** was troublesome. Excess anisaldehyde dimethyl acetal (at least four equivalents) was required to shift the reaction equilibrium toward condensed products. However, this higher concentration also appeared to encourage condensation of anisaldehyde to the remaining primary alcohol, reducing yield of the desired (mono-condensed) product and complicating the purification of these highly acid-sensitive substrates. Furthermore, the isomeric ratio of the expected products **176** and **179**, which differ at the tertiary carbon, had decreased from 9:1 to approximately 2:1. This clearly indicates that under the conditions used for anisaldehyde condensation, the tertiary oxygenated carbon undergoes epimerisation, presumably through formation of carbocation **180** (Scheme 4.5). Despite a substantial loss of yield through these

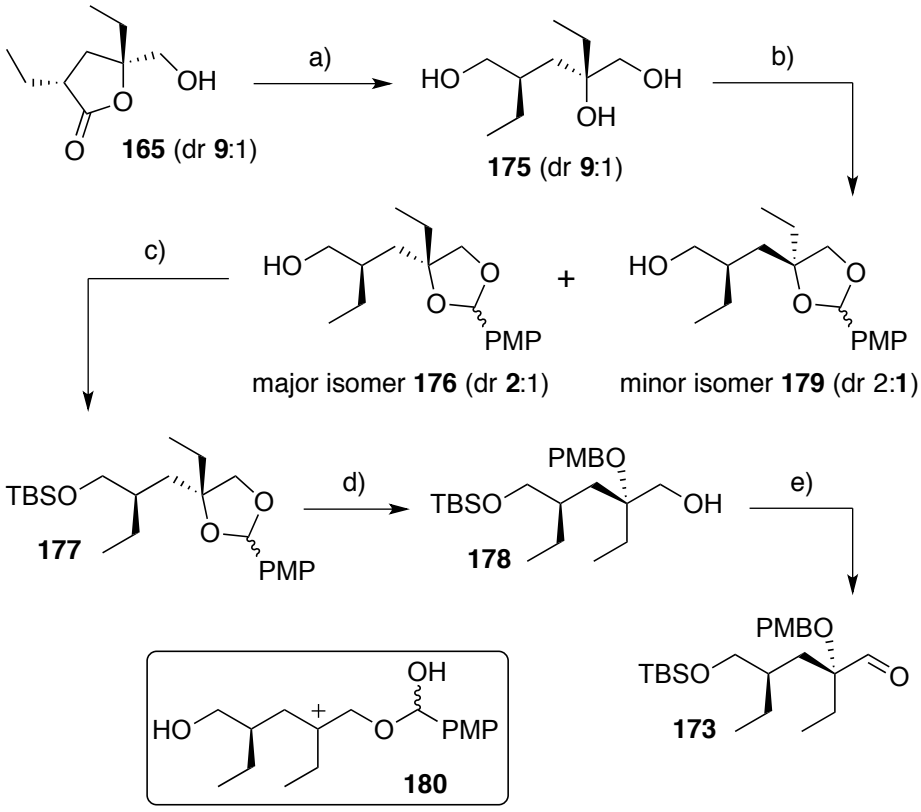

Scheme 4.5: Synthesis of aldehyde **173** from lactone **165**. a) $LiBH_4$, Et_2O, 0 °C, 2 h, 97%; b) $PMPCH(OMe)_2$, TFA, CH_2Cl_2, r.t., 24 h, 59%; c) TBSCl, imidazole, CH_2Cl_2, r.t., 45 min, 99%; d) DIBAL, CH_2Cl_2, 0 °C, 2 h, 96 %; e) $(COCl)_2$, DMSO, CH_2Cl_2, –78 °C, 1 h, then Et_3N, –78 °C to r.t., 30 min, quant.

undesired processes, the acetal epimers **176** and **179** were separable by bench top chromatography and adequate quantities of dioxolane **176** as a single enantiomer were obtained. Finally, Swern oxidation of alcohol **178** afforded aldehyde **173** in good yield.

Unfortunately, the sodio-lithio aldol reaction of aldehyde **173** with methyl 3-oxohexanoate (**145**) under the conditions reported in Chapter 3 gave inconsistent results (Scheme 4.6). The reaction appeared to be complicated through decomposition of the pendent silyl ether, since unknown desilylated products where noticed in the crude material. Furthermore, the reaction products both desired and undesired, were difficult to purify and characterise due to the number of stereoisomers and possibly regioisomers that might have formed in the reaction. As a result, the success of this approach had to be assessed against the quantity of alcohol **174** recovered after the subsequent reactions with DDQ and TFA. Disappointingly, very little of the desired compound could be

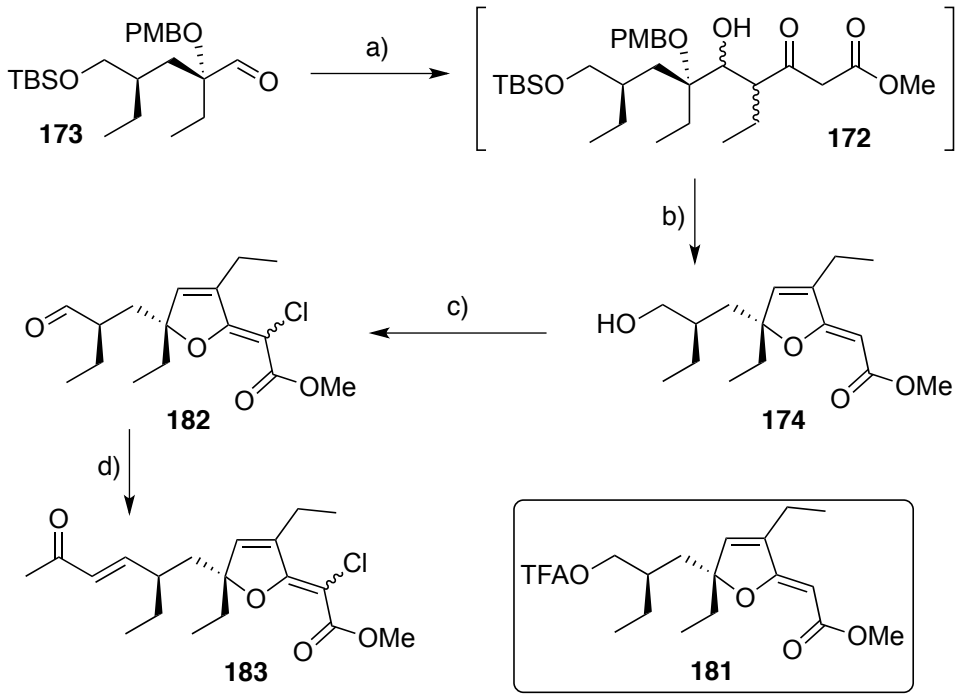

Scheme 4.6: Synthesis of alcohol **174** and an unexpected oxidation followed by Horner-Wadsworth olefination to (*E*/*Z*)-2-chlorogracilioether B (**183**). a) methyl 3-oxohexanoate (treated with NaH and ^{n}BuLi), THF, –78 °C to r.t., 15 h; then b) DDQ, pH 7 phosphate buffer, CH_2Cl_2, r.t., 3 h; then TFA, $CDCl_3$, r.t., 15 h, 25 %; c) $(COCl)_2$, DMSO, CH_2Cl_2, –78 °C, 1 h, then Et_3N, –78 °C to r.t., 30 min, 72%; d) $CH_3COCH_2PO(OEt)_2$, NaH, THF, 0 °C, 3 h, 63%.

recovered after multiple attempts. The TFA ester (**181**) of alcohol **174** was also observed as a product, which presumably formed through silyl cation activation of TFA in the final step.

At this time an opportune sample of furanylidene **174**, which was not characterised further than ^{1}H and ^{13}C NMR, was subject to further conditions in an attempt install a terminal methyl ketone and thereby synthesise a small sample of synthetic gracilioether B (**85**). Obtaining stereochemical information for synthetic **85** prior to method optimisation was considered highly valuable since stereochemical parameters of the current strategy (Section 4.2) could be adjusted promptly to suit the desired outcome, at least for the total synthesis of this target. However, under Swern conditions and with an excess of active oxidant, **174** reacted smoothly to give the chlorinated aldehyde products **182** (Scheme 4.6). It appears that furanylidene heterocycles are sensitive to oxidation at the electron-rich enol ether and that under Swern conditions the electrophilic chlorine intermediate (dimethylsulfonium chloride) reacts at this olefin with loss of the furanyl acetate hydrogen (Scheme 4.7).

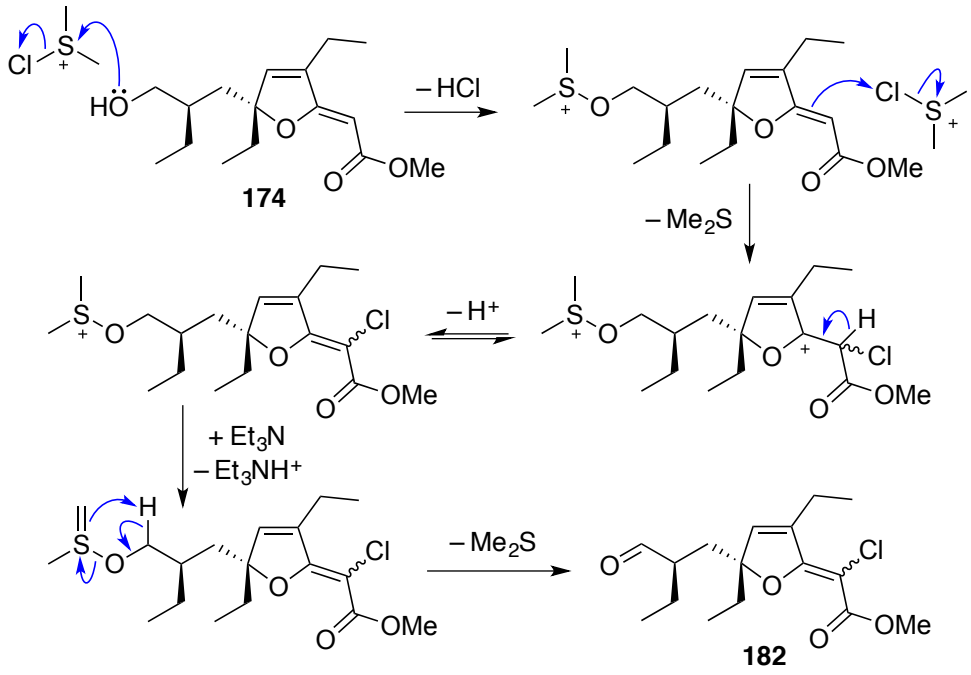

Scheme 4.7: Oxidation and chlorination of furanylidene alcohol **174** on treatment with dimethylsulfonium chloride.

It is also interesting to note that aldehyde **182** was recovered as a mixture of *E*/*Z* isomers. It appears that this lack of selectivity may be a result of poor kinetic control on formation of the vinyl chloride, where under the chlorinating conditions (–78 °C, 1 h) there is not enough time for thermodynamic equilibrium to establish before quenching. Horner-Wadsworth-Emmons olefination of **182** finally yielded a synthetic sample of (*E*/*Z*)-2-chlorogracilioether B (**183**, Scheme 4.6). At this time, furanylidene heterocycles were also found to be sensitive to oxidation with pyridinium chlorochromate (PCC); and these details are discussed further in Chapter 6.

Several issues were now apparent through application of the first-generation approach. Although the conversion of lactone **165** to dioxolane **176** facilitates enrichment of the tertiary oxygenated stereocenter, its synthesis is complicated by epimerisation and poor thermodynamic selectivity for the five-membered dioxolane. The sodio-lithio aldol reaction of aldehyde **173** with methyl 3-oxohexanoate is complicated by the instability of its silyloxy ether to the conditions employed; and difficulties associated with identifying those products that have formed. Finally, furanylidene substrates were found to have some inherent sensitivity to oxidative conditions, which are required to advance late stage furanylidene alcohol **174** to the desired targets. These findings warranted re-examination of the current strategy to address these issues and consequently, aldehyde **173** and alcohol **174** were no longer considered viable intermediates *en route* to the furanylidene metabolites.

4.4 Second-generation ‘acetylene’ approach

A key issue with the first-generation approach (Section 4.3) was failure to obtain useful quantities of desired materials through the sodio-lithio aldol reaction of aldehyde **173** with methyl 3-oxohexanoate before cyclisation to a late stage furanylidene intermediate. This was mostly attributed to instability of the pendent silyloxy ether under the reaction conditions. To address this issue, acetylene **184** was considered an alternate late-stage target and aldehyde **185** was thought to be a suitable aldol precursor (Scheme 4.8). While the terminal acetylene of aldehyde **185** would undoubtedly be base-sensitive, it was envisaged that the use of excess enolate in the aldol reaction might provide *in situ* protection through the formation of a metal acetylide. In turn, the terminal acetylene of **186** might act as a useful functional handle through

hydrometallation with zirconocene hydrochloride (Schwartz reagent)[6] and quenching of the resulting organozirconium intermediate with an appropriate electrophile. Finally, protecting the tertiary alcohol of **185** as a MOM ether might offer a simpler strategy for the application and removal of protecting groups at this site.

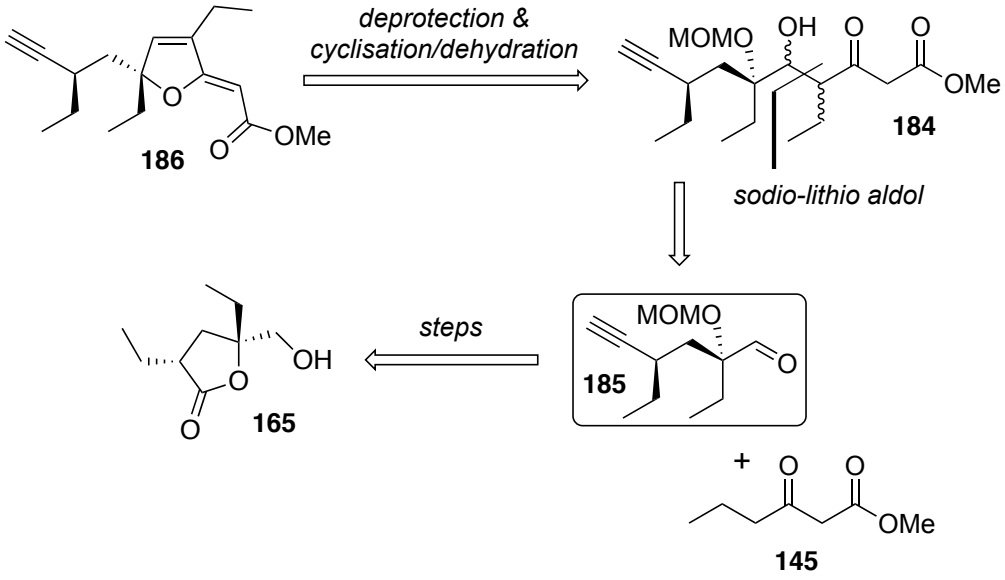

Scheme 4.8: A second-generation approach to the total synthesis of gracilioether furanylidenes via acetylene **184**.

A 9:1 mixture of lactone **165** and **171** was treated with TESCl to obtain the corresponding silyl ether **187** and its C4 epimer, which were fortunately separable by bench top chromatography (Scheme 4.9). DIBAL reduction gave lactol **188** as a single epimer and homologation[7,8] with $TMSCHN_2$ and LDA cleanly afforded acetylene **189** in good yield. Subsequent treatment with MOMCl and DIPEA in CH_2Cl_2 gave the corresponding methoxymethyl ether **190**, which was considered an appropriate compound to test hydrometallation of the terminal acetylene group. However, on exposure to zirconocene hydrochloride **190** underwent complete decomposition. It is unclear why ether **190** is liable to such decomposition under Schwartz' conditions, since it is well documented that silylethers and acetals are generally tolerant.[6]

Although there was scope to pursue this approach and attempt to synthesise furanylidene **186**, the failure for acetylene **190** to undergo controlled hydrometallation was discouraging. Furthermore, if hydrometallation of alkyne **186** was also unsuccessful, it might otherwise be difficult to extend the terminal acetylene and install

a *trans*-olefin. Acetylide alkylation of **186** followed by Birch reduction was considered an alternative method to hydrometallation, however it was expected that Birch conditions might also cause undesired reaction at the unsaturated furanylidene heterocycle. At this time, it was considered that the current method could best be modified to target an aldehyde equivalent of acetylene **186**; and that one-carbon homologation of lactol **188** should be avoided. This strategic revision gave rise to a third-generation approach (Section 4.5) and the 'acetylene' target, although providing some insight to developing an effective synthetic route, was ultimately abandoned.

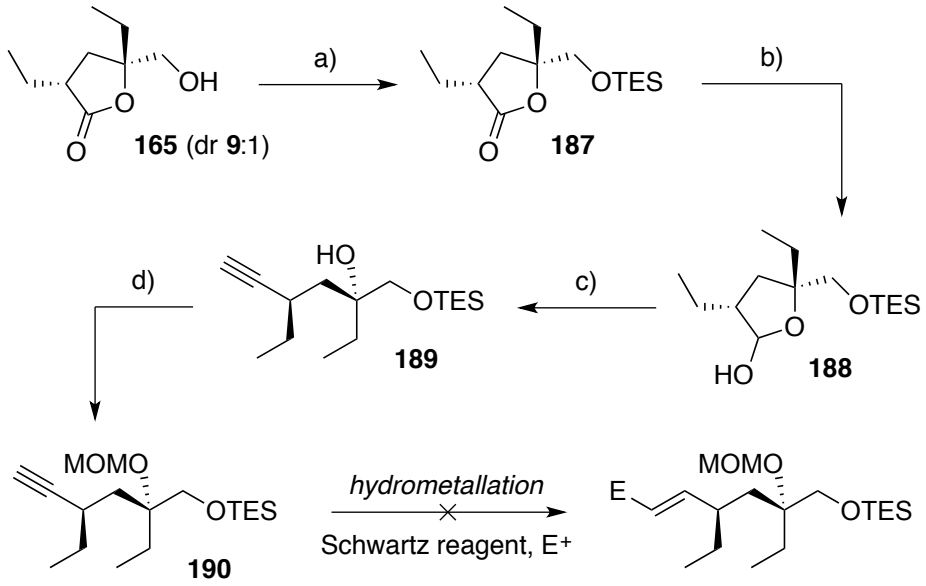

Scheme 4.9: Synthesis of acetylene **190** and decomposition on treatment with zirconocene hydrochloride (Schwartz reagent). a) TESCl, imidazole, CH_2Cl_2, 0 °C to r.t., 90 min, 92%; b) DIBAL, CH_2Cl_2, –78 °C, 60 min, 95%; LDA, $TMSCHN_2$, THF, –78 °C to r.t., 40 min, 75%; MOMCl, DIPEA, CH_2Cl_2, r.t., 5 h, 94%.

4.5 Third-generation 'masked aldehyde' approach

The instability of intermediate compounds; and the application and removal of protecting groups employed in the previous two strategies greatly hindered their success. Rather than attempting to manipulate protecting group chemistry and the order of synthetic steps to find a combination that better suits the chosen reaction conditions, attention focussed on minimising changes in oxidation state. The third-generation and final approach to the synthesis of a versatile late-stage furanylidene intermediate **162** (Scheme 4.1) was based on a notion that the alcohol of lactone **165** should be oxidised

and extended through reaction with methyl 3-oxohexanoate (**145**) without the application of an intermediate protecting group. Futhermore, the lactone carbon should only be reduced once, thereby placing it in the correct oxidation state for olefination at the endgame stage. Hence, furanylidene aldehyde dimethyl acetal **88** was the target in this final approach (Scheme 4.10) and aldehyde **191** was selected as a suitable aldol precursor. The design of this third strategy is unique in that the R and PG groups of the hypothetical furanylidene precursor **162** (Scheme 4.1) are linked as a methyl acetal (**87**). The subsequent biomimetic cascade reaction would therefore take a subtly different form to that described in Chapter 3, involving transacetalisation of the tertiary alcohol group to the nearby ketone, followed by dehydration to afford the conjugated furanylidene heterocycle. The remaining dimethyl acetal, or 'masked aldehyde,' is then poised for further modification without requiring additional changes in oxidation state. The power of this new approach and its application to achieve total synthesis of the furanylidene metabolites gracilioethers B and C in excellent overall yield is presented in Chapter 5.

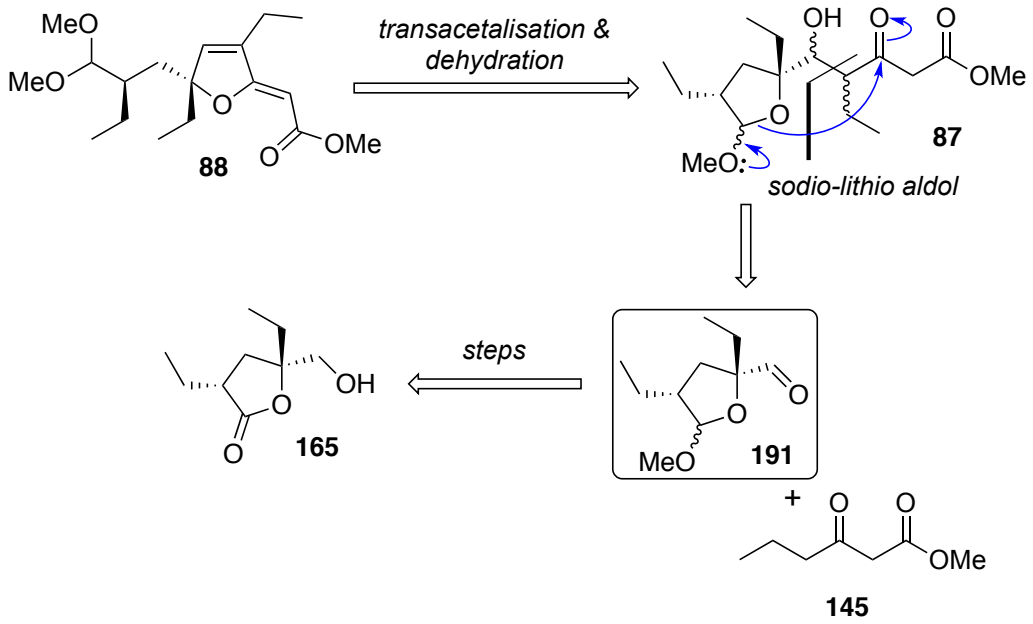

Scheme 4.10: A third-generation approach to the total synthesis of gracilioether furanylidenes via methyl acetal **87**.

4.6 Concluding remarks

Several approaches to the synthesis of a versatile late-stage intermediate *en route* to the total synthesis of related furanylidene metabolites were designed and trialled. A number of advanced synthetic compounds were synthesised in excellent yield and attempts were made to extend these substrates through the aldol methodology developed in Chapter 3. Despite some success, a number of contributing factors including the instability of intermediate compounds; and the application and removal of protecting groups ultimately hindered these efforts. A better understanding of the advantages and limitations of these strategies inspired a third approach (discussed further in Chapter 5), which attempts to address each of the problems encountered in Chapter 4.

4.7 Preparative procedures and analytical data

4.7.1 General experimental details

For general experimental details, including information on reaction solvents, chromatography, analytical equipment and reported data, see Section 3.5.1.

*4.7.2 (2R,4R)-2,4-Diethylpentan-1,2,5-triol (**175**)*

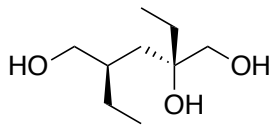

To a stirred solution of **165** (1.87 g, 10.9 mmol) in Et_2O (300 mL) at 0 °C was added $LiBH_4$ (13.6 mL, 2.0 M in THF, 27.2 mmol). The mixture was stirred at 0 °C for 2 h before quenching with the addition of NH_4Cl (satd aq). The organic layer was separated and aqueous extracted with EtOAc. The combined extracts were washed with brine, dried (Na_2SO_4) and concentrated *in vacuo*. Flash chromatography afforded the *title compound* and its C5 epimer (1.85 g, 97%) as an inseparable 9:1 mixture of stereoisomers. R_f (EtOAc) 0.34; ν_{max} (thin film) 3331, 2964, 2934, 2880, 1463, 1381, 1133, 1052 cm^{-1}; δ_H (600 MHz, $CDCl_3$) 3.75 (1H, dd, *J* 3.3, 10.4 Hz, $CHCH_AH_BOH$), 3.55 (1H, d, *J* 10.9 Hz, $C(OH)CH_AH_BOH$), 3.37 (2H, m, $CHCH_AH_BOH$ overlapped with $C(OH)CH_AH_BOH$), 3.17 (3H, br s, OH × 3), 1.74 (1H, m, C*H*), 1.64 (2H, m, CCH_2CH_3),

1.53 (2H, m, CH_2CH(Et)CH_2OH), 1.32 (1H, m, CHC$H_A$$H_B$$CH_3$), 1.24 (1H, m, CHC$H_A$$H_B$$CH_3$), 0.92 (3H, t, *J* 7.4 Hz, C(OH)CH_2CH_3), 0.85 (3H, t, *J* 7.6 Hz, CHCH_2CH_3); diagnostic peaks observed for the minor isomer: 3.64 (1H, d, *J* 11.2 Hz, C(OH)C$H_A$$H_B$OH), 3.45 (1H, d, *J* 11.2 Hz, C(OH)C$H_A$$H_B$OH); δ_C (150 MHz, $CDCl_3$) 74.5, 68.2, 67.6, 39.1, 37.2, 28.4, 26.6, 11.7, 8.6; HRMS (ESI): MNa^+, found 199.1308. $C_9H_{20}NaO_3^+$ requires 199.1310.

*4.7.3 (2R)-2-{[(4R)-4-Ethyl-2-(4-methoxyphenyl)-1,3-dioxolan-4-yl]methyl}butan-1-ol (**176**)*

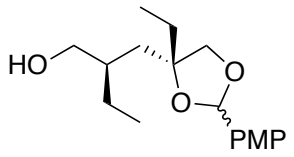

To a stirred solution of **175** (1.79 g, 10.1 mmol) in CH_2Cl_2 (70 mL) at room temperature was added anisaldehyde dimethyl acetal (7.40 mL, 43.5 mmol) and TFA (0.20 mL, 2.6 mmol). The mixture was stirred at room temperature for 24 h before quenching with the addition of $NaHCO_3$ (satd aq). The organic layer was separated and aqueous extracted with CH_2Cl_2. The combined extracts were washed with brine, dried (Na_2SO_4) and concentrated *in vacuo*. Flash chromatography afforded the *title compound* (1.76 g, 59%) as an inseparable 4:5 mixture of stereoisomers. R_f (25% EtOAc/hexanes) 0.21; ν_{max} (thin film) 3437, 2964, 2934, 2878, 1615, 1589, 1518, 1463, 1435, 1394, 1304, 1250, 1171, 1075, 1034, 973, 830 cm^{-1}; δ_H (600 MHz, $CDCl_3$) 7.40 (2H, m), 6.90 (2H, m), 5.86 (0.45H, s), 5.84 (0.55H, s), 4.10 (0.55H, d, *J* 8.3 Hz), 3.94 (0.45H, d, *J* 8.3 Hz), 3.85 (0.45H, d, *J* 8.3 Hz), 3.81 (1.65H, s), 3.80 (1.35H, s), 3.66 (1H, m), 3.63 (0.55H, d, *J* 8.3 Hz), 3.48 (0.55H, m), 3.42 (0.45H, m), 3.31 (0.55H, dd, *J* 4.6, 8.7 Hz), 3.02 (0.45H, dd, *J* 5.5, 8.2 Hz), 1.90 (0.45H, m), 1.81 (2H, m), 1.72 (2.55H, m), 1.38 (1H, m), 1.26 (1H, m), 0.93 (6H, m); δ_C (150 MHz, $CDCl_3$) 160.5, 160.4, 129.6, 129.2, 128.1, 127.8, 113.9, 113.7, 103.9, 103.1, 84.2, 83.9, 75.4, 75.1, 66.8, 66.0, 55.3 (2 peaks), 40.4, 39.7, 38.6 (2 peaks), 29.3, 28.0, 26.3 (2 peaks), 11.7 (2 peaks), 8.9, 8.6; HRMS (ESI): MNa^+, found 317.1731. $C_{17}H_{26}NaO_4^+$ requires 317.1729.

*4.7.4 tert-Butyl[(2R)-2-{[(4R)-4-ethyl-2-(4-methoxyphenyl)-1,3-dioxolan-4-yl]methyl}butoxy]dimethylsilane (**177**)*

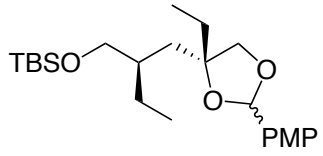

To a stirred solution of **176** (0.57 g, 1.9 mmol) in CH_2Cl_2 (10 mL) at room temperature was added imidazole (0.39 g, 5.7 mmol). After 15 min, a solution of TBSCl (0.39 g, 2.6 mmol) in CH_2Cl_2 (4 mL) was added slowly. Stirring continued for 45 min before quenching with the addition of $NaHCO_3$ (satd aq). The organic layer was separated and aqueous extracted with CH_2Cl_2. The combined extracts were dried (Na_2SO_4) and concentrated *in vacuo*. Flash chromatography afforded the title compound (0.78 g, 99%) as an inseparable 4:5 mixture of stereoisomers. R_f (50% CH_2Cl_2/hexane) 0.37; ν_{max} (thin film) 2957, 2930, 2882, 2857, 1616, 1589, 1518, 1463, 1391, 1303, 1250, 1170, 1078, 1037, 834, 775 cm^{-1}; δ_H (600 MHz, $CDCl_3$) 7.41 (2H, app. d, *J* 7.6 Hz), 6.89 (2H, m), 5.82 (0.55H, s), 5.79 (0.45H, s), 3.94 (1H, app. t, *J* 8.5 Hz), 3.81 (3H, s), 3.78 (0.45H, d, *J* 8.0 Hz), 3.74 (0.55H, d, *J* 8.2 Hz), 3.59 (1.1H, d, *J* 5.2 Hz), 3.51 (0.9H, d, *J* 5.9 Hz), 1.85 (0.55H, dd, *J* 6.6, 14.6 Hz), 1.79 (0.45H, m), 1.72 (2H, app. m), 1.63 (1.1H, app. m), 1.55 (0.45H, dd, *J* 5.5, 14.3 Hz), 1.46 (1.1H, m), 1.37 (1.35H, app. m), 0.96 (3H, app. q, *J* 7.6 Hz), 0.89 (4.95H, s), 0.89 (3H, app. m), 0.88 (4.05H, s), 0.03 (3.3H, s), 0.02 (1.35H, s), 0.01 (1.35, s); δ_C (150 MHz, $CDCl_3$) 160.2 (2 peaks), 130.4, 130.3, 128.1, 128.0, 113.7, 113.6, 103.2, 102.8, 84.2, 84.1, 74.5, 74.0, 65.6, 65.2, 55.3 (2 peaks), 38.1, 37.7, 37.2, 36.2, 30.4, 29.5, 25.9 (2 peaks), 25.1 (2 peaks), 18.3 (2 peaks), 11.3, 11.1, 8.6, 8.3, –5.4 (3 peaks), –5.5; HRMS (ESI): MNa^+, found 431.2606. $C_{23}H_{40}NaO_4Si^+$ requires 431.2594.

*4.7.5 (2R,4R)-4-{[(tert-Butyldimethylsilyl)oxy]methyl}-2-ethyl-2-[(4-methoxyphenyl)methoxy]hexan-1-ol (**178**)*

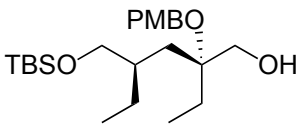

To a stirred solution of **177** (0.77 g, 1.9 mmol) in CH_2Cl_2 (15 mL) at 0 °C was added DIBAL (3.0 mL, 1.0 M in PhMe, 3.0 mmol). The mixture was stirred at 0 °C for

2 h before diluting with CH_2Cl_2 and quenching with the addition of sodium potassium tartrate (1.0 M aq). The organic layer was separated and aqueous extracted with CH_2Cl_2. The combined extracts were washed with brine, dried (Na_2SO_4) and concentrated *in vacuo*. Flash chromatography afforded the *title compound* (0.74 g, 96%) as a colourless oil. R_f (20% EtOAc/hexanes) 0.38; $[\alpha]^{20}_D$ +0.4 (*c* 2.45, $CHCl_3$); ν_{max} (thin film) 3462, 2957, 2931, 2858, 1614, 1515, 1464, 1381, 1302, 1249, 1173, 1078, 1040, 836, 776 cm^{-1}; δ_H (600 MHz, $CDCl_3$) 7.26 (2H, d, *J* 8.6 Hz, Ar*H*), 6.87 (2H, d, *J* 8.6 Hz, Ar*H*), 4.35 (2H, dd, *J* 11.2, 12.1 Hz, CH_2PMP), 3.80 (3H, s, OCH_3), 3.65 (1H, dd, *J* 4.8, 9.7 Hz, CH_AH$_B$OTBS), 3.61 (1H, dd, *J* 5.4, 11.7 Hz, CH_AH$_B$OH), 3.51 (1H, dd, *J* 8.2, 11.7 Hz, CH$_A$$H_B$OH), 3.44 (1H, dd, *J* 4.7, 9.7 Hz, CH$_A$$H_B$OTBS), 2.81 (1H, dd, *J* 5.4, 8.2 Hz, O*H*), 1.74 (1H, m, C*H*CH$_2$OTBS), 1.67 (3H, app. m, CH_AH$_B$CH(CH$_2$OTBS)Et and C(OPMB)CH_2CH$_3$), 1.51 (1H, dd, *J* 4.9, 15.1 Hz, CH$_A$$H_B$CH(CH$_2$OTBS)Et), 1.44 (1H, m, CH(CH$_2$OTBS)CH_AH$_B$CH$_3$), 1.34 (1H, m, CH(CH$_2$OTBS)CH$_A$$H_BCH_3$), 0.92 (3H, t, *J* 7.5 Hz, CHCH$_2$CH_3), 0.90 (9H, s, C(CH_3)$_3$), 0.89 (3H, t, *J* 7.6 Hz, C(OPMB)CH$_2$CH_3), 0.07 (3H, s, SiCH_3), 0.06 (3H, s, SiCH_3); δ_C (150 MHz, $CDCl_3$) 158.9, 131.3, 128.7, 113.7, 79.9, 66.7, 64.0, 62.6, 55.3, 36.7, 33.9, 26.1, 26.0 (2 peaks), 18.4, 11.5, 7.6, –5.4, –5.5; HRMS (ESI): MNa^+, found 433.2750. $C_{23}H_{42}NaO_4Si^+$ requires 433.2750.

*4.7.6 (2R,4R)-4-{[(tert-Butyldimethylsilyl)oxy]methyl}-2-ethyl-2-[(4-methoxyphenyl)methoxy]hexanal (**173**)*

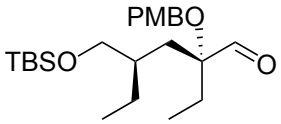

To a stirred solution of DMSO (0.28 mL, 3.9 mmol) in CH_2Cl_2 (18 mL) at –78 °C was added $(COCl)_2$ (1.3 mL, 2.0 M in CH_2Cl_2, 2.6 mmol). The mixture was stirred at –78 °C for 20 min before the addition of **178** (0.71 g, 1.7 mmol) in CH_2Cl_2 (5 mL), followed by Et_3N (1.4 mL, 10 mmol) after another 60 min. Once warmed to room temperature, the reaction was quenched with the addition of NH_4Cl (satd aq). The organic layer was separated and aqueous extracted with CH_2Cl_2. The combined extracts were washed with water, dried (Na_2SO_4) and concentrated *in vacuo*. Flash chromatography afforded the *title compound* (0.71 g, quant.) as a colourless oil. R_f (CH_2Cl_2) 0.56; $[\alpha]^{20}_D$ –14.0 (*c* 1.14, $CHCl_3$); ν_{max} (thin film) 2957, 2929, 2857, 1734, 1614, 1587, 1515, 1463, 1383, 1302, 1250, 1173, 1088, 1039, 837, 776 cm^{-1}; δ_H (600

MHz, $CDCl_3$) 9.63 (1H, s, C*H*O), 7.30 (2H, ds, *J* 8.6 Hz, Ar*H*), 6.89 (2H, d, *J* 8.6 Hz, Ar*H*), 4.42 (1H, d, *J* 10.7 Hz, CH_AH$_B$PMP), 4.36 (1H, d, *J* 10.7 Hz, CH$_A$$H_B$PMP), 3.81 (3H, s, OCH_3), 3.48 (1H, dd, *J* 4.9, 10.0 Hz, CH_AH$_B$OTBS), 3.44 (1H, dd, *J* 5.2, 10.0 Hz, CH$_A$$H_B$OTBS), 1.82 (3H, app. m, CH_AH$_B$CH(CH$_2$OTBS)Et and C(OPMB)CH_2CH$_3$), 1.67 (1H, dd, *J* 5.0, 15.1 Hz, CH$_A$$H_B$CH(CH$_2$OTBS)Et), 1.59 (1H, m, C*H*CH$_2$CH$_3$), 1.41 (1H, m, CHCH_AH$_B$CH$_3$), 1.33 (1H, m, CHCH$_A$$H_BCH_3$), 0.89 (3H, t, *J* 7.4 Hz, C(OPMP)CH$_2$CH_3), 0.88 (9H, s, C(CH$_3$)$_3$), 0.87 (3H, t, *J* 7.5 Hz, CHCH$_2$CH_3), 0.01 (6H, s, Si(CH_3)$_2$); δ_C (150 MHz, $CDCl_3$) 159.1, 130.4, 128.9, 113.8, 85.0, 64.7 (3 peaks), 55.3, 37.0, 33.2, 25.9, 25.3, 24.9, 18.3, 11.2, 7.2, –5.5 (2 peaks); HRMS (ESI): MNa$^+$, found 431.2600. $C_{23}H_{40}NaO_4Si^+$ requires 431.2594.

*4.7.7 Methyl 2-[(2Z,5R)-3,5-diethyl-5-[(2R)-2-ethyl-3-hydroxypropyl]-2(5H)-furanylidene]ethanoate (**174**)*

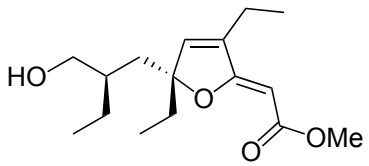

NaH (0.040 g, 60% in mineral oil, 1.0 mmol) was washed with hexane and suspended in THF (3.0 mL). To the stirred slurry at 0 °C was added methyl 3-oxohexanoate (0.070 g, 0.49 mmol), followed by ^{n}BuLi (0.26 mL, 1.7 M in hexane, 0.44 mmol) after 30 min. The mixture was stirred at 0 °C for a further 30 min before cooling to –78 °C and adding a solution of **173** (0.10 g, 0.24 mmol) in THF (1.0 mL). After warming to room temperature, stirring continued for 15 h before quenching with the addition of NH_4Cl (satd aq). The organic layer was separated and aqueous extracted with Et_2O. The combined extracts were washed with brine, dried (Na_2SO_4) and concentrated *in vacuo*. Flash chromatography afforded a complex mixture of products (0.067 g). The mixture was diluted in CH_2Cl_2 (4.3 mL) and aqueous pH 7 phosphate buffer (0.59 mL). DDQ (0.042 g, 0.19 mmol) was added and the biphasic mixture stirred rapidly at room temperature for 3 h before diluting with CH_2Cl_2 and quenching with the addition of $NaHCO_3$ (satd aq). The organic layer was separated and aqueous extracted with CH_2Cl_2. The combined extracts were washed with brine, dried (Na_2SO_4), filtered through a small pad of buffered silica (washing with excess Et_2O) and concentrated *in vacuo*. The crude material was diluted with $CDCl_3$ (0.5 mL) and shaken vigorously in an NMR tube after the addition of TFA (0.03 mL, 0.39 mmol). After

standing for 15 h, the solution was diluting with CH_2Cl_2 quenched with the addition of $NaHCO_3$ (satd aq). The organic layer was separated and aqueous extracted with CH_2Cl_2. The combined extracts were washed with brine, dried (Na_2SO_4) and concentrated *in vacuo*. Flash chromatography afforded a crude sample of the *title compound*, which was difficult to separate from anisaldehyde, a reaction byproduct. The material was used without further purification. R_f (30% EtOAc/hexane) 0.51; δ_H (600 MHz, $CDCl_3$) 6.31 (1H, s), 4.88 (1H, s), 3.88 (1H, dd, *J* 11.7, 2.9 Hz), 3.69 (3H, s), 3.51 (1H, dd, *J* 11.7, 5.5 Hz), 2.16 (2H, dd, *J* 14.7, 7.0 Hz), 1.96–1.90 (1H, m), 1.88–1.83 (1H, m), 1.82 (1H, dd, *J* 14.9, 3.5 Hz), 1.69–1.63 (1H, m), 1.47 (1H, dd, *J* 14.9, 10.5 Hz), 1.42–1.34 (1H, m), 1.27–1.20 (1H, m), 1.16 (3H, t, *J* 7.3 Hz), 0.91 (3H, t, *J* 7.5 Hz), 0.80 (3H, t, *J* 7.5 Hz). No further analytical data was recorded for this compound.

*4.7.8 Methyl (E)-2-chloro-2-((R)-3,5-diethyl-5-((R)-2-formylbutyl)-2(5H)-furanylidene)ethanoate (**182**)*

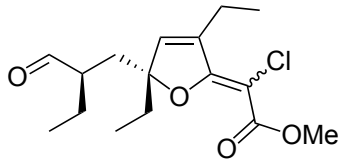

To a stirred solution of DMSO (0.10 mL, 1.4 mmol) in CH_2Cl_2 (6.0 mL) at –78 °C was added $(COCl)_2$ (0.35 mL, 2.0 M in CH_2Cl_2, 0.70 mmol). The mixture was stirred at –78 °C for 20 min before the addition of **174** (0.010 g, 0.04 mmol) in CH_2Cl_2 (1.0 mL), followed by Et_3N (0.52 mL, 3.7 mmol) after another 60 min. Once warmed to room temperature, the reaction was quenched with the addition of NH_4Cl (satd aq). The organic layer was separated and aqueous extracted with CH_2Cl_2. The combined extracts were washed three times with water, dried (Na_2SO_4) and concentrated *in vacuo*. Flash chromatography afforded the *title compound* (0.08 g, 72%) as a mixture of *E* and *Z* isomers, which decomposed on storage. First *E* or *Z* isomer δ_H (600 MHz, $CDCl_3$) 9.54 (1H, d, *J* 1.8 Hz), 6.22 (1H, t, *J* 1.5 Hz), 3.78 (3H, s), 2.50–2.44 (2H, m), 2.28 (1H, dd, *J* 14.5, 9.0 Hz), 2.15–2.11 (1H, m), 1.87–1.81 (2H, overlapping), 1.79–1.74 (1H, m), 1.68–1.63 (1H, m), 1.52–1.47 (1H, m), 1.05 (3H, t, *J* 7.3 Hz), 0.92 (3H, t, *J* 7.5 Hz), 0.81 (3H, t, *J* 7.5 Hz); δ_C (150 MHz, $CDCl_3$) 204.0, 166.7, 164.4, 143.0, 140.2, 96.2, 94.1, 52.3, 47.9, 35.1, 31.6, 22.9, 21.7, 13.0, 11.1, 8.0; second *E* or *Z* isomer δ_H (600 MHz, $CDCl_3$) 9.53 (1H, d, *J* 1.8 Hz), 6.24 (1H, t, *J* 1.7 Hz), 3.79 (3H, s), 2.64–2.60 (2H, m), 2.23 (1H, dd, *J* 14.3, 9.2 Hz), 2.20–2.16 (1H, m), 1.88–1.82 (2H,

m), 1.78–1.72 (1H, m), 1.67–1.62 (1H, m), 1.53–1.46 (1H, m), 1.13 (3H, t, *J* 7.3 Hz), 0.90 (3H, t, *J* 7.7 Hz), 0.82 (3H, t, *J* 7.3 Hz). No further analytical data was recorded for these compounds.

*4.7.9 Methyl (E/Z)-2-chloro-2-[(R)-3,5-diethyl-5-{(R,E)-2-ethyl-5-oxohex-3-en-1-yl}-2(5H)-furanylidene]ethanoate (**183**)*

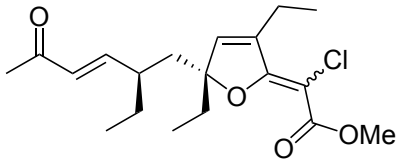

A solution of **182** (0.007 g, 0.02 mmol) in THF (1.5 mL) was added dropwise to a stirred suspension of NaH (0.040 g, 60% in mineral oil, 1.0 mmol; washed with hexane before use), diethyl 2-oxophosphonate (0.10 mL, 0.5 mmol) and THF (2.0 mL) at 0 °C. Stirring continued at 0 °C for 3 h before quenching with the addition of NH_4Cl (50% satd aq). The organic layer was separated and aqueous extracted with Et_2O. The combined extracts were washed with brine, dried (Na_2SO_4) and concentrated *in vacuo*. Flash chromatography afforded the title compound (0.005 g, 63%) as a mixture of *E* and *Z* isomers, which decomposed on storage. First *E* or *Z* isomer δ_H (600 MHz, $CDCl_3$) 6.52 (1H, dd, *J* 16.0, 9.4 Hz), 6.24 (1H, t, *J* 1.7 Hz), 5.93 (1H, d, *J* 16.0 Hz), 3.79 (3H, s), 2.54–2.48 (1H, m), 2.42–2.36 (1H, m), 2.23 (3H, s), 2.14–2.09 (1H, m), 2.03 (1H, dd, *J* 14.7, 3.3 Hz), 1.83–1.75 (2H, overlapping), 1.74–1.68 (1H, m), 1.50–1.46 (1H, m), 1.35–1.30 (1H, m), 1.05 (3H, t, *J* 7.3 Hz), 0.83 (3H, t, *J* 7.5 Hz), 0.79 (3H, t, *J* 7.3 Hz); second *E* or *Z* isomer δ_H (600 MHz, $CDCl_3$) 6.51 (1H, dd, *J* 16.0, 9.4 Hz), 6.23 (1H, t, *J* 1.8 Hz), 5.92 (1H, d, *J* 16.0 Hz), 3.79 (3H, s), 2.69–2.62 (1H, m), 2.56–2.49 (1H, m), 2.23 (3H, s), 2.13–2.07 (1H, m), 2.05 (1H, dd, *J* 14.7, 3.3 Hz), 1.84–1.77 (2H, overlapping), 1.73–1.67 (1H, m), 1.52–1.45 (1H, m), 1.35–1.28 (1H, m), 1.11 (3H, t, *J* 7.2 Hz), 0.81 (3H, t, *J* 7.3 Hz), 0.80 (3H, t, *J* 7.3 Hz); combined isomers: HRMS (ESI): MNa^+, found 377.1510. $C_{19}H_{27}NaO_4Cl^+$ requires 377.1496. No further analytical data was recorded for these compounds.

*4.7.10 (3R,5R)-3,5-Diethyl-5-[{(triethylsilyl)oxy}methyl]dihydro-2(3H)-furanone (**187**)*

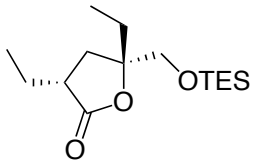

TESCl (0.13 mL, 0.77 mmol) in CH_2Cl_2 (1.0 mL) was added dropwise to a stirred solution of **165** (0.099 g, 0.58 mmol) and imidazole (0.12 g, 1.7 mmol) in CH_2Cl_2 (3.5 mL) at 0 °C. The resulting mixture was brought to room temperature and stirred for a further 90 min before quenching with the addition of $NaHCO_3$ (50% satd aq). The organic phase was separated and aqueous extracted with CH_2Cl_2. The combined extracts were dried (Na_2SO_4) and concentrated *in vacuo*. Flash chromatography afforded the title compound (0.14 g, 92%) as a colourless oil. R_f (40% hexane/CH_2Cl_2) 0.44; $[\alpha]^{20}_D$ –21 (*c* 0.10, $CHCl_3$); ν_{max} (thin film) 2956, 2926, 2877, 1771, 1643, 1463, 1215, 1110, 1011 cm^{-1}; δ_H (600 MHz, $CDCl_3$) 3.65 (1H, d, *J* 10.8 Hz, CH_AH$_B$OTES), 3.53 (1H, d, *J* 10.8 Hz, CH$_A$$H_B$OTES), 2.64–2.57 (1H, m, C*H*CH$_2$CH$_3$), 2.09–1.99 (2H, m, CHCH_2CCH$_2$OTES), 1.94–1.86 (1H, m, CHCH_AH$_B$CH$_3$), 1.72–1.60 (2H, m, CCH_2CH$_3$), 1.57–1.49 (1H, m, CHCH$_A$$H_BCH_3$), 0.99 (3H, t, *J* 7.4 Hz, CHCH$_2$CH_3), 0.98–0.93 (12H, overlapping, CCH$_2$CH_3, Si(CH$_2$CH_3)$_3$), 0.63–0.58 (6H, q, *J* 7.9 Hz, Si(CH_2CH$_3$)$_3$); δ_C (150 MHz, $CDCl_3$) 179.0, 86.5, 66.8, 42.0, 32.3, 29.2, 24.3, 11.8, 7.6, 6.7 (3 overlapping), 4.3 (3 overlapping); HRMS (ESI): MNa^+, found 309.1855. $C_{15}H_{30}NaO_3Si^+$ requires 309.1862.

*4.7.11 (3R,5R)-3,5-Diethyl-5-[{(triethylsilyl)oxy}methyl]tetrahydrofuran-2-ol (**188**)*

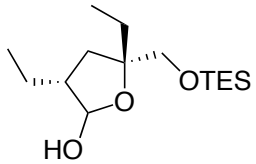

DIBAL (0.57 mL, 1.0 M in PhMe, 0.57 mmol) was added dropwise to a stirred solution of **187** (0.14 g, 0.48 mmol) in CH_2Cl_2 (3.0 mL) at –78 °C. After 60 min, MeOH (0.40 mL) was added dropwise and the mixture was brought to room temperature before quenching with the addition of sodium potassium tartrate (50% satd aq). The resulting mixture was stirred vigorously for 30 min and extracted with CH_2Cl_2. The combined extracts were dried (Na_2SO_4) and concentrated *in vacuo*. Flash chromatography afforded

the *title compound* (0.13 g, 95%) as a colourless oil. R_f (10% EtOAc/hexane) 0.45; $[\alpha]^{20}_D$ +8 (*c* 0.13, $CHCl_3$); ν_{max} (thin film) 3431, 2956, 2876, 1725, 1643, 1463, 1273, 1108, 1017 cm^{-1}; δ_H (600 MHz, $CDCl_3$) 5.15 (1H, dd, *J* 9.9, 4.3 Hz, C*H*OH), 4.03 (1H, d, *J* 9.9 Hz, CHO*H*), 3.54 (1H, d, *J* 10.1 Hz, C$H_A$$H_B$OTES), 3.35 (1H, d, *J* 10.1 Hz, CH$_A$$H_B$OTES), 2.06–1.98 (1H, m, C*H*CH_2CH_3), 1.74–1.66 (2H, m, CHC$H_2$$CH_2$OTES), 1.57–1.51 (1H, m, CHC$H_A$$H_B$$CH_3$), 1.51–1.43 (2H, m, CC$H_2$$CH_3$), 1.43–1.32 (1H, m, CHC$H_2$$H_B$$CH_3$), 0.99 (9H, t, *J* 8.2 Hz, Si(CH_2CH_3)$_3$), 0.94 (3H, t, *J* 7.6 Hz, CHCH_2CH_3), 0.91 (3H, t, *J* 7.6 Hz, CCH_2CH_3), 0.67 (6H, q, *J* 7.9 Hz, Si(C$H_2$$CH_3$)$_3$); δ_C (150 MHz, $CDCl_3$) 99.3, 86.8, 67.0, 48.0, 32.4, 30.2, 22.4, 12.9, 8.0, 6.6 (3 overlapping), 4.1 (3 overlapping); HRMS (ESI): MNa^+, found 311.2007. $C_{15}H_{32}NaO_3Si^+$ requires 311.2018.

*4.7.12 (3R,5R)-5-Ethyl-3-[{(triethylsilyl)oxy}methyl]hept-6-yn-3-ol (**189**)*

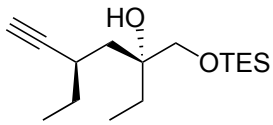

^{n}BuLi (0.47 mL, 2.5 M in hexane, 1.2 mmol) was added dropwise to a stirred solution of DIPA (0.20 mL, 1.4 mmol) in THF (4.1 mL) at –78 °C. After 30 min, $TMSCHN_2$ (0.29 mL, 0.58 mmol) was added dropwise followed by a solution of **188** (0.13 g, 0.45 mmol) in THF (1.0 mL) 5 min later. The mixture was allowed to gradually warm to room temperature over 40 min before quenching with the addition of NH_4Cl (50% satd aq). The organic phase was separated and aqueous extracted with Et_2O. The combined extracts were washed with brine, dried (Na_2SO_4) and concentrated *in vacuo*. Flash chromatography afforded the title compound (0.96 g, 75%) as a colourless oil. R_f (10% EtOAc/hexane) 0.43; $[\alpha]^{20}_D$ no observed rotation (*c* 0.08, $CHCl_3$); ν_{max} (thin film) 3435, 2957, 2929, 2877, 1643, 1460, 1272, 1095 cm^{-1}; δ_H (600 MHz, $CDCl_3$) 3.65 (1H, d, *J* 9.8 Hz, C$H_A$$H_B$OTES), 3.43 (1H, d, *J* 9.8 Hz, CH$_A$$H_B$OTES), 2.56 (1H, s, O*H*), 2.48–2.42 (1H, m, C*H*CH_2CH_3), 2.09 (1H, d, *J* 2.5 Hz, CH_2CHCC*H*), 1.72 (1H, dd, *J* 14.2, 10.0 Hz, CHC$H_A$$H_B$COH), 1.67–1.58 (2H, overlapping, CHC$H_A$$H_B$COH, C(OH)C$H_A$$H_B$$CH_3$), 1.58–1.43 (3H, overlapping, C(OH)C$H_A$$H_B$$CH_3$, CHC$H_2$$CH_3$), 1.02 (3H, t, *J* 7.4 Hz, CHCH_2CH_3), 0.98–0.95 (9H, overlapping, Si(CH_2CH_3)$_3$), 0.89 (3H, t, *J* 7.6 Hz, C(OH)CH_2CH_3), 0.61 (6H, q, *J* 7.9 Hz, Si(C$H_2$$CH_3$)$_3$); δ_C (150 MHz, $CDCl_3$)

88.7, 74.2, 69.7, 67.2, 40.6, 29.7, 29.4, 27.7, 11.4, 8.0, 6.7 (3 overlapping), 4.4 (3 overlapping); HRMS (ESI): MNa^+, found 307.2067. $C_{16}H_{32}NaO_2Si^+$ requires 307.2069.

*4.7.13 (R)-6,8,8-Triethyl-6-[(R)-2-ethylbut-3-yn-1-yl]-2,4,7-trioxa-8-siladecane (**190**)*

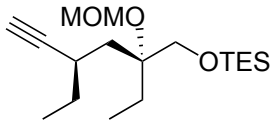

MOMCl (0.06 mL, 0.8 mmol) was added dropwise to a stirred solution of **189** (0.094 g, 0.33 mmol) and DIPEA (0.23 mL, 1.3 mmol) in CH_2Cl_2 (3.0 mL) at 0 °C. Stirring continued for 5 h before quenching with the addition of $NaHCO_3$ (50% satd aq). The organic phase was separated and aqueous extracted with CH_2Cl_2. The combined organic extracts were dried (Na_2SO_4) and concentrated *in vacuo*. Flash chromatography afforded the *title compound* (0.10 g, 94%) as a colourless oil. R_f (10% EtOAc/hexane) 0.54; $[\alpha]^{20}_D$ no observed rotation (*c* 0.14, $CHCl_3$); ν_{max} (thin film) 2954, 2877, 1645, 1463, 1272, 1239, 1100, 1035 cm^{-1}; δ_H (600 MHz, $CDCl_3$) 4.79 (1H, d, *J* 7.1 Hz, $OCH_AH_BOCH_3$), 4.72 (1H, d, *J* 7.1 Hz, $OCH_AH_BOCH_3$), 3.69 (dd, *J* 15.7, 10.4 Hz, CH_2OTES), 3.38 (3H, s, OCH_2OCH_3), 2.49–2.44 (1H, m, $CHCH_2CH_3$), 2.02 (1H, dd, *J* 2.5 Hz, CH_2CHCCH), 1.84 (1H, dd, *J* 14.4, 9.4 Hz, $CHCH_AH_BCOMOM$), 1.77–1.70 (1H, m, $C(OTES)CH_AH_BCH_3$), 1.67 (1H, dd, *J* 14.4, 2.9 Hz, $CHCH_AH_BCOMOM$), 1.65–1.58 (1H, m, $C(OTES)CH_AH_BCH_3$), 1.57–1.51 (1H, m, $CHCH_AH_BCH_3$), 1.51–1.43 (1H, m, $CHCH_AH_BCH_3$), 1.02 (3H, t, *J* 7.4 Hz, $CHCH_2CH_3$), 0.98–0.94 (9H, overlapping, $Si(CH_2CH_3)_3$), 0.89 (3H, t, *J* 7.7 Hz, $C(OMOM)CH_2CH_3$), 0.60 (6H, q, *J* 7.9 Hz, $Si(CH_2CH_3)_3$); δ_C (150 MHz, $CDCl_3$) 91.1, 88.7, 80.5, 68.9, 65.8, 55.5, 38.9, 29.9, 27.5, 26.5, 11.5, 7.6, 6.8 (3 overlapping), 4.4 (3 overlapping); HRMS (ESI): MNa^+, found 351.2322. $C_{18}H_{36}NaO_3Si^+$ requires 351.2331.

4.8 Chapter summary

Chapter 4 outlines an extensive effort to understand the advantages and limitations associated with different approaches toward the synthesis of more complex furanylidene scaffolds. The aldol methodology and biomimetic cyclisation/double dehydration cascade reaction developed in Chapter 3 was applied to an analogous aldehyde substrate, which was poised to generate a late stage intermediate to many related furanylidene-containing metabolites. Although this target was achieved, the

yield and reproducibility of the key aldol and cyclisation events was poor; and the target itself, which requires oxidation of the pendent alcohol for extension of the lipophilic tether, was sensitive to unwanted oxidation reactions of the furanylidene heterocycle under Swern conditions and on treatment with PCC (Chapter 6).

Finally, the failed attempts outlined in Chapter 4 led rationally to the design of a final strategy, which aimed to capitalise on the advantages and address limitations of the first approaches. Importantly, this new strategy avoids the application and removal of protecting groups that are unstable to conditions for the sodio-lithio aldol reaction and cyclisation/dehydration cascade; and attempts to minimise changes in oxidation state throughout the synthesis to improve step economy and yield (Chapter 5).

4.9 References and notes

1. M. D. Norris and M. V. Perkins, *Tetrahedron*, 2013, **69**, 9813.
2. E. A. Santos, A. L. Quintela, E. G. Ferreira, T. S. Sousa, F. d. C. L. Pinto, E. Hajdu, M. S. Carvalho, S. Salani, D. D. Rocha, D. V. Wilke, M. d. C. M. Torres, P. C. Jimenez, E. R. Silveira, J. J. La Clair, O. D. L. Pessoa and L. V. Costa-Lotufo, *J. Nat. Prod.*, 2015, **78**, 996.
3. E. W. Schmidt and D. J. Faulkner, *Tetrahedron Lett.*, 1996, **37**, 6681.
4. M. Akiyama, Y. Isoda, M. Nishimoto, A. Kobayashi, D. Togawa, N. Hirao, A. Kuboki and S. Ohira, *Tetrahedron Lett.*, 2005, **46**, 7483.
5. P. R. Allen, M. A. Brimble and H. Prabaharan, *J. Chem. Soc., Perkins Trans. 1*, 2001, 379.
6. P. Wipf and C. Kendall, *Topics Organomet. Chem.*, 2008, **8**, 1; and references therein.
7. K. Miwa, T. Aoyama and T. Shioiri, *Synlett*, 1994, 107.
8. A. B. Smith, S. Dong, R. J. Fox, J. B. Brenneman, J. A. Vanecko and T. Maegawa, *Tetrahedron*, 2011, **67**, 9809.

5. Biomimetic total synthesis of gracilioethers B and C

After developing an effective method for constructing the [2(5*H*)-furanylidene] ethanoate (furanylidene) core of spongosoritin A and the gracilioethers (Chapter 3); and extensive efforts to validate a strategy for the total synthesis of these natural products (Chapter 4), an efficient and enantioselective route to the polyketide metabolites gracilioethers B and C was finally established. Notably, issues regarding the oxidation state adjustments of synthetic intermediates *en route* to the natural products were solved by masking aldehydes as methyl acetals; and the key biomimetic transformation, a cyclisation/dehydration cascade, was re-engineered to maximise step economy and tolerate non-participating functional groups.

Chapter 5 details the 'biomimetic total synthesis of gracilioethers B and C' as prepared in an article with the same title and published in the refereed journal *Organic Letters*, American Chemical Society on 26 February 2015 (DOI: 10.1021/ol503695j). Preparative procedures and analytical data (Section 5.5) presented in this chapter/publication were collected by the candidate at the Department of Chemistry, Princeton University while enrolled externally at Flinders University and with the support of the Fulbright Alumni (WG Walker) Postgraduate Scholarship. The candidate researched, planned, executed and prepared the following chapter/published article with full intellectual and practical contribution with due guidance and only minor textual editing from co-authors throughout manuscript preparation and final publishing; and is listed as the primary author of this work.

5.1 Biomimetic total synthesis of gracilioethers B and C

Total syntheses of the marine polyketide metabolites gracilioethers B and C have been realised in 9 steps (40% overall yield) and 10 steps (34% overall yield), respectively. The [2(5*H*)-furanylidene]ethanoate (furanylidene) motif was constructed in a transacetalisation/dehydration cascade of an advanced β-ketoester intermediate, which was designed to mimic a postulated biosynthetic precursor to the natural products (Scheme 5.1). The relative and absolute configurations of gracilioethers B and C are confirmed as (6*R*,8*R*) and (6*R*,8*R*,11*S*), respectively.

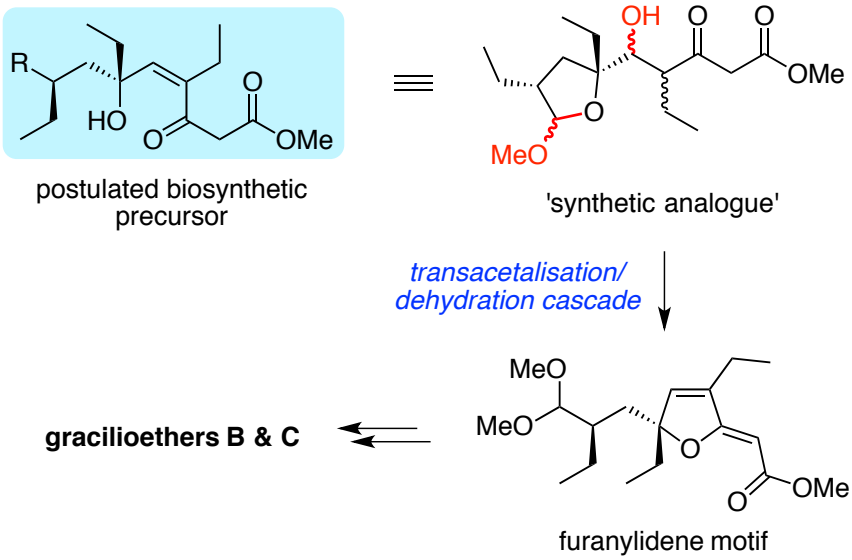

Scheme 5.1: Biomimetic total synthesis of gracilioethers B and C.

5.2 Introduction

The polyketide secondary metabolites gracilioethers A–K, plakilactones A–H,[1–5] and a number of related compounds[6–13] were recently isolated from marine sponges of the genera *Plakortis*, *Plakinastrella* and *Agelas*. A number of these have shown significant antimalarial activity,[1,3] moderate inhibition of *Leishmaniasis major*,[1,11] pregnane-X-receptor (PXR) agonistic activity,[4] and antifungal properties.[12] Gracilioethers B (**85**) and C (**86**) (Figure 5.1) were also identified as agonists of peroxisome proliferator-activated receptor γ (PPARγ).[2] To date, few studies have

focused on developing methods for the synthetic preparation of metabolites in this family.[14–18]

We recently proposed a plausible biosynthetic origin of metabolites containing the [2(5*H*)-furanylidene]ethanoate (furanylidene) motif by Kornblum–DeLaMare rearrangement,[19,20] cyclisation, and dehydration of related endoperoxides (Scheme 5.2) and demonstrated the utility of hydroxy β-ketoesters such as **192** in the synthesis of furanylidene scaffolds (Chapter 3).[16] Herein we report application of this methodology to achieve total synthesis of gracilioethers B (**85**) and C (**86**).

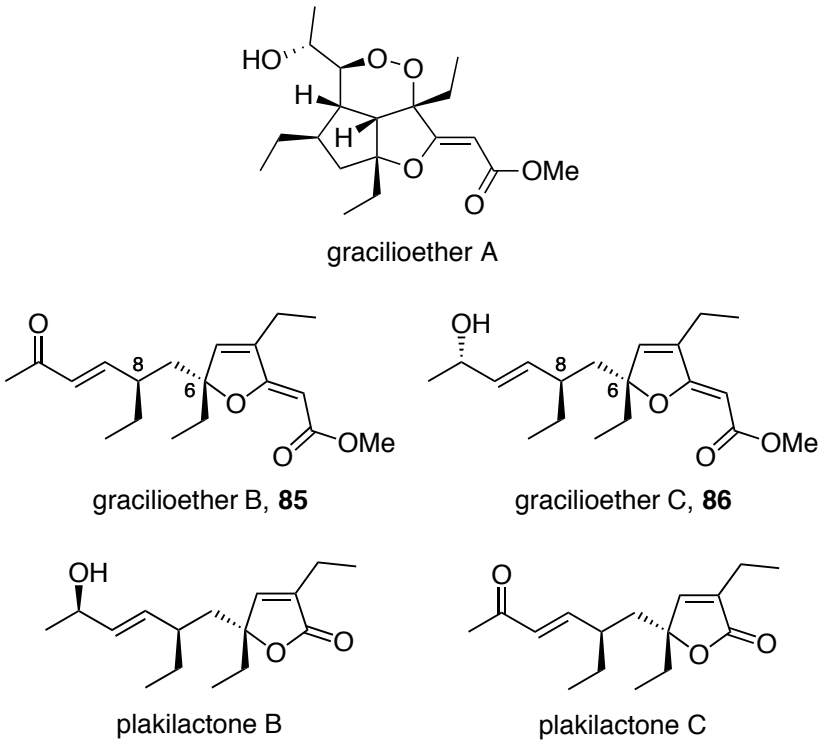

Figure 5.1: Reported structures of gracilioethers B and C with (*R*,*R*) configuration assumed at C6 and C8; and the oxygenated co-isolates gracilioether A, plakilactone B and plakilactone C.

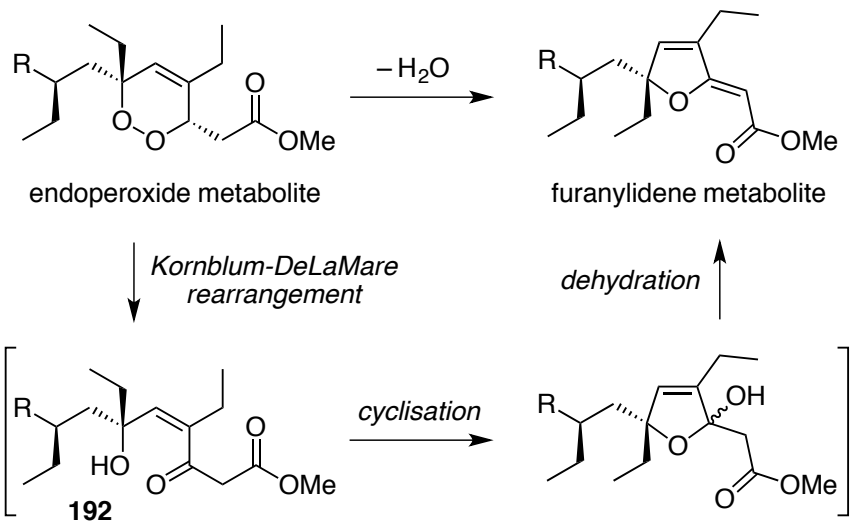

Scheme 5.2: Postulated biosynthetic origin of furanylidene metabolites.

5.3 Results and discussion

We reasoned that the relative and absolute configurations of both gracilioethers B and C at C6 and C8 were most likely to be (*R*,*R*). Our assumption was based, first, on the total synthesis and stereochemical elucidation of a similar metabolite,[14] '*des*-hydroxygracilioether C,' found unequivocally to have (6*R*,8*R*) configuration and, second, the likelihood that gracilioethers B and C share a common biosynthetic origin to the endoperoxide co-isolate gracilioether A, whose relative and absolute configuration was determined as (6*R*,8*R*) by chemical derivatisation and NMR analysis.[1] Compound **85** was thus identified as the structure most likely to be consistent with natural gracilioether B and became the primary target of our strategy, since selective reduction to the corresponding allyl alcohol **86** might be possible by methods of asymmetric carbonyl hydrogenation developed by Noyori.[21,22]

Disconnection of the unsaturated methyl ketone of **85**, which may be installed by Horner–Wadsworth–Emmons olefination, unveiled aldehyde dimethyl acetal **88** as a key late stage intermediate (Scheme 5.3). We envisaged that the furanylidene ring system and correct oxidation state of **88** might be reached in a single cascade reaction of alcohol **87** (a synthetic analogue of **192**) by transacetalisation to the putative intermediate **193** before dehydration. Presumably this would occur via a number of stabilised carbocation intermediates, which we have described previously (Chapter 3).[16] Another advantage of our design was the potential to access alcohol **87** directly from the

aldol reaction of methyl 3-oxohexanoate with aldehyde **191** that could be assembled in a number of steps from olefin **169**.

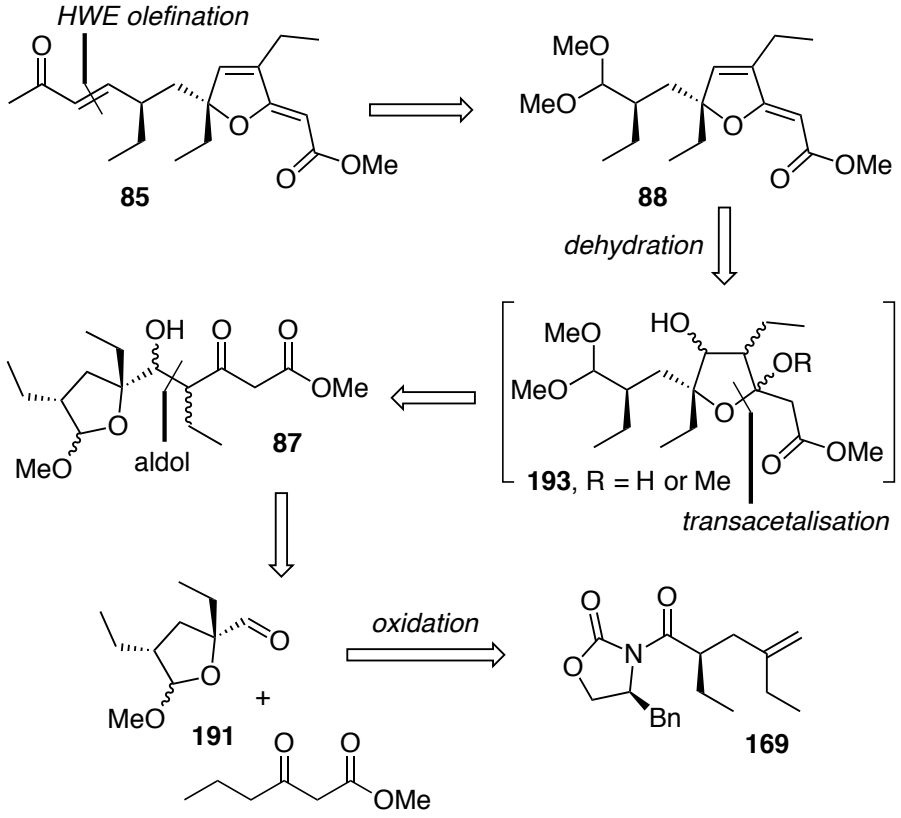

Scheme 5.3: Strategy for a biomimetic total synthesis of gracilioether B.

To begin, **169** was prepared in good yield and as a single diastereomer by alkylation of the readily available oxazolidinone **170** with known allyl iodide 2-(iodomethyl)but-1-ene [23] (Scheme 5.4). Capitalising on Brimble's[23] finding of reverse Sharpless-mnemonic dihydroxylation of a substrate similar to **169**, treatment with catalytic $K_2OsO_4 \cdot 2H_2O$ and $(DHQ)_2PHAL$ with K_2CO_3 and $K_3[Fe(CN)_6]$ (purchased as commercially available AD-mix-α) in a 1:1 mixture of ^{t}BuOH and H_2O at –5 °C effected oxidation and concomitant lactonisation with good selectivity (9:1) for the desired *syn*-lactone **165** (Chapter 4), which was inseparable from the minor *anti*-diastereomer (with (*S*) configuration at C4). Reduction with DIBAL was followed immediately by conversion of the resulting lactol isomers to the configurationally stable methyl acetal **194** (as a 3:1 mixture of acetal stereoisomers), and the corresponding C4-epimer in a combined yield of 83%. Oxidation with catalytic TPAP and NMO under standard conditions developed by Ley[24] cleanly afforded aldehyde **195**, still as an

inseparable mixture. Despite attempts to remove the undesired epimers produced in this sequence, separation of the C4-epimer was not possible by column chromatography.

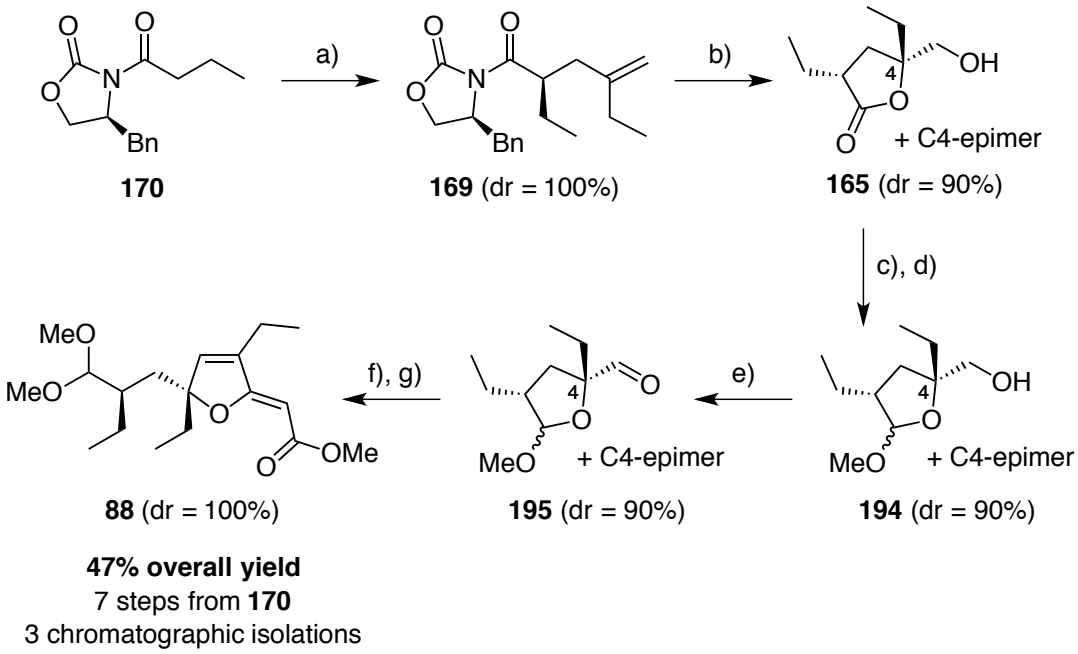

Scheme 5.4: Synthesis of aldehyde **195**, aldol condensation and transacetalisation/ dehydration to furanylidene aldehyde dimethyl acetal **88**. a) LDA, THF, –78 °C to r.t., 20 min, then 2-(iodomethyl)but-1-ene, –78 °C to r.t., 3 h, 80%; b) AD-mix-α, ^{t}BuOH, H_2O, –5 °C, 15 h, 99%; c) DIBAL, CH_2Cl_2, –78 °C, 2.5 h; then d) CH_3OH, AcCl, $CH(OCH_3)_3$, 0 °C, 4 h, 83% over 2 steps; e) TPAP, NMO, 4 Å MS, CH_2Cl_2, r.t., 1 h, 97%; f) methyl 3-oxohexanoate (treated with NaH and ^{n}BuLi), THF, –78 °C to r.t., 3 h; then g) CH_3OH, AcCl, $CH(OCH_3)_3$, r.t., 15 h, 74 % over 2 steps.

Aldehyde **195** was then added to a solution of the sodio-lithio dianion of methyl 3-oxohexanoate, preformed by treating the parent β-ketoester with NaH followed by ^{n}BuLi.[25] Gratifyingly, the anticipated aldol reaction appeared to proceed smoothly on warming from –78 °C to room temperature yielding a complex isomeric mixture of alcohol **87**. Rather than attempting to isolate intermediates, the resulting mixture was simply treated with dry HCl (generated in situ from acetyl chloride), MeOH, and excess $CH(OMe)_3$ at 20 °C overnight (15 h). Remarkably, NMR analysis of this final material showed that the complex series of spectral peaks observed on completion of the aldol reaction had mostly resolved to a single set, which was identified as aldehyde dimethyl acetal **88** and isolated in 74% yield as a single isomer after flash chromatography.

Consistent with our previous study of furanylidene ring systems, we observed complete selectivity for *Z* geometry of the exocyclic olefin (Chapter 3).[26]

We were also pleased to find that the aldehyde dimethyl acetal expected to arise from aldol reaction and transacetalisation/dehydration of the C4-epimer of **195** was not isolated. It appears that reaction of the C4-epimeric aldehydes does not proceed readily under our reaction conditions. This has allowed us to streamline the middle section of our strategy by removing the need to attempt chromatographic isolation of **194** and **195**. Furanylidene **88**, a pivotal late stage intermediate in our strategy, was thus prepared in 47% yield over seven preparative steps from **170** and required only three applications of chromatographic purification.

Transacetalisation[27] of **88** with catalytic $In(OTf)_3$ and Me_2CO followed immediately by Horner–Wadsworth–Emmons olefination with diethyl (2-oxopropyl)phosphonate afforded **85** (Scheme 5.5, Figure 5.2). The ^1H and ^{13}C NMR data (Section 8.1.1) obtained were consistent with that reported for natural gracilioether B[1] (Table 5.1), and optical rotation confirmed that **85** had the same absolute configuration. We were also pleased to find that reduction of the pendant methyl ketone with catalytic $RuCl_2$[(*R*)-Xylbinap][(*R*)-Daipen] under H_2 (4 atm), which has been shown to give excellent selectivity for generating the corresponding (*S*)-allyl alcohol,[21,22] yielded **86** directly (Scheme 5.6, Figure 5.3). Spectroscopic analysis revealed overwhelming similarity with that reported for natural gracilioether C (Section 8.1.2, Table 5.2) and once again, optical rotation measurements confirmed the same absolute configuration.[29] The assignment 11*S* is also consistent with the Mosher's ester analysis of natural gracilioether C.

It was also possible to selectively reduce **85** with the enantiomeric catalyst $RuCl_2$[(*S*)-Xylbinap][(*S*)-Daipen] under H_2 (4 atm) yielding **196** and thus demonstrating that asymmetric induction is under catalyst control. Similarly, reduction of **85** with $NaBH_4$ and $CeCl_3 \cdot 7H_2O$ in MeOH at 0 °C yielded **86** and **196** in approximately the ratio 1:1, further demonstrating a lack of facial bias. The ^1H and ^{13}C NMR spectra of **196** in CD_3OD, although very similar to the spectra of **86**, were inconsistent with those of the natural material (Table 5.2). Hence, the structures as well as relative and absolute configurations of gracilioethers B and C are confirmed as (6*R*,8*R*)-**85** and (6*R*,8*R*,11*S*)-**86**, respectively.

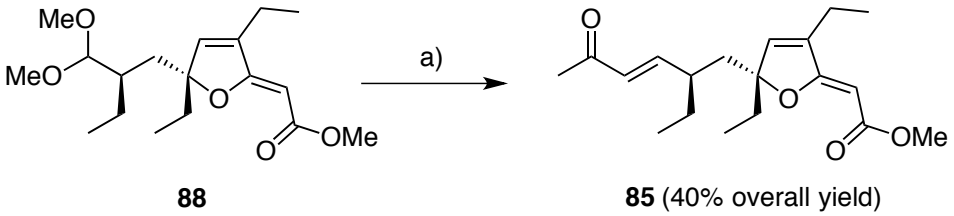

88 **85** (40% overall yield)

Scheme 5.5: Synthesis of **85** from **88**. a) $In(OTf)_3$, $(CH_3)_2CO$, r.t., 1 h; then $CH_3COCH_2PO(OEt)_2$, NaH, THF, 0 °C, 3 h, 86% over 2 steps.

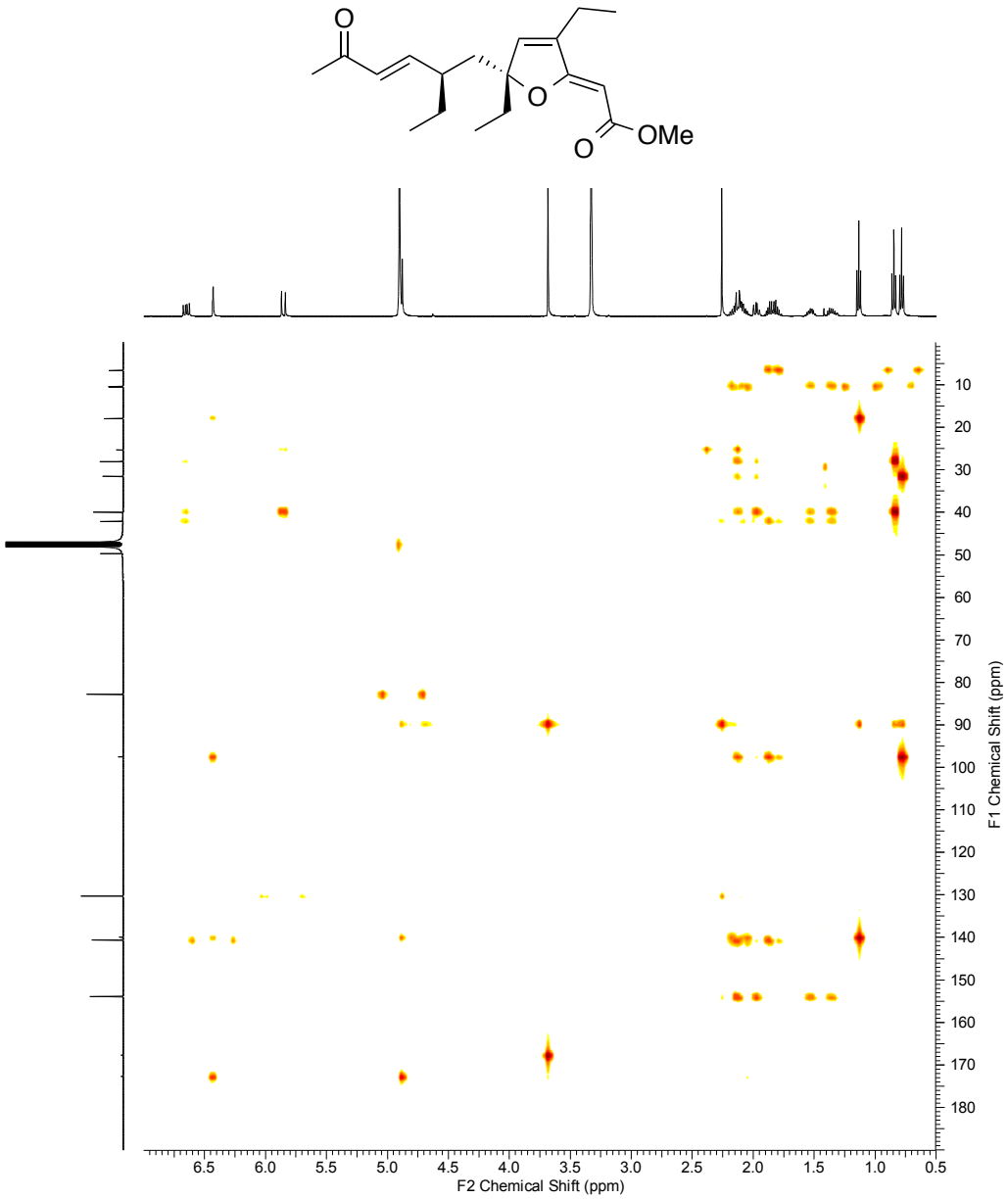

Figure 5.2: HMBC spectrum of synthetic gracilioether B (**85**) with 1D ^{1}H NMR (500 MHz, CD_3OD) and ^{13}C NMR (125 MHz, CD_3OD) projections.

Table 5.1: Tabulated ^{1}H NMR and ^{13}C NMR data of **85** with direct comparison to natural gracilioether B.

Carbon	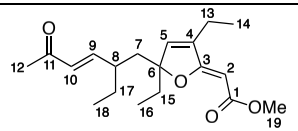		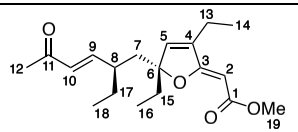		
	Natural gracilioether B[1]		Synthetic **85**		
	δ_H (600 MHz, CD_3OD) (ppm)	δ_C (150 MHz, CD_3OD) (ppm)	δ_H (500 MHz, CD_3OD) (ppm)	δ_C (125 MHz, CD_3OD) (ppm)	$\Delta\delta_C$ (ppm)
1		168.8		169.2	+0.4
2	4.85 (1H, s)	84.3	4.88 (1H, s)	84.3	+0.0
3		174.1		174.1	+0.0
4		142.1		141.4	–0.7
5	6.40 (1H, s)	142.1	6.43 (1H, s)	142.1	+0.0
6		99.0		99.0	+0.0
7	2.08 (1H, m)	43.6	2.21–2.03 (1H, overlapping)	43.6	+0.0
	1.94 (1H, m)		2.01–1.93 (1H, m)		
8	2.08 (1H, m)	41.4	2.21–2.03 (1H, overlapping)	41.4	+0.0
9	6.62 (1H, dd, *J* 15.8, 8.9 Hz)	155.3	6.65 (1H, dd, *J* 16.0, 9.3 Hz)	155.3	+0.0
10	5.82 (1H, d, *J* 15.8 Hz)	131.7	5.85 (1H, d, *J* 16.0 Hz)	131.7	+0.0
11		204.2[a]		201.3	–2.9[a]
12	2.23 (3H, s)	26.8	2.26 (3H, s)	26.8	+0.0
13	2.13 (1H, m)	19.4	2.21–2.03 (2H, overlapping)	19.4	+0.0
	2.05 (1H, m)				
14	1.10 (3H, t, *J* 7.6 Hz)	12.0	1.13 (3H, t, *J* 7.4 Hz)	12.0	+0.0
15	1.83 (1H, p, *J* 7.6 Hz)	33.0	1.87 (1H, p, *J* 7.2 Hz)	33.0	+0.0
	1.78 (1H, p, *J* 7.6 Hz)		1.82 (1H, p, *J* 7.2 Hz)		
16	0.75 (3H, t, *J* 7.6 Hz)	8.1	0.78 (3H, t, *J* 7.4 Hz)	8.1	+0.0
17	1.50 (1H, m)	29.5	1.58–1.48 (1H, m)	29.5	+0.0
	1.32 (1H, m)		1.41–1.30 (1H, m)		
18	0.82 (3H, t, *J* 7.6 Hz)	11.8	0.85 (3H, t, *J* 7.4 Hz)	11.8	+0.0
19	3.65 (3H, s)	51.1	3.68 (3H, s)	51.1	+0.0

[a] The HMBC spectrum of natural gracilioether B clearly shows a chemical shift for carbon 11 less than 204.2 ppm and it appears that this was incorrectly reported in the article describing its isolation.[1]

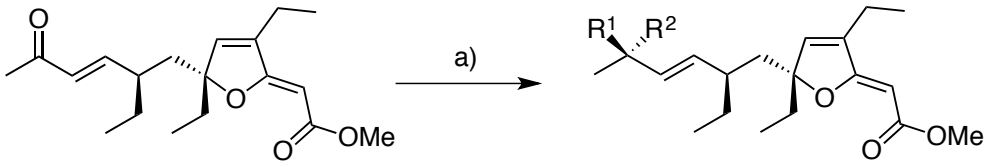

85

86 R^1 = H, R^2 = OH (cat. **A**, 85%)
196 R^1 = OH, R^2 = H (cat. **B**, 91%)

Scheme 5.6: Synthesis of **86** and **196**. a) cat. **A** ($RuCl_2$[(*R*)-Xylbinap][(*R*)-Daipen]) or cat. **B** ($RuCl_2$[(*S*)-Xylbinap][(*S*)-Daipen]) (1.6 mol%), H_2 (4 atm), K_2CO_3, ^{i}PrOH, 30 °C, 48 h.

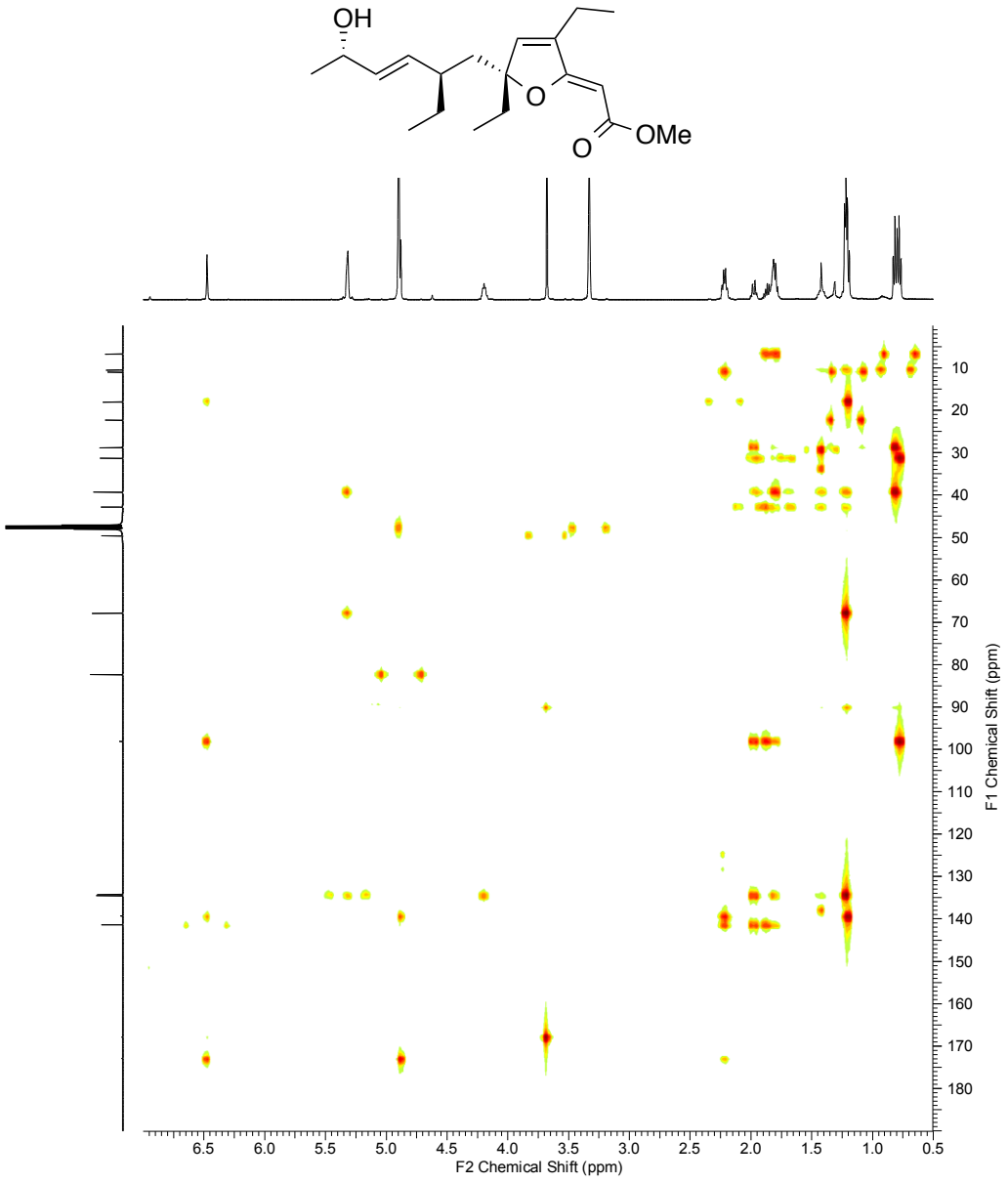

Figure 5.3: HMBC spectrum of synthetic gracilioether C (**86**) with 1D ^{1}H NMR (500 MHz, CD_3OD) and ^{13}C NMR (125 MHz, CD_3OD) projections.

Table 5.2: Tabulated ^{1}H NMR and ^{13}C NMR data of **86** and **196** with direct comparison to natural gracilioether C (most significant differences highlighted in blue).

Carbon	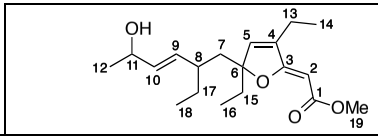		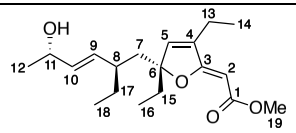			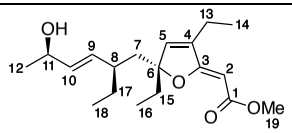		
	Natural gracilioether C[1]		Synthetic **86**			Synthetic **196**		
	δ_H (600 MHz, CD_3OD) (ppm)	δ_C (150 MHz, CD_3OD) (ppm)	δ_H (500 MHz, CD_3OD) (ppm)	δ_C (125 MHz, CD_3OD) (ppm)	$\Delta\delta_C$ (ppm)	δ_H (500 MHz, CD_3OD) (ppm)	δ_C (125 MHz, CD_3OD) (ppm)	$\Delta\delta_C$ (ppm)
1		169.0		169.3	+0.3		169.3	+0.3
2	4.82 (1H, s)	83.8	4.85 (1H, s)	83.8	+0.0	4.85 (1H, s)	83.8	+0.0
3		174.3		174.3	+0.0		174.3	+0.0
4		140.7		140.7	+0.0		140.7	+0.0
5	**6.44 (1H, s)**	**142.8**	**6.44 (1H, s)**	**142.8**	**+0.0**	**6.42 (1H, d, *J* 1.7 Hz)**	**142.7**	**–0.1**
6		99.6		99.6	+0.0		99.5	–0.1
7	1.94 (1H, d, *J* 10.3 Hz) 1.78 (1H, m)	44.3	1.95 (1H, dd, *J* 17.9, 7.1 Hz) 1.81–1.75 (1H, overlapping)	44.3	+0.0	1.97–1.93 (1H, m) 1.87–1.72 (1H, overlapping)	44.3	+0.0
8	1.78 (1H, m)	40.7	1.81–1.75 (1H, overlapping)	40.7	+0.0	1.87–1.72 (1H, overlapping)	40.6	–0.1
9	**5.29 (1H, m)**	**135.7**	**5.29 (1H, overlapping)**	**135.7**	**+0.0**	**5.33 (1H, dd, *J* 15.5, 7.5 Hz)**	**135.6**	**–0.1**
10	**5.29 (1H, m)**	**135.9**	**5.29 (1H, overlapping)**	**135.9**	**+0.0**	**5.27 (1H, dd, *J* 15.5, 5.4 Hz)**	**135.6**	**–0.3**
11	4.16 (1H, p, *J* 6.2, 5.5 Hz)	69.3	4.19–4.14 (1H, m)	69.3	+0.0	4.16 (1H, m)	69.1	–0.2
12	1.19 (3H, d, *J* 6.2 Hz)	23.7	1.22–1.16 (3H, overlapping)	23.7	+0.0	1.19 (3H, d, *J* 6.2 Hz)	23.9	+0.2
13	**2.18 (2H, m)**	**19.5**	**2.21–2.16 (2H, m)**	**19.5**	**+0.0**	**2.18 (2H, qd, *J* 7.4, 1.7 Hz)**	**19.5**	**+0.0**
14	1.17 (3H, t, *J* 7.2 Hz)	12.4	1.22–1.16 (3H, overlapping)	12.4	+0.0	1.17 (3H, t, *J* 7.4 Hz)	12.4	+0.0
15	1.83 (1H, m, *J* 7.2 Hz) 1.78 (1H, m)	32.8	1.86–1.80 (1H, m) 1.81–1.75 (1H, overlapping)	32.7	–0.1	1.87–1.72 (2H, overlapping)	33.0	+0.2
16	0.75 (3H, t, *J* 7.2 Hz)	8.1	0.75 (3H, t, *J* 7.2 Hz)	8.2	+0.1	0.75 (3H, t, *J* 7.4 Hz)	8.1	+0.0
17	1.39 (1H, m) 1.21 (1H, m)	30.2	1.42–1.37 (1H, m) 1.22–1.16 (1H, overlapping)	30.2	+0.0	1.42–1.36 (1H, m) 1.26–1.18 (1H, m)	30.3	+0.1
18	0.78 (3H, t, *J* 7.2 Hz)	11.9	0.79 (3H, t, *J* 7.6 Hz)	11.9	+0.0	0.80 (3H, *J* 7.4 Hz)	11.9	+0.0
19	3.65 (1H, s)	51.1	3.65 (3H, s)	51.1	+0.0	3.65 (3H, s)	51.1	+0.0

5.4 Concluding remarks

In summary, total syntheses of gracilioethers B and C were accomplished in 9 steps (40% overall yield) and 10 steps (34% overall yield), respectively. The [2(5*H*)-furanylidene]ethanoate (furanylidene) motif was installed in a facile biomimetic transacetalisation/dehydration cascade, allowing the development of an exceptionally short and high yielding synthetic route to the natural products. The structures as well as relative and absolute configurations of gracilioethers B and C are confirmed as (6*R*,8*R*)-**85** and (6*R*,8*R*,11*S*)-**86**, respectively.

5.5 Preparative procedures and analytical data

5.5.1 General experimental details

For general experimental details, including information on reaction solvents, chromatography, analytical equipment and reported data, see Section 3.5.1. Circular dichroism measurements were obtained on a Chirascan CD Spectrometer with MeOH as solvent for each analyte.

*5.5.2 (4S)-4-Benzyl-3-[(2R)-2-ethyl-4-methylidenehexanoyl]-1,3-oxazolidin-2-one (**169**)*

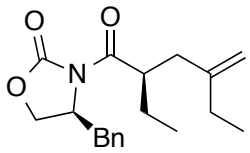

^{n}BuLi (23.1 mL, 1.6 M in hexane, 37.0 mmol) was added dropwise to a stirred solution of (^{i}Pr)$_2$NH (5.27 mL, 37.6 mmol) in THF (50 mL) at –78 °C. Stirring continued at –78 °C for 30 min before dropwise addition of (4*S*)-4-benzyl-3-butanoyl-1,3-oxazolidin-2-one (**170**) (8.45 g, 34.2 mmol) in THF (25 mL) followed by warming to room temperature (20 °C) over 20 min. The mixture was cooled to –78 °C before dropwise addition of 2-(iodomethyl)but-1-ene (7.41 g, 37.8 mmol) in THF (25 mL) followed by warming to room temperature (20 °C) over 3 h and quenching with the addition of NH_4Cl (satd aq). The organic layer was separated and aqueous extracted with Et_2O. The combined extracts were washed with brine, dried (Na_2SO_4) and concentrated *in vacuo*. Flash chromatography yielded the *title compound* (8.63 g, 80%)

as a colourless oil: R_f (20% EtOAc/hexane) 0.41; $[\alpha]^{20}_D$ +24.7 (*c* 0.16, $CHCl_3$); ν_{max} (thin film) 2968, 2935, 2878, 1776, 1698, 1455, 1390, 1351, 1212, 1107, 1029, 703 cm^{-1}; δ_H (500 MHz, $CDCl_3$) 7.33 (2H, m, Ar*H*), 7.27 (1H, m, Ar*H*), 7.22 (2H, m, Ar*H*), 4.79 (2H, s, C=CH_2), 4.70 (1H, tdd, *J* 3.3, 7.5, 9.8 Hz, C*H*Bn), 4.15 (2H, m, CH_2Ph), 4.05 (1H, tt, *J* 6.0, 8.5 Hz, C*H*CH_2CH_3), 3.27 (1H, dd, *J* 3.3, 13.4 Hz, C$H_A$$H_B$O), 2.67 (1H, dd, *J* 9.8, 13.4 Hz, $CH_A$$H_B$O), 2.53 (1H, dd, *J* 8.5, 14.1 Hz, C$H_A$$H_B$C=$CH_2$), 2.20, (1H, dd, *J* 6.0, 14.1 Hz, $CH_A$$H_B$C=$CH_2$), 2.09 (2H, m, CC$H_2$$CH_3$), 1.70 (1H, qdd, *J* 7.4, 8.5, 21.2 Hz, CHC$H_A$$H_B$$CH_3$), 1.56 (1H, dqd, *J* 6.0, 7.4, 21.2 Hz, $CHCH_A$$H_B$$CH_3$), 1.05 (3H, t, *J* 7.4 Hz, $CCH_2C$$H_3$), 0.93 (3H, t, *J* 7.4 Hz, $CHCH_2CH_3$); δ_C (125 MHz, $CDCl_3$) 176.4, 153.2, 148.7, 135.4, 129.4, 128.9, 127.3, 109.9, 65.8, 55.4, 42.2, 38.7, 37.9, 28.6, 25.4, 12.2, 11.6; HRMS (ESI): MH^+, found 316.1906. $C_{19}H_{26}NO_3^+$ requires 316.1907.

*5.5.3 (3R,5R)-3,5-Diethyl-5-(hydroxymethyl)oxolan-2-one (**165**)*

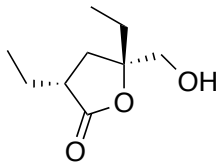

AD-mix-α (18.5 g, 0.17 mol% $K_2OsO_4.2H_2O$; Sigma Aldrich) was added in small portions to a rapidly stirred suspension of **169** (5.14 g, 29.8 mmol), ^{t}BuOH (27 mL) and water (27 mL) at –5 °C. Stirring continued at –5 °C for 15 h before quenching with the addition of Na_2SO_3 (2.5 g), water (50 mL) and EtOAc (70 mL). The phases were partitioned, organic layer separated and aqueous extracted with EtOAc. The combined extracts were washed with brine, dried (Na_2SO_4) and concentrated *in vacuo*. Purification by column chromatography yielded the *title compound* and its C5 epimer (2.78 g, 99%) as an inseparable 9:1 mixture of stereoisomers: R_f (50% EtOAc/hexane) 0.31; ν_{max} (thin film) 3444, 2969, 2937, 2880, 1753, 1464, 1384, 1214, 1158, 1115, 1067, 969, 956 cm^{-1}; δ_H (500 MHz, $CDCl_3$) major isomer 3.75 (1H, dd, *J* 12.2, 4.3 Hz, C$H_A$$H_B$OH), 3.46 (1H, dd, *J* 12.2, 7.3 Hz, $CH_A$$H_B$OH), 2.67 (1H, tdd, *J* 10.2, 9.3, 4.7 Hz, C*H*CH_2), 2.12 (1H, dd, *J* 12.9, 10.2 Hz, C$H_A$$H_B$$CCH_2$OH), 2.01 (1H, br, O*H*), 1.99 (1H, dd, *J* 12.9, 10.2 Hz, $CH_A$$H_B$$CCH_2$OH), 1.91 (1H, dtd, *J* 13.8, 7.5, 4.6 Hz, CHC$H_A$$H_B$$CH_3$), 1.69 (2H, q, *J* 7.6 Hz, C(CH_2OH)C$H_2$$CH_3$), 1.54 (1H, ddt, *J* 13.8, 9.3, 7.5 Hz, $CHCH_A$$H_B$$CH_3$), 0.99 (3H, t, *J* 7.5 Hz, $CHCH_2C$$H_3$), 0.95 (3H, t, *J* 7.6 Hz, C(CH_2OH)$CH_2C$$H_3$); diagnostic peaks observed for the minor isomer 3.70 (1H, dd, *J* 11.9, 5.0 Hz, C$H_A$$H_B$OH), 3.58 (1H, dd, *J* 11.9, 4.6 Hz, $CH_A$$H_B$OH), 2.82 (1H, m,

C*H*CH_2), 2.35 (1H, dd, *J* 13.0, 10.1 Hz, C$H_A$$H_B$$CH_2OH$), 1.72 (1H, dd, *J* 10.1, 6.0 Hz, $CH_A$$H_B$$CH_2OH$); δ_C (125 MHz, $CDCl_3$) 178.8, 86.8, 66.5, 41.9, 31.8, 28.8, 24.1, 11.7, 7.8; HRMS (ESI): MNa^+, found 195.0989. $C_9H_{16}NaO_3^+$ requires 195.0992.

*5.5.4 [(2R,4R)-2,4-Diethyl-5-methoxyoxolan-2-yl]methanol (**194**)*

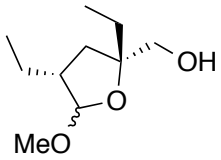

DIBAL (6.9 mL, 1.0 M in PhMe; 6.9 mmol) was added dropwise to a rapidly stirred solution of **165** (9:1 ratio of C5 epimers from previous reaction, 0.50 g, 2.9 mmol) in CH_2Cl_2 (35 mL) at –78 °C. Stirring continued at –78 °C for 2.5 h before quenching with the addition of MeOH. Once brought to room temperature (20 °C) the mixture was poured into a rapidly stirred suspension of sodium potassium tartrate (50% satd aq) and CH_2Cl_2. After 1 h the organic phase was separated and aqueous extracted with CH_2Cl_2. The combined extracts were dried (Na_2SO_4) and concentrated *in vacuo*. The crude material was diluted in MeOH (30 mL), $CH(OMe)_3$ (0.64 mL, 5.9 mmol) and cooled to 0 °C before dropwise addition of AcCl (0.12 mL, 1.7 mmol). Stirring continued at 0 °C for 4 h before quenching with the addition of K_2CO_3 (0.40 g, 2.9 mmol) and concentrating to approximately 5 mL *in vacuo*. The residue was diluted with $NaHCO_3$ (50% satd aq) and extracted with CH_2Cl_2. The combined extracts were dried (Na_2SO_4) and concentrated *in vacuo* to yield the *title compound* (0.46 g, 83% over 2 steps) as a separable pair of acetal stereoisomers in a 3:1 ratio, each of which were inseparable from their corresponding C4 epimer (chromatography was employed for characterisation of each pair of acetal diastereomers however, the crude mixture of isomers was otherwise used in the next step without further purification): major (2*R*,4*R*) isomer R_f (20% EtOAc/hexane) 0.36; δ_H (500 MHz, $CDCl_3$) 4.78 (1H, d, *J* 4.7 Hz, C*H*OCH_3), 3.52 (1H, dd, *J* 11.2, 2.9 Hz, C$H_A$$H_B$OH), 3.41 (3H, s, OC$H_3$), 3.37 (1H, dd, *J* 11.2, 8.7 Hz, $CH_A$$H_B$OH), 2.82 (1H, dd, *J* 8.7, 2.9 Hz, CH_2O*H*), 2.10 (1H, m, $CHCH_2CH_3$), 1.76 (2H, apparent d, *J* 10.4 Hz, C$H_2$$CHCH_2CH_3$), 1.57–1.45 (3H, overlapping peaks, $CH_2CCH_2CH_3$, CHC$H_A$$H_B$$CH_3$), 1.41 (1H, m, $CHCH_A$$H_B$$CH_3$), 0.90 (6H, overlapping peaks, $CH_2CCH_2CH_3$, $CHCH_2CH_3$); δ_C (125 MHz, $CDCl_3$) 106.2, 88.3, 67.5, 55.5, 46.8, 32.9, 30.0, 21.7, 12.9, 8.3; minor (2*R*,4*R*) isomer R_f (20% EtOAc/hexane) 0.26; δ_H (500 MHz, $CDCl_3$) 4.65 (1H, d, *J* 3.2 Hz, C*H*OCH_3), 3.58 (1H,

dd, *J* 11.5, 4.5 Hz, CH_AH$_B$OH), 3.41–3.34 (4H, overlapping peaks, CH$_A$$H_BOH, OCH_3$), 2.12 (1H, pd, *J* 8.0, 3.2 Hz, CHCH$_2$CH$_3$), 1.94 (1H, dd, *J* 12.6, 8.0 Hz, CH_AH$_B$CHCH$_2$CH$_3$), 1.88 (1H, dd, *J* 7.9, 4.5 Hz, CH$_2$OH), 1.78–1.67 (1H, m, CH$_2$CCH_AH$_B$CH$_3$), 1.65–1.48 (3H, overlapping peaks, CH$_A$$H_B$CHCH$_2CH_3$, CHC$H_AH_BCH_3$, CH$_2CCH_A$$H_BCH_3$), 1.41–1.29 (1H, m, CHCH$_A$$H_BCH_3$), 0.92 (3H, t, *J* 7.4 Hz, CHCH$_2$CH_3), 0.88 (3H, t, *J* 7.6 Hz, CH$_2$CCH$_2$CH_3); δ_C (125 MHz, CDCl$_3$) 111.2, 87.3, 66.2, 55.5, 47.7, 35.8, 30.3, 26.0, 12.6, 8.8; combined isomers ν_{max} (thin film) 3452, 2961, 2932, 2877, 2830, 1462, 1377, 1195, 1164, 1028, 962, 872, 791, 761 cm^{-1}; HRMS (ESI): MNa$^+$, found 211.1307. C$_{10}$H$_{20}$NaO$_3^+$ requires 211.1305.

*5.5.5 (2R,4R)-2,4-Diethyl-5-methoxyoxolane-2-carbaldehyde (**195**)*

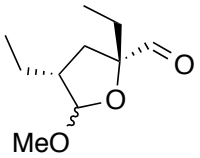

TPAP (0.039 g, 0.11 mmol) was added in a single portion to a stirred suspension of **194** (mixture of stereoisomers from previous reaction, 0.44 g, 2.3 mmol), NMO (0.42 g, 3.6 mmol), 4 Å MS (1.1 g; oven dried) and CH$_2$Cl$_2$ (5.0 mL) at room temperature (20 °C). After 1 h the mixture was passed through a thick pad of silica (eluting with excess CH$_2$Cl$_2$) and concentrated *in vacuo* to yield the *title compound* (0.42 g, 97%) as an inseparable mixture of expected stereoisomers, which were used in the next step without further purification: R_f (50% CH$_2$Cl$_2$/hexane) 0.38; ν_{max} (thin film) 2965, 2936, 2879, 1706, 1461, 1413, 1377, 1164, 1084, 1024, 940, 780 cm^{-1}; δ_H (500 MHz, CDCl$_3$) major (2*R*, 4*R*) isomer 9.57 (1H, s, CHO), 4.90 (1H, d, *J* 4.4 Hz, CHOCH$_3$), 3.39 (3H, s, OCH_3), 2.11–2.00 (1H, m, CHCH$_2$CH$_3$), 1.92–1.80 (2H, m, CH_2CCH$_2$CH$_3$), 1.80–1.66 (1H, m, CH$_2$CCH_AH$_B$CH$_3$), 1.65–1.57 (1H, m, CH$_2$CCH$_A$$H_BCH_3$), 1.54–1.45 (1H, m, CHC$H_AH_BCH_3$), 1.45–1.34 (1H, m, CHCH$_A$$H_BCH_3$), 0.95–0.85 (6H, overlapping peaks, CHCH$_2$CH_3, CCH$_2$CH_3); diagnostic peaks observed for the minor (2*R*, 4*R*) isomer 9.63 (1H, s, CHO), 4.80 (1H, s, CHOCH$_3$), 3.40 (3H, s, OCH_3); δ_C (125 MHz, CDCl$_3$) major (2*R*,4*R*) isomer: 204.4, 106.5, 89.5, 55.1, 46.1, 34.4, 28.0, 21.5, 12.8, 7.5; observed peaks for the minor (2*R*,4*R*) isomer: 204.4, 110.4, 91.0, 55.0, 47.0, 36.0, 30.6, 25.0, 12.1, 8.3; HRMS (ESI): M(–CHO)$^+$, found 157.1223. C$_9$H$_{17}$O$_2^+$ requires 157.1223.

*5.5.6 Methyl 2-[(2Z,5R)-5-[(2R)-2-(dimethoxymethyl)butyl]-3,5-diethyl-2(5H)-furanylidene]ethanoate (**88**)*

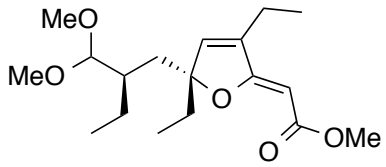

Methyl 3-oxohexanoate (0.50 g, 3.5 mmol) was added dropwise to a stirred suspension of NaH (0.28 g 60% in mineral oil, 7.0 mmol; washed with hexane before use) and THF (18 mL) at 0 °C. Stirring continued at 0 °C for 30 min before dropwise addition of ^{n}BuLi (1.2 mL, 2.5 M in hexane, 3.0 mmol) and another 30 min before dropwise addition of **195** (0.25 g, 1.4 mmol) in THF (6 mL) at −78 °C. Stirring continued for 3 h once warmed to room temperature (20 °C) before quenching with the addition of NH_4Cl (50% satd aq). The organic layer was separated and aqueous extracted with Et_2O. The combined extracts were washed with brine, dried (Na_2SO_4) and concentrated *in vacuo*. The crude material was diluted in MeOH (42 mL) and $CH(OMe)_3$ (1.4 mL, 13 mmol) before dropwise addition of AcCl (0.42 mL, 5.9 mmol) at room temperature (20 °C). Stirring continued at room temperature (20 °C) for 15 h before quenching with the addition of K_2CO_3 (1.2 g, 8.7 mmol) and concentrating to approximately 5 mL *in vacuo*. The residue was diluted with $NaHCO_3$ (50% satd aq) and extracted with CH_2Cl_2. The combined extracts were dried (Na_2SO_4) and concentrated *in vacuo*. Purification by column chromatography yielded the *title compound* (0.33 g, 74% over 2 steps) as a yellow oil: R_f (20% EtOAc/hexane) 0.30; $[\alpha]^{20}_{D}$ −122 (*c* 1.65, $CHCl_3$); ν_{max} (thin film) 2935, 2878, 2831, 1712, 1686, 1624, 1460, 1433, 1376, 1270, 1156, 1068, 1037, 963, 854, 804, 721 cm^{-1}; δ_H (500 MHz, $CDCl_3$) 6.21 (1H, s, C*H*=CCH_2CH_3), 4.81 (1H, s, C*H*CO_2CH_3), 4.15 (1H, d, *J* 4.1 Hz, C*H*$(OCH_3)_2$), 3.68 (3H, s, CO_2CH_3), 3.37 (3H, s, $CH(OCH_3)_A(OCH_3)_B$), 3.29 (3H, s, $CH(OCH_3)_A(OCH_3)_B$), 2.18 (2H, qd, *J* 7.6, 1.2 Hz, CH=CCH_2CH_3), 1.94–1.83 (2H, overlapping peaks, $CH_AH_BCHCH_2CH_3$, $CH_2CCH_AH_BCH_3$), 1.80–1.69 (2H, overlapping peaks, $CH_AH_BCHCH_2CH_3$, $CH_2CCH_AH_BCH_3$), 1.47–1.31 (3H, overlapping peaks, C*H*CH_2CH_3, CHCH_2CH_3), 1.17 (3H, t, *J* 7.4 Hz, CH=CCH_2CH_3), 0.86 (3H, t, *J* 7.3 Hz, $CHCH_2CH_3$), 0.80 (3H, t, *J* 7.4 Hz, $CH_2CCH_2CH_3$); δ_C (125 MHz, $CDCl_3$) 171.7, 166.9, 140.2, 140.0, 107.9, 98.1, 83.7, 55.7, 54.8, 50.5, 37.8, 35.7, 31.9, 23.4, 18.5, 12.2, 11.2, 8.1; HRMS (ESI): MNa^+, found 349.1983. $C_{18}H_{30}NaO_5^+$ requires 349.1985.

*5.5.7 Gracilioether B (**85**)*

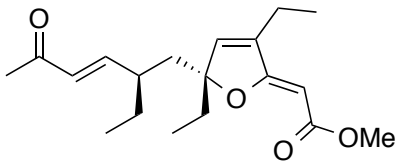

$In(OTf)_3$ (0.006 g, 0.01 mmol) was added in a single portion to a stirred solution of **88** (0.32 g, 1.0 mmol) in Me_2CO (10 mL) at room temperature (20 °C). After 1 h volatiles were removed and the mixture passed through a thick pad of silica (washing with excess 50% Et_2O/CH_2Cl_2) before concentrating *in vacuo*. The crude material was diluted in THF (5 mL) and added dropwise to a stirred suspension of NaH (0.12 g 60% in mineral oil, 3.0 mmol; washed with hexane before use), diethyl 2-oxopropylphosponate (0.39 mL, 2.0 mmol) and THF (8 mL) at 0 °C. Stirring continued at 0 °C for 3 h before quenching with the addition of NH_4Cl (50% satd aq). The organic layer was separated and aqueous extracted with Et_2O. The combined extracts were washed with brine, dried (Na_2SO_4) and concentrated *in vacuo*. Flash chromatography yielded the *title compound* (0.27 g, 86% over 2 steps) as a pale yellow oil: R_f (25% EtOAc/hexane) 0.23; $[\alpha]^{20}_D$ –370 (*c* 0.46, MeOH), lit.[1] $[\alpha]^{34.6}_D$ –120 (*c* 0.03, MeOH); $[\theta]_{218}$ +97640 (max), $[\theta]_{248}$ +74530 (max), $[\theta]_{286}$ –160420 (max); ν_{max} (thin film) 2968, 2936, 2879, 1737, 1710, 1671, 1621, 1450, 1433, 1358, 1251, 1159, 1089, 1036, 975, 870, 805, 782 cm^{-1}; δ_H (500 MHz, CD_3OD) 6.65 (1H, dd, *J* 16.0, 9.3 Hz, C*H*=CHCOCH$_3$), 6.43 (1H, s, C*H*=CCH$_2$CH$_3$), 5.85 (1H, d, *J* 16.0 Hz, C*H*COCH$_3$), 4.88 (1H, s, C*H*CO$_2$CH$_3$), 3.68 (3H, s, OC*H*$_3$), 2.26 (3H, s, COC*H*$_3$), 2.21–2.03 (4H, overlapping peaks, CH=CC*H*$_2$CH$_3$, C*H*CH$_2$CH$_3$, C*H*$_A$H$_B$CHCH$_2$CH$_3$), 2.01–1.93 (1H, m, CH$_A$*H*$_B$CHCH$_2$CH$_3$), 1.87 (1H, p, *J* 7.2 Hz, CH$_2$CC*H*$_A$H$_B$CH$_3$), 1.82 (1H, p, *J* 7.2 Hz, CH$_2$CCH$_A$*H*$_B$CH$_3$), 1.58–1.48 (1H, m, CHC*H*$_A$H$_B$CH$_3$), 1.41–1.30 (1H, m, CHCH$_A$*H*$_B$CH$_3$), 1.13 (3H, t, *J* 7.4 Hz, CH=CCH$_2$C*H*$_3$), 0.85 (3H, t, *J* 7.4 Hz, CHCH$_2$C*H*$_3$), 0.78 (3H, t, *J* 7.4 Hz, CH$_2$CCH$_2$C*H*$_3$); δ_C (125 MHz, CD_3OD) 201.3, 174.1, 169.2, 155.3, 142.1, 141.4, 131.7, 99.0, 84.3, 51.1, 43.6, 41.4, 33.0, 29.5, 26.8, 19.4, 12.0, 11.8, 8.1; HRMS (ESI): MNa^+, found 343.1882. $C_{19}H_{28}NaO_4^+$ requires 343.1880.

*5.5.8 Gracilioether C (**86**)*

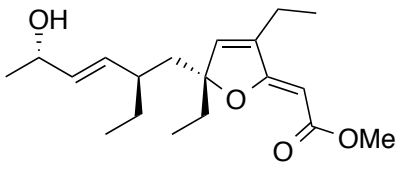

85 (0.021 g, 0.069 mmol), $RuCl_2$[(*R*)-xylbinap][(*R*)-daipen] (0.0014 g, 1.7 mol%), K_2CO_3 (0.024 g, 0.17 mmol) and ^{i}PrOH (1.0 mL) were stirred at 30 °C under an atmosphere of H_2 (4 atm) in a sealed vessel for 48 h. Volatiles were removed and the mixture passed through a thick pad of silica (washing with excess 50% EtOAc/hexane) before concentrating *in vacuo*. Flash chromatography yielded the *title compound* (0.018 g, 85%) as a colourless oil. R_f (20% EtOAc/hexane) 0.17; $[\alpha]^{20}_D$ –196 (*c* 0.45, MeOH), lit.[1] $[\alpha]^{31.7}_D$ –24 (*c* 0.02, MeOH); $[\theta]_{207}$ +50390 (max), $[\theta]_{231}$ –19420 (max), $[\theta]_{285}$ –53660 (max); ν_{max} (thin film) 3493, 2966, 2924, 2877, 1698, 1620, 1457, 1434, 1377, 1276, 1160, 1037, 970, 861, 803 cm^{-1}; δ_H (500 MHz, CD_3OD) 6.44 (1H, s, C*H*=CCH_2CH_3), 5.29 (2H, overlapping peaks, C*H*=C*H*CHOH), 4.85 (1H, s, C*H*CO_2CH_3), 4.19–4.14 (1H, m, C*H*OH), 3.65 (3H, s, OCH_3), 2.21–2.16 (2H, m, CH=CCH_2CH_3), 1.95 (1H, dd, *J* 17.9, 7.1 Hz, CH_AH_BCHCH_2CH_3), 1.86–1.80 (1H, m, CHCCH_AH_BCH_3), 1.81–1.75 (3H, overlapping peaks, CH_AH_BCHCH_2CH_3, C*H*CH_2CH_3, CHCCH_AH_BCH_3), 1.42–1.37 (1H, m, CHCH_AH_BCH_3), 1.22–1.16 (7H, overlapping peaks, CH(OH)CH_3, CH=CCH_2CH_3, CHCH_AH_BCH_3), 0.79 (3H, t, *J* 7.6 Hz, CHCH_2CH_3), 0.75 (3H, t, *J* 7.2 Hz, CHCCH_2CH_3); δ_C (125 MHz, CD_3OD) 174.3, 169.3, 142.8, 140.7, 135.9, 135.7, 99.6, 83.8, 69.3, 51.1, 44.3, 40.7, 32.7, 30.2, 23.7, 19.5, 12.4, 11.9, 8.2; HRMS (ESI): MNa^+, found 345.2037. $C_{19}H_{30}NaO_4^+$ requires 345.2036.

*5.5.9 11-epi-Gracilioether C (**196**)*

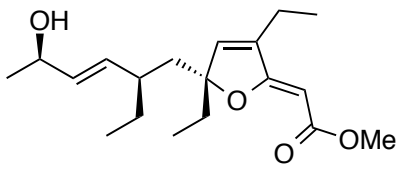

85 (0.023 g, 0.072 mmol), $RuCl_2$[(*S*)-xylbinap][(*S*)-daipen] (0.0014 g, 1.6 mol%), K_2CO_3 (0.017 g, 0.12 mmol) and ^{i}PrOH (1.0 mL) were stirred at 30 °C under an atmosphere of H_2 (4 atm) in a sealed vessel for 48 h. Volatiles were removed and the mixture passed through a thick pad of silica (washing with excess 50%

EtOAc/hexane) before concentrating *in vacuo*. Flash chromatography yielded the *title compound* (0.021 g, 91%) as a colourless oil. R_f (20% EtOAc/hexane) 0.13; $[\alpha]^{20}_{D}$ –271 (*c* 0.39, MeOH); $[\theta]_{209}$ +54170 (max), $[\theta]_{231}$ –19630 (max), $[\theta]_{285}$ –58840 (max); ν_{max} (thin film) 3488, 2967, 2925, 2877, 1696, 1620, 1457, 1434, 1376, 1275, 1161, 1036, 971, 857, 803 cm^{-1}; δ_H (500 MHz, CD_3OD) 6.42 (1H, d, *J* 1.7 Hz, C*H*=CCH_2CH_3), 5.33 (1H, dd, *J* 15.5, 7.5 Hz, C*H*=CHCH(OH)CH_3), 5.27 (1H, dd, *J* 15.5, 5.4 Hz, CH=C*H*CH(OH)CH_3), 4.85 (1H, s, C*H*CO_2CH_3), 4.16 (1H, m, C*H*OH), 3.65 (3H, s, OCH_3), 2.18 (2H, qd, *J* 7.4, 1.7 Hz, CH=CH_2CH_3), 1.97–1.93 (1H, m, C$H_A$$H_B$$CHCH_2CH_3$), 1.87–1.72 (4H, overlapping peaks, $CH_AH_BCHCH_2CH_3$, C*H*CH_2CH_3, $CHCCH_2CH_3$), 1.42–1.36 (1H, m, $CHCH_AH_BCH_3$), 1.26–1.18 (1H, m, $CHCH_AH_BCH_3$), 1.19 (3H, d, *J* 6.2 Hz, CH(OH)CH_3), 1.17 (3H, t, *J* 7.4 Hz, $CH=CCH_2CH_3$), 0.80 (3H, t, *J* 7.4 Hz, $CHCH_2CH_3$), 0.75 (3H, t, *J* 7.4 Hz, $CHCCH_2CH_3$); δ_C (125 MHz, CD_3OD) 174.3, 169.3, 142.7, 140.7, 135.6 (2 peaks), 99.5, 83.8, 69.1, 51.1, 44.3, 40.6, 33.0, 30.3, 23.8, 19.5, 12.4, 11.9, 8.1; HRMS (ESI): MNa^+, found 345.2036. $C_{19}H_{30}NaO_4^+$ requires 345.2036.

5.5.10 Luche reduction of ***85***

$NaBH_4$ (0.026 g, 0.69 mmol) was added in a single portion to a stirred solution of **85** (0.030 g, 0.094 mmol), $CeCl_3.7H_2O$ (0.080 g, 0.21 mmol) and MeOH (0.4 mL) at 0 °C. Stirring continued at 0 °C for 2 h before quenching with the addition of NH_4Cl (50% satd aq) and Et_2O (5mL). The phases were partitioned, organic layer separated and aqueous extracted with Et_2O. The combined extracts were washed with brine, dried (Na_2SO_4) and concentrated *in vacuo* to yield **86** and **196** (0.024 g, 80%) in approximately the ratio 1:1. Flash chromatography allowed separation, spectra reported above.

5.6 Chapter summary

Chapter 5 reports the first enantioselective total synthesis and stereochemical elucidation of the marine sponge metabolites gracilioethers B and C, known to have therapeutic potential as antimalarial agents and for use in the treatment of type II diabetes. The design and execution of this work represents a unique inclusion to the chemical literature with a novel approach to the synthesis of two complex natural structures; and strategic optimisation of the linear sequence to limit changes in

oxidation state and use of protecting groups. The key biomimetic reaction, re-engineered from that presented in Chapters 3 and 4, further demonstrates the inherent structural rearrangements of hydroxy β-ketoesters, which have been implicated as intermediates arising from the base-mediated decomposition of related endoperoxides.

Finally, an operationally simple and high yielding route to aldehyde dimethyl acetal **88**, which has great potential as a versatile advanced synthetic intermediate, provides an opportunity for the semi-synthesis of many related polyketide metabolites and synthetic analogues of great relevance in the context of drug development.

5.7 References and notes

1. R. Ueoka, Y. Nakao, S. Kawatsu, J. Yaegashi, Y. Matsumoto, S. Matsunaga, K. Furihata, R. W. M. van Soest and N. Fusetani, *J. Org. Chem.*, 2009, **74**, 4203.
2. C. Festa, G. Lauro, S. De Marino, M. V. D'Auria, M. C. Monti, A. Casapullo, C. D'Amore, B. Renga, A. Mencarelli, S. Petek, G. Bifulco, S. Fiorucci and A. Zampella, *J. Med. Chem.*, 2012, **55**, 8303.
3. C. Festa, S. De Marino, M. V. D'Auria, E. Deharo, G. Gonzalez, C. Deyssard, S. Petek, G. Bifulco and A. Zampella, *Tetrahedron*, 2012, **68**, 10157.
4. C. Festa, C. D'Amore, B. Renga, G. Lauro, S. De Marino, M. V. D'Auria, G. Bifulco, A. Zampella and S. Fiorucci, *Mar. Drugs*, 2013, **11**, 2314.
5. S. Di Micco, A. Zampella, M. V. D'Auria, C. Festa, S. De Marino, R. Riccio, C. P. Butts and G. Bifulco, *Beilstein J. Org. Chem.*, 2013, **9**, 2940.
6. D. B. Stierle and D. J. Faulkner, *J. Org. Chem.*, 1980, **45**, 3396.
7. M. V. D'Auria, L. G. Paloma, L. Minale, R. Riccio, A. Zampella and C. Debitus, *J. Nat. Prod.*, 1993, **56**, 418.
8. R. S. Compagnone, I. C. Pina, R. R. Hector, F. Dagger, A. I. Suarez, M. V. R. Reddy and D. J. Faulkner, *Tetrahedron*, 1998, **54**, 3057.
9. R. J. Capon, S. Singh, S. Ali and S. Sotheeswaran, *Aust. J. Chem.*, 2005, **58**, 18.
10. R. Epifanio, L. Pinheiro and N. Alves, *J. Braz. Chem. Soc.*, 2005, **16**, 1367.
11. X.-F. Liu, Y. Shen, F. Yang, M. T. Hamann, W.-H. Jiao, H.-J. Zhang, W.-S. Chen and H.-W. Lin, *Tetrahedron*, 2012, **68**, 4635.
12. S.-J. Piao, Y.-L. Song, W.-H. Jiao, F. Yang, X-.F. Liu, W.-S. Chen, B.-N. Han and H.-W. Lin, *Org. Lett.*, 2013, **15**, 3526.

13. F. Rahm, P. Y. Hayes and W. Kitching, *Heterocycles*, 2004, **64**, 523.
14. M. Akiyama, Y. Isoda, M. Nishimoto, A. Kobayashi, D. Togawa, N. Hirao, A. Kuboki and S. Ohira, *Tetrahedron Lett*., 2005, **46**, 7483.
15. M. Akiyama, Y. Isoda, M. Nishimoto, M. Narazaki, H. Oka, A. Kuboki and S. Ohira, *Tetrahedron Lett*., 2006, **47**, 2287.
16. M. D. Norris and M. V. Perkins, *Tetrahedron*, 2013, **69**, 9813.
17. C. M. Rasik and M. K. Brown, *Angew. Chem., Int. Ed*., 2014, **53**, 14522.
18. S. A. Ruider, T. Sandmeier and E. M. Carreira, *Angew. Chem., Int. Ed*., 2015, **54**, 2378.
19. N. Kornblum and H. DeLaMare, *J. Am. Chem. Soc*., 1951, **73**, 880.
20. N. Kornblum and H. DeLaMare, *J. Am. Chem. Soc*., 1952, **74**, 3029.
21. R. Noyori and T. Ohkuma, *Angew. Chem. Int. Ed*., 2001, **40**, 40.
22. T. Ohkuma, M. Koizumi, H. Doucet, T. Pham, M. Kozawa, K. Murata, E. Katayama, T. Yokozawa, T. Ikariya and R. Noyori, *J. Am. Chem. Soc*., 1998, **120**, 13529.
23. P. R. Allen, M. A. Brimble and H. Prabaharan, *J. Chem. Soc., Perkin Trans. 1*, 2001, 379.
24. S. V. Ley, J. Norman, W. P. Griffith and S. P. Marsden, *Synthesis*, 1994, 639.
25. S. N. Huckin and L. Weiler, *Can. J. Chem*., 1974, **52**, 2157.
26. B. T. Gregg, K. C. Golden and J. F. Quinn, *J. Org. Chem*., 2007, **72**, 5890.

6. Oxidation of the gracilioether furanylidenes

While exploring the total synthesis of gracilioethers B and C (Chapters 4 and 5); and through considering divergent strategies toward the synthesis of related targets, it was discovered that the chromate oxidant pyridinium chlorochromate (PCC, also known as the Corey-Suggs reagent) is capable of effecting a novel C–C bond cleavage reaction of furanylidene heterocycles to the corresponding γ-butenolide. The utility of this reaction, where natural butenolide congeners of the gracilioether metabolites may be accessed from the same late-stage synthetic intermediate (**88**), ultimately led to the first enantioselective total synthesis and stereochemical elucidation of three butenolide natural products; and further inspired total synthesis of the putative biosynthetic precursor to hippolachnin A.

Chapter 6 details the 'total synthesis of plakilactones C, B and *des*-hydroxy plakilactone B by the oxidative cleavage of gracilioether furanylidenes' as prepared in an article with the same title and published in the refereed journal *Journal of Organic Chemistry*, American Chemical Society on 30 June 2016 (DOI: 10.1021/acs.joc.6b01196). The candidate researched, planned, executed and prepared the following chapter/published article with full intellectual and practical contribution with due guidance and only minor textual editing from co-authors throughout manuscript preparation and final publishing; and is listed as the primary author of this work.

6.1 Total synthesis of plakilactones C, B and *des*-hydroxyplakilactone B by the oxidative cleavage of gracilioether furanylidenes

A chemoselective oxidative cleavage of synthetic gracilioether B, 11-*epi*-gracilioether C benzoate and *des*-hydroxygracilioether C with pyridinium chlorochromate (PCC), which proceeds with loss of the furanyl acetate, has enabled total synthesis and stereochemical elucidation of the marine sponge metabolites (4*R*,6*R*)-plakilactone C, (4*R*,6*R*,9*R*)-plakilactone B and (4*R*,6*R*)-*des*-hydroxyplakilactone B (Scheme 6.1). *des*-Hydroxygracilioether C, the putative biosynthetic precursor to hippolachnin A, was also found to undergo a facile ene cyclisation on treatment with $SnCl_4$.

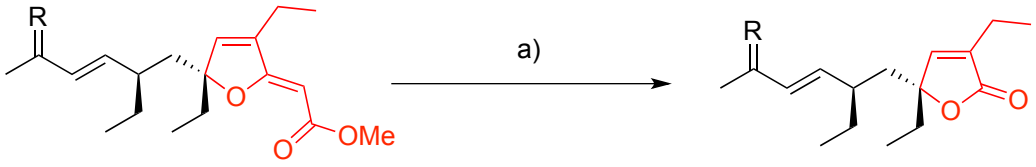

gracilioether furanylidene — **plakilactone butenolide**

gracilioether B (R = O) — plakilactone C (R = O)
11-*epi*-gracilioether C benzoate (R = (*R*)-OBz, H) — plakilactone B benzoate (R = (*R*)-OBz, H)
des-hydroxygracilioether C (R = H, H) — *des*-hydroxyplakilactone B (R = H, H)

Scheme 6.1: Total synthesis of plakilactones C, B and *des*-hydroxyplakilactone B by the oxidative cleavage of gracilioether furanylidenes. a) PCC (9 equiv.), 4 Å MS, $(CH_2Cl)_2$, reflux, 15 h, 71–82%.

6.2 Introduction

The polyketide secondary metabolites gracilioethers A–K and plakilactones A–H were recently isolated from marine sponges of the genera *Plakortis*, *Plakinastrella* and *Agelas*.[1–5] Several of these compounds, and other related natural products,[6–15] are known to be agonists of peroxisome proliferator-activated receptor γ (PPARγ) and pregnane-X-receptor (PXR); and exhibit antimalarial, antileishmanial and antifungal properties. Metabolites in this family are notable for having unique polyoxygenated carbon scaffolds and can be classified as complex polycycles, such as gracilioether A (**92**) and hippolachnin A (**98**); butenolides, which include plakilactones C (**197**), B (**198**) and *des*-hydroxyplakilactone B (**91**); and the furanylidenes, consisting of

gracilioethers B (**85**), C (**86**), *des*-hydroxygracilioether C (**90**) and spongosoritin A (**139**) (Figure 6.1).[16] In recent years, several groups have targeted their synthesis,[17–22] but few have focused on the synthesis or structural elucidation of the plakilactone butenolides.

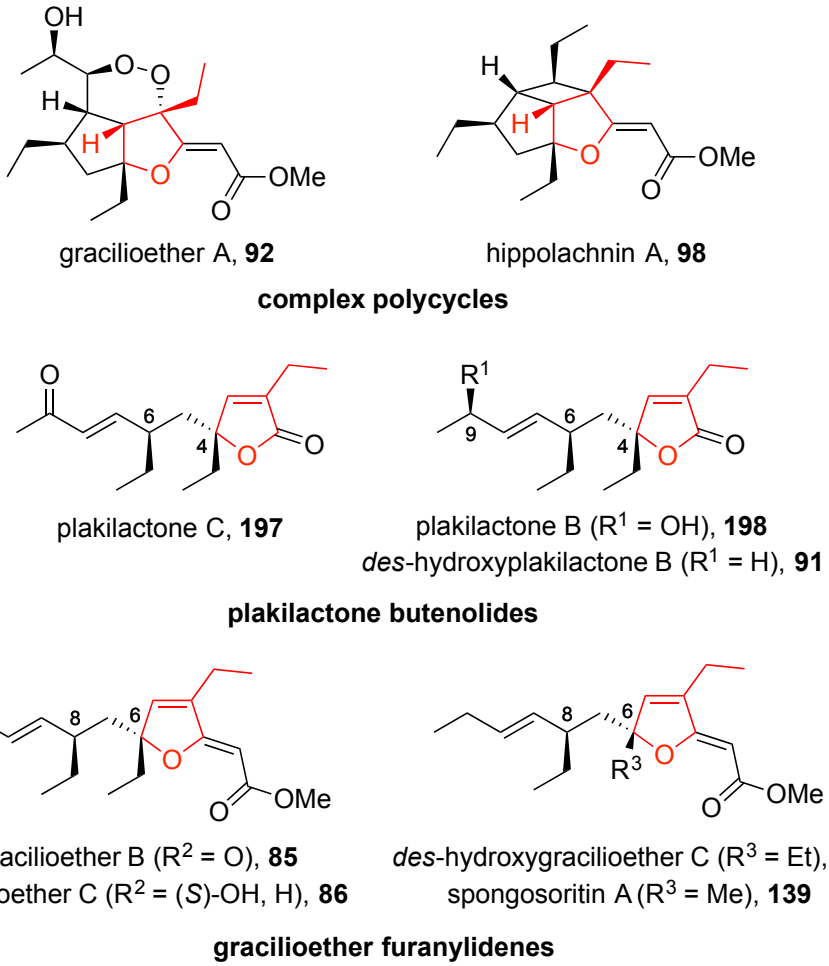

Figure 6.1: Complex polycycles, butenolides and furanylidenes isolated from marine sponges. Common furanyl heterocycle highlighted in red.

We have recently reported the first total synthesis of **85** and **86** using an approach modelled on a theory for the biogenesis of furanylidene metabolites (Chapter 5).[23,24] With a short and high-yielding route to aldehyde dimethyl acetal **88**, we sought to extend the scope of this advanced intermediate to include synthesis of the related butenolides **197**, **198** and **91** (Scheme 6.2). Herein, we report the total synthesis and structural elucidation of **197**, **198** and **91** from acetal **88** featuring a novel and chemoselective oxidation with pyridinium chlorochromate (PCC).

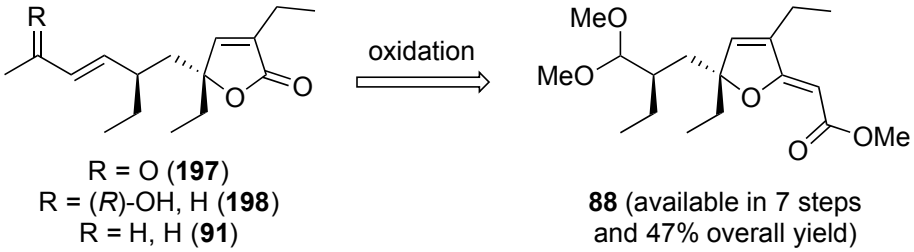

Scheme 6.2: Aldehyde dimethyl acetal **88** as an advanced intermediate for the synthesis of butenolides **197**, **198** and **91**.

6.3 Results and discussion

The polyketide natural products shown in Figure 6.1 each have a common furanyl heterocycle, which we have proposed to originate from the dehydrative ring contraction of related endoperoxide metabolites.[16,23,24] Since the carbon structures of many plakilactone butenolides and gracilioether furanylidenes appear to correlate, we suspect they may be linked biosynthetically by oxidative scission of the furanylidene enol ether.[16] This prompted us to examine the oxidation of furanylidenes **85**, **86** and **90** to their corresponding butenolides, **197**, **198** and **91**.

While there are many reagents capable of oxidative C–C bond cleavage,[25] these methods often lack selectivity in the presence of multiple alkenes and other sensitive functional groups. We thus became interested in the use of chromate oxidants, especially PCC, which are known to be effective for the oxidation of electron-rich enol ethers,[26–29] with great potential for chemoselectivity (Scheme 6.3).[27] However, application of this methodology to a complex system, such as the gracilioether furanylidenes, had not been explored.

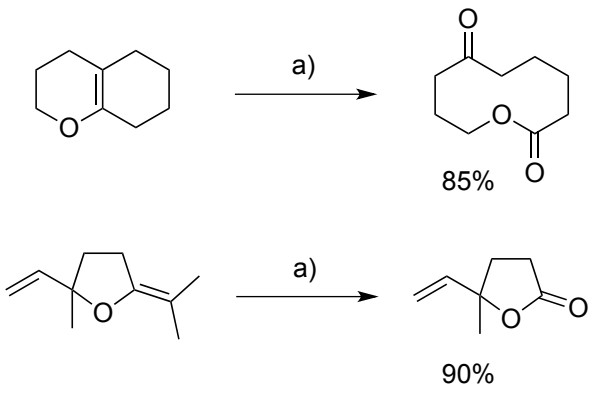

Scheme 6.3: Oxidation of cyclic enol ethers with PCC. a) PCC (4 equiv.), celite, CH_2Cl_2, r.t., 1–2 h.

With synthetic gracilioether B (**85**) already in hand (Chapter 5),[24] we attempted oxidation with PCC (1.5 equivalents) and 4 Å MS in CH_2Cl_2 at ambient temperature but only recovered starting material. After further experimentation, we were pleased to find that increasing the loading of PCC to a 9-fold excess, changing the solvent to $(CH_2Cl)_2$ and heating the mixture at reflux temperature for 15 h gave excellent conversion to butenolide **197** in 73% isolated yield (Scheme 6.4, Figure 6.2). Notably, oxidation was selective for the electron-rich enol ether, as desired. While the ^{1}H NMR spectrum, ^{13}C NMR spectrum (Section 8.1.3) and sign of specific rotation ($[\alpha]^{20}_D$ –165, *c* 0.65, $CHCl_3$; lit.[1b] $[\alpha]^{25}_D$ –64, *c* 0.11, $CHCl_3$) of synthetic **197** were consistent with that reported for plakilactone C,[2,30] we wanted to confirm our assignment through synthesis of the isomeric compound, **199** (Scheme 6.5).

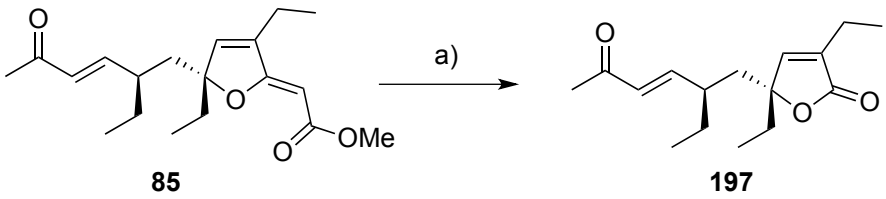

Scheme 6.4: Chemoselective PCC oxidation of gracilioether B (**85**) to plakilactone C (**197**). a) PCC (9 equiv.), 4 Å MS, $(CH_2Cl)_2$, reflux, 15 h, 73%.

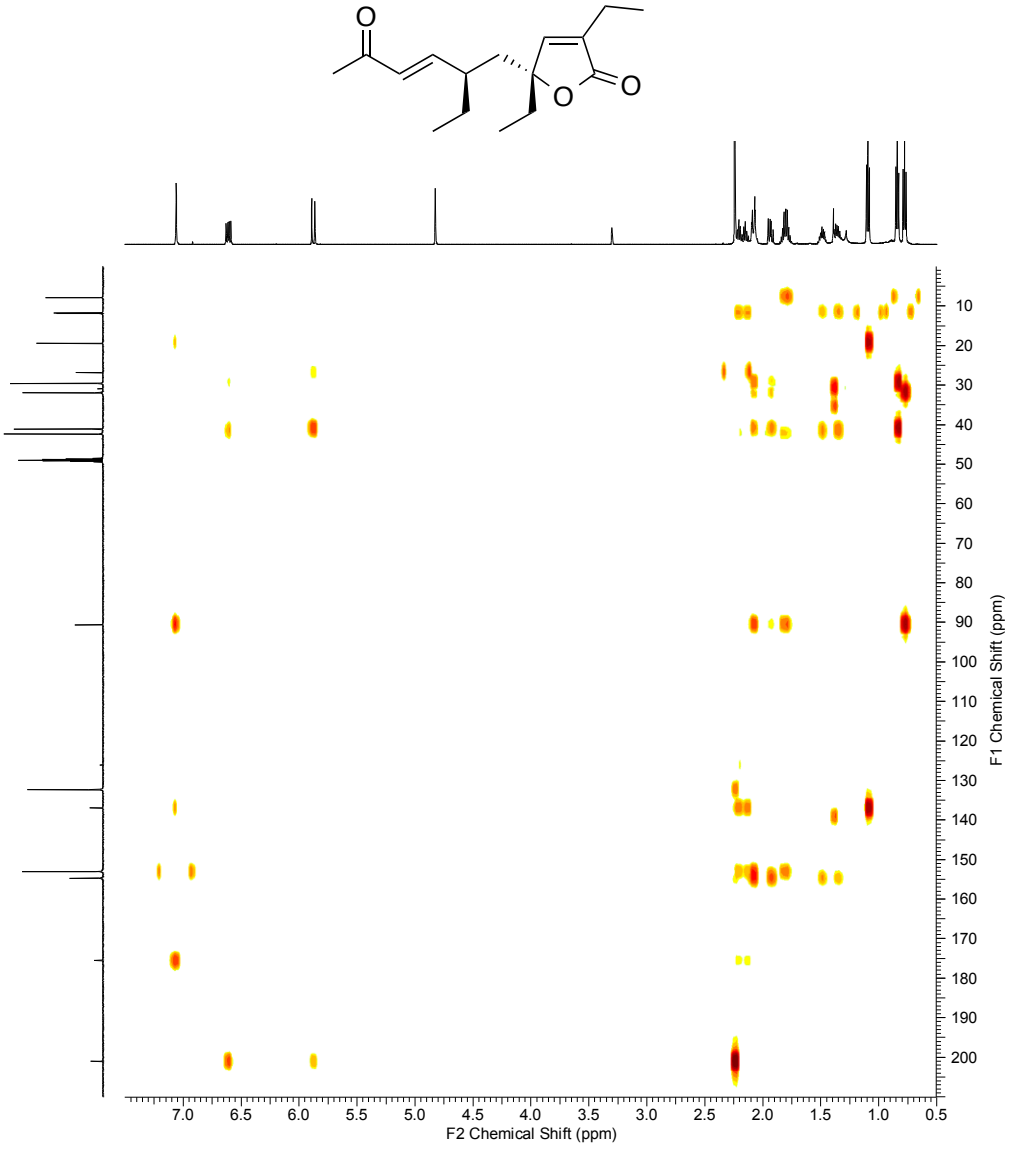

Figure 6.2: HMBC spectrum of synthetic plakilactone C (**197**) with 1D ^{1}H NMR (600 MHz, CD_3OD) and ^{13}C NMR (150 MHz, CD_3OD) projections.

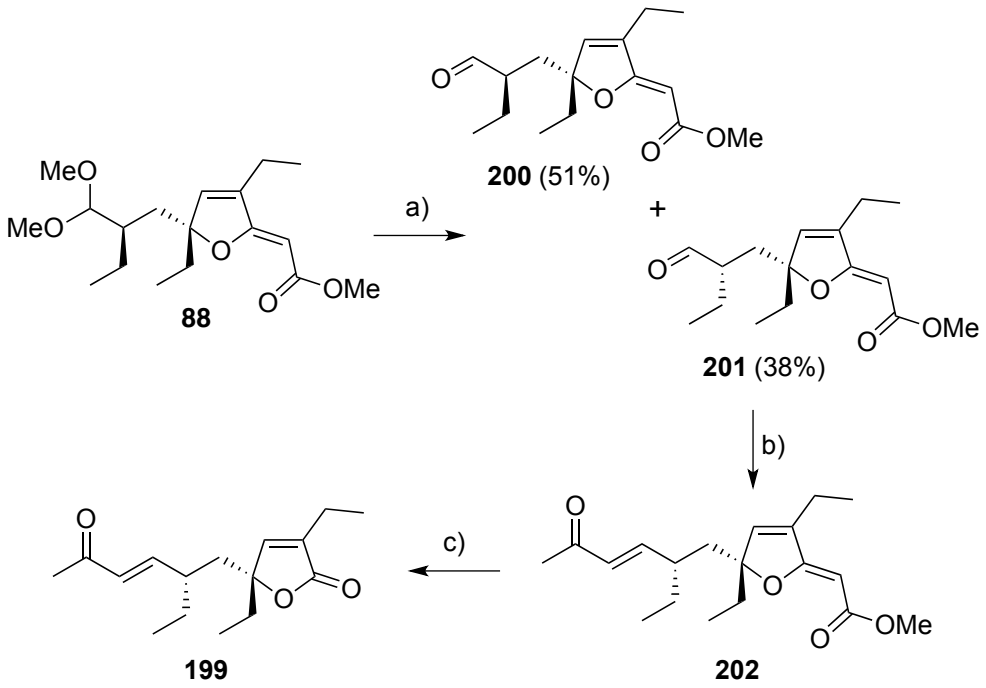

Scheme 6.5: Synthesis of **199** and **202**. a) HCl, H_2O, THF, r.t., 15 h; b) $CH_3COCH_2PO(OEt)_2$, Et_3N, CH_3CN, Et_2O, r.t., 15 h, 85%; c) PCC (9 equiv.), 4 Å MS, $(CH_2Cl)_2$, reflux, 15 h, 77%.

Acetal **88** was hydrolysed to give aldehyde **200** and useful quantities of the C8 epimer, **201**. Horner-Wadsworth-Emmons olefination[31] afforded **202** and oxidation with PCC under our optimised conditions gave **199** in 77% yield. The ^{1}H NMR and ^{13}C NMR of **199** did not match that of the natural product, thus supporting our initial structural and configurational assignment of plakilactone C as (4*R*,6*R*)-**197** (Table 6.1).[30] Additionally, the ^{1}H NMR and ^{13}C NMR of **202** did not match that of gracilioether B[1] (Table 6.2), which supports our original assignment of the natural product as (6*R*,8*R*)-**85** (Chapter 5).[24]

Table 6.1: Tabulated ^{1}H NMR and ^{13}C NMR data of **197** and **199** with direct comparison to natural plakilactone C (most significant differences highlighted in blue).

Carbon	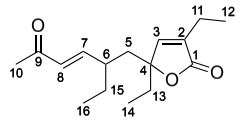 Natural plakilactone C[a]		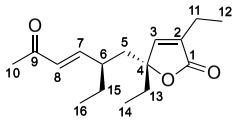 Synthetic **197**			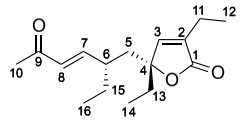 Synthetic **199**		
	δ_H (500 MHz, CD_3OD) (ppm)	δ_C (125 MHz, CD_3OD) (ppm)	δ_H (600 MHz, CD_3OD) (ppm)[b]	δ_C (150 MHz, CD_3OD) (ppm)	$\Delta\delta_C$ (ppm)	δ_H (600 MHz, CD_3OD) (ppm)[b]	δ_C (150 MHz, CD_3OD) (ppm)	$\Delta\delta_C$ (ppm)
1		175.6		175.6	+0.0		175.5	–0.1
2		137.0		136.9	–0.1		138.0	+1.0
3	**7.07 (1H, broad t, *J* 1.4 Hz)**	**153.1**	**7.07 (1H, s)**	**153.1**	**+0.0**	**7.14 (1H, s)**	**151.7**	**–1.4**
4		90.7		90.6	–0.1		91.1	+0.4
5	2.09 (1H, overlapping)	42.4	2.10–2.08 (1H, overlapping)	42.4	+0.0	2.06–2.01 (2H, overlapping)	42.0	–0.4
	1.94 (1H, dd, *J* 14.9, 9.9 Hz)		1.94 (1H, dd, *J* 15.0, 10.1 Hz)					
6	**2.08 (1H, overlapping)**	**41.1**	**2.10–2.08 (1H, overlapping)**	**41.1**	**+0.0**	**2.06–2.01 (1H, overlapping)**	**42.9**	**+1.8**
7	**6.62 (1H, dd, *J* 16.0, 9.4 Hz)**	**154.8**	**6.62 (1H, dd, *J* 16.0, 9.4 Hz)**	**154.7**	**–0.1**	**6.54 (1H, dd, *J* 16.0, 9.1 Hz)**	**154.3**	**–0.5**
8	**5.88 (1H, d, *J* 16.0 Hz)**	**132.3**	**5.88 (1H, d, *J* 16.0 Hz)**	**132.3**	**+0.0**	**5.71 (1H, d, *J* 16.0 Hz)**	**131.7**	**–0.6**
9		201.1		201.0	–0.1		201.3	+0.2
10	**2.25 (3H, s)**	**26.9**	**2.25 (3H, s)**	**26.9**	**+0.0**	**2.23 (3H, s)**	**26.3**	**–0.6**
11	2.22 (2H, m)	19.5	2.24–2.19 (1H, m)	19.5	+0.0	2.23–2.19 (2H, m)	19.4	–0.1
			2.19–2.13 (1H, m)					
12	**1.10 (3H, t, *J* 7.4 Hz)**	**11.9**	**1.10 (3H, t, *J* 7.5 Hz)**	**11.9**	**+0.0**	**1.16 (3H, t, *J* 7.5 Hz)**	**12.4**	**+0.5**
13	**1.83 (2H, m)**	**32.0**	**1.86–1.76 (2H, m)**	**32.0**	**+0.0**	**1.83 (1H, dq, *J* 14.5, 7.5 Hz)**	**32.5**	**+0.5**
						1.74 (1H, dq, *J* 14.5, 7.5 Hz)		
14	0.79 (3H, t, *J* 7.4 Hz)	7.9	0.79 (3H, t, *J* 7.5 Hz)	7.9	+0.0	0.79 (3H, t, *J* 7.5 Hz)	7.8	–0.1
15	1.50 (1H, m)	29.6	1.53–1.47 (1H, m)	29.6	+0.0	1.54–1.47 (1H, m)	29.3	–0.3
	1.37 (1H, m)		1.39–1.33 (1H, m)			1.37–1.31 (1H, m)		
16	0.85 (3H, t, *J* 7.4 Hz)	11.7	0.85 (3H, t, *J* 7.4 Hz)	11.7	+0.0	0.84 (3H, t, *J* 7.4 Hz)	11.7	+0.0

[a] Amended tabulated data for natural plakilactone C provided by C. Festa and A. Zampella, authors of ref. 2 (Festa, C.; Lauro, G.; De Marino, S.; D'Auria, M. V.; Monti, M. C.; Casapullo, A.; D'Amore, C.; Renga, B.; Mencarelli, A.; Petek, S.; Bifulco, G.; Fiorucci, S.; Zampella, A. *J. Med. Chem.* **2012**, *55*, 8303). [b] ^{1}H NMR data for synthetic compound is presented as referenced for residual CD_3OH (δ_H 3.31) instead of CD_3OH (δ_H 3.30), for direct comparison to the data reported for the natural product.

Table 6.2: Tabulated ^{1}H NMR and ^{13}C NMR data of **85** and **202** with direct comparison to natural gracilioether B (most significant differences highlighted in blue).

Carbon	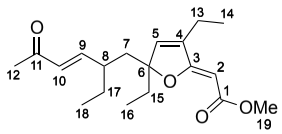		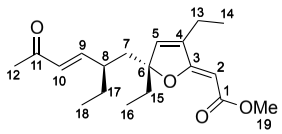			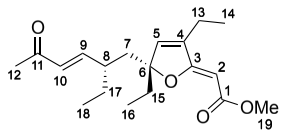		
	Natural gracilioether B[1]		Synthetic **85**[22]			Synthetic **202**		
	δ_H (600 MHz, CD_3OD) (ppm)	δ_C (150 MHz, CD_3OD) (ppm)	δ_H (500 MHz, CD_3OD) (ppm)	δ_C (125 MHz, CD_3OD) (ppm)	$\Delta\delta_C$ (ppm)	δ_H (600 MHz, CD_3OD) (ppm)	δ_C (150 MHz, CD_3OD) (ppm)	$\Delta\delta_C$ (ppm)
1		168.8		169.2	+0.4		169.0	+0.2
2	**4.85 (1H, s)**	**84.3**	**4.88 (1H, s)**	**84.3**	**+0.0**	**4.77 (1H, s)**	**84.7**	**+0.4**
3		174.1		174.1	+0.0		173.9	–0.2
4		142.1		141.4	–0.7		142.4	+0.3
5	**6.40 (1H, s)**	**142.1**	**6.43 (1H, s)**	**142.1**	**+0.0**	**6.46 (1H, s)**	**141.1**	**–1.0**
6		99.0		99.0	+0.0		99.5	+0.5
7	2.08 (1H, m) 1.94 (1H, m)	43.6	2.21–2.03 (1H, overlapping) 2.01–1.93 (1H, m)	43.6	+0.0	2.13–2.11 (1H, overlapping) 2.03 (1H, dd, *J* 14.7, 2.8 Hz)	43.8	+0.2
8	**2.08 (1H, m)**	**41.4**	**2.21–2.03 (1H, overlapping)**	**41.4**	**+0.0**	**1.99–1.94 (1H, m)**	**43.1**	**+1.7**
9	6.62 (1H, dd, *J* 15.8, 8.9 Hz)	155.3	6.65 (1H, dd, *J* 16.0, 9.3 Hz)	155.3	+0.0	6.56 (1H, dd, *J* 16.0, 9.7 Hz)	155.2	–0.1
10	5.82 (1H, d, *J* 15.8 Hz)	131.7	5.85 (1H, d, *J* 16.0 Hz)	131.7	+0.0	5.60 (1H, d, *J* 16.0 Hz)	131.2	–0.5
11		204.2[a]		201.3	–2.9[a]		201.7	–2.5
12	**2.23 (3H, s)**	**26.8**	**2.26 (3H, s)**	**26.8**	**+0.0**	**2.13–2.11 (3H, overlapping)**	**25.9**	**–0.9**
13	2.13 (1H, m) 2.05 (1H, m)	19.4	2.21–2.03 (2H, overlapping)	19.4	+0.0	2.18–2.13 (2H, m)	19.4	+0.0
14	1.10 (3H, t, *J* 7.6 Hz)	12.0	1.13 (3H, t, *J* 7.4 Hz)	12.0	+0.0	1.18 (3H, t, *J* 7.4 Hz)	12.6	+0.6
15	1.83 (1H, p, *J* 7.6 Hz) 1.78 (1H, p, *J* 7.6 Hz)	33.0	1.87 (1H, p, *J* 7.2 Hz) 1.82 (1H, p, *J* 7.2 Hz)	33.0	+0.0	1.88–1.82 (1H, m) 1.79–1.73 (1H, m)	33.4	+0.4
16	0.75 (3H, t, *J* 7.6 Hz)	8.1	0.78 (3H, t, *J* 7.4 Hz)	8.1	+0.0	0.75 (3H, t, *J* 7.4 Hz)	7.9	–0.2
17	1.50 (1H, m) 1.32 (1H, m)	29.5	1.58–1.48 (1H, m) 1.41–1.30 (1H, m)	29.5	+0.0	1.51–1.44 (1H, m) 1.36–1.29 (1H, m)	29.3	–0.2
18	0.82 (3H, t, *J* 7.6 Hz)	11.8	0.85 (3H, t, *J* 7.4 Hz)	11.8	+0.0	0.81 (3H, t, *J* 7.4 Hz)	11.8	+0.0
19	3.65 (3H, s)	51.1	3.68 (3H, s)	51.1	+0.0	3.60 (3H, s)	51.1	+0.0

[a]The HMBC spectrum of natural gracilioether B clearly shows a chemical shift for C11 less than 204.2 ppm and it appears that this was incorrectly reported in the article describing its isolation.[22]

Further expanding the scope of our approach, Steglich esterification[32] of synthetic gracilioether C (**86**)[24] with benzoic acid followed by PCC oxidative cleavage gave butenolide **203** in 70% yield over two steps; and without epimerisation of the allylic alcohol stereocentre (Scheme 6.6). Hydrolysis of the resulting benzoate ester with KOH and CH_3OH cleanly afforded **204**. However, the ^{1}H NMR and ^{13}C NMR of **204** showed subtle differences to that reported for plakilactone B[2,33] (Table 6.3). With the same strategy, **196**[24] was advanced to **205** in 68% yield over two steps and hydrolysis of the benzoate ester gave butenolide **198**[34] (Figure 6.3). The ^{1}H NMR and ^{13}C NMR (Section 8.1.4) of **198** matched those reported for plakilactone B[2] (Table 6.3) and the sign of specific rotation ($[\alpha]^{20}_D$ –66, *c* 0.64, $CHCl_3$; lit.[2] $[\alpha]^{25}_D$ –25, *c* 0.05, $CHCl_3$) was consistent, thereby elucidating the structure and absolute configuration of the natural product as (4*R*,6*R*,9*R*)-**198**.[33,35] It is interesting to note that the relative configuration of plakilactone B (**198**) does not match that of gracilioether C (**86**). We speculate that **198** might, therefore, be derived biosynthetically from oxidative cleavage of the C11 furanylidene epimer **196**.

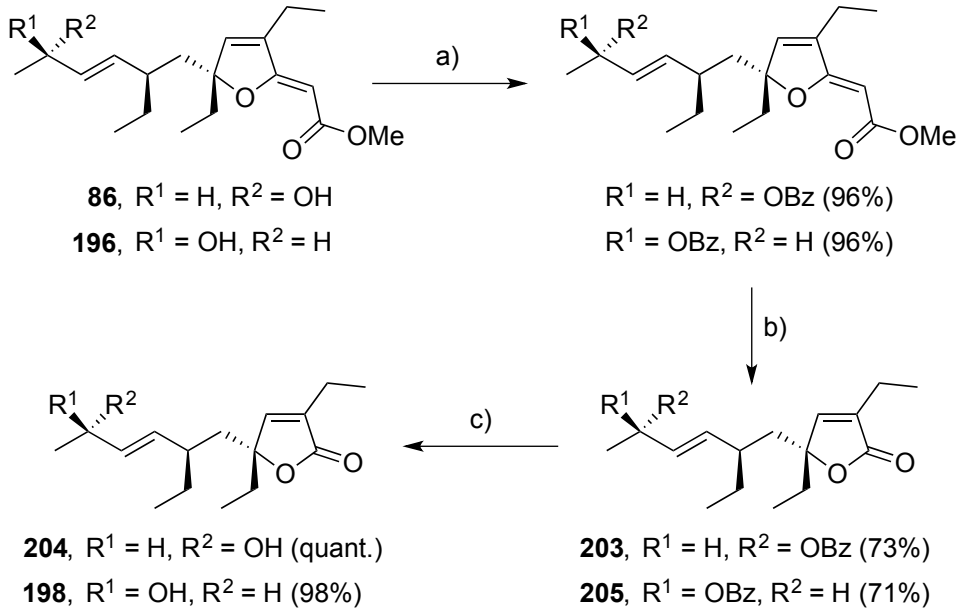

Scheme 6.6: Synthesis of **204** and plakilactone B (**198**). a) $PhCO_2H$, DCC, DMAP, THF, r.t., 3 h; b) PCC (9 equiv.), 4 Å MS, $(CH_2Cl)_2$, reflux, 15 h; c) KOH, CH_3OH, r.t., 1 h.

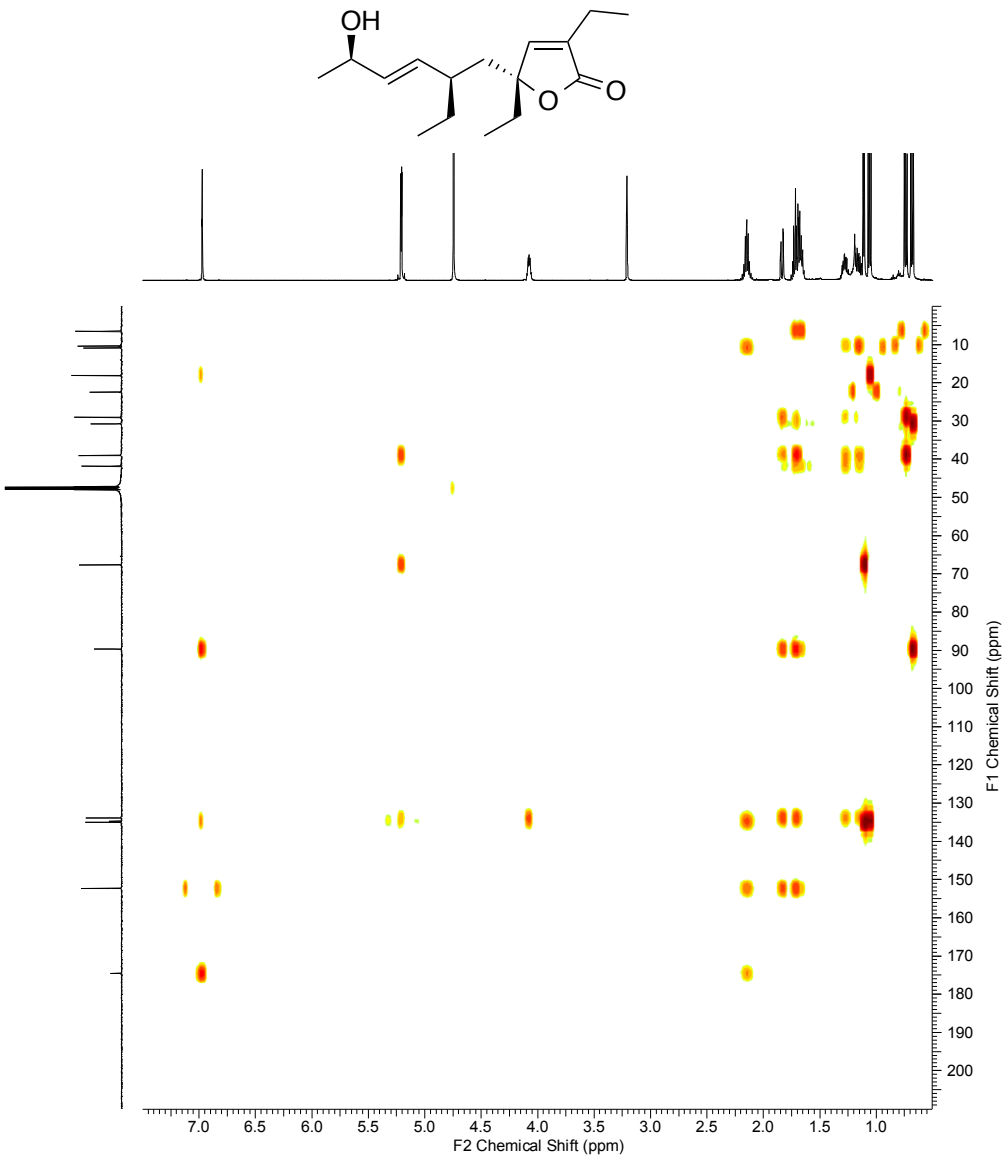

Figure 6.3: HMBC spectrum of synthetic plakilactone B (**198**) with 1D ^{1}H NMR (600 MHz, CD_3OD) and ^{13}C NMR (150 MHz, CD_3OD) projections.

Table 6.3: Tabulated ^{1}H NMR and ^{13}C NMR data of **198** and **204** with direct comparison to natural plakilactone B (most significant differences highlighted in blue).

Carbon	Natural plakilactone B[a]		Synthetic **198**			Synthetic **204**		
	δ_H (500 MHz, CD_3OD) (ppm)	δ_C (125 MHz, CD_3OD) (ppm)	δ_H (600 MHz, CD_3OD) (ppm)[b]	δ_C (150 MHz, CD_3OD) (ppm)	$\Delta\delta_C$ (ppm)	δ_H (600 MHz, CD_3OD) (ppm)[b]	δ_C (150 MHz, CD_3OD) (ppm)	$\Delta\delta_C$ (ppm)
1		175.8		176.0	+0.2		176.0	+0.2
2		136.0		136.1	+0.1		136.2	+0.2
3	**7.07 (1H, broad t, *J* 1.5 Hz)**	**153.7**	**7.07 (1H, t, *J* 1.6 Hz)**	**153.7**	**+0.0**	**7.10 (1H, t, *J* 1.5 Hz)**	**153.7**	**+0.0**
4		91.1		91.1	+0.0		91.2	+0.1
5	1.95 (1H, dd, *J* 14.0, 2.3 Hz)	43.3	1.94 (1H, dd, *J* 14.1, 2.6 Hz)	43.3	+0.0	1.93 (1H, dd, *J* 14.7, 3.1 Hz)	43.3	+0.0
	1.82 (1H, overlapping)		1.85–1.74 (1H, overlapping)			1.86–1.72 (1H, overlapping)		
6	1.79 (1H, overlapping)	40.4	1.85–1.74 (1H, overlapping)	40.4	+0.0	1.86–1.72 (1H, overlapping)	40.5	+0.1
7	5.29 (1H, overlapping)	135.4	5.34–5.28 (2H, overlapping)	135.3	–0.1	5.33–5.27 (1H, overlapping)	135.3	–0.1
8	5.31 (1H, overlapping)	136.4	5.34–5.28 (2H, overlapping)	136.4	+0.0	5.33–5.27 (1H, overlapping)	136.5	+0.1
9	4.18 (1H, m)	69.0	4.20–4.16 (1H, m)	69.1	+0.1	4.20–4.16 (1H, m)	69.1	+0.1
10	1.21 (3H, d, *J* 6.4 Hz)	23.9	1.21 (3H, d, *J* 6.4 Hz)	23.8	–0.1	1.21 (3H, d, *J* 6.4 Hz)	23.8	–0.1
11	**2.25 (2H, m)**	**19.6**	**2.30–2.20 (2H, m)**	**19.5**	**–0.1**	**2.26 (2H, qd, *J* 7.5, 1.5 Hz)**	**19.4**	**–0.2**
12	1.16 (3H, t, *J* 7.4 Hz)	12.3	1.16 (3H, t, *J* 7.4 Hz)	12.3	+0.0	1.16 (3H, t, *J* 7.5 Hz)	12.3	+0.0
13	1.80 (1H, overlapping)	32.2	1.85–1.74 (2H, overlapping)	32.2	+0.0	1.86–1.72 (2H, overlapping)	32.2	+0.0
	1.77 (1H, overlapping)							
14	0.78 (3H, t, *J* 7.4 Hz)	8.0	0.78 (3H, t, *J* 7.4 Hz)	8.0	+0.0	0.79 (3H, t, *J* 7.4 Hz)	8.0	+0.0
15	1.37 (1H, m)	30.4	1.42–1.34 (1H, m)	30.4	0.0	1.42–1.34 (1H, m)	30.4	0.0
	1.27 (1H, m)		1.28–1.23 (1H, m)			1.27–1.20 (1H, m)		
16	**0.84 (3H, t, *J* 7.5 Hz)**	**11.8**	**0.84 (3H, t, *J* 7.4 Hz)**	**11.8**	**+0.0**	**0.82 (3H, t, *J* 7.4 Hz)**	**11.8**	**+0.0**

[a] Amended tabulated data for natural plakilactone C provided by C. Festa and A. Zampella, authors of ref. 2 (Festa, C.; Lauro, G.; De Marino, S.; D'Auria, M. V.; Monti, M. C.; Casapullo, A.; D'Amore, C.; Renga, B.; Mencarelli, A.; Petek, S.; Bifulco, G.; Fiorucci, S.; Zampella, A. *J. Med. Chem.* **2012**, *55*, 8303). [b] ^{1}H NMR data for synthetic compound is presented as referenced for residual CD_3OH (δ_H 3.31) instead of CD_3OH (δ_H 3.30), for direct comparison to the data reported for the natural product.

Finally, Julia-Kocienski olefination[36] of aldehyde **200** with sulfone **206** afforded furanylidene **90** (Scheme 6.7, Figure 6.4) and the corresponding *Z* isomer in a 4:1 (*E*/*Z*) mixture (ratio determined by ^{1}H NMR). Although difficult to purify, it was possible to obtain useable quantities of furanylidene **90** through silver-modified silica chromatography.[37–39] The ^{1}H NMR and ^{13}C NMR (Section 8.1.5) of **90** matched those reported for *des*-hydroxygracilioether C[2,6] and the sign of specific rotation ($[\alpha]^{20}_{D}$ –271, *c* 0.35, $CHCl_3$; lit.[2] $[\alpha]^{25}_{D}$ –282, *c* 0.40, $CHCl_3$) was consistent, thus confirming the structure and absolute configuration of the natural product as (6*R*,8*R*).[40] Once again, PCC oxidation afforded the corresponding butenolide **91** in good yield (Scheme 6.8, Figure 6.5). The ^{1}H NMR (Section 8.1.6) of **91** matched that reported for *des*-hydroxyplakilactone B[2,6] and the sign of specific rotation ($[\alpha]^{20}_{D}$ –90, *c* 0.30, CH_3OH; lit.[2] $[\alpha]^{25}_{D}$ –11, *c* 0.10, CH_3OH) was also consistent.[41]

We also found that simply exposing compound **90** to an atmosphere of oxygen in a sealed tube for 14 days and with ambient light gave trace quantities of butenolide **91** (Scheme 6.8), presumably through oxidation with singlet oxygen.[42,43] The apparent sensitivity of furanylidene substrates to selective oxidation of the enol ether, on exposure to oxygen (for compound **90**) and also PCC, would appear to demonstrate a clear biogenetic link between the gracilioether furanylidenes and plakilactone butenolides.

As illustrated in Scheme 6.9, we presume that the reaction of PCC with furanylidene heterocycles begins with oxidative addition of chlorochromate to the electron-rich alkene.[26–29] Hydrolysis of the resulting chromium(IV) ester (**207**) and uptake of a second chlorochromate species may then give rise to a β-hydroxylated chromium(VI) ester (such as **208**), which is activated toward oxidative C–C bond cleavage.[44–50]

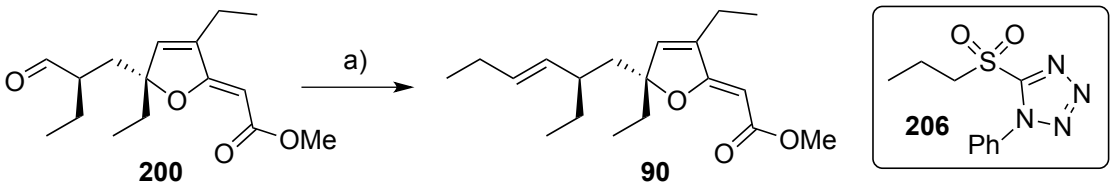

Scheme 6.7: Synthesis of *des*-hydroxygracilioether C (**90**). a) **206**, LHMDS, THF, DMF, –78 °C to r.t., 30 min, 69%.

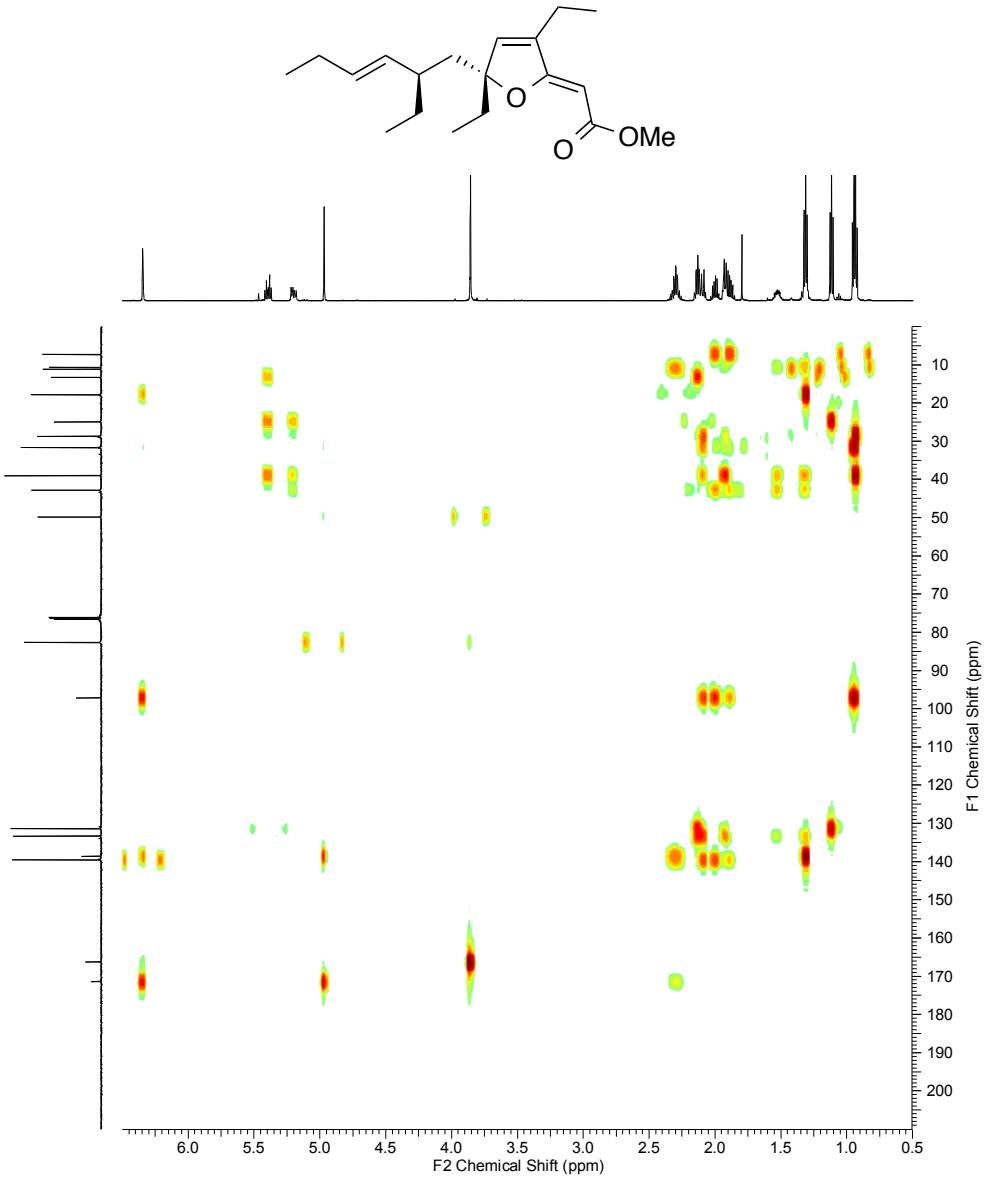

Figure 6.4: HMBC spectrum of synthetic *des*-hydroxygracilioether C (**90**) with 1D ^{1}H NMR (600 MHz, $CDCl_3$) and ^{13}C NMR (150 MHz, $CDCl_3$) projections.

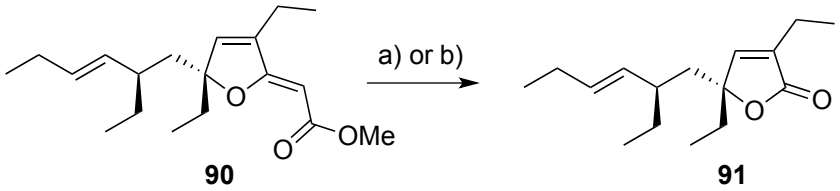

Scheme 6.8: Synthesis of *des*-hydroxyplakilactone B (**91**). a) PCC (9 equiv.), 4 Å MS, $(CH_2Cl)_2$, reflux, 15 h, 82%; b) O_2 (1 atm), CH_3CN, ambient light, r.t., 14 d, trace product.

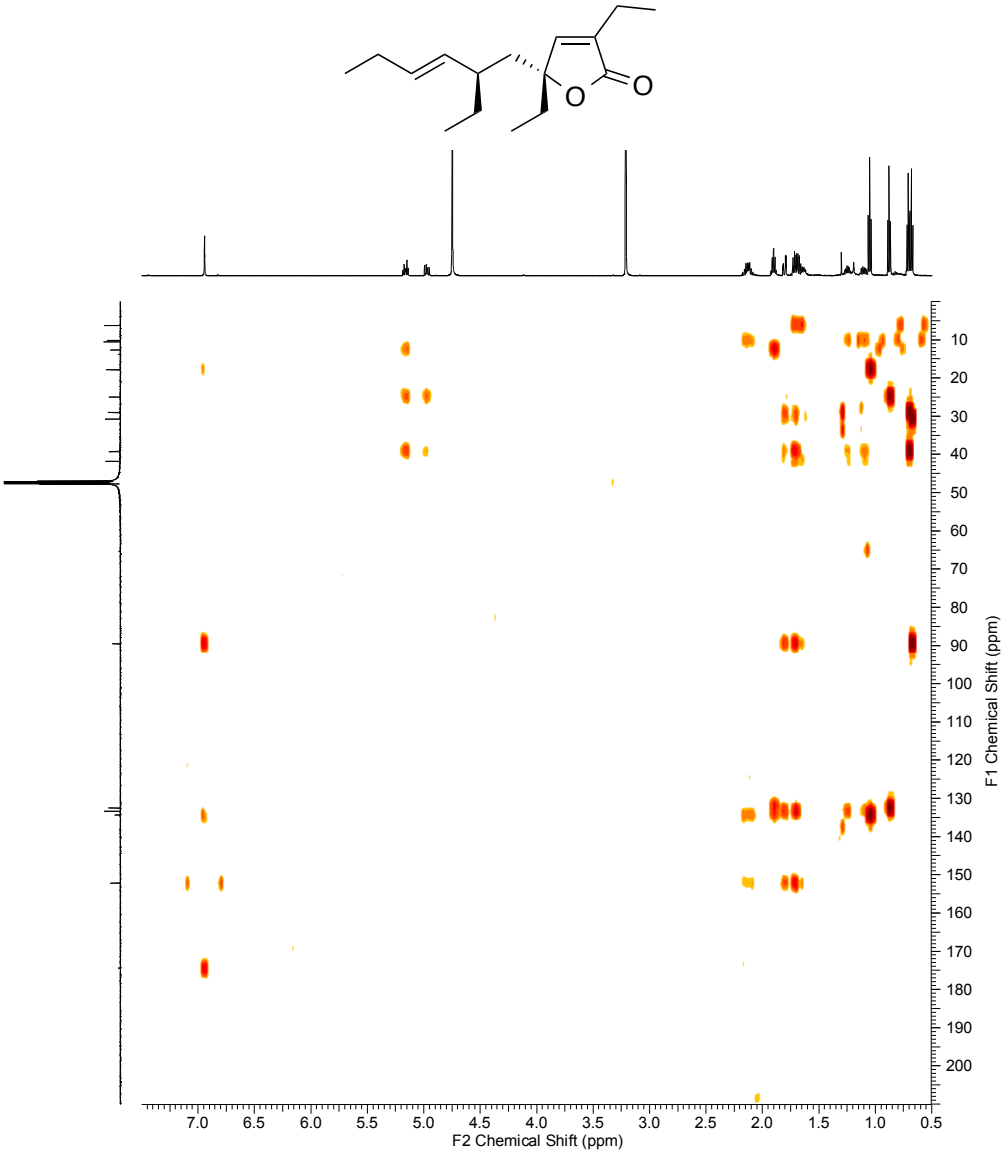

Figure 6.5: HMBC spectrum of synthetic *des*-hydroxyplakilactone B (**91**) with 1D ^{1}H NMR (600 MHz, CD_3OD) and ^{13}C NMR (150 MHz, CD_3OD) projections.

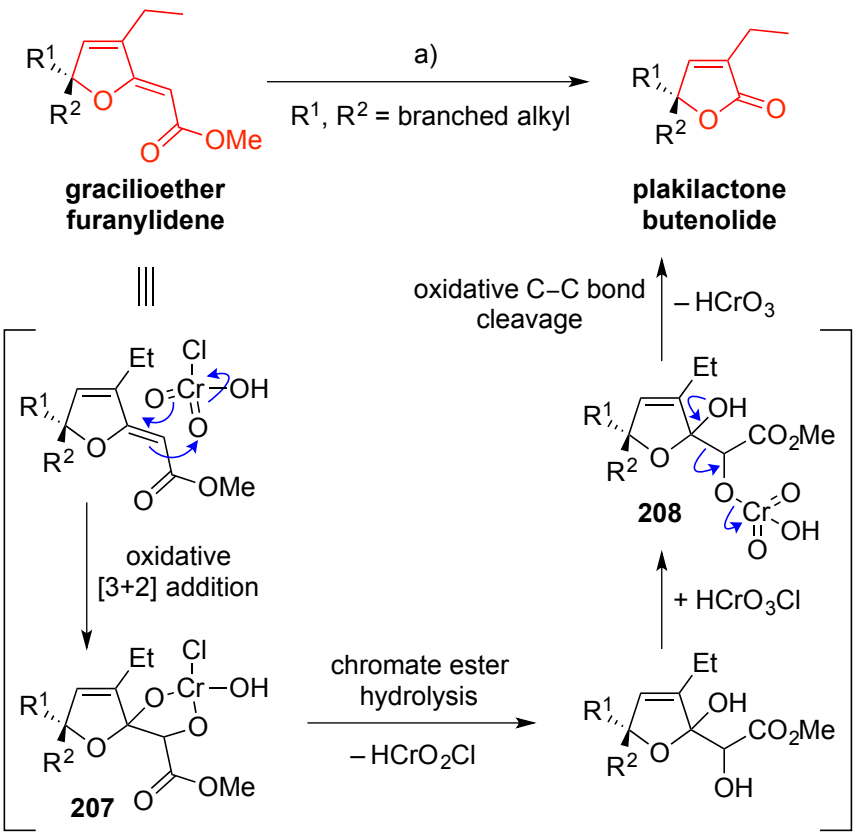

Scheme 6.9: Suggested mechanism for PCC oxidation of furanylidene substrates. a) PCC (9 equiv.), 4 Å MS, $(CH_2Cl)_2$, reflux, 15 h.

Following our synthesis of *des*-hydroxygracilioether C (**90**), we also became interested in the possibility that **90** may be a direct biogenetic precursor to hippolachnin A (**98**) through intramolecular [2+2] annulation, as postulated by Lin.[12] Several attempts at photo-induced cyclisation[21] (250W sunlamp, methylene blue/Me_2CO or 350 nm lamp) only caused epimerisation of the conjugated enol ether or tethered olefin. Treatment with radical initiators, including AIBN/Se_2Ph_2 and Weitz' aminium salt (tris(4-bromophenyl)aminium hexachloroantimonate), or the photoredox catalyst $Ru(bipy)_3Cl_2$ also gave disappointing results. Heating in xylene (140 °C) failed to instigate a stepwise (ionic) cycloaddition;[51–56] and similar results were found when screening conditions with common Lewis acids, including $BF_3{\cdot}OEt_2$, $TiCl_4$, $Ti(O^iPr)_4$, $AlCl_3$, $FeCl_3$ and $In(OTf)_3$. However, on treatment with $SnCl_4$ we discovered that **90** undergoes a facile ene cyclisation at low temperature, yielding the novel [3.3.0]-bicycle **209** (Scheme 6.10, Figure 6.6).[57] Key HMBCs, shown as dashed blue arrows in Scheme 6.10, clearly indicated shift of the furan olefin to the adjacent ethyl substituent and a new bond linking C5 and C9. NOEs, shown as red arrows in Scheme 6.10, were

observed between the hydrogen atoms connected to C2 and C13, and between C5 and C14. Thus, the alkene geometries at C2 and C13 of compound **209** are *Z* and *E*, respectively. Further NOEs appeared between the hydrogen atoms connected to C5 and C9, and between C5 and C7, demonstrating that the C9 stereocenter is in the *S* configuration. The dihedral coupling constant ($J_{5,9}$ 9.9 Hz) observed for the hydrogen atoms connected to C5 and C9 was also consistent with that reported for the analogous bridgehead hydrogen atoms of gracilioether A (*J* 10.7 Hz),[1] E (*J* 10.1 Hz), F (*J* 10.2 Hz), G (*J* 9.3 Hz), H (*J* 9.8 Hz), and I (*J* 10.3 Hz),[2] which all contain a similar [3.3.0]-bicyclic arrangement. Despite many efforts, we are yet to achieve direct [2+2] annulation of furanylidene **90**.

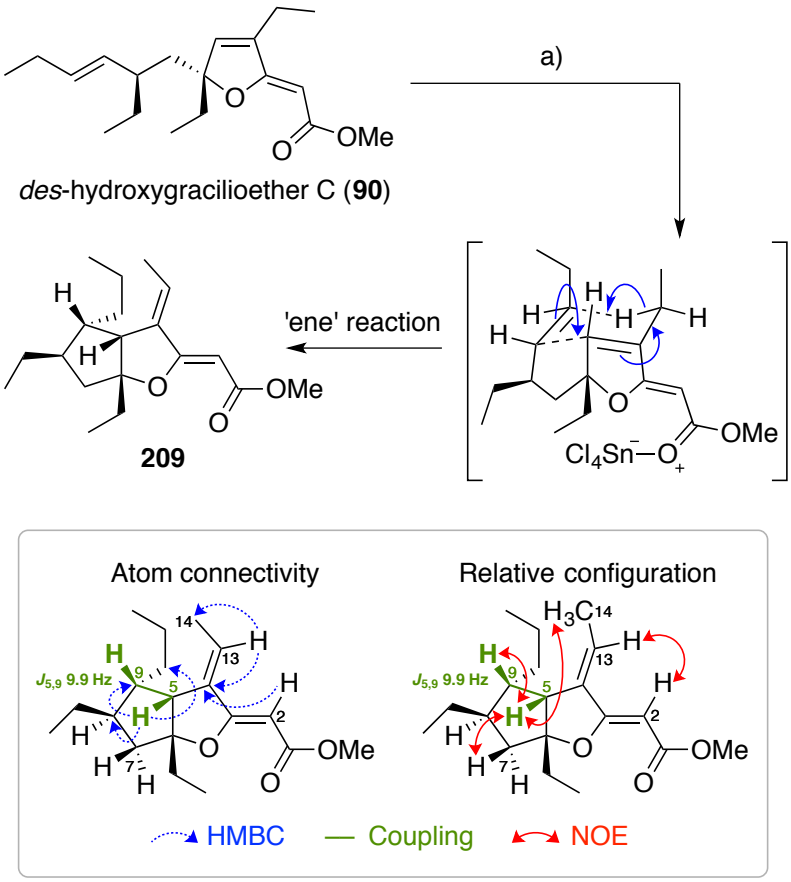

Scheme 6.10: $SnCl_4$-promoted ene reaction of *des*-hydroxygracilioether C (**90**). a) $SnCl_4$, CH_2Cl_2, –78 °C to r.t., 2.5 h, 47%.

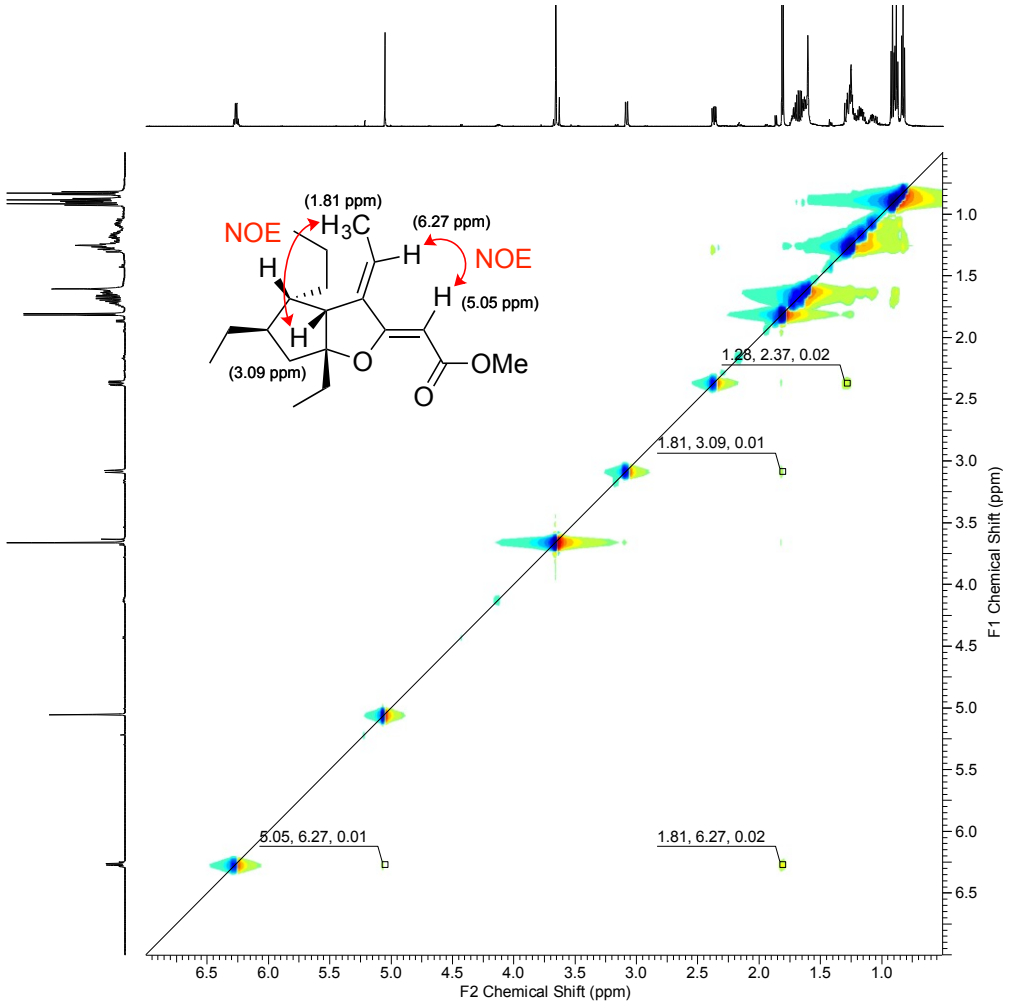

Figure 6.6: NOESY spectrum of ene adduct **209** with 1D ^{1}H NMR (600 MHz, $CDCl_3$) projections as evidence of the depicted stereochemical relationship.

6.4 Concluding remarks

In summary, a novel and chemoselective oxidation of synthetic gracilioether B (**85**), 11-*epi*-gracilioether C (**196**) benzoate and *des*-hydroxygracilioether C (**90**) with PCC has enabled total synthesis and stereochemical elucidation of the marine sponge metabolites plakilactones C, B and *des*-hydroxyplakilactone B. The structures and absolute configuration of the natural products were determined as (4*R*,6*R*)-**197**, (4*R*,6*R*,9*R*)-**198**, and (4*R*,6*R*)-**91**, respectively. Compound **90**, the putative biosynthetic precursor to hippolachnin A (**98**), was also found to undergo a facile $SnCl_4$-promoted ene cyclisation yielding a novel [3.3.0]-bicycle (**209**) with a similar carbon structure to several oxygenated gracilioether polycycles.

6.5 Preparative procedures and analytical data

6.5.1 General experimental details

For general experimental details, including information on reaction solvents, chromatography, analytical equipment and reported data, see Section 3.5.1. Silver-modified silica, when required, was prepared according to literature method.[31]

6.5.2 General procedure for PCC oxidation of furanylidene substrates

PCC (9.0 mmol) is added in a single portion to a stirred suspension of the furanylidene (1.0 mmol), 4 Å MS (1.94 g) and $(CH_2Cl)_2$ (19.4 mL) at room temperature. The mixture is heated at reflux temperature for 15 h. Once cooled, the crude residue is passed through a thick pad of silica (washing with excess 50% Et_2O/CH_2Cl_2) and concentrated *in vacuo*. Purification by flash chromatography yields the corresponding butenolide.

*6.5.3 Plakilactone C (**197**)*

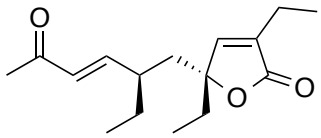

Prepared from furanylidene **85** (0.043 g, 0.13 mmol) according to the general procedure for PCC oxidation of furanylidene substrates (Section 6.5.2). Isolated as a colourless oil (0.026 g, 73%): R_f (25% EtOAc/hexane) 0.25; $[\alpha]^{20}_D$ –165 (*c* 0.65, $CHCl_3$); ν_{max} (thin film) 2969, 2926, 2880, 1746, 1697, 1672, 1623, 1461, 1359, 1254, 1143, 1090, 1045, 954, 883, 803, 781 cm^{-1}; δ_H (600 MHz, CD_3OD) 7.06 (1H, s, C*H*=CCH_2CH_3), 6.61 (1H, dd, *J* 16.0, 9.4 Hz, C*H*=CHC(O)CH_3), 5.87 (1H, d, *J* 16.0 Hz, CH=C*H*C(O)CH_3), 2.24 (3H, s, C(O)CH_3), 2.23–2.18 (1H, m, CH=CC$H_A$$H_B$$CH_3$), 2.18–2.12 (1H, m, CH=C$CH_A$$H_B$$CH_3$), 2.09–2.07 (2H, overlapping peaks, C*H*CH_2CH_3, C$H_A$$H_B$$CCH_2CH_3$), 1.93 (1H, dd, *J* 15.0, 10.1 Hz, $CH_A$$H_B$$CCH_2CH_3$), 1.85–1.75 (2H, m, $CH_2CCH_2CH_3$), 1.52–1.46 (1H, m, CHC$H_A$$H_B$$CH_3$), 1.38–1.32 (1H, m $CHCH_A$$H_B$$CH_3$), 1.09 (3H, t, *J* 7.5 Hz, CH=CCH_2CH_3), 0.84 (3H, t, *J* 7.4 Hz, $CHCH_2CH_3$), 0.78 (3H, t, *J* 7.5 Hz, $CH_2CCH_2CH_3$); δ_C (150 MHz, CD_3OD) 201.0, 175.6, 154.7, 153.1, 136.9, 132.3, 90.6,

42.4, 41.1, 32.0, 29.6, 26.9, 19.5, 11.9, 11.7, 7.9; HRMS (ESI): MNa^+, found 287.1624. $C_{16}H_{24}NaO_3^+$ requires 287.1623.

6.5.4 *Methyl 2-[(2Z,5R)-3,5-diethyl-5-[(2R)-2-ethyl-3-oxopropyl]-2(5H)-furanylidene]ethanoate (**200**) and methyl 2-[(2Z,5R)-3,5-diethyl-5-[(2S)-2-ethyl-3-oxopropyl]-2(5H)-furanylidene]ethanoate (**201**)*

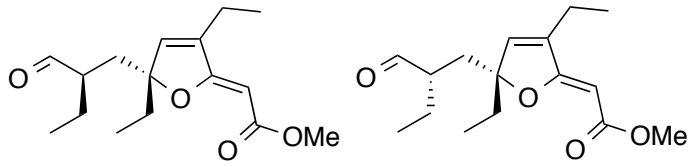

HCl (1.0 mL, 10% aq) was added to a stirred solution of **88** (0.15 g, 0.47 mmol) in THF (10 mL) at room temperature. Stirring continued for 24 h before quenching with slow addition of $NaHCO_3$ (satd aq). The organic phase was separated and aqueous extracted with Et_2O. The combined organic extracts were washed with brine, dried (Na_2SO_4) and concentrated *in vacuo*. Flash chromatography afforded **200** (0.067 g, 51%) and **201** (0.050 g, 38%), each as pale yellow oils. **200**: R_f (20% EtOAc/hexane) 0.31; $[\alpha]^{20}_D$ –98 (*c* 0.35, $CHCl_3$); ν_{max} (thin film) 2969, 2938, 2880, 1713, 1687, 1625, 1460, 1434, 1377, 1274, 1159, 1089, 1037, 975, 852, 806 cm^{-1}; δ_H (600 MHz, $CDCl_3$) 9.53 (1H, d, *J* 1.8 Hz, C*H*O), 6.11 (1H, s, C*H*=CCH_2CH_3), 4.84 (1H, s, C*H*CO_2CH_3), 3.69 (3H, s, OCH_3), 2.26 (1H, dd, *J* 14.3, 9.0 Hz, C$H_A$$H_B$$CCH_2CH_3$), 2.19–2.15 (1H, m, C*H*CH_2CH_3), 2.16–2.12 (2H, m, CH=CC$H_2$$CH_3$), 1.93–1.87 (2H, overlapping peaks, $CH_A$$H_B$$CCH_2CH_3$, $CH_2CC$$H_A$$H_B$$CH_3$), 1.78 (1H, dq, *J* 14.4, 7.3 Hz, $CH_2CCH_A$$H_B$$CH_3$), 1.68–1.60 (1H, m, $CHCH_A$$H_B$$CH_3$), 1.55–1.50 (1H, m, $CHCH_A$$H_B$$CH_3$), 1.12 (3H, t, *J* 7.4 Hz, $CH=CCH_2C$$H_3$), 0.90 (3H, t, *J* 7.4 Hz, $CHCH_2C$$H_3$), 0.81 (3H, t, *J* 7.3 Hz, $CH_2CCH_2C$$H_3$); δ_C (150 MHz, $CDCl_3$) 204.3, 171.2, 166.7, 140.8, 139.1, 96.8, 84.5, 50.6, 48.1, 35.8, 31.7, 23.2, 18.5, 11.9, 11.0, 8.1; HRMS (ESI): MNa^+, found 303.1564. $C_{16}H_{24}NaO_4^+$ requires 303.1572. **201**: R_f (20% EtOAc/hexane) 0.17; $[\alpha]^{20}_D$ –83 (*c* 0.27, $CHCl_3$); ν_{max} (thin film) 2969, 2924, 2880, 2850, 1714, 1689, 1627, 1461, 1435, 1377, 1274, 1169, 1037, 975, 917, 875, 807 cm^{-1}; δ_H (600 MHz, $CDCl_3$) 9.45 (1H, d, *J* 3.7 Hz, C*H*O), 6.13 (1H, s, C*H*=CCH_2CH_3), 4.85 (1H, s, C*H*CO_2CH_3), 3.67 (3H, s, OCH_3), 2.39 (1H, dd, *J* 14.8, 9.6 Hz, C$H_A$$H_B$$CCH_2CH_3$), 2.20–2.15 (2H, m, CH=CC$H_2$$CH_3$), 2.07–2.02 (1H, m, C*H*CH_2CH_3), 1.93–1.80 (1H, m, $CH_2CC$$H_A$$H_B$$CH_3$), 1.80–1.72 (2H, overlapping peaks, C$H_A$$H_B$$CCH_2CH_3$, $CH_2CCH_A$$H_B$$CH_3$), 1.62–1.55 (1H, m, $CHC$$H_A$$H_B$$CH_3$), 1.48–1.42 (1H, m, $CHCH_A$$H_B$$CH_3$), 1.16 (3H, t, *J* 7.4 Hz,

CH=CCH$_2$C*H*$_3$), 0.85 (3H, t, *J* 7.4 Hz, CHCH$_2$C*H*$_3$), 0.80 (3H, t, *J* 7.4 Hz, CH$_2$CCH$_2$C*H*$_3$); δ_C (150 MHz, CDCl$_3$) 203.5, 170.4, 166.5, 141.5, 137.9, 96.6, 85.2, 50.6, 48.8, 37.6, 31.7, 23.0, 18.5, 12.0, 11.1, 7.9; HRMS (ESI): MNa$^+$, found 303.1562. $C_{16}H_{24}NaO_4^+$ requires 303.1572.

*6.5.5 8-epi-Gracilioether B (**202**)*

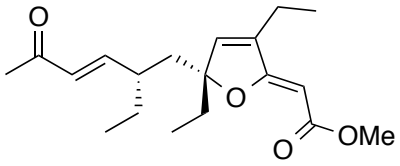

Et$_3$N (0.16 mL, 1.2 mmol) was added to a solution of **201** (0.12 g, 0.44 mmol), diethyl 2-oxopropylphosphonate (0.16 mL, 0.83 mmol) and LiCl (0.048 g, 1.1 mmol) in MeCN (9.4 mL) at room temperature. Stirring continued for 24 h (progress monitored by TLC until completion) before partitioning between NH$_4$Cl (satd aq) and CH$_2$Cl$_2$. The organic phase was separated and aqueous extracted with CH$_2$Cl$_2$. The combined extracts were dried (Na$_2$SO$_4$) and concentrated *in vacuo*. Flash chromatography afforded the *title compound* (0.12 g, 85%) as a colourless waxy solid: R_f (40% EtOAc/hexane) 0.41; $[\alpha]^{20}_D$ –269 (*c* 0.36, CHCl$_3$); ν_{max} (thin film) 2969, 2937, 2879, 1709, 1672, 1625, 1460, 1434, 1356, 1254, 1166, 1037, 974, 874, 805 cm^{-1}; δ_H (600 MHz, CD$_3$OD) 6.56 (1H, dd, *J* 16.0, 9.7 Hz, C*H*=CHC(O)CH$_3$), 6.46 (1H, s, C*H*=CCH$_2$CH$_3$), 5.60 (1H, d, *J* 16.0 Hz, CH=C*H*C(O)CH$_3$), 4.77 (1H, s, C*H*CO$_2$CH$_3$), 3.60 (3H, s, OC*H*$_3$), 2.18–2.13 (2H, m, CH=CC*H*$_2$CH$_3$), 2.13–2.11 (4H, overlapping peaks, C(O)C*H*$_3$, C*H*$_A$H$_B$CCH$_2$CH$_3$), 2.03 (1H, dd, *J* 14.7, 2.8 Hz, CH$_A$*H*$_B$CCH$_2$CH$_3$), 1.99–1.94 (1H, m, C*H*CH$_2$CH$_3$), 1.88–1.82 (1H, m, CH$_2$CC*H*$_A$H$_B$CH$_3$), 1.79–1.73 (1H, m, CH$_2$CCH$_A$*H*$_B$CH$_3$), 1.51–1.44 (1H, m, CHC*H*$_A$H$_B$CH$_3$), 1.36–1.29 (1H, m, CHCH$_A$*H*$_B$CH$_3$), 1.18 (3H, t, *J* 7.4 Hz, CH=CCH$_2$C*H*$_3$), 0.81 (3H, t, *J* 7.4 Hz, CHCH$_2$C*H*$_3$), 0.75 (3H, t, *J* 7.4 Hz, CH$_2$CCH$_2$C*H*$_3$); δ_C (150 MHz, CD$_3$OD) 201.7, 173.9, 169.0, 155.2, 142.4, 141.1, 131.2, 99.5, 84.7, 51.1, 43.8, 43.1, 33.4, 29.3, 25.9, 19.4, 12.6, 11.8, 7.9; HRMS (ESI): MNa$^+$, found 343.1884. $C_{19}H_{28}NaO_4^+$ requires 343.1885.

6.5.6 6-epi-Plakilactone C (**199**)

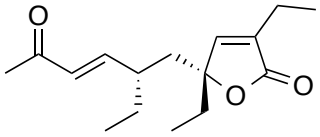

Prepared from furanylidene **202** (0.044 g, 0.14 mmol) according to the general procedure for PCC oxidation of furanylidene substrates (Section 6.5.2). Isolated as a colourless waxy solid (0.028 g, 77%): R_f (25% EtOAc/hexane) 0.21; $[\alpha]^{20}_D$ –6 (*c* 0.70, $CHCl_3$); ν_{max} (thin film) 2969, 2926, 2879, 1748, 1698, 1672, 1625, 1461, 1361, 1254, 1138, 1044, 954, 877, 808, 780 cm^{-1}; δ_H (600 MHz, CD_3OD) 7.13 (1H, s, C*H*=CCH_2CH_3), 6.53 (1H, dd, *J* 16.0, 9.1 Hz, C*H*=CHC(O)CH_3), 5.70 (1H, d, *J* 16.0 Hz, CH=C*H*C(O)CH_3), 2.22 (3H, s, C(O)CH_3), 2.22–2.18 (2H, m, CH=CCH_2CH_3), 2.05–2.00 (3H, overlapping peaks, C*H*CH_2CH_3, CH_2CH_2CH_3), 1.82 (1H, dq, *J* 14.5, 7.5 Hz, $CH_2CCH_AH_BCH_3$), 1.73 (1H, dq, *J* 14.5, 7.5 Hz, $CH_2CCH_AH_BCH_3$), 1.53–1.46 (1H, m, $CHCH_AH_BCH_3$), 1.36–1.30 (1H, m, $CHCH_AH_BCH_3$), 1.15 (3H, t, *J* 7.5 Hz, CH=CCH_2CH_3), 0.83 (3H, t, *J* 7.4 Hz, $CHCH_2CH_3$), 0.78 (3H, t, *J* 7.5 Hz, $CH_2CCH_2CH_3$); δ_C (150 MHz, CD_3OD) 201.3, 175.5, 154.3, 151.7, 138.0, 131.7, 91.1, 42.9, 42.0, 32.5, 29.3, 26.3, 19.4, 12.4, 11.7, 7.8; HRMS (ESI): MNa^+, found 287.1622. $C_{16}H_{24}NaO_3^+$ requires 287.1623.

6.5.7 Gracilioether C (**86**) benzoate

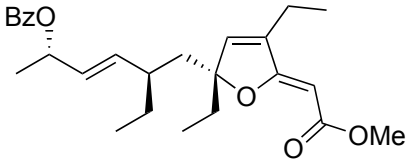

DMAP (0.063 g, 0.52 mmol) was added in a single portion to a stirred solution of **86** (0.026 g, 0.08 mmol), $PhCO_2H$ (0.16 g, 1.3 mmol) and DCC (0.17 g, 0.8 mmol) in THF (4.0 mL) at room temperature. Stirring continued for 3 h before quenching with the addition of $NaHCO_3$ (50% satd aq). The mixture was filtered, organic phase separated and aqueous extracted with Et_2O. The combined extracts were dried (Na_2SO_4), concentrated *in vacuo* and triturated with 50% Et_2O/hexane. Flash chromatography afforded the *title compound* (0.033 g, 96%) as a pale yellow oil: R_f (25% Et_2O/hexane) 0.25; $[\alpha]^{20}_D$ –279 (*c* 0.19, $CHCl_3$); ν_{max} (thin film) 2925, 2857, 1715, 1627, 1453, 1377, 1269, 1162 cm^{-1}; δ_H (600 MHz, $CDCl_3$) 8.04 (2H, apparent d, *J* 8.3 Hz, Ar*H*), 7.56 (1H,

apparent t, *J* 7.6 Hz, Ar*H*), 7.44 (2H, apparent t, *J* 7.6 Hz, Ar*H*), 6.12 (1H, s, C*H*=CCH$_2$CH$_3$), 5.53 (1H, apparent p, *J* 6.6 Hz, C*H*(OBz)CH$_3$), 5.45 (1H, dd, *J* 15.4, 8.4 Hz, C*H*=CHCH(OBz)CH$_3$), 5.35 (1H, dd, *J* 15.4, 7.2 Hz, CH=C*H*CH(OBz)CH$_3$), 4.78 (1H, s, C*H*CO$_2$CH$_3$), 3.68 (3H, s, OC*H*$_3$), 2.03–1.97 (3H, overlapping peaks, CH=CC*H*$_2$CH$_3$, C*H*$_A$H$_B$CCH$_2$CH$_3$), 1.85–1.77 (3H, overlapping peaks, CH$_A$*H*$_B$CCH$_2$CH$_3$, CH$_2$CC*H*$_A$H$_B$CH$_3$, C*H*CH$_2$CH$_3$), 1.69 (1H, dq, *J* 14.4, 7.3 Hz, CH$_2$CCH$_A$*H*$_B$CH$_3$), 1.45–1.38 (1H, m, CHC*H*$_A$H$_B$CH$_3$), 1.40 (3H, d, *J* 6.4 Hz, CH(OBz)C*H*$_3$), 1.24–1.16 (1H, m, CHCH$_A$*H*$_B$CH$_3$), 0.97 (3H, t, *J* 7.4 Hz, CH=CCH$_2$C*H*$_3$), 0.78 (3H, t, *J* 7.3 Hz, CHCH$_2$C*H*$_3$), 0.74 (3H, t, *J* 7.4 Hz, CH$_2$CCH$_2$C*H*$_3$); δ_C (150 MHz, CDCl$_3$) 171.9, 166.9, 165.8, 140.0, 139.5, 138.3, 132.8, 130.8, 129.9, 129.5 (2 peaks), 128.3 (2 peaks), 97.6, 83.5, 72.0, 50.5, 43.2, 39.3, 32.4, 29.1, 20.8, 18.5, 11.9, 11.3, 7.9; HRMS (ESI): MNa$^+$, found 449.2299. $C_{26}H_{34}NaO_5^+$ requires 449.2304.

*6.5.8 9-epi-Plakilactone B benzoate (**203**)*

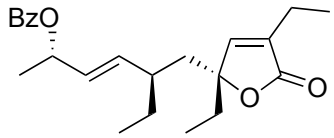

Prepared from furanylidene **86** benzoate (0.030 g, 0.07 mmol) according to the general procedure for PCC oxidation of furanylidene substrates (Section 6.5.2). Isolated as a pale yellow oil (0.019 g, 73%): R_f (20% Et$_2$O/hexane) 0.26; $[\alpha]^{20}_D$ –104 (*c* 0.37, CHCl$_3$); ν_{max} (thin film) 2925, 2856, 1755, 1716, 1603, 1452, 1315, 1269, 1110 cm^{-1}; δ_H (600 MHz, CDCl$_3$) 8.04 (2H, d, *J* 7.2 Hz, Ar*H*), 7.57 (1H, apparent t, *J* 7.2 Hz, Ar*H*), 7.45 (2H, apparent t, *J* 7.8 Hz, Ar*H*), 6.71 (1H, t, *J* 1.6 Hz, C*H*=CCH$_2$CH$_3$), 5.52 (1H, apparent p, *J* 6.6 Hz, C*H*(OBz)CH$_3$), 5.44 (1H, dd, *J* 15.4, 8.4 Hz, C*H*=CHCH(OBz)CH$_3$), 5.32 (1H, dd, *J* 15.4, 7.3 Hz, CH=C*H*CH(OBz)CH$_3$), 2.14–2.05 (2H, m, CH=CC*H*$_2$CH$_3$), 1.95 (1H, apparent q, *J* 18.9, 6.8 Hz, C*H*$_A$H$_B$CCH$_2$CH$_3$), 1.81–1.73 (3H, overlapping peaks, CH$_A$*H*$_B$CCH$_2$CH$_3$, C*H*CH$_2$CH$_3$, CH$_2$CC*H*$_A$H$_B$CH$_3$), 1.67 (1H, dq, *J* 14.4, 7.4 Hz, CH$_2$CCH$_A$*H*$_B$CH$_3$), 1.41 (3H, d, *J* 6.4 Hz, CH(OBz)C*H*$_3$), 1.40–1.34 (1H, m, CHC*H*$_A$H$_B$CH$_3$), 1.25–1.18 (1H, m, CHCH$_A$*H*$_B$CH$_3$), 0.92 (3H, t, *J* 7.4 Hz, CH=CCH$_2$C*H*$_3$), 0.79 (3H, t, *J* 7.3 Hz, CHCH$_2$C*H*$_3$), 0.77 (3H, t, *J* 7.3 Hz, CH$_2$CCH$_2$C*H*$_3$); δ_C (150 MHz, CDCl$_3$) 173.6, 165.9, 150.8, 138.2, 135.1, 132.9, 131.0,

130.7, 129.5 (2 peaks), 128.3 (2 peaks), 89.0, 72.0, 42.4, 38.9, 31.8, 29.3, 20.9, 18.5, 11.8, 11.4, 7.7; HRMS (ESI): MNa^+, found 393.2053. $C_{23}H_{30}NaO_4^+$ requires 393.2042.

*6.5.9 9-epi-Plakilactone B (**204**)*

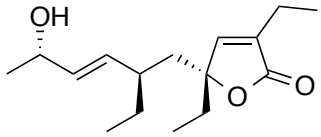

KOH (0.11 g, 1.9 mmol) was added in a single portion to a stirred solution of **203** (0.014 g, 0.05 mmol) in MeOH (1.0 mL) at room temperature. Stirring continued for 1 h before quenching with the addition of NH_4Cl (satd aq) and Et_2O. The organic phase was separated and aqueous extracted with Et_2O. The combined extracts were washed with $NaHCO_3$ (50% satd aq), brine, dried (Na_2SO_4) and concentrated *in vacuo*. Flash chromatography afforded the *title compound* (0.010 g, quant.) as a colourless oil: R_f (25% EtOAc/hexane) 0.25; $[\alpha]^{20}_D$ –46 (*c* 0.54, $CHCl_3$); ν_{max} (thin film) 3445, 3057, 2968, 2926, 2878, 1733, 1461, 1368, 1267, 1139, 1051 cm^{-1}; δ_H (600 MHz, CD_3OD) 7.09 (1H, t, *J* 1.5 Hz, C*H*=CCH_2CH_3), 5.32–5.26 (2H, overlapping peaks, C*H*=CHCH(OH)CH_3, CH=C*H*CH(OH)CH_3), 4.19–4.15 (1H, m, C*H*(OH)CH_3), 2.25 (2H, qd, *J* 7.5, 1.5 Hz, CH=CCH_2CH_3), 1.92 (1H, dd, *J* 14.7, 3.1 Hz, CH_AH_BCCH_2CH_3), 1.85–1.71 (4H, overlapping peaks, CH_AH_BCCH_2CH_3, C*H*CH_2CH_3, $CH_2CCH_2CH_3$), 1.41–1.33 (1H, m, CHC$H_AH_B$$CH_3$), 1.26–1.19 (1H, m, $CHCH_AH_B$$CH_3$), 1.20 (3H, d, *J* 6.4 Hz, CH(OH)CH_3), 1.15 (3H, t, *J* 7.5 Hz, CH=CCH_2CH_3), 0.81 (3H, t, *J* 7.4 Hz, $CHCH_2CH_3$), 0.78 (3H, t, *J* 7.4 Hz, $CH_2CCH_2CH_3$), missing O*H*; δ_C (150 MHz, CD_3OD) 176.0, 153.7, 136.5, 136.2, 135.3, 91.2, 69.1, 43.3, 40.5, 32.2, 30.4, 23.8, 19.4, 12.3, 11.8, 8.0; HRMS (ESI): MNa^+, found 289.1773. $C_{16}H_{26}NaO_3^+$ requires 289.1780.

*6.5.10 11-epi-Gracilioether C (**196**) benzoate*

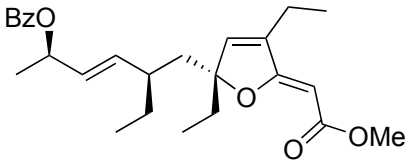

DMAP (0.073 g, 0.60 mmol) was added in a single portion to a stirred solution of **196** (0.034 g, 0.11 mmol) and DCC (0.20 g, 0.96 mmol) in THF (5.0 mL) at room temperature. Stirring continued for 3 h before quenching with the addition of $NaHCO_3$

(50% satd aq). The organic phase was separated and aqueous extracted with Et_2O. The combined extracts were washed with water, brine, dried (Na_2SO_4) and concentrated *in vacuo*. Flash chromatography afforded the *title compound* (0.043 g, 96%) as a colourless oil: R_f (25% Et_2O/hexane) 0.25; $[\alpha]^{20}_D$ –167 (*c* 0.30, $CHCl_3$); ν_{max} (thin film) 3060, 2927, 2858, 1715, 1634, 1493, 1452, 1266, 1160, 1050 cm^{-1}; δ_H (600 MHz, $CDCl_3$) 8.03 (2H, apparent d, *J* 7.2 Hz, Ar*H*), 7.55 (1H, apparent t, *J* 7.9 Hz, Ar*H*), 7.44 (2H, apparent t, *J* 7.7 Hz, Ar*H*), 6.17 (1H, s, C*H*=CCH_2CH_3), 5.53 (1H, apparent p, *J* 6.3 Hz, C*H*(OBz)CH_3), 5.45 (1H, dd, *J* 15.5, 8.7 Hz, C*H*=CHCH(OBz)CH_3), 5.39 (1H, dd, *J* 15.5, 6.0 Hz, CH=C*H*CH(OBz)CH_3), 4.81 (1H, s, C*H*CO_2CH_3), 3.69 (3H, s, OCH_3), 2.14 (2H, apparent q, *J* 7.7 Hz, CH=CCH_2CH_3), 1.97 (1H, dd, *J* 14.2, 3.2 Hz, C$H_A$$H_B$$CCH_2CH_3$), 1.87–1.75 (3H, overlapping peaks, $CH_AH_BCCH_2CH_3$, C*H*CH_2CH_3, $CH_2CCH_AH_BCH_3$), 1.70 (1H, dq, *J* 14.3, 7.3 Hz, $CH_2CCH_AH_BCH_3$), 1.43–1.37 (1H, m, $CHCH_AH_BCH_3$), 1.41 (3H, d, *J* 6.4 Hz, CH(OBz)CH_3), 1.25–1.17 (1H, m, $CHCH_AH_BCH_3$), 1.13 (3H, t, *J* 7.4 Hz, CH=CCH_2CH_3), 0.77 (3H, t, *J* 7.3 Hz, $CHCH_2CH_3$), 0.76 (3H, t, *J* 7.3 Hz, $CH_2CCH_2CH_3$); δ_C (150 MHz, $CDCl_3$) 171.8, 166.8, 165.8, 139.9, 139.7, 137.5, 132.8, 130.8, 129.6, 129.5 (2 peaks), 128.3 (2 peaks), 97.5, 83.6, 71.3, 50.5, 43.0, 39.2, 32.3, 29.0, 20.5, 18.6, 11.9, 11.3, 7.9; HRMS (ESI): MNa^+, found 449.2296. $C_{26}H_{34}NaO_5^+$ requires 449.2304.

*6.5.11 Plakilactone B benzoate (**205**)*

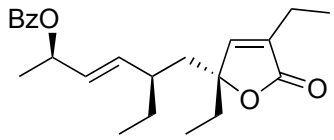

Prepared from furanylidene **196** benzoate (0.034 g, 0.09 mmol) according to the general procedure for PCC oxidation of furanylidene substrates (Section 6.5.2). Isolated as a pale yellow oil (0.021 g, 71%): R_f (20% Et_2O/hexane) 0.26; $[\alpha]^{20}_D$ –44 (*c* 0.25, $CHCl_3$); ν_{max} (thin film) 2968, 2927, 2859, 1751, 1716, 1603, 1494, 1452, 1270, 1111, 1050 cm^{-1}; δ_H (600 MHz, $CDCl_3$) 8.04 (2H, apparent d, *J* 8.2 Hz, Ar*H*), 7.56 (1H, apparent t, *J* 7.5 Hz, Ar*H*), 7.45 (2H, apparent t, *J* 7.8 Hz, Ar*H*), 6.77 (1H, t, *J* 1.6 Hz, C*H*=CCH_2CH_3), 5.53 (1H, m, C*H*(OBz)CH_3), 5.44–5.37 (2H, overlapping peaks, C*H*=CHCH(OBz)CH_3, CH=C*H*CH(OBz)CH_3), 2.33–2.21 (2H, m, CH=CCH_2CH_3), 1.94 (1H, dd, *J* 14.4, 2.7 Hz, C$H_A$$H_B$$CCH_2CH_3$), 1.83–1.65 (4H, overlapping peaks, $CH_AH_BCCH_2CH_3$, C*H*CH_2CH_3, C$H_2CCH_2CH_3$), 1.42 (3H, d, *J* 6.6 Hz, CH(OBz)CH_3),

1.40–1.33 (1H, m, CHCH_AH$_B$CH$_3$), 1.27–1.20 (1H, m, CHCH$_A$$H_BCH_3$), 1.14 (3H, t, *J* 7.4 Hz, CH=CCH$_2$CH_3), 0.79 (3H, t, *J* 7.4 Hz, CH$_2$CCH$_2$CH_3), 0.78 (3H, t, *J* 7.4 Hz, CHCH$_2$CH_3); δ_C (150 MHz, CDCl$_3$) 173.6, 165.8, 150.6, 137.0, 135.4, 132.9, 130.7, 130.6, 129.5 (2 peaks), 128.3 (2 peaks), 89.0, 71.2, 42.2, 38.9, 31.6, 29.3, 20.5, 18.6, 11.9, 11.3, 7.8; HRMS (ESI): MNa$^+$, found 393.2041. $C_{23}H_{30}NaO_4^+$ requires 393.2042.

*6.5.12 Plakilactone B (**198**)*

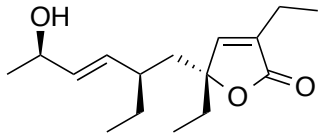

KOH (0.095 g, 1.7 mmol) was added in a single portion to a stirred solution of **205** (0.017 g, 0.05 mmol) in MeOH (1.0 mL) at room temperature. Stirring continued for 1 h before quenching with the addition of NH_4Cl (satd aq) and Et_2O. The organic phase was separated and aqueous extracted with Et_2O. The combined extracts were washed with $NaHCO_3$ (50% satd aq), brine, dried (Na_2SO_4) and concentrated *in vacuo*. Flash chromatography afforded the *title compound* (0.012 g, 98%) as a colourless oil: R_f (25% EtOAc/hexane) 0.25; $[\alpha]^{20}_D$ –66 (*c* 0.64, $CHCl_3$); ν_{max} (thin film) 3445, 2968, 2926, 2857, 1739, 1494, 1456, 1051 cm^{-1}; δ_H (600 MHz, CD_3OD) 7.06 (1H, t, *J* 1.6 Hz, C*H*=CCH$_2$CH$_3$), 5.33–5.27 (2H, overlapping peaks, C*H*=CHCH(OH)CH$_3$, CH=C*H*CH(OH)CH$_3$), 4.19–4.15 (1H, m, C*H*(OH)CH$_3$), 2.29–2.19 (2H, m, CH=CCH_2CH$_3$), 1.93 (1H, dd, *J* 14.1, 2.6 Hz, CH_AH$_B$CCH$_2$CH$_3$), 1.84–1.73 (4H, overlapping peaks, CH$_A$$H_BCCH_2CH_3$, C*H*CH$_2CH_3$, CH$_2CCH_2CH_3$), 1.41–1.33 (1H, m, CHC$H_AH_BCH_3$), 1.27–1.22 (1H, m, CHCH$_A$$H_BCH_3$), 1.20 (3H, d, *J* 6.4 Hz, CH(OH)CH_3), 1.15 (3H, t, *J* 7.4 Hz, CH=CCH$_2$CH_3), 0.83 (3H, t, *J* 7.4 Hz, CHCH$_2$CH_3), 0.77 (3H, t, *J* 7.4 Hz, CH$_2$CCH$_2$CH_3), missing O*H*; δ_C (150 MHz, CD_3OD) 176.0, 153.7, 136.4, 136.1, 135.3, 91.1, 69.1, 43.3, 40.4, 32.2, 30.4, 23.8, 19.5, 12.3, 11.8, 8.0; HRMS (ESI): MNa$^+$, found 289.1780. $C_{16}H_{26}NaO_3^+$ requires 289.1780.

*6.5.13 des-Hydroxygracilioether C (**90**)*

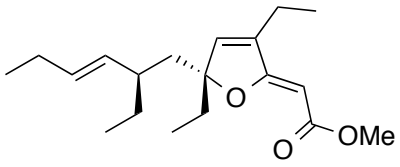

LHMDS (0.35 mL, 1.0 M in THF; 0.35 mmol) was added dropwise over 30 s to a stirred solution of sulfone **206** (0.10 g, 0.40 mmol) in DMF (3.0 mL) and DMPU (1.0 mL) at –60 °C. After 120 s, a solution of **200** (0.040 g, 0.14 mmol) in DMF (0.2 mL) was added dropwise. The mixture was stirred at –60 °C for 1 h before gradually warming to room temperature and quenching with the addition of NH_4Cl (satd aq) and Et_2O. The organic phase was separated and aqueous extracted with Et_2O. The combined extracts were washed with water, brine, dried (Na_2SO_4) and concentrated *in vacuo*. Silver-modified silica chromatography[31] afforded the *title compound* (0.030 g, 69%) as a pale yellow oil: R_f (10% EtOAc/hexane) 0.40 (non-modified silica); $[\alpha]^{20}_D$ –271 (*c* 0.35, $CHCl_3$); ν_{max} (thin film) 2966, 2935, 2877, 1713, 1687, 1625, 1460, 1434, 1376, 1272, 1159, 1087, 1039, 973, 853, 804 cm^{-1}; δ_H (600 MHz, $CDCl_3$) 6.17 (1H, s, C*H*=CCH_2CH_3), 5.22 (1H, dt, *J* 15.3, 6.4 Hz, CH=C*H*CH_2CH_3), 5.03 (1H, dd, *J* 15.3, 8.5 Hz, C*H*=$CHCH_2CH_3$), 4.80 (1H, s, C*H*CO_2CH_3), 3.68 (3H, s, OCH_3), 2.18–2.08 (2H, m, CH=CCH_2CH_3), 1.98–1.90 (3H, m, CH=CHCH_2CH_3, C$H_A$$H_B$$CCH_2CH_3$), 1.86–1.80 (1H, m, $CH_2CCH_A$$H_B$$CH_3$), 1.77–1.68 (3H, overlapping peaks, $CH_2CCH_A$$H_B$$CH_3$, C*H*$CH_2CH_3$ $CH_A$$H_B$$CCH_2CH_3$), 1.39–1.32 (1H, m, CHC$H_A$$H_B$$CH_3$), 1.18–1.11 (1H, m, $CHCH_A$$H_B$$CH_3$), 1.14 (3H, t, *J* 7.3 Hz, CH=CCH_2CH_3), 0.94 (3H, t, *J* 7.5 Hz, CH=$CHCH_2CH_3$), 0.78–0.75 (6H, overlapping peaks, $CHCH_2CH_3$, $CH_2CCH_2CH_3$); δ_C (150 MHz, C_6D_6) 171.5, 166.2, 139.7, 139.5, 134.5, 131.9, 97.2, 84.7, 50.3, 43.6, 39.9, 32.5, 29.7, 25.9, 18.6, 14.2, 11.8, 11.6, 7.9; HRMS (ESI): MNa^+, found 329.2092. $C_{19}H_{30}NaO_3^+$ requires 329.2093.

*6.5.14 des-Hydroxyplakilactone B (**91**)*

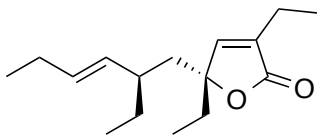

Prepared from furanylidene **90** (0.006 g, 0.02 mmol) according to the general procedure for PCC oxidation of furanylidene substrates (Section 6.5.2). Isolated as a

colourless oil (0.004 g, 82%): R_f (10% EtOAc/hexane) 0.44; $[\alpha]^{20}_D$ –90 (*c* 0.30, CH_3OH); ν_{max} (thin film) 3056, 2968, 2933, 2877, 1749, 1461, 1266, 1086, 1047, 970 cm^{-1}; δ_H (600 MHz, CD_3OD) 7.03 (1H, t, *J* 1.7 Hz, C*H*=CCH_2CH_3), 5.25 (1H, dt, *J* 15.2, 6.4 Hz, CH=C*H*CH_2CH_3), 5.06 (1H, ddt, *J* 15.2, 8.8, 1.5 Hz, C*H*=$CHCH_2CH_3$), 2.28–2.16 (2H, m, CH=CC$H_2$$CH_3$), 2.02–1.97 (2H, m, CH=CHC$H_2$$CH_3$), 1.89 (1H, dd, *J* 14.3, 2.9 Hz, C$H_A$$H_B$$CCH_2CH_3$), 1.84–1.69 (4H, overlapping peaks, $CH_A$$H_B$$CCH_2CH_3$, C*H*$CH_2CH_3$, $CH_2CC$$H_2$$CH_3$), 1.38–1.30 (1H, m, CHC$H_A$$H_B$$CH_3$), 1.23–1.15 (1H, m, $CHCH_A$$H_B$$CH_3$), 1.14 (3H, t, *J* 7.5 Hz, CH=$CCH_2C$$H_3$), 0.97 (3H, t, *J* 7.4 Hz, CH=$CHCH_2C$$H_3$), 0.80 (3H, t, *J* 7.5 Hz, $CHCH_2C$$H_3$), 0.77 (3H, t, *J* 7.4 Hz, $CH_2CCH_2C$$H_3$); δ_C (150 MHz, CD_3OD) 176.1, 153.8, 136.0, 135.0, 134.2, 91.2, 43.5, 40.9, 32.4, 30.7, 26.6, 19.5, 14.3, 12.1, 11.8, 7.9; HRMS (ESI): MNa^+, found 273.1834. $C_{16}H_{26}NaO_2^+$ requires 273.1831.

*6.5.15 Methyl (Z)-2-[(3aR,4S,5R,6aR,E)-5,6a-diethyl-3-ethylidene-4-propylhexahydro-2(2H)-cyclopenta[b]furanylidene]ethanoate (**208**)*

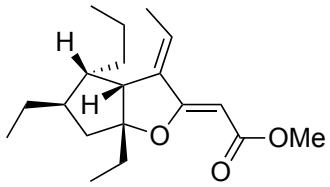

$SnCl_4$ (0.03 mL 0.3 mmol) was added dropwise to a stirred solution of **90** (0.015 g, 0.05 mmol) in CH_2Cl_2 (5 mL) at –78 °C. Stirring continued as the mixture warmed from –78 °C to room temperature over a period of 2.5 h, before quenching with the addition of $NaHCO_3$ (satd aq). The organic phase was separated and aqueous extracted with CH_2Cl_2. The combined extracts were dried (Na_2SO_4) and concentrated *in vacuo*. Flash chromatography afforded the *title compound* (0.007 g, 47%) as a colourless oil: R_f (10% EtOAc/hexane) 0.32; $[\alpha]^{20}_D$ +54 (*c* 0.39, $CHCl_3$); ν_{max} (thin film) 3055, 2962, 2927, 2874, 1705, 1627, 1436, 1371, 1263 cm^{-1}; δ_H (600 MHz, $CDCl_3$) 6.27 (1H, apparent qd, *J* 7.1, 1.5 Hz, C=C*H*CH_3), 5.05 (1H, s, C*H*CO_2CH_3), 3.66 (3H, s, OCH_3), 3.08 (1H, d, *J* 9.9 Hz, C*H*C=$CHCH_3$), 2.37 (1H, dd, *J* 13.6, 5.5 Hz, C$H_A$$H_B$$CCH_2CH_3$), 1.81 (3H, d, *J* 7.1 Hz, C=CHCH_3), 1.75–1.60 (5H, overlapping peaks, CHC$H_A$$H_B$$CH_3$, $CH_2CC$$H_2$$CH_3$, C*H*$CH_2CH_3$, C*H*$CH_2CH_2CH_3$), 1.30–1.22 (4H, overlapping peaks, CHC$H_A$$H_B$$CH_2CH_3$, $CHCH_2C$$H_2$$CH_3$, $CH_A$$H_B$$CCH_2CH_3$), 1.21–1.14 (1H, m, $CHCH_A$$H_B$$CH_2CH_3$), 1.11–1.04 (1H, m, $CHCH_A$$H_B$$CH_3$), 0.91 (3H, t, *J* 7.5 Hz,

$CH_2CCH_2CH_3$), 0.88 (3H, t, *J* 7.3 Hz, $CHCH_2CH_3$), 0.83 (3H, t, *J* 7.2 Hz, $CHCH_2CH_2CH_3$); δ_C (150 MHz, $CDCl_3$) 169.4, 167.0, 139.0, 125.6, 101.3, 81.3, 50.4, 50.1, 48.4, 45.1, 41.9, 31.9, 31.5, 26.8, 22.1, 16.3, 14.5, 12.4, 8.8; HRMS (ESI): MNa^+, found 329.2090. $C_{19}H_{30}NaO_3^+$ requires 329.2093.

6.6 Chapter summary

Chapter 6 reports a new entry to understanding the chemical reactivity of polyunsaturated non-aromatic heterocyclic systems and the oxidative potential of pyridinium chlorochromate. The findings expand on a limited pool of literature regarding the oxidative C–C bond cleavage of electron-rich enol ethers with chromate reagents; and establishes aldehyde dimethyl acetal **88** as a versatile late-stage intermediate in the synthesis of furanylidene and furanylidene-related sponge metabolites of broad interest. The first enantioselective total syntheses of four natural products, known to have therapeutic potential, were accomplished. The absolute configuration of each natural product, where required, was also determined through the synthesis of possible stereoisomers.

Finally, a continued effort to explore and understand the biosynthesis and structural similarity of sponge metabolites in this class has provided some insight to the origin of the plakilactone butenolides. Preliminary results also suggest that *des*-hydroxygracilioether C may, in fact, not be a direct biogenetic precursor to the complex polycyclic metabolite hippolachnin A, as suggested in current literature.

6.7 References and notes

1. R. Ueoka, Y. Nakao, S. Kawatsu, J. Yaegashi, Y. Matsumoto, S. Matsunaga, K. Furihata, R. W. M. van Soest and N. Fusetani, *J. Org. Chem.*, 2009, **74**, 4203.
2. C. Festa, G. Lauro, S. De Marino, M. V. D'Auria, M. C. Monti, A. Casapullo, C. D'Amore, B. Renga, A. Mencarelli, S. Petek, G. Bifulco, S. Fiorucci and A. Zampella, *J. Med. Chem.*, 2012, **55**, 8303.
3. C. Festa, S. De Marino, M. V. D'Auria, E. Deharo, G. Gonzalez, C. Deyssard, S. Petek, G. Bifulco and A. Zampella, *Tetrahedron*, 2012, **68**, 10157.

4. C. Festa, C. D'Amore, B. Renga, G. Lauro, S. De Marino, M. V. D'Auria, G. Bifulco, A. Zampella and S. Fiorucci, *Mar. Drugs*, 2013, **11**, 2314.
5. S. Di Micco, A. Zampella, M. V. D'Auria, C. Festa, S. De Marino, R. Riccio, C. P. Butts and G. Bifulco, *Beilstein J. Org. Chem.*, 2013, **9**, 2940.
6. D. B. Stierle and D. J. Faulkner, *J. Org. Chem.*, 1980, **45**, 3396.
7. M. V. D'Auria, L. G. Paloma, L. Minale, R. Riccio, A. Zampella and C. Debitus, *J. Nat. Prod.*, 1993, **56**, 418.
8. R. S. Compagnone, I. C. Pina, R. R. Hector, F. Dagger, A. I. Suarez, M. V. R. Reddy and D. J. Faulkner, *Tetrahedron*, 1998, **54**, 3057.
9. R. J. Capon, S. Singh, S. Ali and S. Sotheeswaran, *Aust. J. Chem.*, 2005, **58**, 18.
10. R. Epifanio, L. Pinheiro and N. Alves, *J. Braz. Chem. Soc.*, 2005, **16**, 1367.
11. X.-F. Liu, Y. Shen, F. Yang, M. T. Hamann, W.-H. Jiao, H.-J. Zhang, W.-S. Chen and H.-W. Lin, *Tetrahedron*, 2012, **68**, 4635.
12. S.-J. Piao, Y.-L. Song, W.-H. Jiao, F. Yang, X-.F. Liu, W.-S. Chen, B.-N. Han and H.-W. Lin, *Org. Lett.*, 2013, **15**, 3526.
13. G. Chianese, B.-B. Gu, F. Yang, W.-H. Jiao, Y.-W. Guo, H.-W. Lin and O. Taglialetella-Scafati, *RSC Adv.*, 2015, **5**, 63372.
14. E. A. Santos, A. L. Quintela, E. G. Ferreira, T. S. Sousa, F. d. C. L. Pinto, E. Hajdu, M. S. Carvalho, S. Salani, D. D. Rocha, D. V. Wilke, M. d. C. M. Torres, P. C. Jimenez, E. R. Silveira, J. J. La Clair, O. D. L. Pessoa and L. V. Costa-Lotufo, *J. Nat. Prod.*, 2015, **78**, 996.
15. F. Rahm, P. Y. Hayes and W. Kitching, *Heterocycles*, 2004, **64**, 523.
16. M. D. Norris and M. V. Perkins, *Nat. Prod. Rep.*, DOI:10.1039/c5np00142k.
17. M. Akiyama, Y. Isoda, M. Nishimoto, A. Kobayashi, D. Togawa, N. Hirao, A. Kuboki and S. Ohira, *Tetrahedron Lett.*, 2005, **46**, 7483.
18. C. M. Rasik and M. K. Brown, *Angew. Chem., Int. Ed.*, 2014, **53**, 14522.
19. S. A. Ruider, T. Sandmeier and E. M. Carreira, *Angew. Chem., Int. Ed.*, 2015, **54**, 2378.
20. S. A. Ruider and E. M. Carreira, *Org. Lett.*, 2016, **18**, 220.
21. R. Datta, R. J. Dixon and S. Ghosh, *Tetrahedron Lett.*, 2016, **57**, 29.
22. McCallum, M. E.; Rasik, C. M.; Wood, J. L.; Brown, M. K. *J. Am. Chem. Soc.* **2016**, *138*, 2437.
23. M. D. Norris and M. V. Perkins, *Tetrahedron*, 2013, **69**, 9813.
24. M. D. Norris, M. V. Perkins and E. J. Sorensen, *Org. Lett.*, 2015, **17**, 688.

25. A. Rajagopalan, M. Lara and W. Kroutil, *Adv. Synth. Catal.*, 2013, **355**, 3321, and references therein.

26. G. Piancatelli, A. Scettri and M. D'Auria, *Tetrahedron Lett.*, 1977, **39**, 3483.

27. S. Baskaran, I. Islam, M. Raghavan and S. Chandrasekaran, *Chem. Lett.*, 1987, **6**, 1175.

28. M. Fetizon, P. Goulaouic and I. Hanna, *Tetrahedron Lett.*, 1988, **29**, 6261.

29. T. Naito, N. Kojima, O. Miyata, I. Ninomiya, M. Inoue and M. Doi, *J. Chem. Soc., Perkin Trans. I*, 1990, **5**, 1271.

30. In a personal communication with the authors of ref. 2 (C. Festa and A. Zampella) slight anomalies were noted with the published data (ref. 2) for natural plakilactone C. Copies of the ^{1}H and ^{13}C NMR spectra and amended tabulated data for natural plakilactone C was provided (Table 6.1) and the corrected data for natural plakilactone C follows: δ_H (400 MHz, CD_3OD) 7.07 (1H, broad t, C*H*=CCH_2CH_3), 6.62 (1H, dd, *J* 16.0, 9.4 Hz, C*H*=CHC(O)CH_3), 5.88 (1H, d, *J* 16.0 Hz, CH=C*H*C(O)CH_3), 2.25 (3H, s, C(O)CH_3), 2.22 (2H, m, CH=CCH_2CH_3), 2.09 (1H, overlapping, C$H_AH_BCCH_2CH_3$), 2.08 (1H, overlapping, C*H*CH_2CH_3), 1.94 (1H, dd, *J* 14.9, 9.9 Hz, $CH_AH_BCCH_2CH_3$), 1.83 (2H, m, $CH_2CCH_2CH_3$), 1.50 (1H, m, CHC$H_AH_BCH_3$), 1.37 (1H, m $CHCH_AH_BCH_3$), 1.10 (3H, t, *J* 7.4 Hz, CH=CCH_2CH_3), 0.85 (3H, t, *J* 7.4 Hz, CHCH_2CH_3), 0.79 (3H, t, *J* 7.5 Hz, $CH_2CCH_2CH_3$); δ_C (100 MHz, CD_3OD) 201.1, 175.6, 154.8, 153.1, 137.0, 132.3, 90.7, 42.4, 41.1, 32.0, 29.6, 26.9, 19.5, 11.9, 11.7, 7.9. On close examination it was verified that the ^{1}H NMR and ^{13}C NMR of synthetic compound **197** matches that of natural plakilactone C; and that synthetic compound **199** is different.

31. M. W. Rathke and M. Nowak, *J. Org. Chem.*, 1985, **50**, 2624.

32. B. Neises and W. Steglich, *Angew. Chem. Int. Ed.*, 1978, **17**, 522.

33. In a personal communication with the authors of ref. 2 (C. Festa and A. Zampella) slight anomalies were noted with the published data (ref. 2) for natural plakilactone B. A copy of the ^{1}H NMR spectrum and amended tabulated data (^{1}H and ^{13}C NMR) for natural plakilactone B was provided (Table 6.3) and the corrected data for natural plakilactone B follows: δ_H (500 MHz, CD_3OD), 7.07 (1H, broad t, *J* 1.5 Hz, C*H*=CCH_2CH_3), 5.31 (1H, overlapping, CH=C*H*CH(OH)CH_3), 5.29 (1H, overlapping, C*H*=CHCH(OH)CH_3), 4.18 (1H, m, C*H*(OH)CH_3), 2.25 (2H, m, CH=CCH_2CH_3), 1.95 (1H, dd, *J* 14.0, 2.3 Hz,

$CH_AH_BCCH_2CH_3$), 1.82 (1H, overlapping, $CH_AH_BCCH_2CH_3$), 1.80 (1H, overlapping, $CH_2CCH_AH_BCH_3$), 1.79 (1H, overlapping, $CHCH_2CH_3$), 1.77 (1H, overlapping, $CH_2CCH_AH_BCH_3$), 1.37 (1H, m, $CHCH_AH_BCH_3$), 1.27 (1H, m, $CHCH_AH_BCH_3$), 1.21 (3H, d, *J* 6.4 Hz, $CH(OH)CH_3$), 1.16 (3H, t, *J* 7.4 Hz, $CH=CCH_2CH_3$), 0.84 (3H, t, *J* 7.5 Hz, $CHCH_2CH_3$), 0.78 (3H, t, *J* 7.4 Hz, $CH_2CCH_2CH_3$); δ_C (125 MHz, CD_3OD) 175.8, 153.7, 136.4, 136.0, 135.4, 91.1, 69.0, 43.3, 40.4, 32.2, 30.4, 23.9, 19.6, 12.3, 11.8, 8.0. On close examination it was verified that the ^1H NMR and ^{13}C NMR of synthetic compound **198** matches that of natural plakilactone B; and that synthetic compound **204** is different.

34. Itsuno-Corey reduction of **197** with the enantiomeric catalysts (*R*)- and (*S*)-2-methyl-CBS-oxazaborolidine also yielded **204** and **198** with good selectivity for the desired isomer. However, in each case we were unable to separate the remaining minor isomer. This necessitated the protecting group strategy outlined in Scheme 6.6.
35. The assignment 9*R* is also consistent with the Mosher's ester analysis of plakilactone B, see ref. 2.
36. J. Pospisil, *Tetrahedron Lett*., 2011, **52**, 2348.
37. T.-S. Li, J.-T. Li and H.-Z. Li, *J. Chromatogr. A*, 1995, **715**, 372.
38. C. M. Williams and L. N. Mander, *Tetrahedron* **2001**, *57*, 425.
39. L. N. Mander and C. M. Williams, *Tetrahedron* **2016**, *72*, 1133.
40. This is also in agreement with the configurational analysis of Faulkner, see E. W. Schmidt and D. J. Faulkner, *Tetrahedron Lett*., 1996, **37**, 6681.
41. The stereochemical relationship of compounds **91** and **90** were previously determined to be equivalent by chemical degradation, see ref. 2.
42. A. L. Baumstark, M. Moghaddari and M. L. Chamblee, *Heteroat. Chem*., 1990, **1**, 175.
43. E. L. Clennan and A. Pace, *Tetrahedron*, 2005, **61**, 6665.
44. R. Antonioletti, M. D'Auria, A. DeMico, G. Piancatelli and A. Scettri, *Synthesis*, 1983, **11**, 890.
45. T. Sugimura and L. A. Paquete, *J. Am. Chem. Soc*., 1987, **109**, 3017.
46. A. Rubello and P. Vogel, *Helv. Chim. Acta*, 1988, **71**, 1268.
47. H. Morita, K. Simizu, H. Takizawa, R. Aiyama and H. Itokawa, *Chem. Pharm. Bull*., 1988, **36**, 3156.

48. D. R. Williams, D. L. Brown and J. W. Benbow, *J. Am. Chem. Soc.*, 1989, **111**, 1923.
49. M. Tori, M. Sono and Y. Asakawa, *Chem. Pharm. Bull.*, 1989, **37**, 534.
50. T. G. Waddell, A. D. Carter, T. J. Miller and R. Pagni, *J. Org. Chem.*, 1992, **57**, 381.
51. B. B. Snider, D. J. Rodini and J. van Straten, *J. Am. Chem. Soc.*, 1980, **102**, 5872.
52. P. G. Gassman, S. P. Chavan and L. B. Fertel, *Tetrahedron Lett.*, 1990, **31**, 6489.
53. P. G. Gassman and A. C. Lottes, *Tetrahedron Lett.*, 1992, **33**, 157.
54. C. Ko, J. B. Feltenberger, S. K. Ghosh and R. P. Hsung, *Org. Lett.*, 2008, **10**, 1971.
55. X. Li and Y. R. Lee, *Org. Biomol. Chem.*, 2014, **12**, 1250.
56. Y. J. Hong and D. J. Tantillo, *Chem. Soc. Rev.*, 2014, **43**, 5042.
57. The Lewis acid catalysed ene reaction of compound **90** in Scheme 6.10 is drawn to proceed through a concerted mechanism. However, it is possible that this reaction might proceed in a stepwise manner via discrete carbocation intermediates. Furthermore, we expect that the olefin at C13 is able to isomerise under the reaction conditions, and its geometry is thus under thermodynamic control.

7. Conclusions and future challenges

Peroxide and peroxide-derived metabolites have been isolated from the extracts of marine sponges since the late 1970s – yet the compound class is still emerging as a novel target for the treatment of infectious diseases, cancers and physiological disorders of the human body. Despite a number of recent advances in the chemical synthesis of peroxide-derived molecules, their complex scaffolds are in short supply and our understanding of their therapeutic potential remains limited. There is a great need for general and efficient synthetic routes to compounds in this class, which are amenable to the synthesis of analogous substrates for SAR analysis and further development as drug candidates in a research setting.

The work outlined in this thesis aims to provide a better understanding the biosynthetic origins and inherent structural rearrangements of peroxide and peroxide-derived metabolites from marine sponges. Insight gathered from a comprehensive and critical review of literature (Chapter 2) drove the development of a cascade reaction modelled on a revised theory of the biogenesis of furanylidene metabolites (Chapter 3). Application of this method through a number of revised strategies (Chapter 4) ultimately led to the synthesis of a versatile late-stage synthetic intermediate, which was quickly advanced to the natural products gracilioether B, gracilioether C (Chapter 5) and *des*-hydroxygracilioether C. Finally, a novel and chemoselective oxidative cleavage reaction of furanylidene heterocycles with pyridinium chlorochromate allowed total synthesis of the related butenolides plakilactone B, *des*-hydroxyplakilactone B and plakilactone C (Chapter 6).

These methods provide a foundation to explore the chemical basis and structural limitations of these compounds as potential drug candidates. As already demonstrated in this work, modification of late-stage intermediate **88** is easily achieved by extension of the pendant aldehyde dimethyl acetal and oxidation of the furanylidene heterocycle; and further derivatisation of the resulting butenolides may be possible (Scheme 7.1). The ability to access synthetic isomers through controlled epimerisation could also provide valuable SAR data, especially since other related natural products such as plakortin (**1**) and **80** (Scheme 2.19) have *anti*-configuration rather than *syn*.

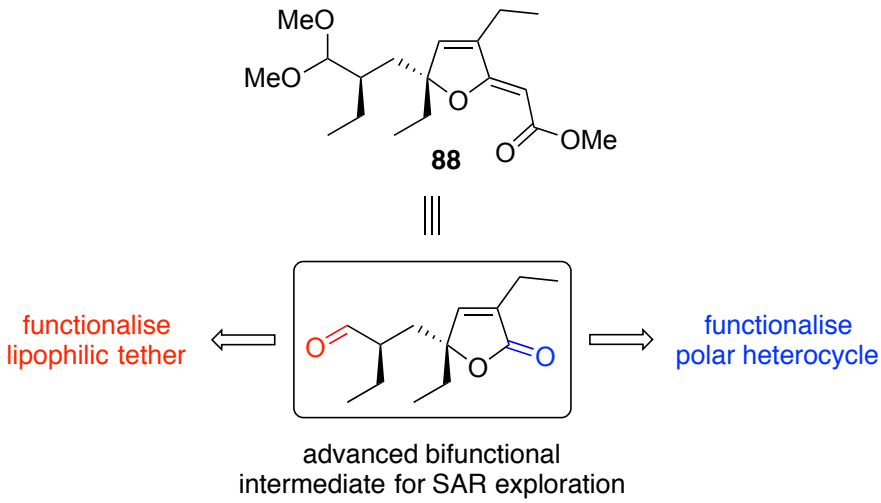

Scheme 7.1: Illustration of the utility of aldehyde dimethyl acetal **88** as an advanced bifunctional intermediate for SAR exploration.

The total synthesis and structural elucidation of other gracilioether and plakilactone metabolites may also be achievable from **88** in only a few steps. Plakilactones G (**209**) and H (**210**) may be accessed though asymmetric epoxidation and regioselective ring-opening of *des*-hydroxyplakilactone B (**91**, Scheme 7.2). The synthesis of gracilioether D (**211**) and plakorfuran A (**212**) could be possible through propionate homologation via the enol of aldehyde **200** (Scheme 7.3). Spiroplakortone (**213**) has an unprecedented spiroketal moiety, which appears to be related to the furanylidene metabolites; it is also conceivable that this compound might be accessible via intermediate **88** in a number of steps (Scheme 7.4).

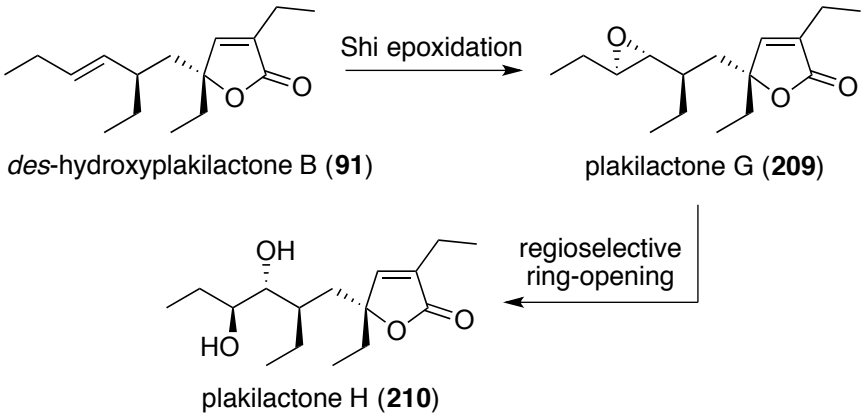

Scheme 7.2: Proposed synthesis of plakilactone G (**209**) and H (**210**) by Shi epoxidation and regioselective ring-opening of *des*-hydroxyplakilactone B (**90**).

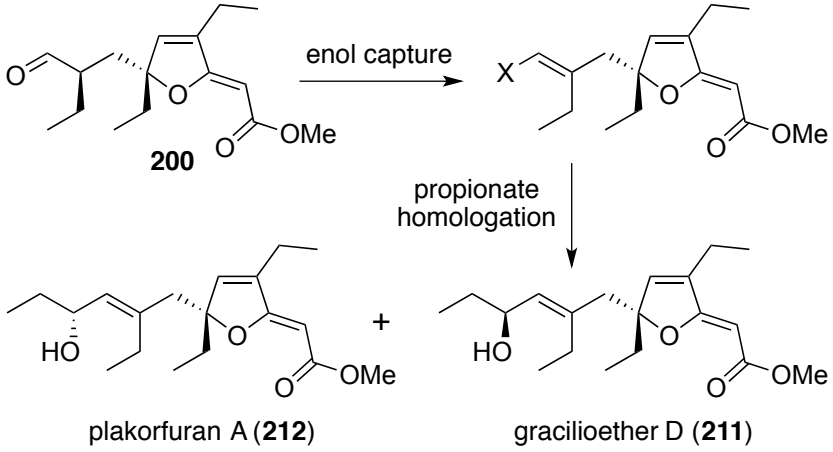

Scheme 7.3: Proposed synthesis of gracilioether D (**211**) and plakorfuran A (**212**) by enol capture and propionate homologation of aldehyde **200**. X = activating group.

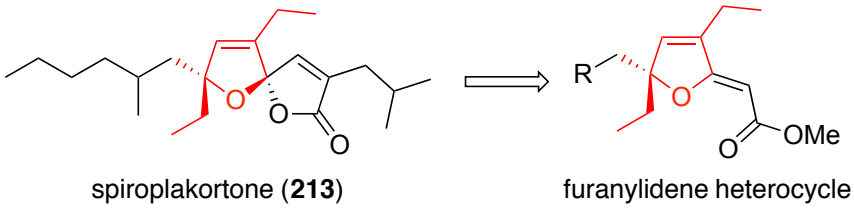

Scheme 7.4: Possible extension of the end-game strategy to achieve total synthesis of spiroplakortone (**213**) from a late-stage furanylidene intermediate. Absolute configuration not implied.

Unfortunately, many attempts to effect intramolecular [2+2] annulation of *des*-hydroxygracilioether C (**90**) failed to yield the corresponding cyclobutane, hippolachnin A (**98**, Chapter 6). Despite the obvious structural and stereochemical similarity of these two metabolites, it appears that they may not be directly linked by this hypothetical reaction. While it is possible that the conversion might be achieved under laboratory conditions yet to be tested or be aided through enzyme catalysis, perhaps the biosynthetic origin of hippolachnin A (**98**) is parallel to that of *des*-hydroxygracilioether C (**90**) rather than orthogonal. Alkene-alkene [2+2] cycloadditions are well known and in some cases are accelerated by neighbouring groups that donate electron density to a Lewis acid catalyst. The association of a Lewis acid, electron-donating group and the two alkenes brings the pi bonds in close proximity and facilitates photo-induced [2+2] cycloaddition. Following the discussion in this thesis, which argues that *des*-hydroxygracilioether C (**90**) originates from haterumadioxin A (**7**) methyl ester by dehydrative ring contraction, it follows that hippolachnin A (**98**) might in fact be a direct adduct of **7** (Scheme 7.5). Photo-induced [2+2] annulation of haterumadioxin A (**7**) methyl ester, possibly facilitated by the

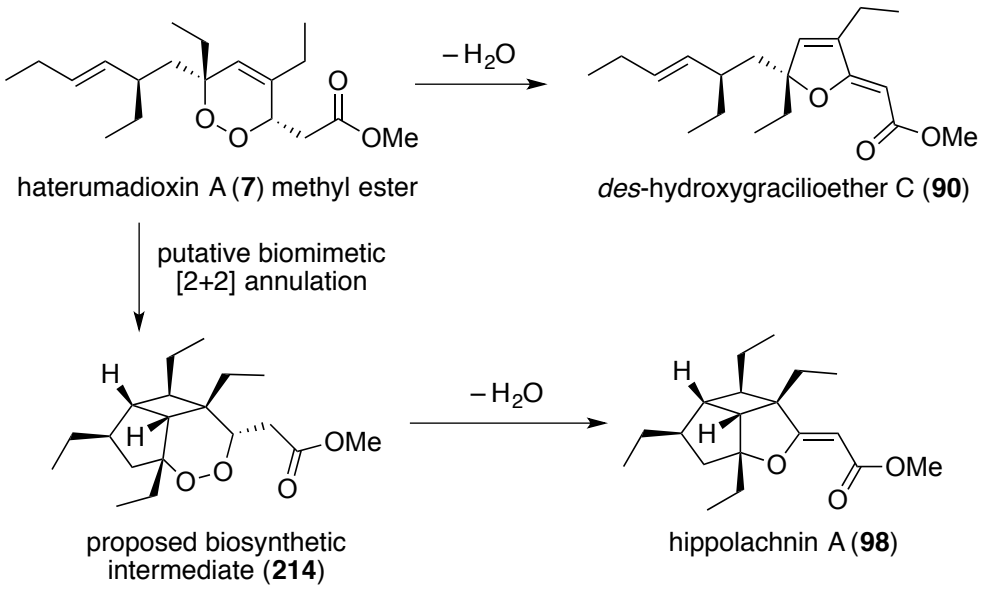

Scheme 7.5: Biosynthesis of *des*-hydroxygracilioether C (**90**) by dehydrative ring contraction as argued in this thesis and a revised theory of the biogenetic origin of hippolachnin A (**98**) by photochemical [2+2] cycloaddition and dehydrative ring contraction of the putative endoperoxide intermediate **214**.

neighbouring peroxyether through coordination with a Lewis acid could yield endoperoxide **214**, which might then undergo dehydrative ring contraction to afford hippolachnin A (**98**). This hypothesis constitutes a new theory for the biogenesis of hippolachnin A in light of the results presented in this thesis.

Finally, expanding the utility of aldehyde dimethyl acetal **88** toward efficient synthetic routes to related targets and to facilitate exploration of their structure-activity relationships is a significant future challenge. Evaluation of the compounds in this class as effective treatments for infectious diseases, cancers and physiological disorders is a larger collaborative project for future consideration; yet, the work presented in this thesis provides a sturdy foundation for further studies and introduces a chemical supply of furanylidene and related butenolides that was previously beyond the knowledge reported in scientific literature.

8. Appendix

The appendix includes full copies of the 1D and 2D ^{1}H and ^{13}C NMR spectra for each of the synthesised natural products. All raw data presented in this chapter is provided in support of the thesis body. This data is also available on the publishers' websites through the supporting information files of the article reporting their synthesis.

8.1 Analytical data for the synthesised natural products

8.1.1 Synthetic gracilioether B

^{1}H NMR (500 MHz, CD_3OD)

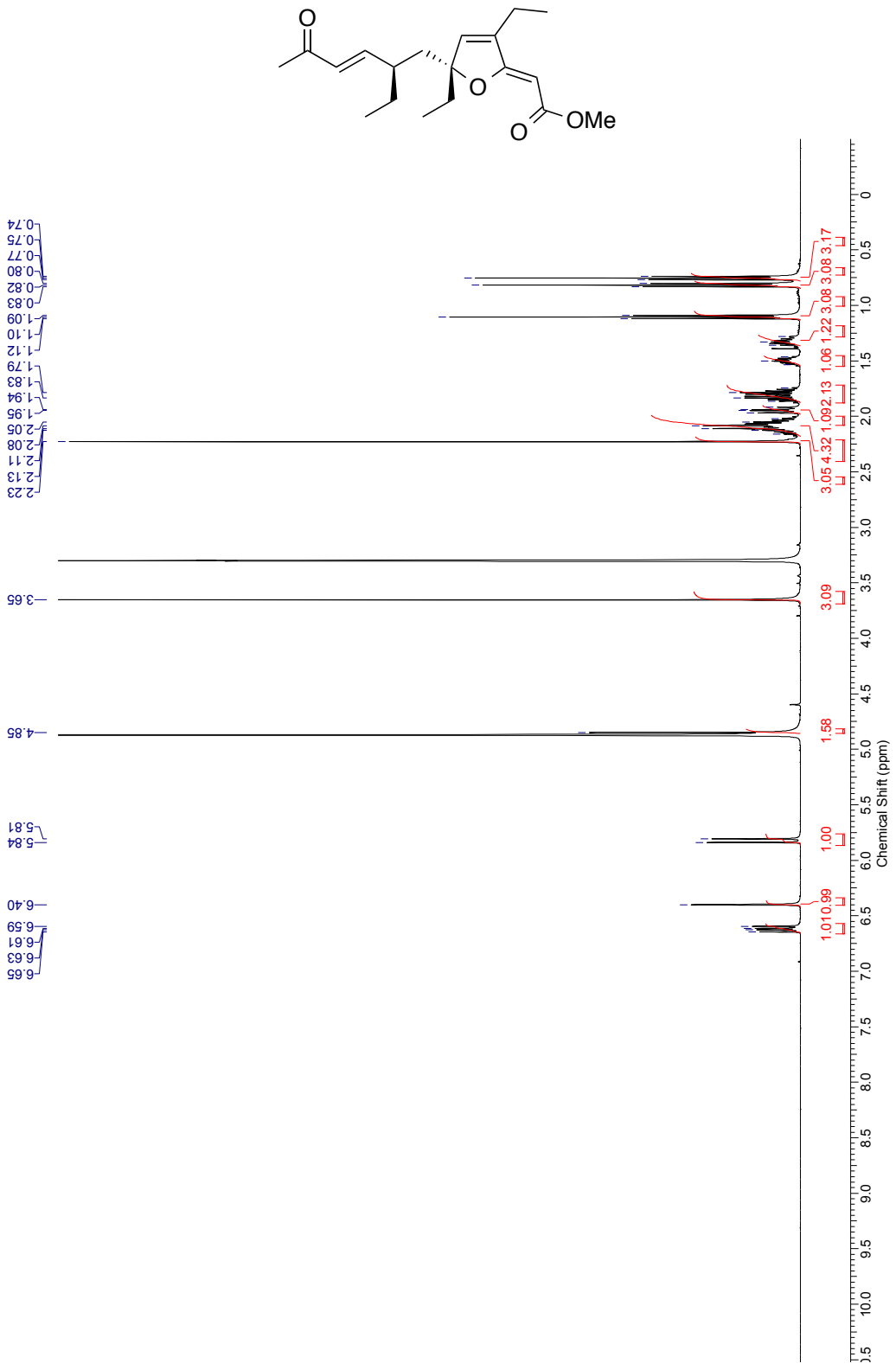

^{13}C NMR (125 MHz, CD_3OD)

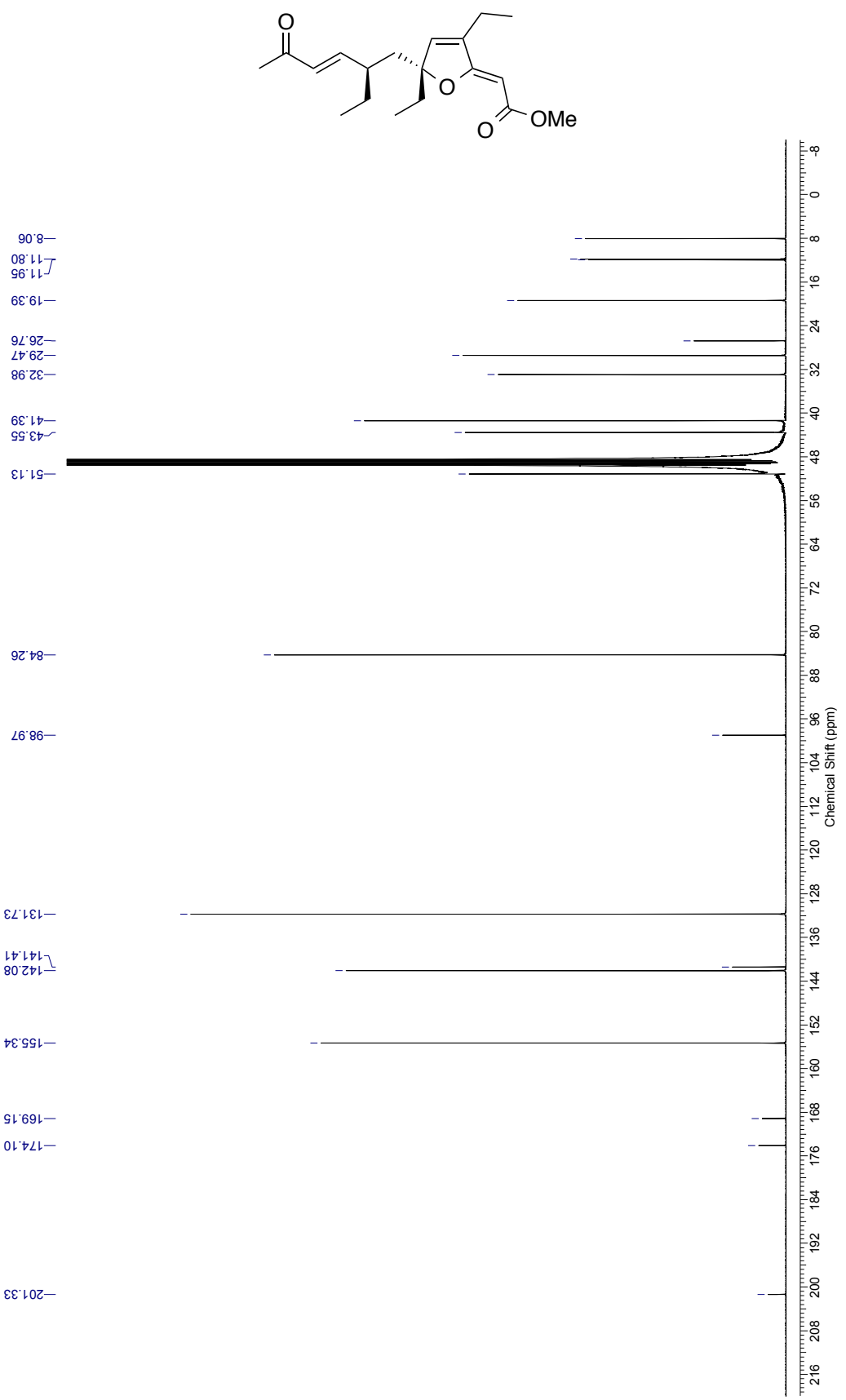

COSY (500 × 500 MHz, CD_3OD)

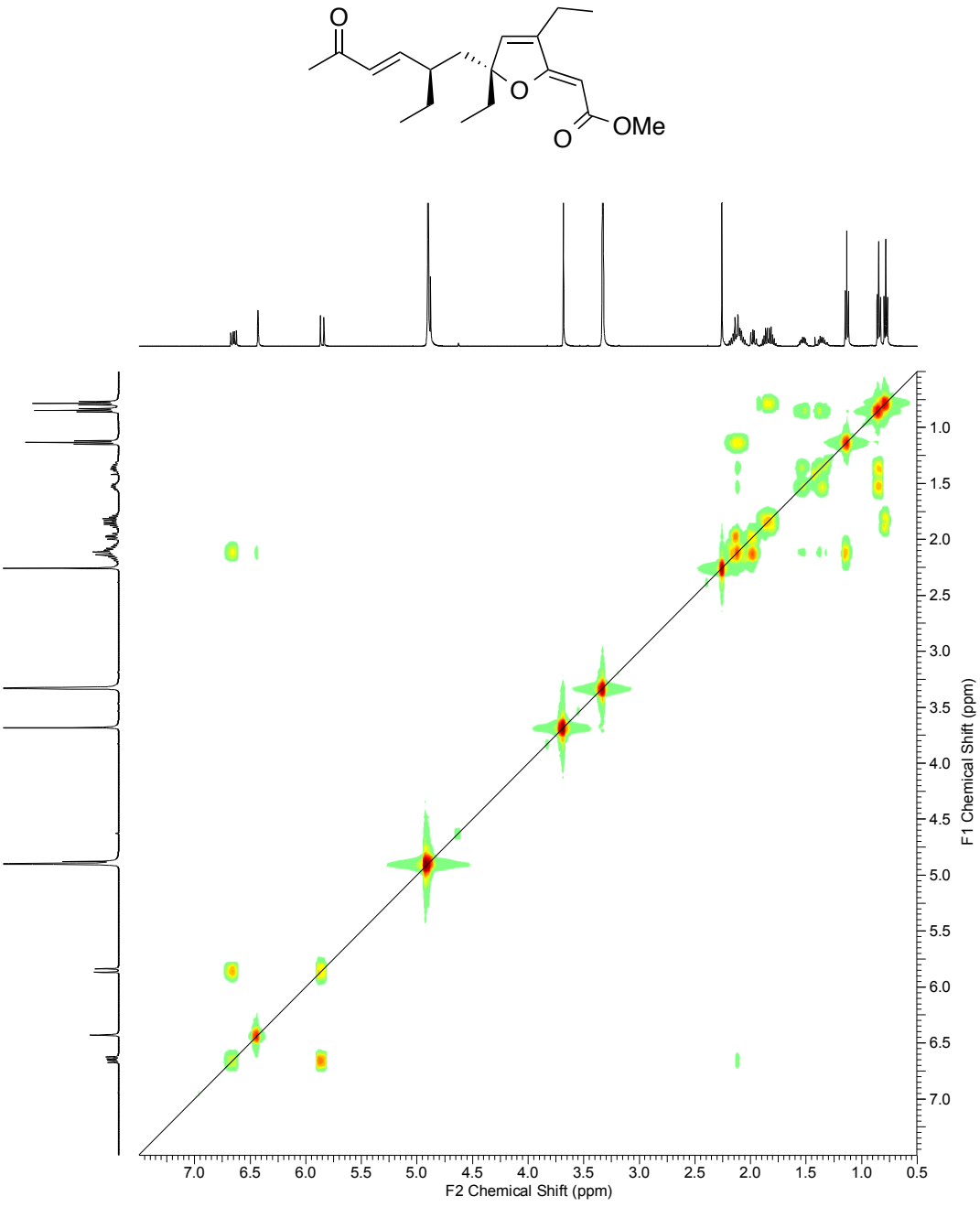

HSQC (500 × 125 MHz, CD_3OD)

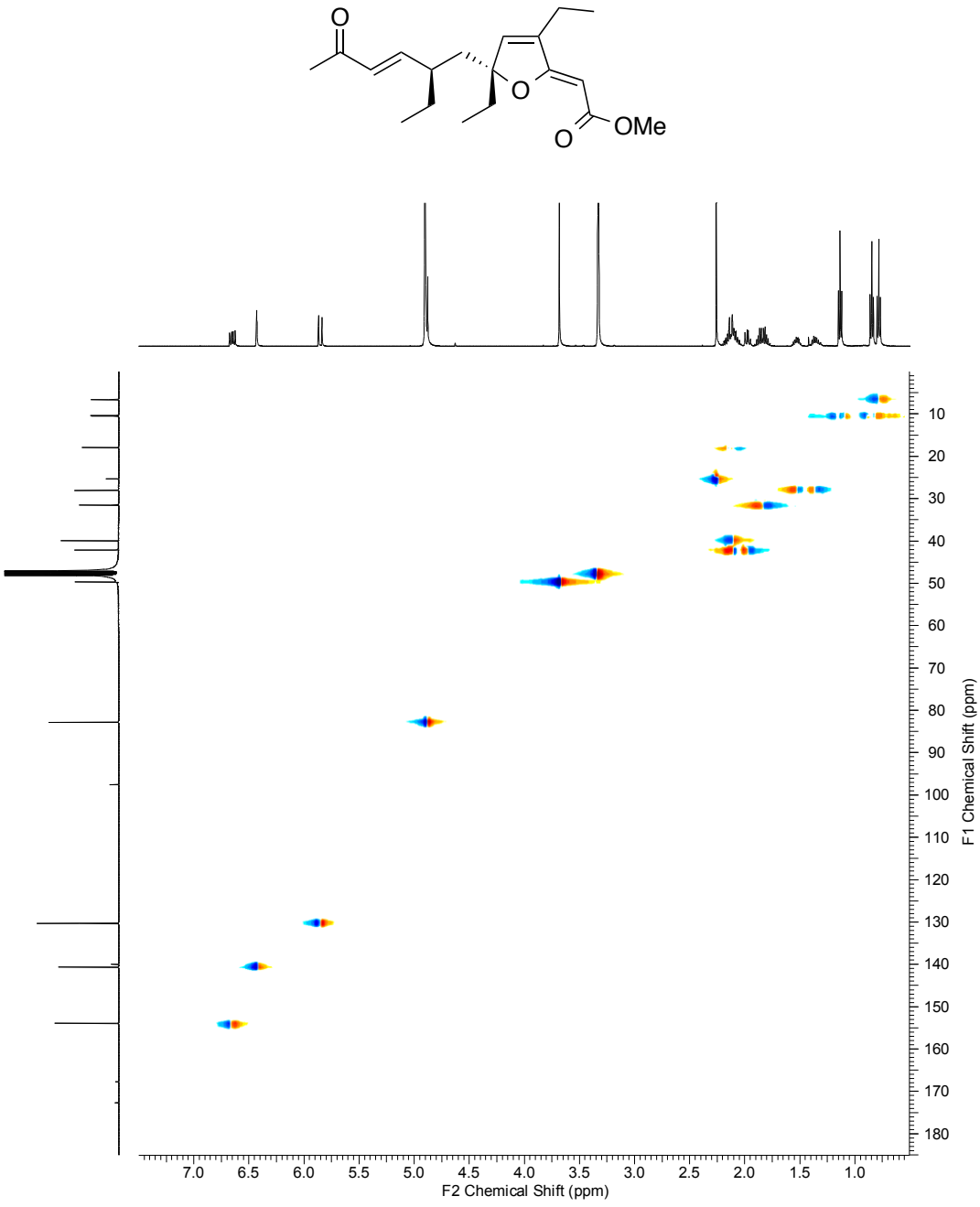

HMBC (500 × 125 MHz, CD_3OD)

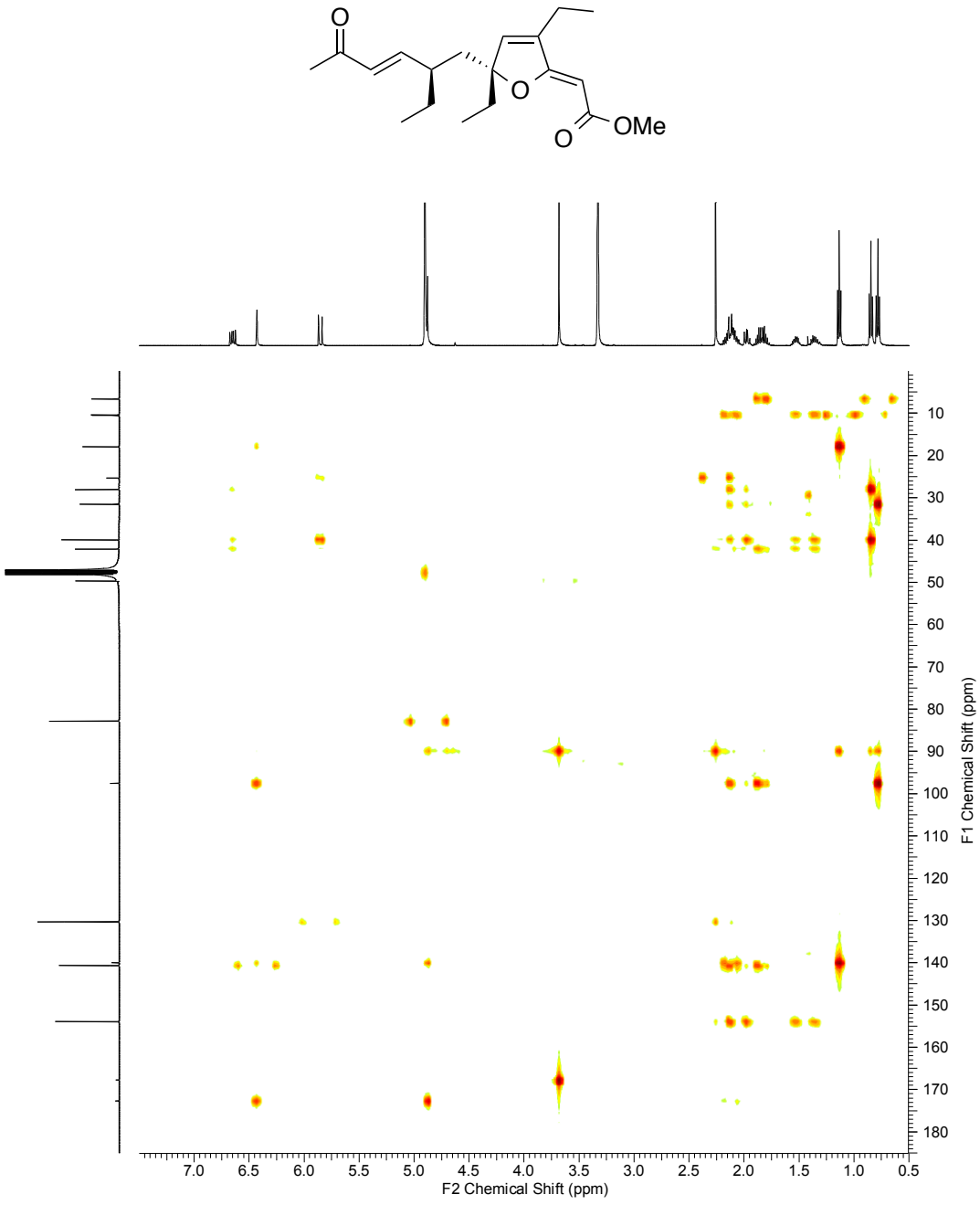

HRMS (ESI)

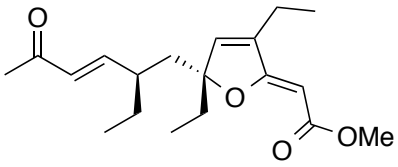

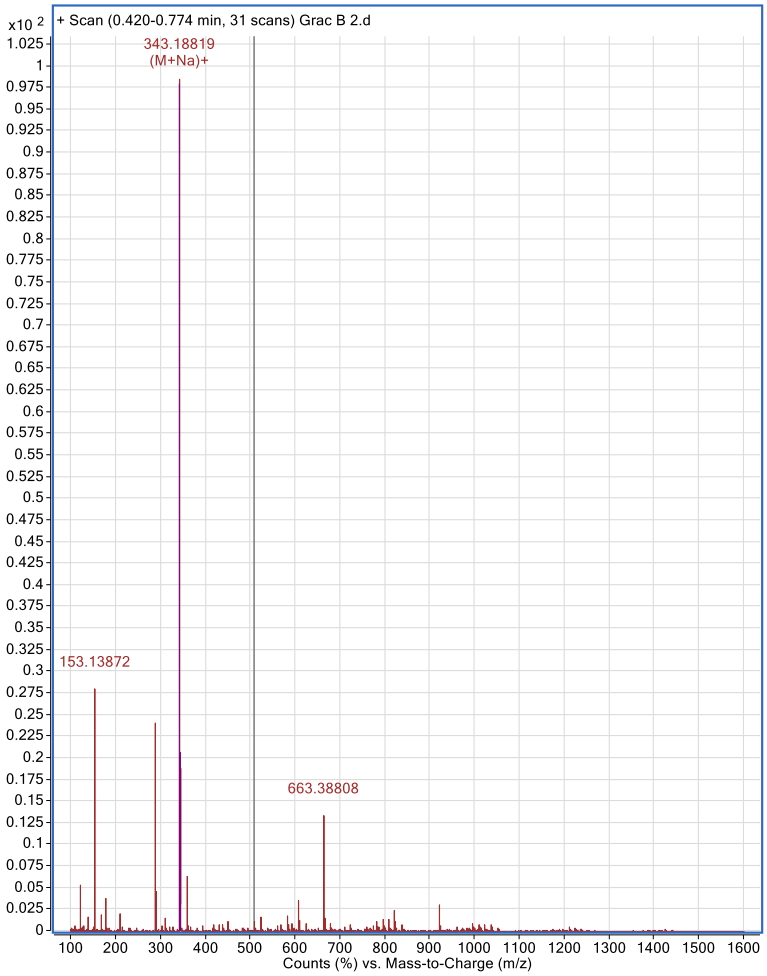

Formula (M)	Ion	Ion Formula	Mass	Calc Mass	Difference (ppm)	Abs Diff (ppm)
C19H28O4	(M+Na)+	C19H28NaO4+	343.18819	343.18799	-0.64	0.64

CD (380–200 nm)

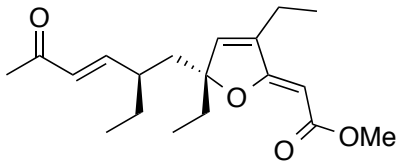
O
O
O
OMe

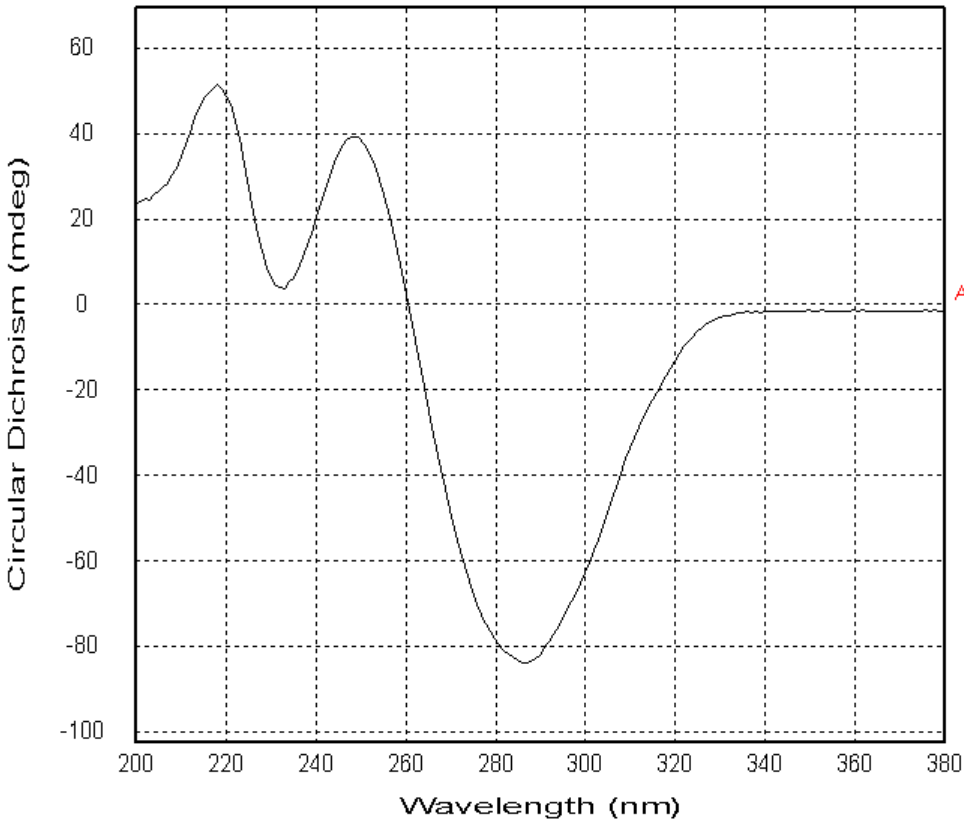
Circular Dichroism (mdeg)
60
40
20
0
-20
-40
-60
-80
-100
200
220
240
260
280
300
320
340
360
380
Wavelength (nm)

8.1.2 Synthetic gracilioether C

^{1}H NMR (500 MHz, CD_3OD)

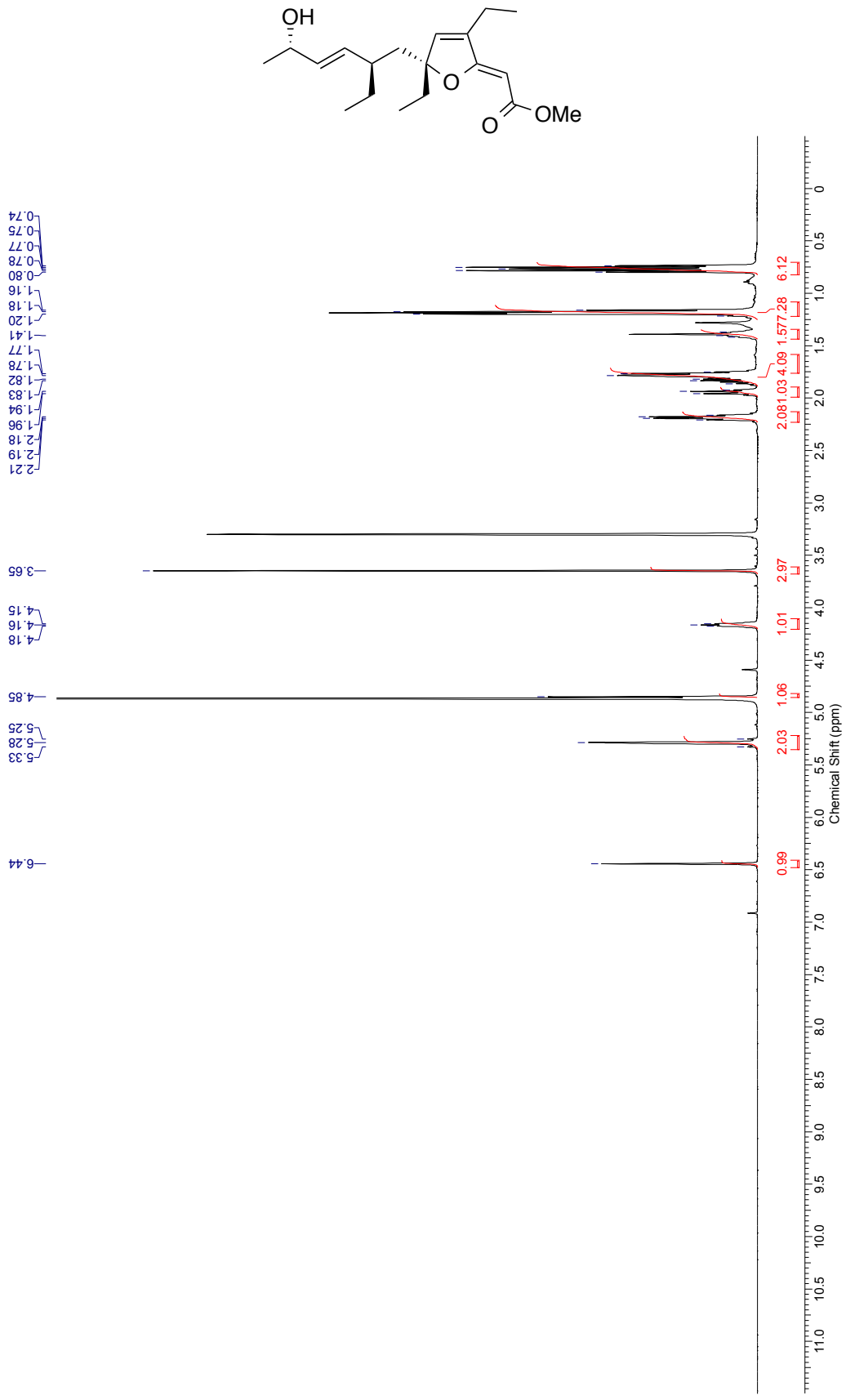

^{13}C NMR (125 MHz, CD_3OD)

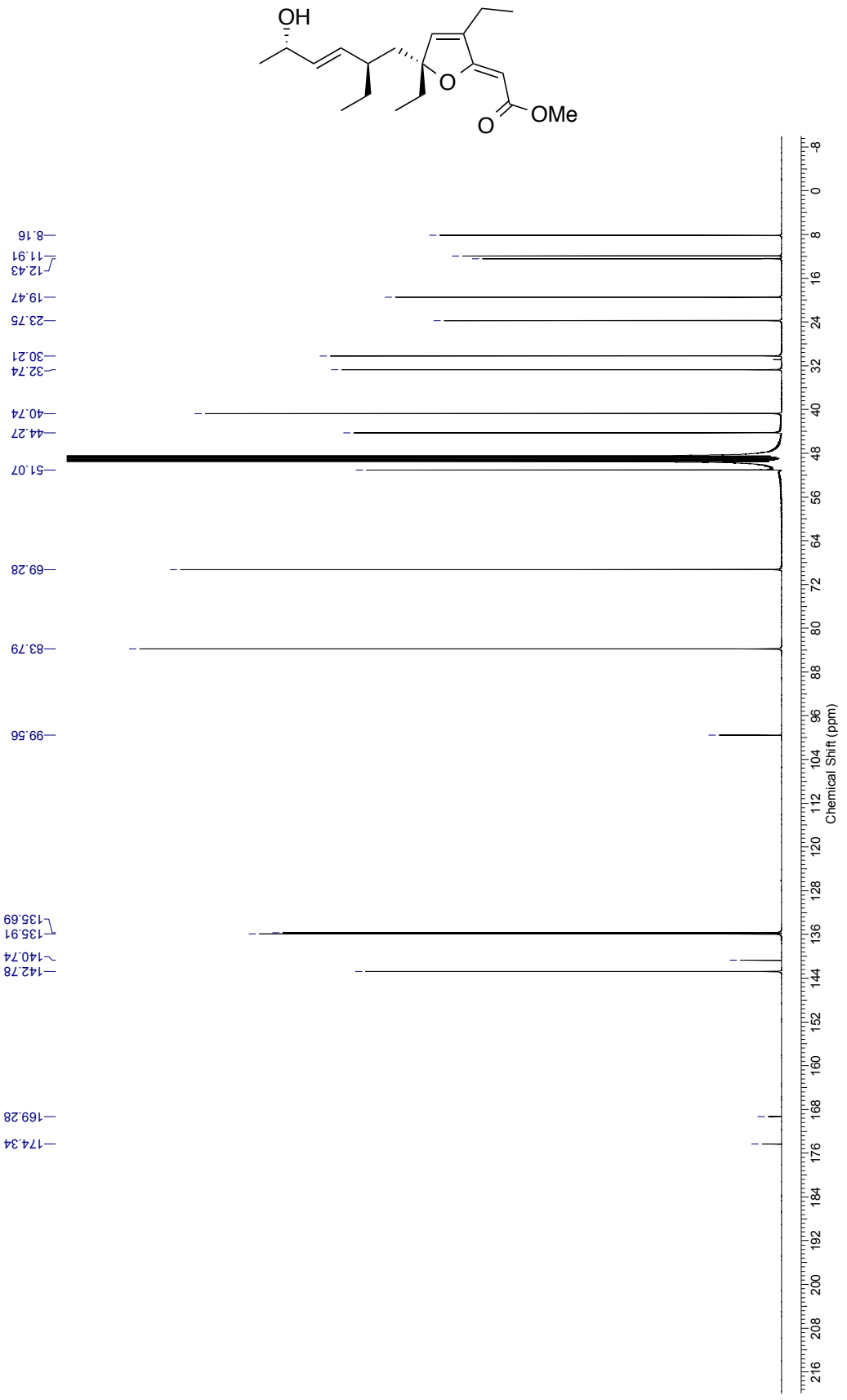

COSY (500 × 500 MHz, CD_3OD)

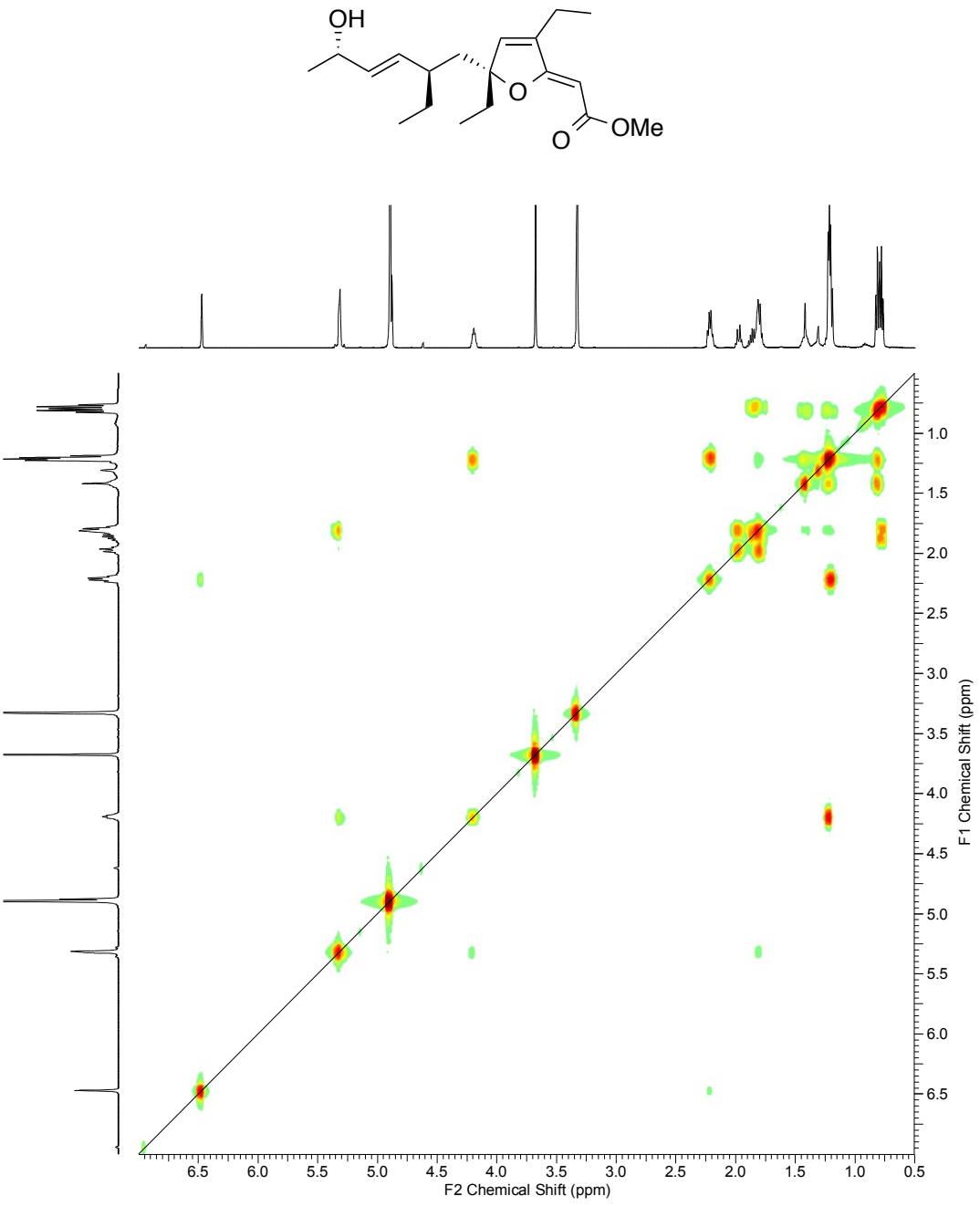

HSQC (500 × 125 MHz, CD_3OD)

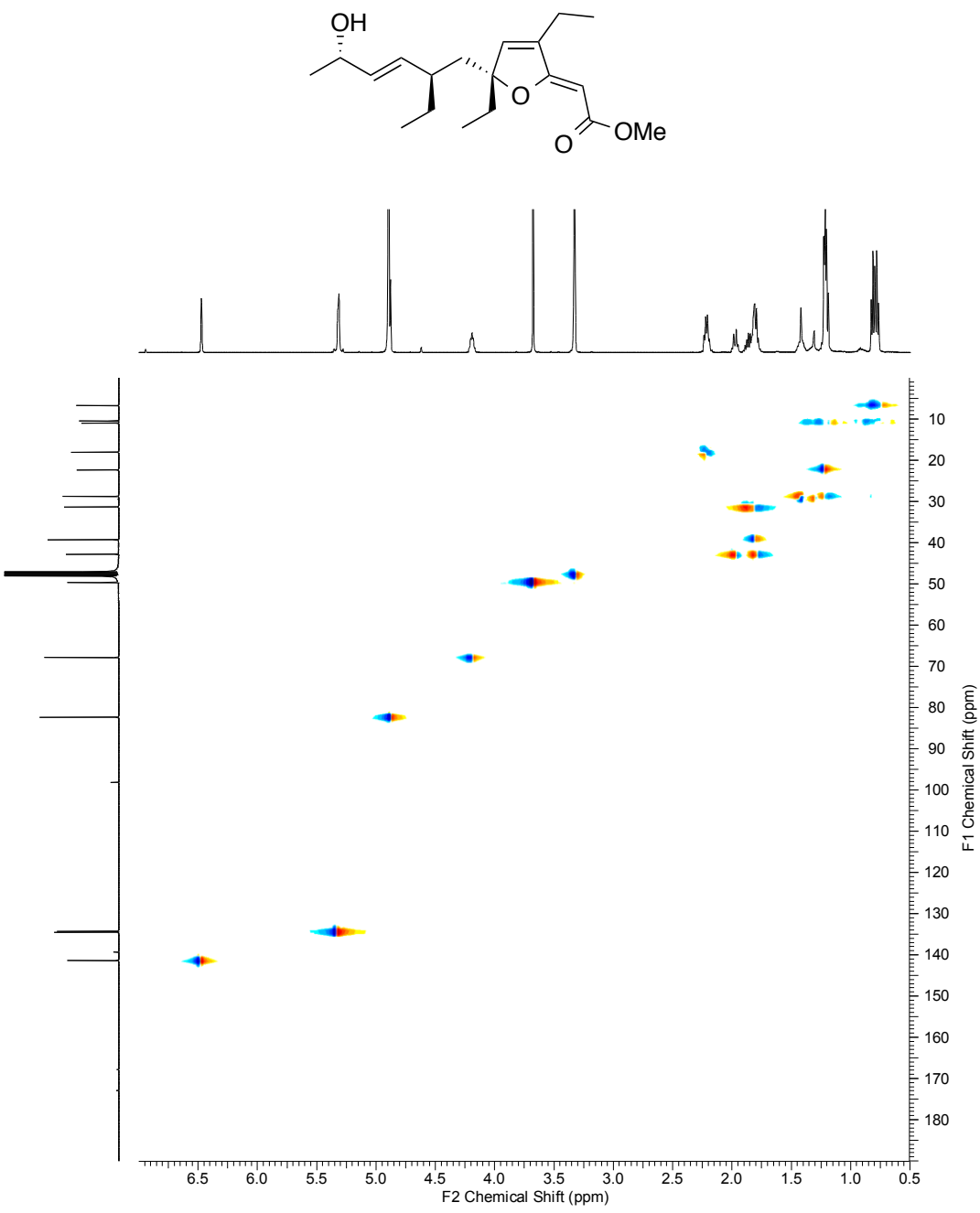

HMBC (500 × 125 MHz, CD_3OD)

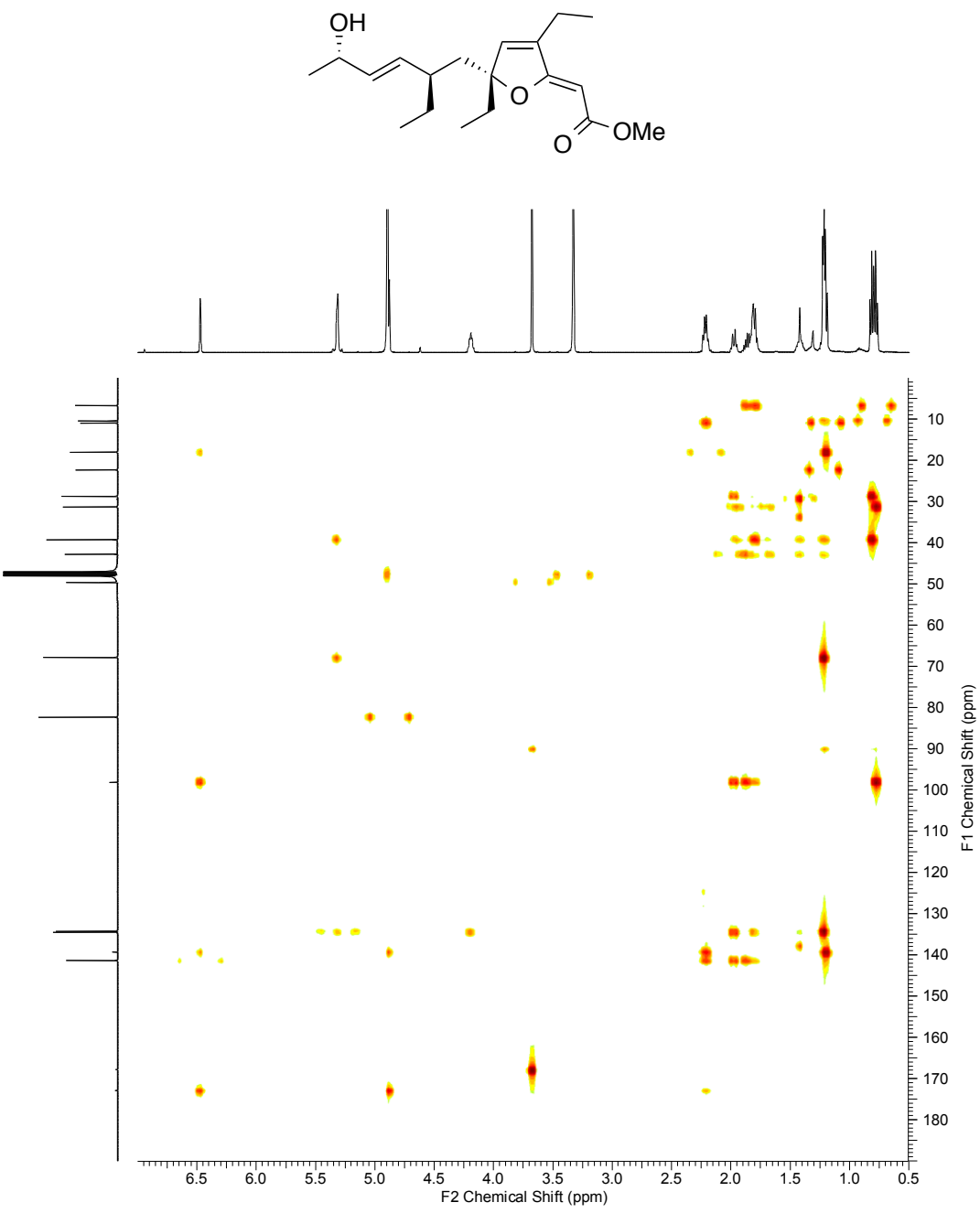

HRMS (ESI)

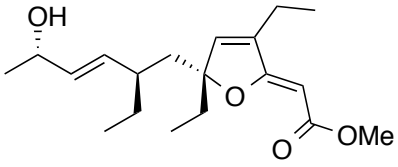

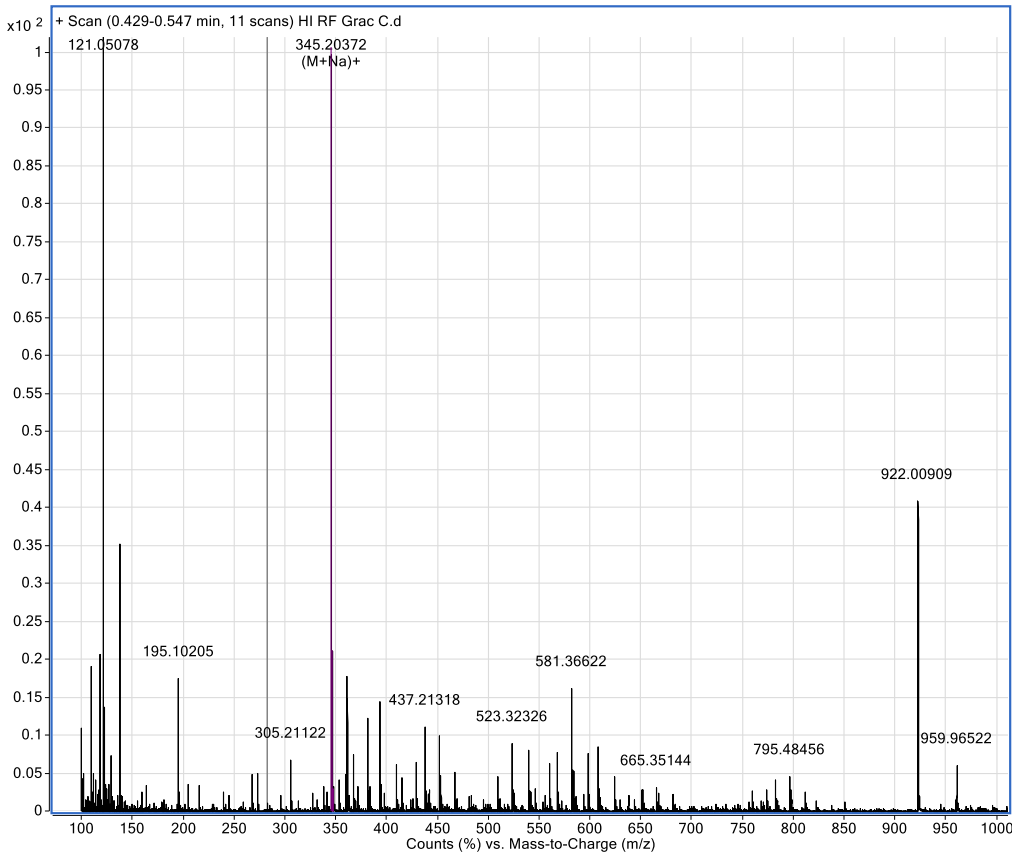

Formula (M)	Ion	Ion Formula	Mass	Calc Mass	Difference (ppm)	Abs Diff (ppm)
C19H30O4	(M+Na)+	C19H30NaO4+	345.2037	345.2036	-0.28	0.28

CD (380–200 nm)

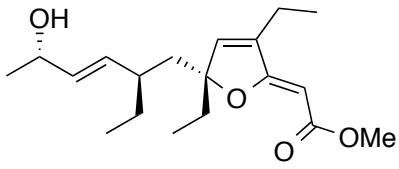
OH
O
O
OMe

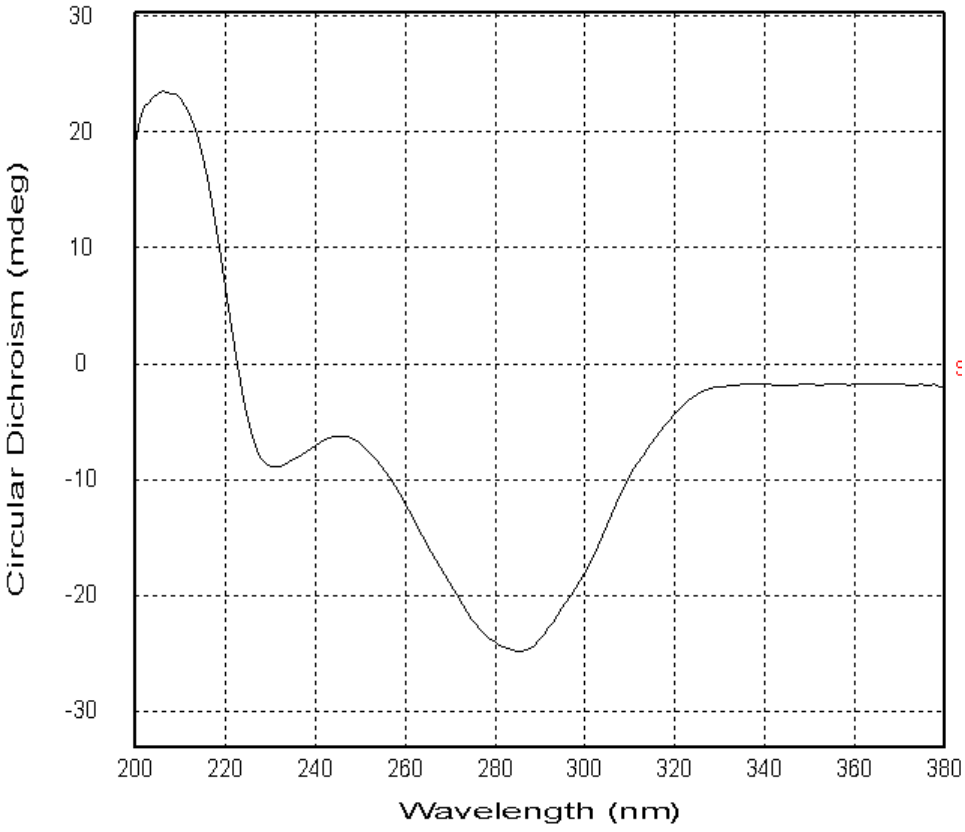
Circular Dichroism (mdeg)
30
20
10
0
-10
-20
-30
200
220
240
260
280
300
320
340
360
380
Wavelength (nm)

8.1.3 Synthetic plakilactone C

^{1}H NMR (600 MHz, CD_3OD)

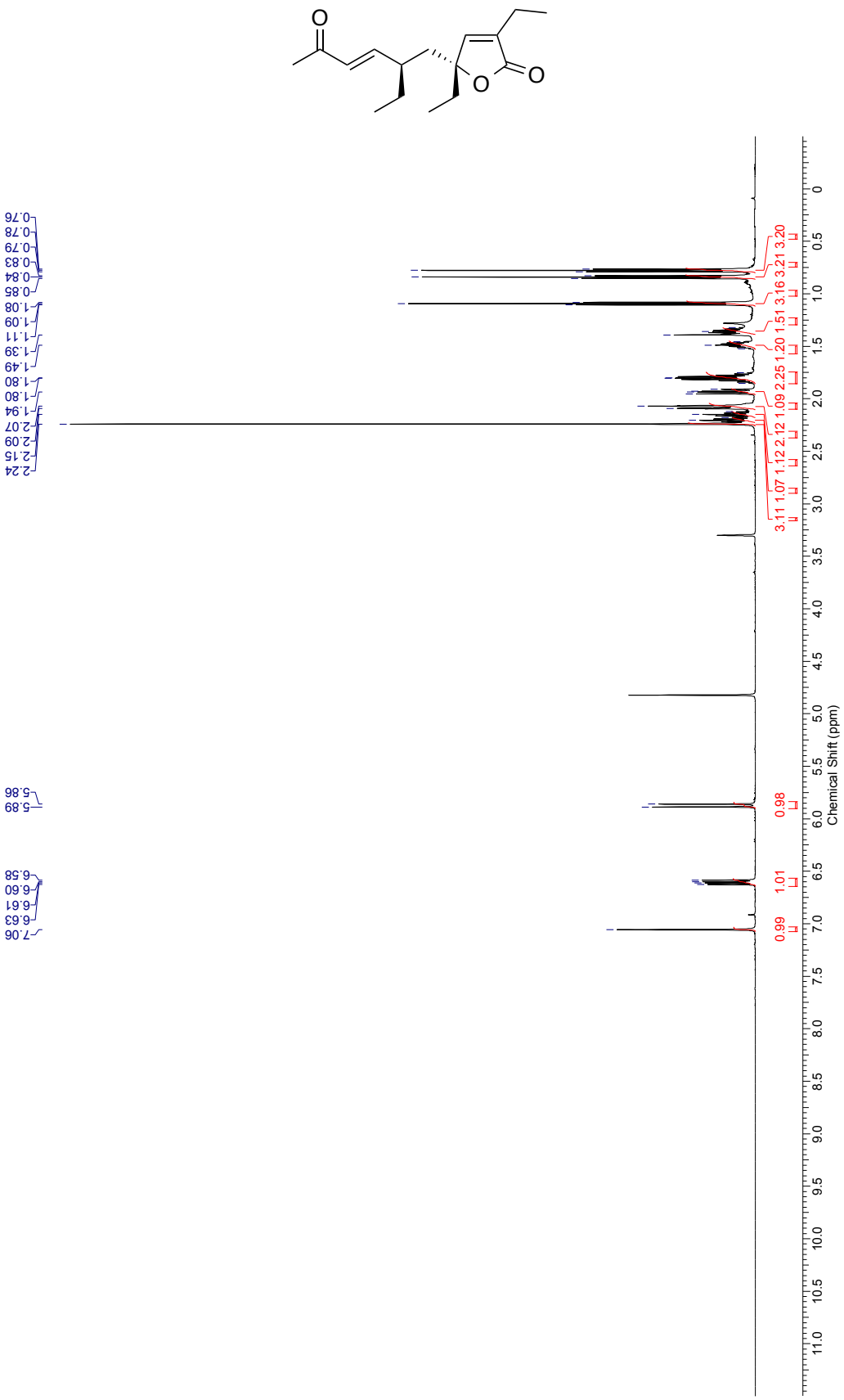

^{13}C NMR (150 MHz, CD_3OD)

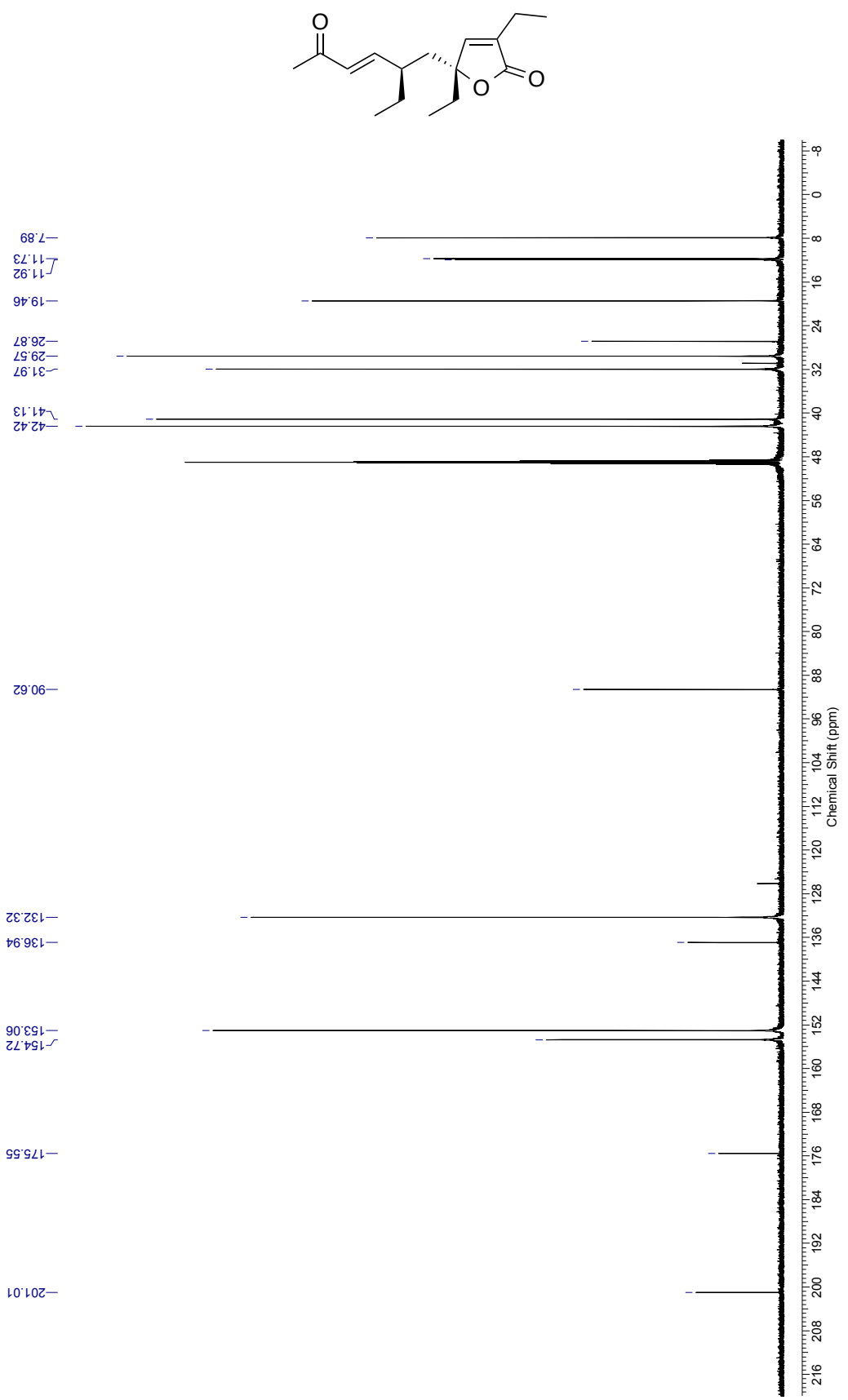

COSY (600 × 600 MHz, CD_3OD)

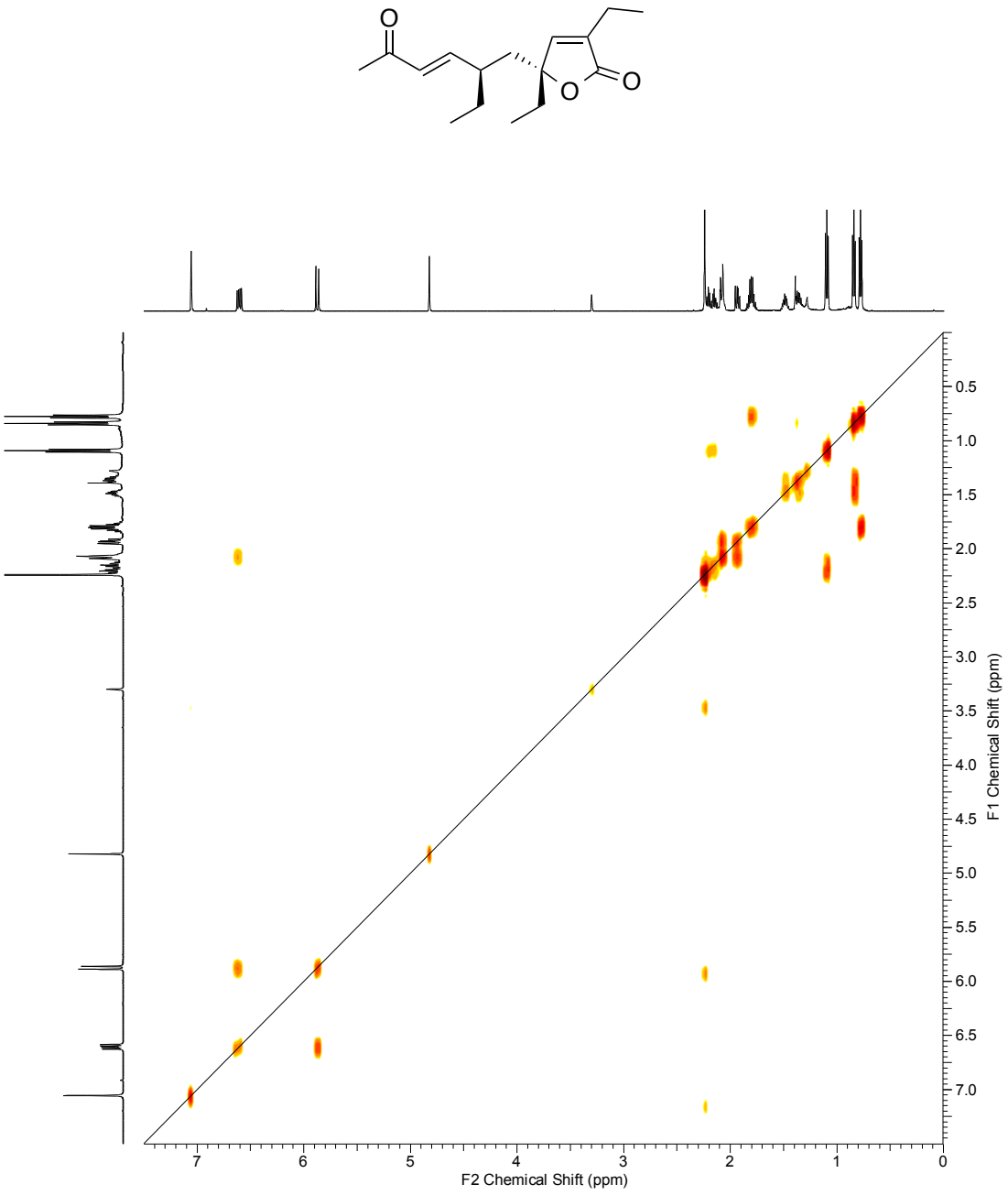

HSQC (600 × 150 MHz, CD_3OD)

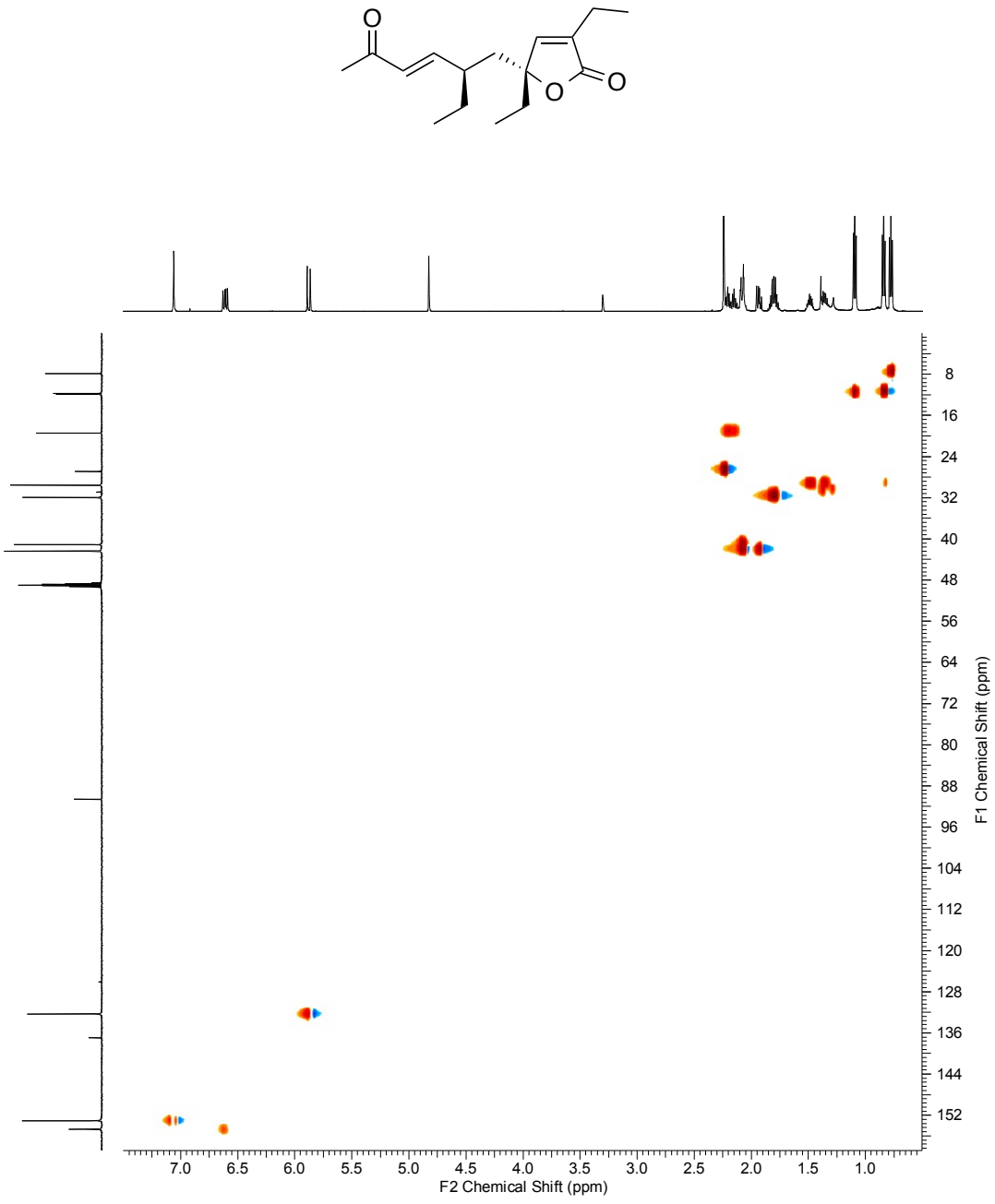

HMBC (600 × 150 MHz, CD_3OD)

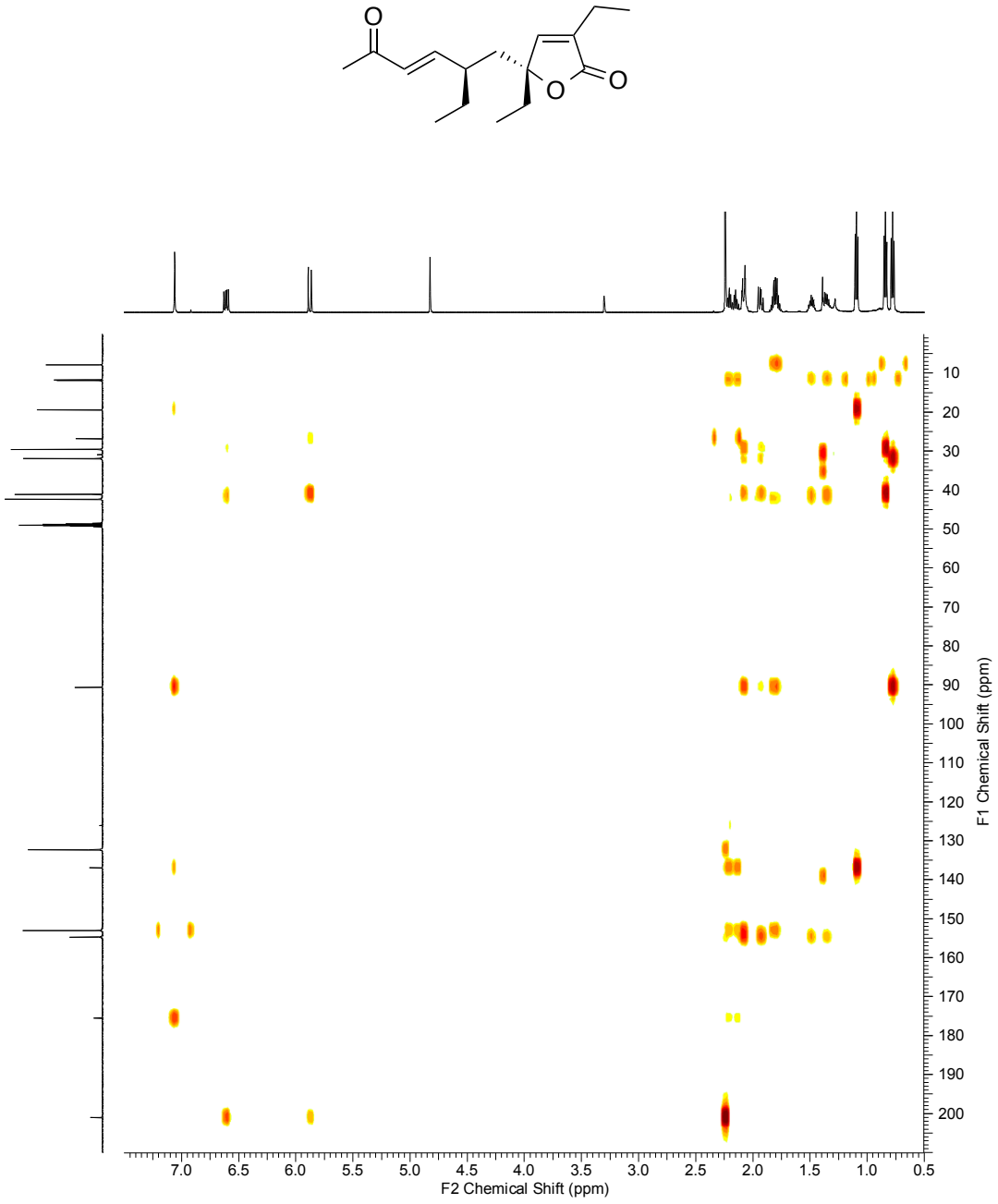

HRMS (ESI)

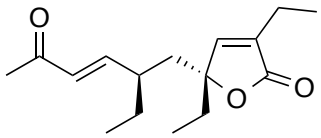

High Resolution Spectra
Positive ion

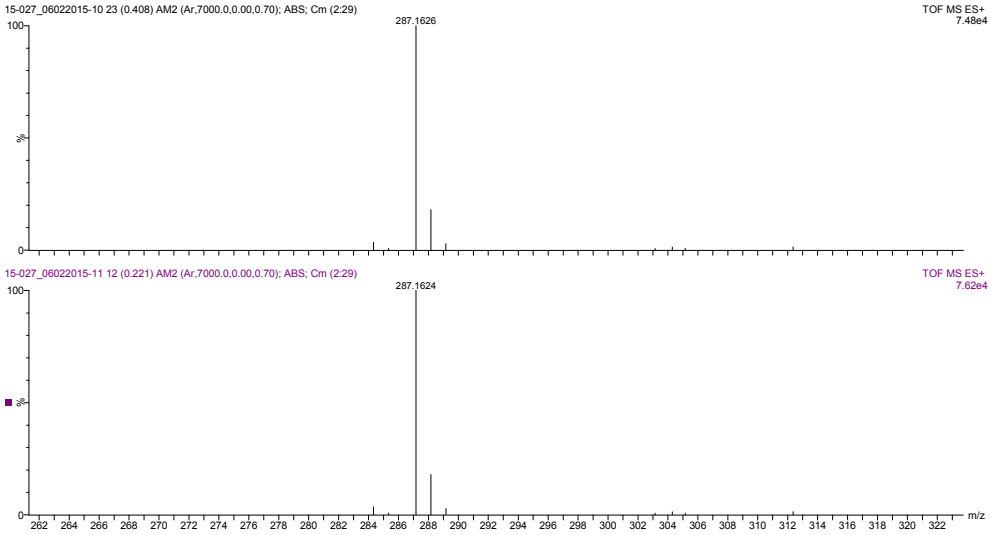

Accurate Mass Data

Observed Mass	Formula $[M+Na]^+$	Calculated mass	Difference (ppm)	iFiT (norm)
287.1624	C16H24O3Na	287.1623	0.3	2.5
287.1626	C16H24O3Na	287.1623	1.0	0.6

8.1.4 Synthetic plakilactone B

^{1}H NMR (600 MHz, CD_3OD)

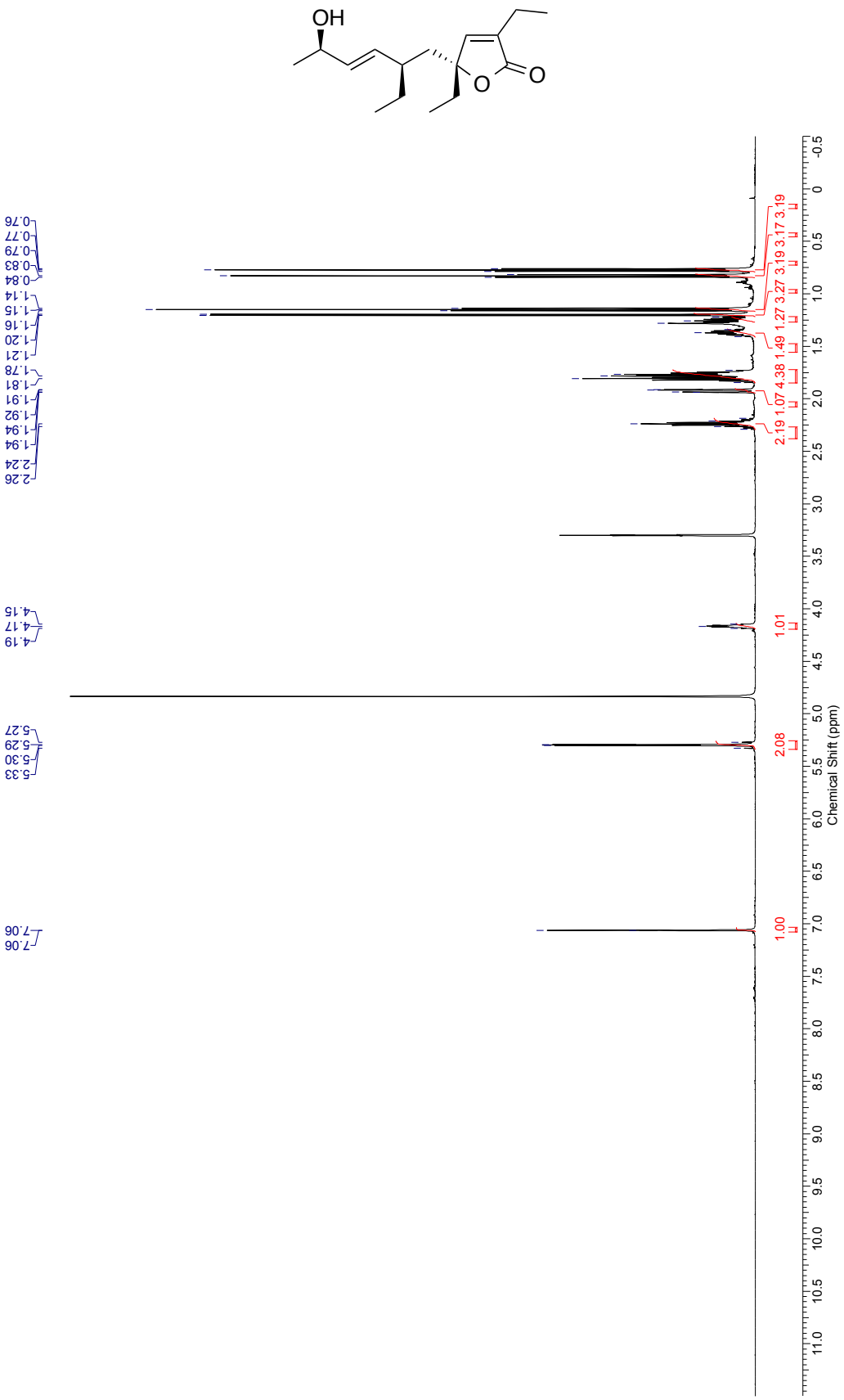

^{13}C NMR (150 MHz, CD_3OD)

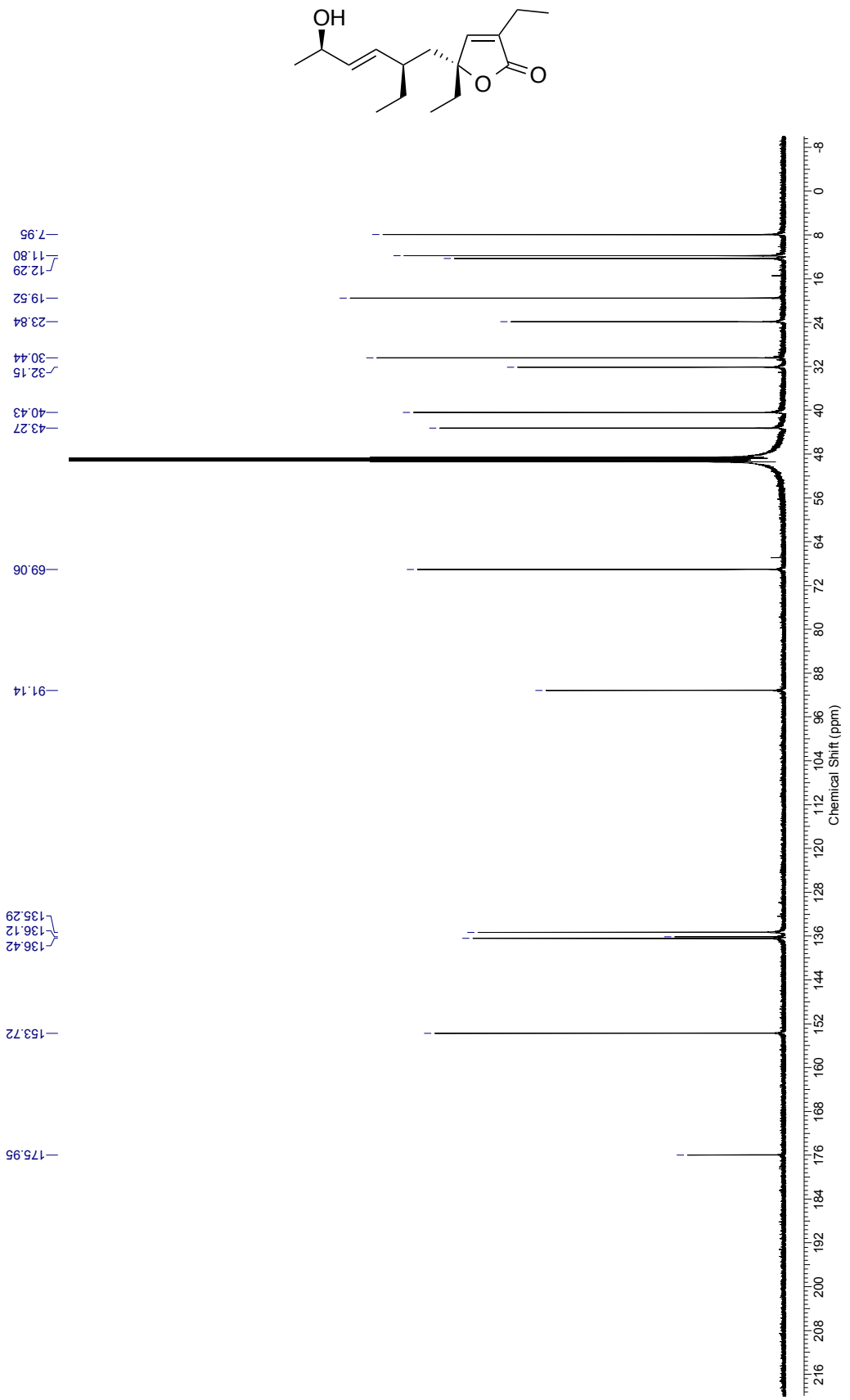

COSY (600 × 600 MHz, CD_3OD)

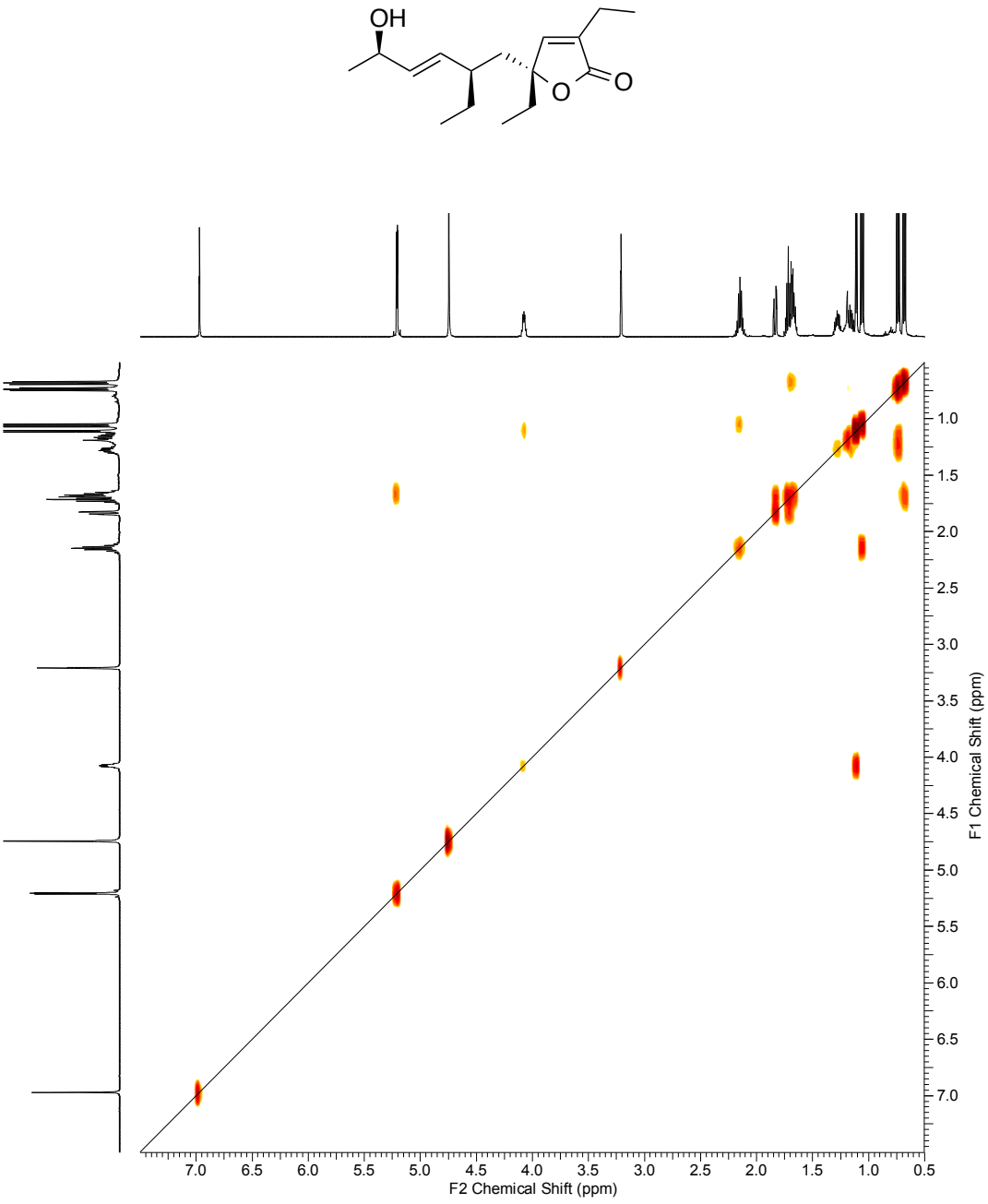

HSQC (600 × 150 MHz, CD_3OD)

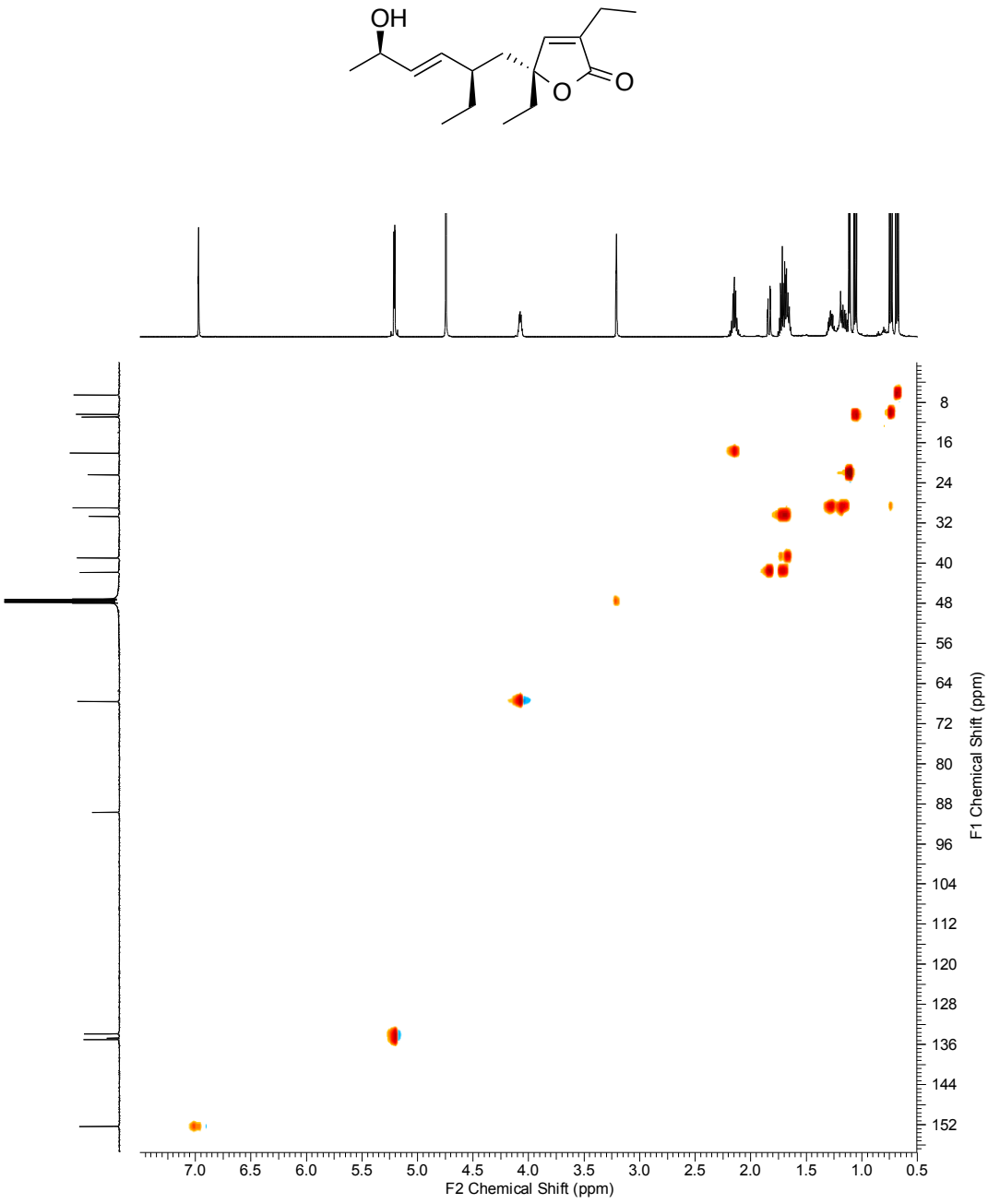

HMBC (600 × 150 MHz, CD_3OD)

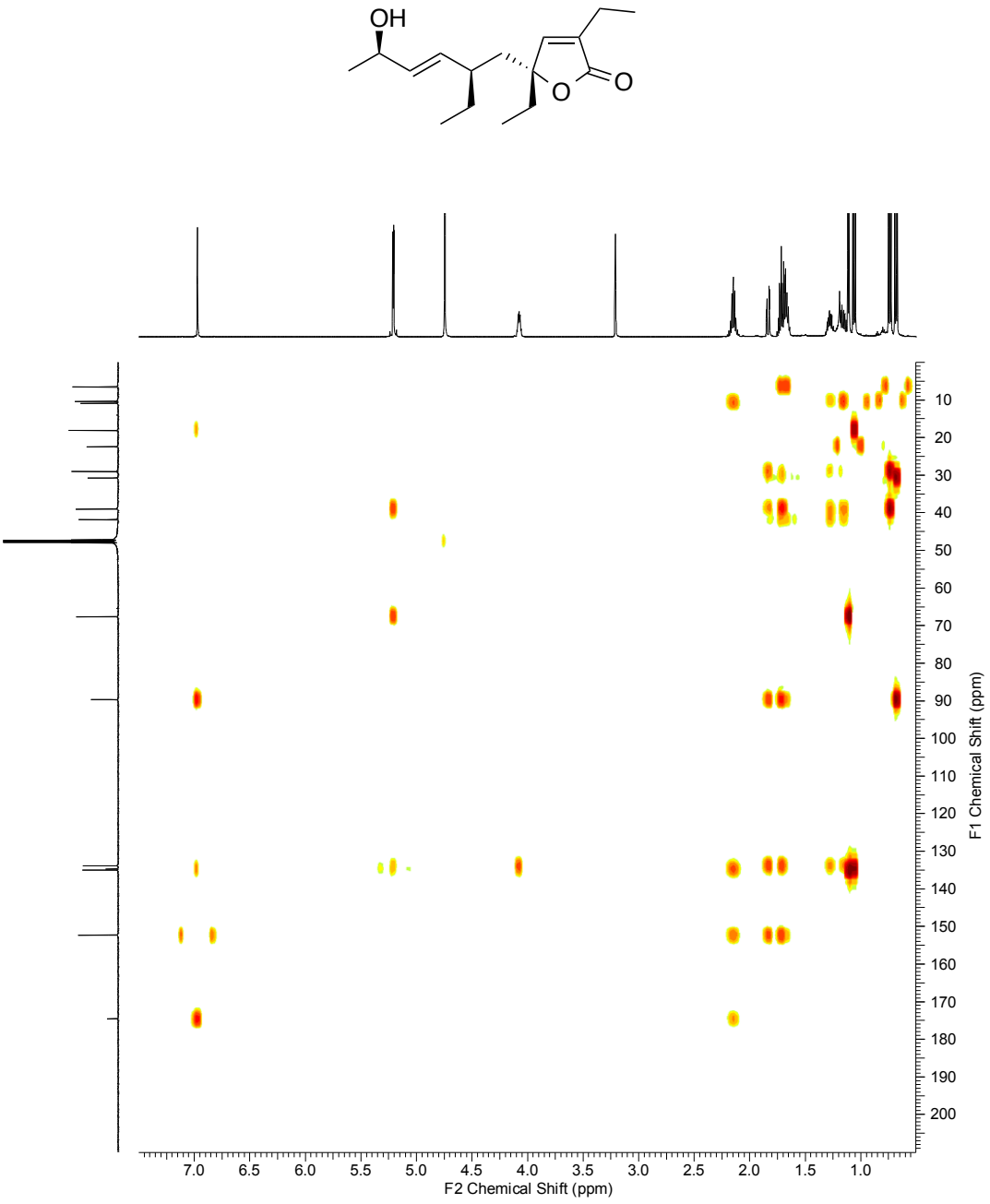

HRMS (ESI)

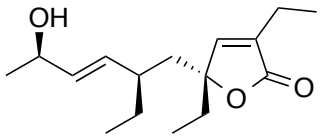

High Resolution Spectra
Positive ion

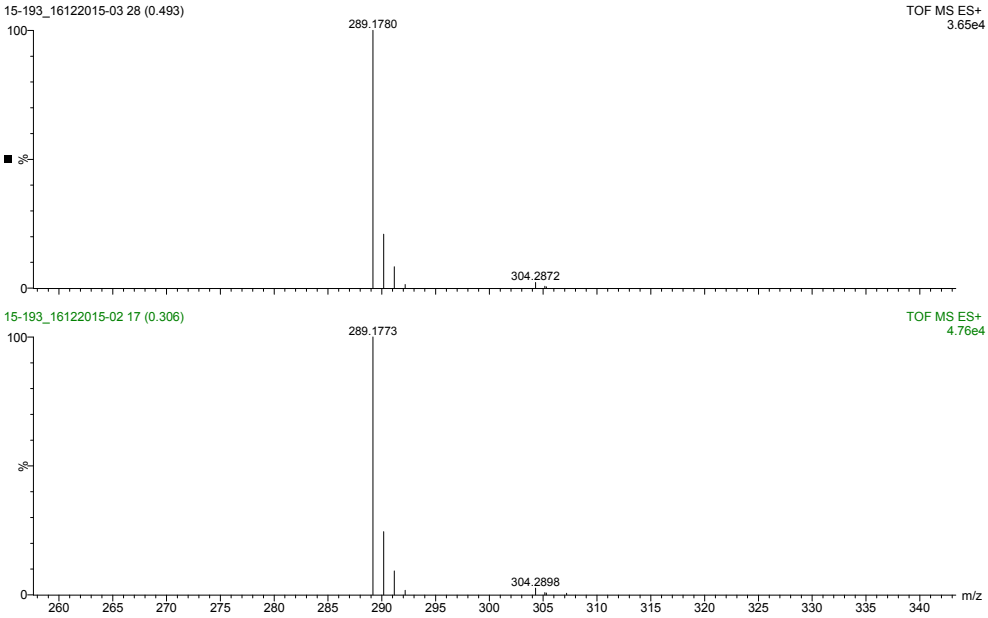

Accurate Mass Data

Observed Mass	Formula $[M+Na]^+$	Calculated mass	Difference (ppm)	iFiT (norm)
289.1773	C16H26O3Na	289.1780	-2.4	0.7
289.1780	C16H26O3Na	289.1780	0.0	0.7

8.1.5 *Synthetic des-hydroxygracilioether C*

^{1}H NMR (600 MHz, $CDCl_3$)

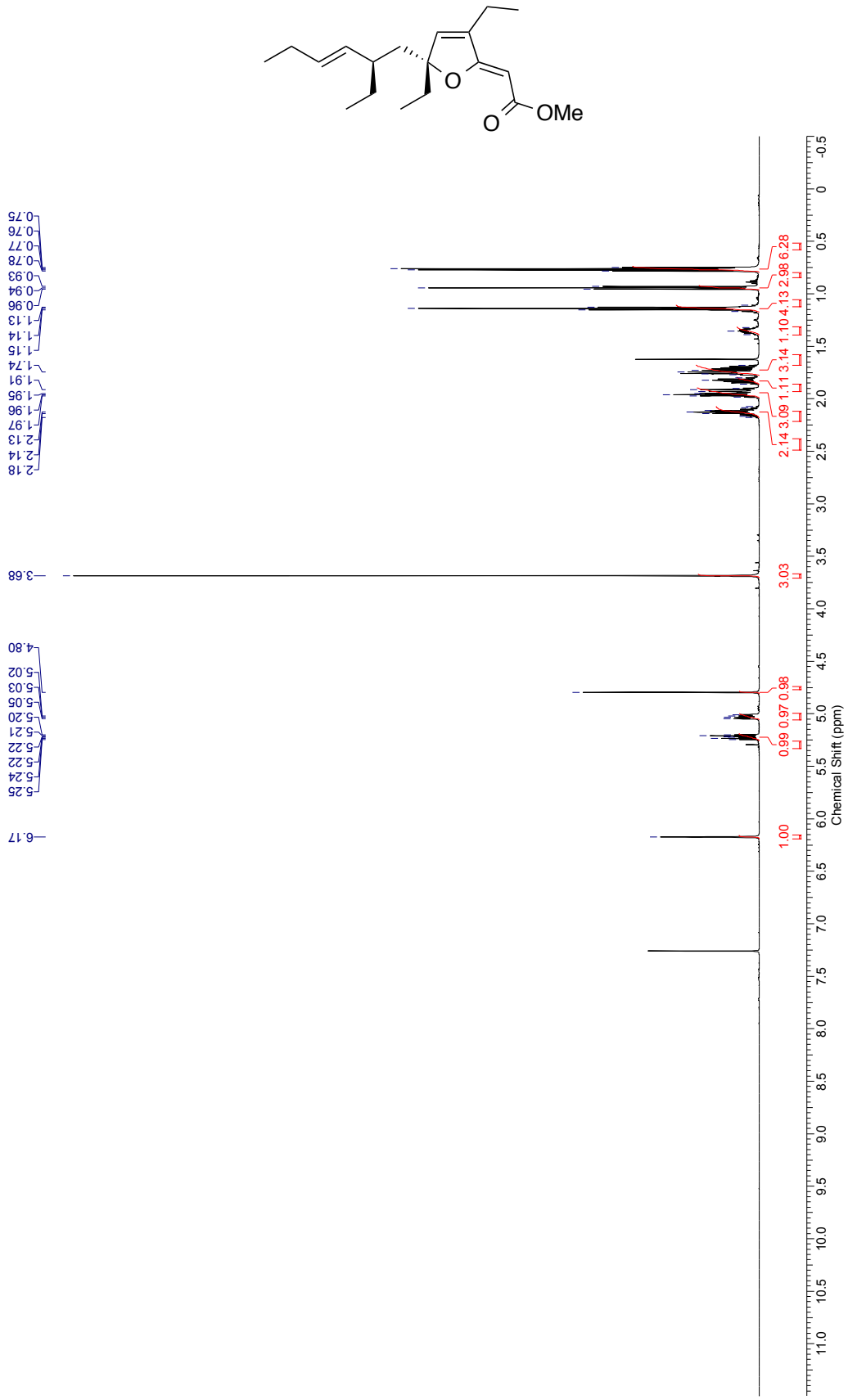

^{13}C NMR (150 MHz, $CDCl_3$)

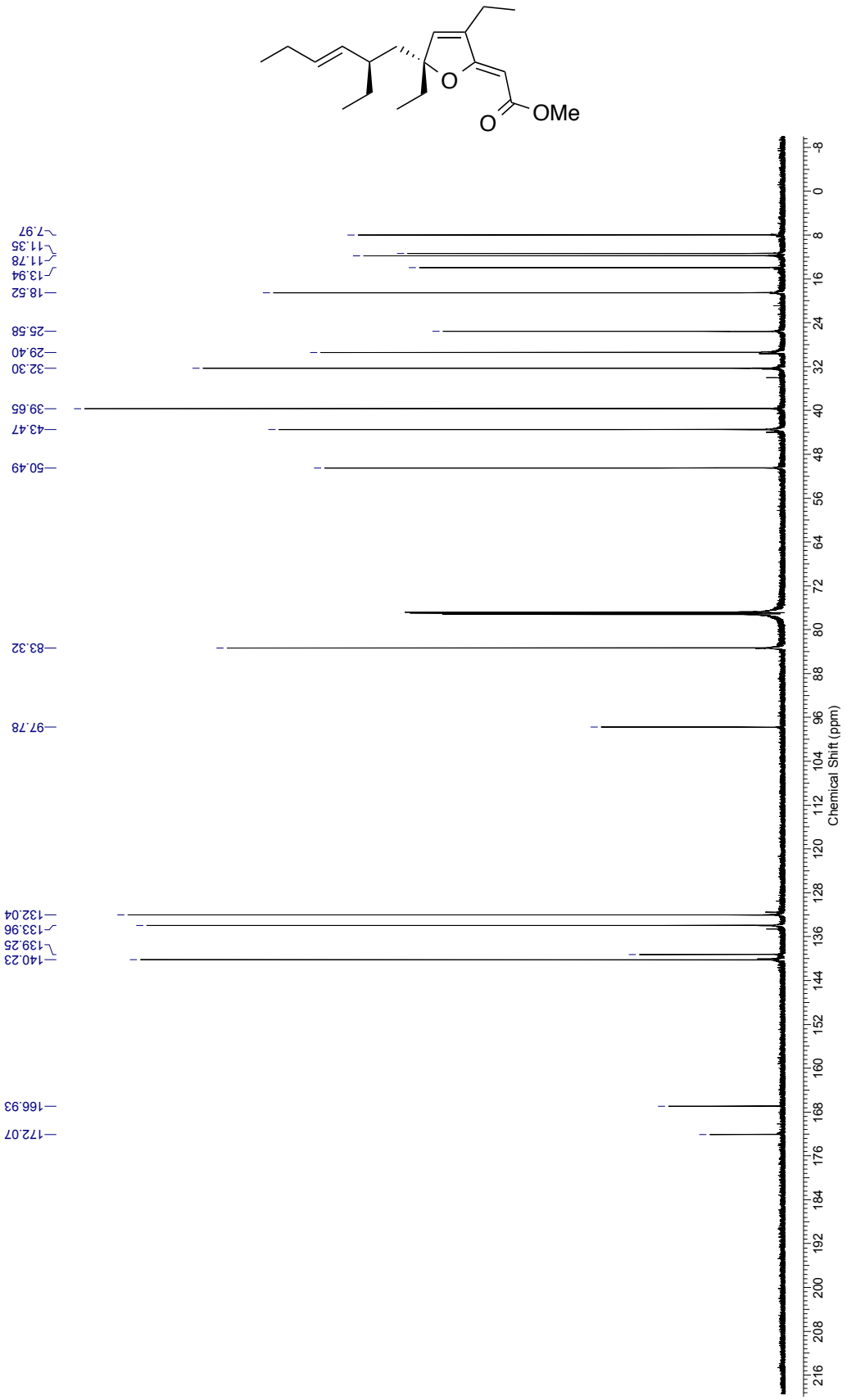

^{13}C NMR (150 MHz, C_6D_6)

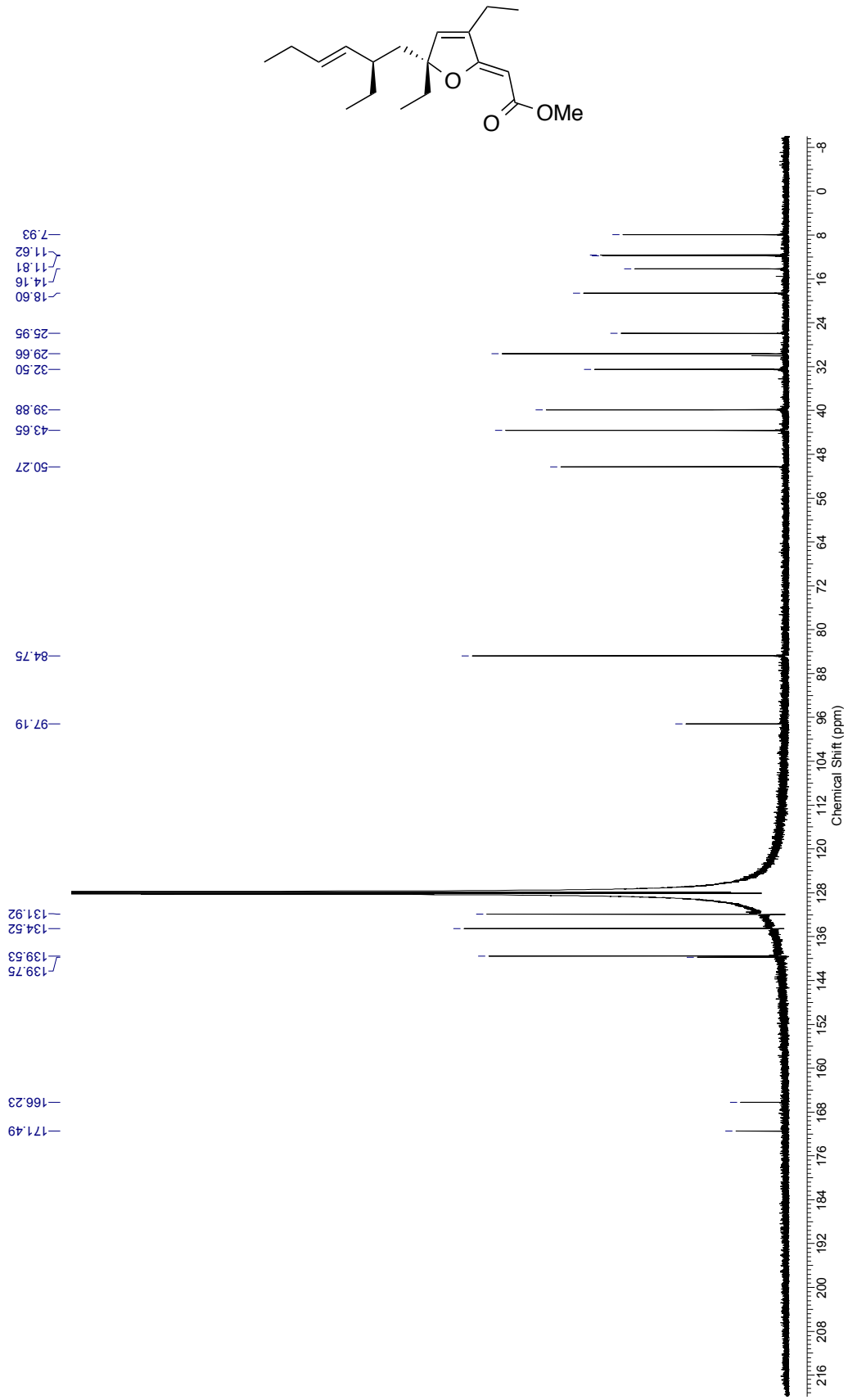

COSY (600 × 600 MHz, $CDCl_3$)

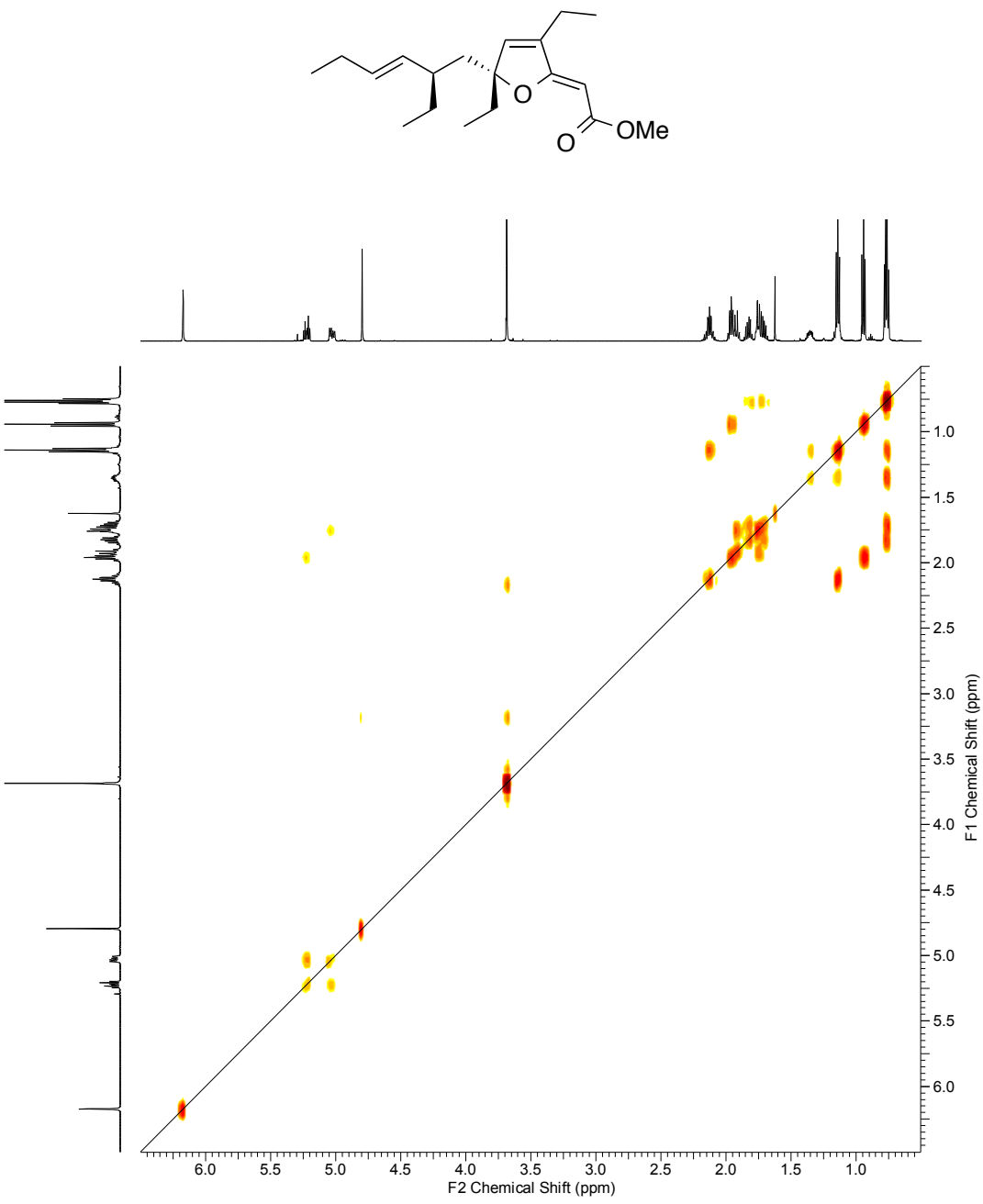

HSQC (600 × 150 MHz, $CDCl_3$)

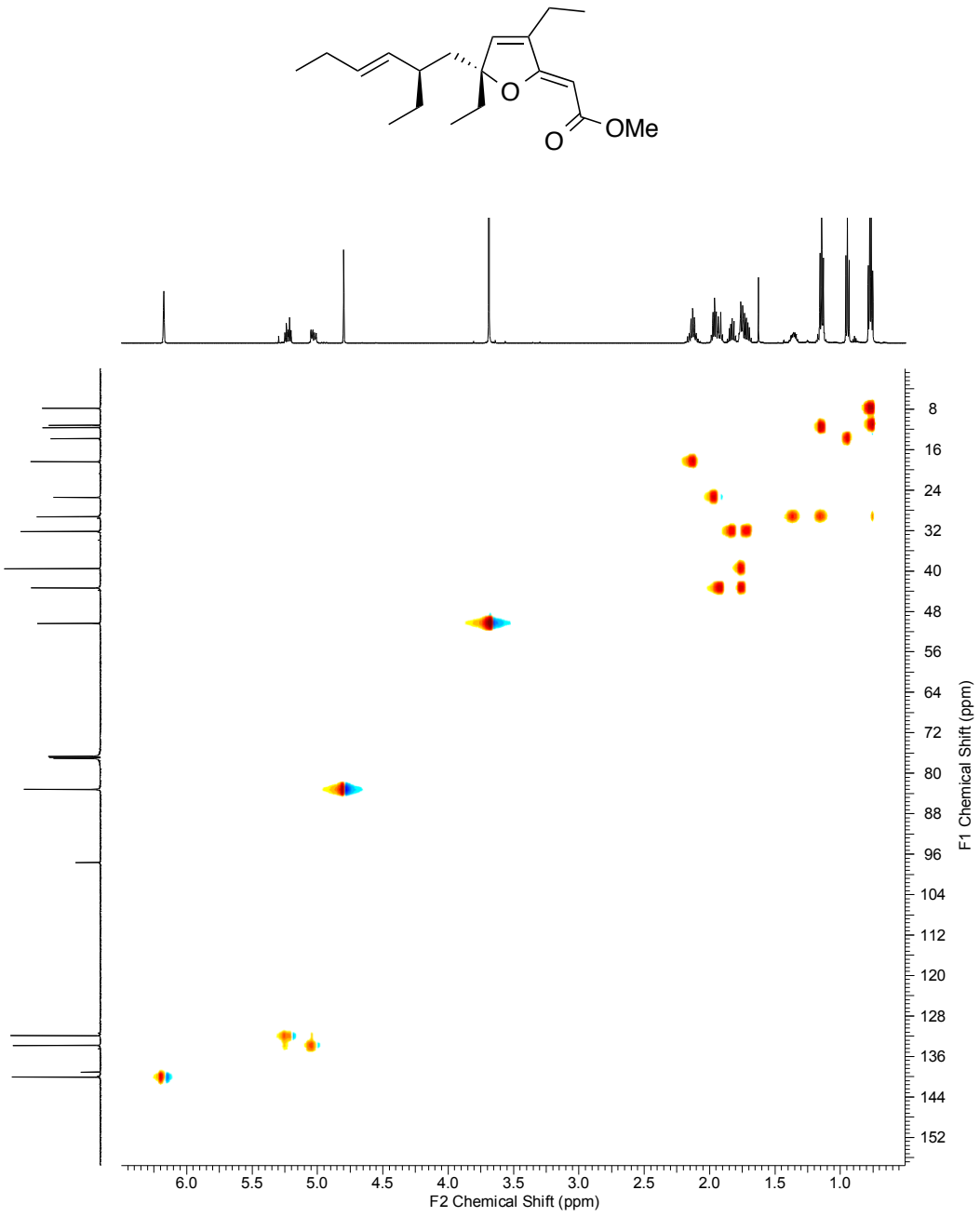

HMBC (600 × 150 MHz, $CDCl_3$)

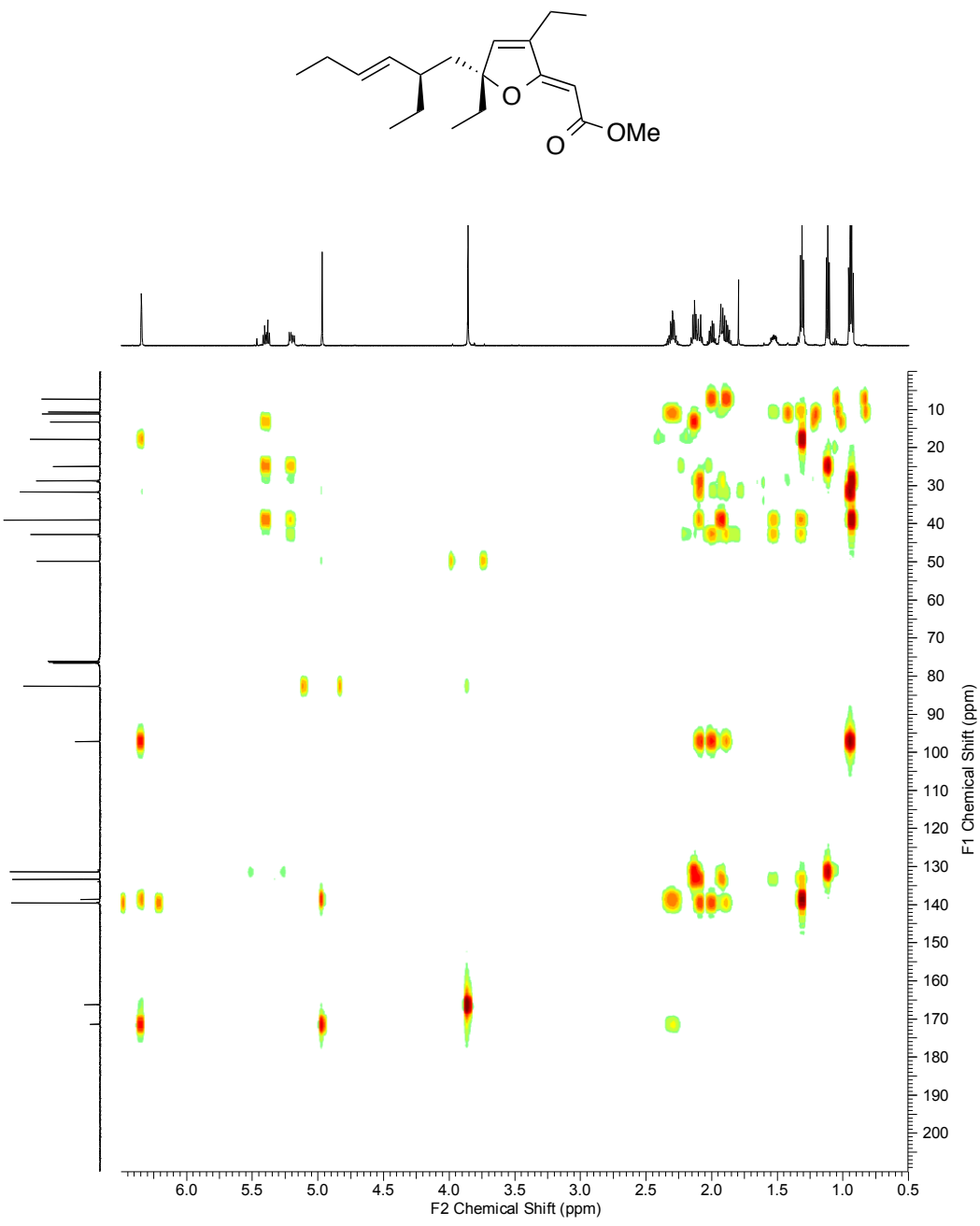

HRMS (ESI)

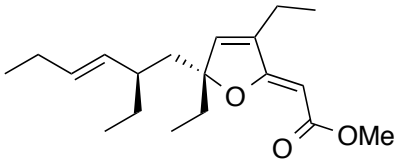

High Resolution Spectra
Positive ion

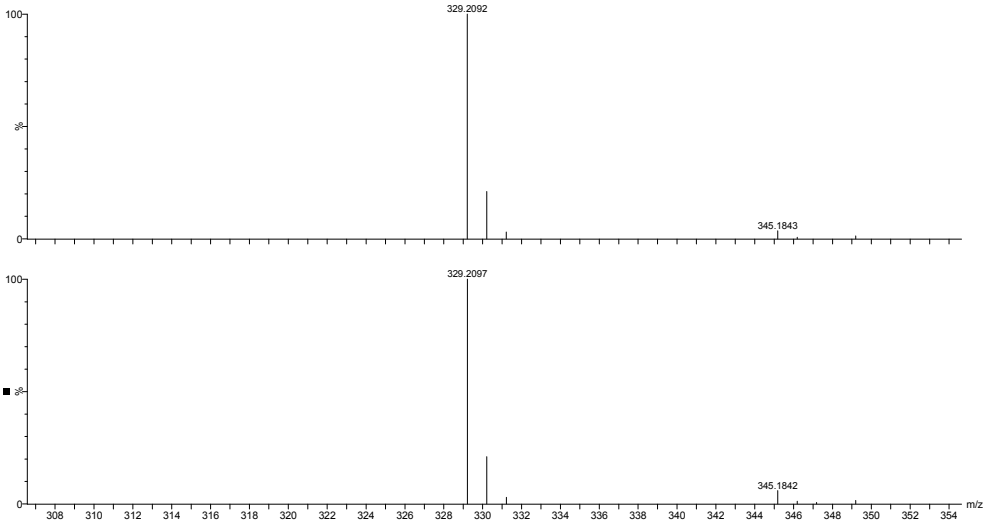

Accurate Mass Data

Observed Mass	Formula $[M+Na]^+$	Calculated mass	Difference (ppm)	iFiT (norm)
329.2097	C19H30O3Na	329.2093	1.2	0.6
329.2092	C19H30O3Na	329.2093	-0.3	1.3

8.1.6 *Synthetic des-hydroxyplakilactone B*

^{1}H NMR (600 MHz, CD_3OD)

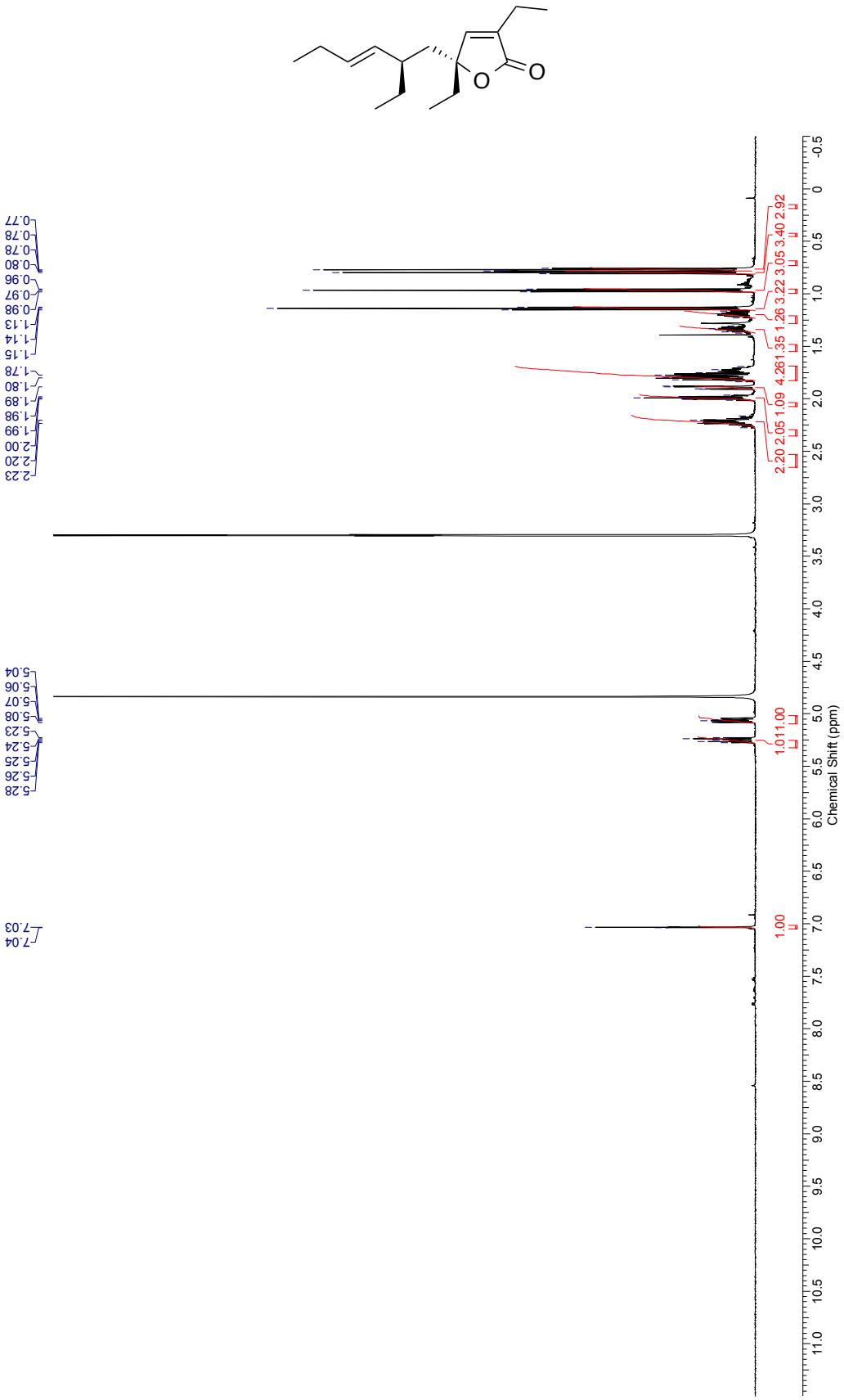

^{13}C NMR (150 MHz, CD_3OD)

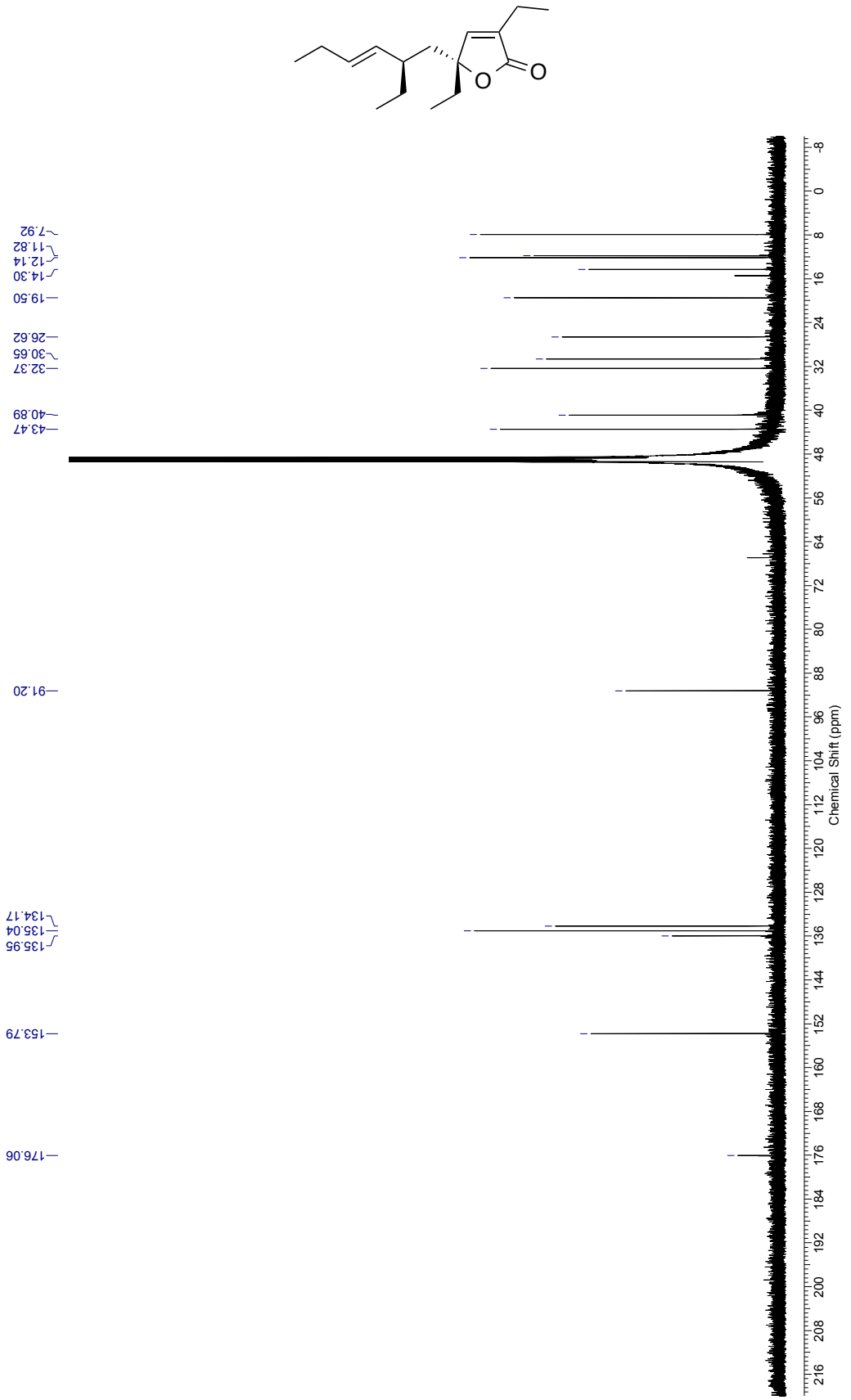

COSY (600 × 600 MHz, CD_3OD)

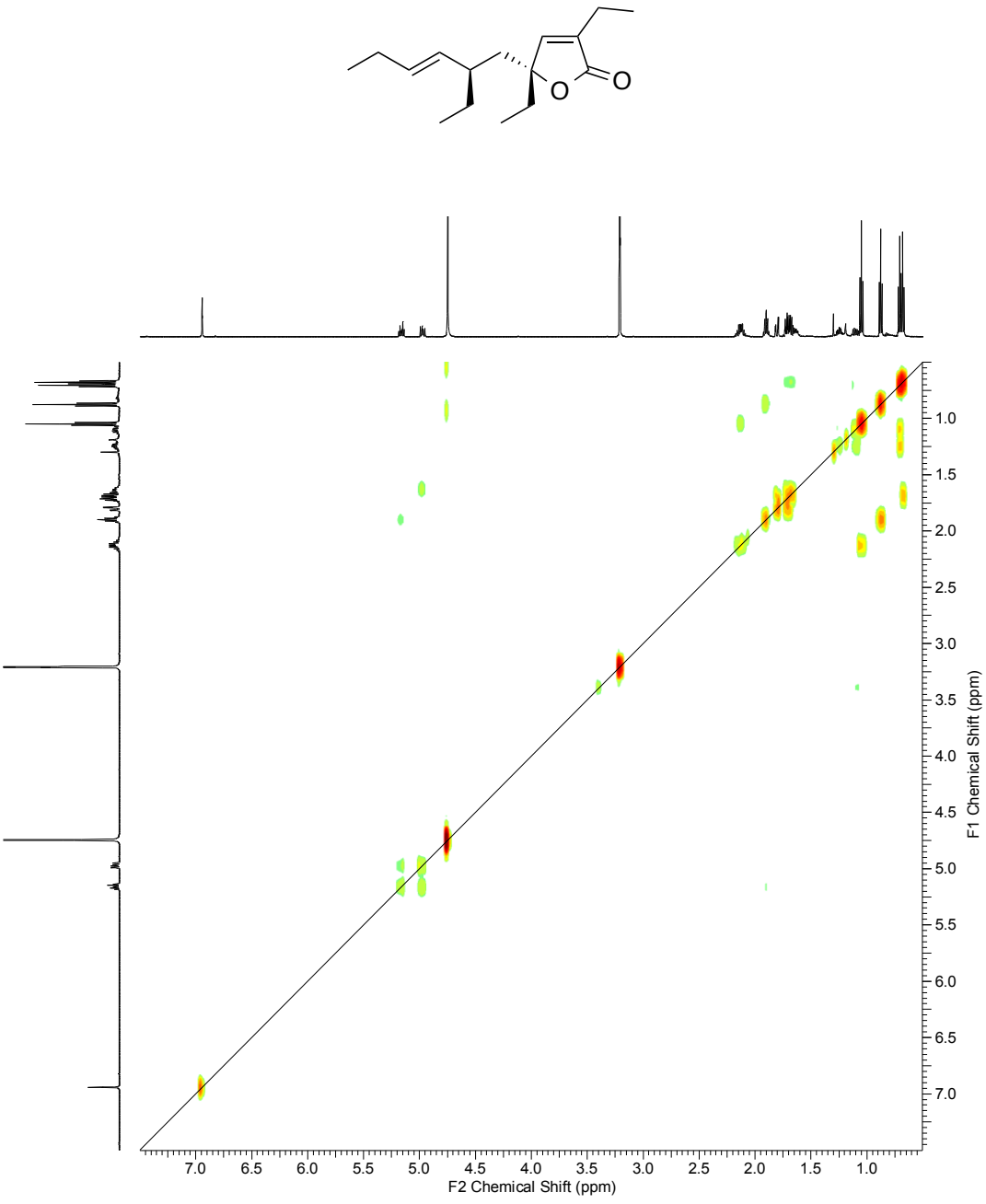

HSQC (600 × 150 MHz, CD_3OD)

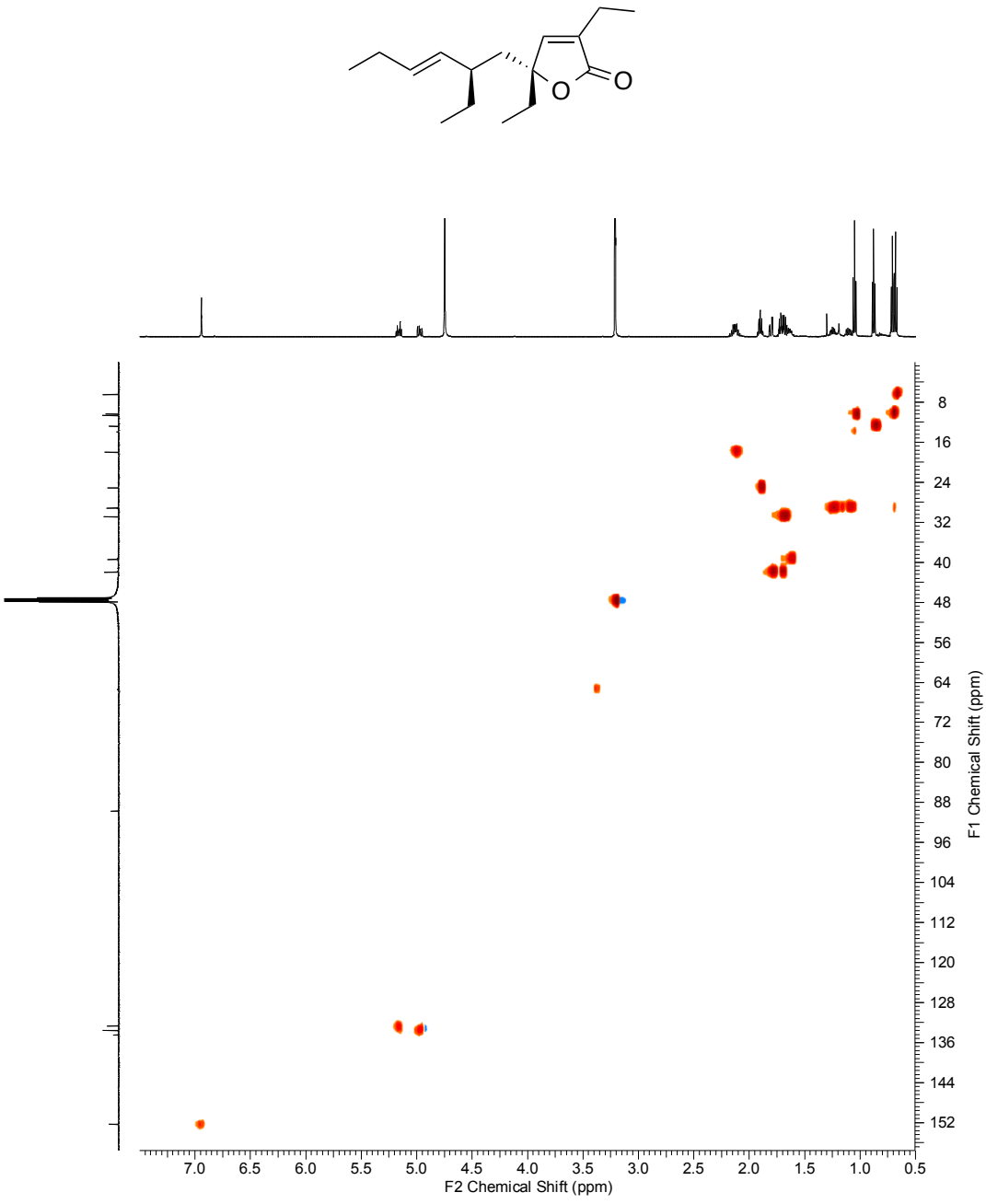

HMBC (600 × 150 MHz, CD_3OD)

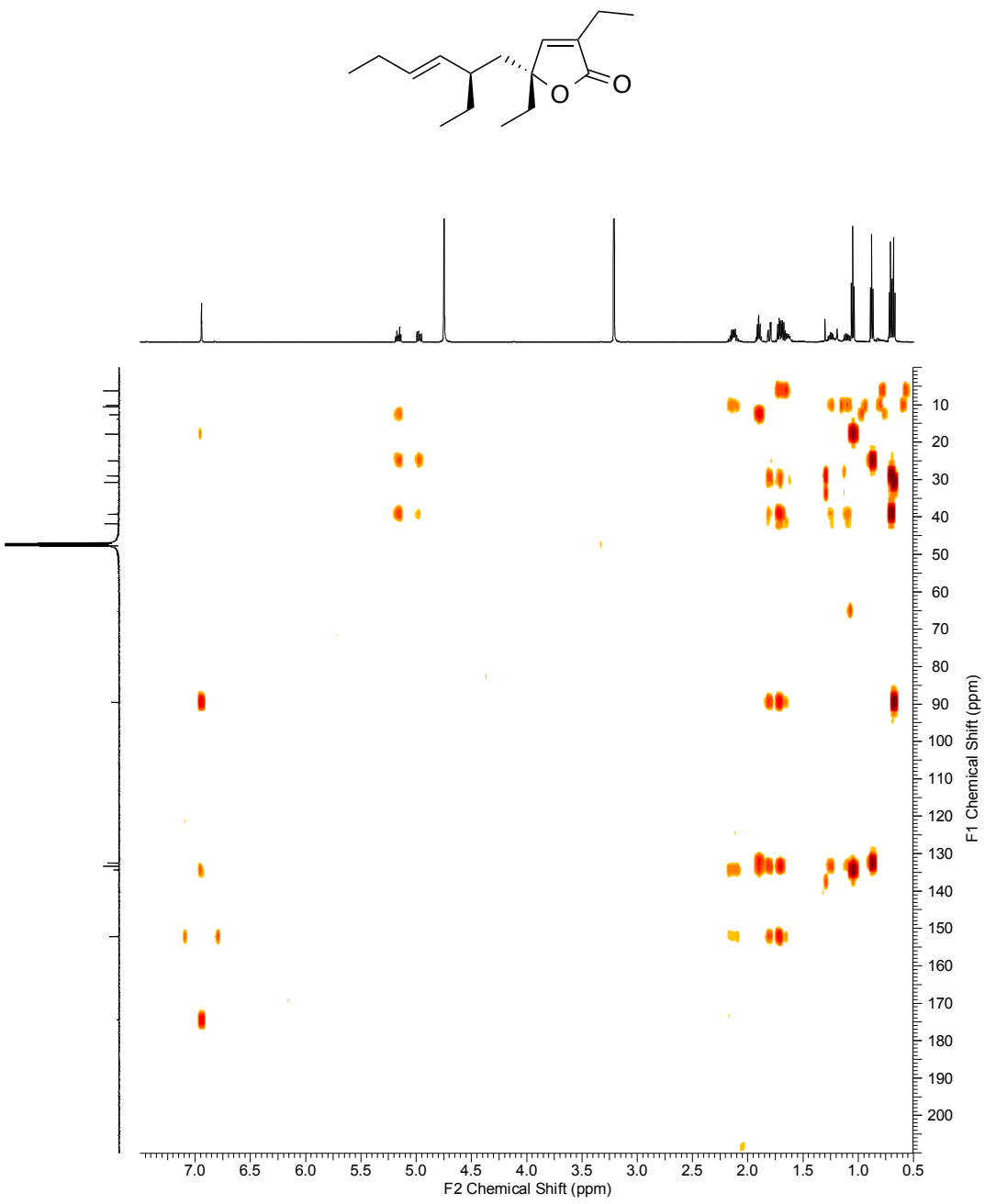

HRMS (ESI)

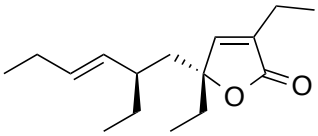

High Resolution Spectra
Positive ion

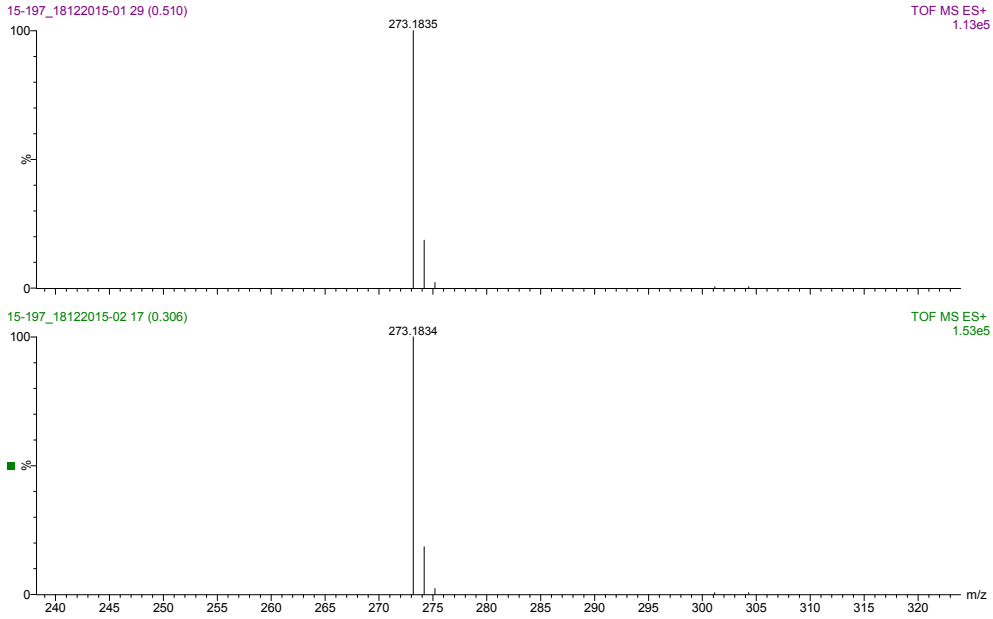

Accurate Mass Data

Observed Mass	Formula $[M+Na]^+$	Calculated mass	Difference (ppm)	iFiT (norm)
273.1834	C16H26O2Na	273.1831	1.1	0.0
273.1835	C16H26O2Na	273.1831	1.5	0.0